Republic of Iraq
Ministry of Higher Education
& Scientific Research
University of Misan
College of Science
Department of Physics

Measurement of Radioactivity Levels and Assessment of Radiological Risks in the Soils of Al-Majar and Kalaat Saleh Cities of Misan Province – Iraq

A Thesis

submitted to the Council of the College of Science, Misan University

in Partial Fulfillment of the Requirements for the Degree of Master of Science in Physics

By

Duaa Mohammed Kadhem

[B.Sc., Wasit University, 2010]

Supervised by

Prof. Dr. Zahraa Abd Al-Hussein Ismail.

2026 A.D. **1448 H.D.**

{وسِعَ رَبُّنا كُلَّ شَيْءٍ عِلْمًا عَلى اللَّهِ تَوَكَّلْنا }

صدق الله العلي العظيم

سورة الأعراف الآية (89)

Supervisor Certification

I certify that the preparation of this thesis, entitled" **Measurement of Radioactivity Levels and Assessment of Radiological Risks in the Soils of Al-Majar and Kalaat Saleh Cities of Misan Province-Iraq** " was made under our supervision by **"Duaa Mohammed Kadhem"** at the College of sciences, University of Misan, in partial fulfilment for the requirements for the degree of the M.Sc. in physics.

Signature:

Name: **Prof. Dr. Zahraa Abd Al-Hussein Ismail**

Titel: Professor

Address: College of Sciences / University of Misan

Date : / / 2026

In view of the available recommendations, I forward this thesis for debate by the examining committee.

Signature:

Name: **Asst. Prof. Dr. Ahmed khalaf**

Title: Assist. Professor

Head of Physics Department/ College of Sciences.

Misan University

Date: / / 2026

Examination Committee Certification

We certify that we have read this thesis "**Measurement of Radioactivity Levels and Assessment of Radiological Risks in the Soils of Al-Majar and Kalaat Saleh Cities of Misan Province-Iraq**" as an examining committee, examined the student "**Duaa Mohammed Kadhem**" in its contents and in our opinion meets the standard of a thesis for the degree of Master in Physics with **(Excellent)** grade.

Signature
Assistant Professor
Dr. Mohammed Kazem Hamad
College of Education
University of Misan
Date: / /2026
(Chairman)

Signature
Assistant Professor
Dr. Sawsan Sherif Fleifl
College of Education for pure sciences
University of Basrah
Date: / /2026
(Member)

Signature
Assistant Professor
Dr. Salih Hassan Jazza
College of Science
University of Misan
Date: / /2026
(Member)

Signature
Profess
Dr. Zahraa Abd Al-Hussein Ismail
College of Science
University of Misan
Date: / /2026
(Supervisor and Member)

Approved for the College Committee of graduate Studies

Signature
Professor
Dr. Tahseen Saddam Fandi
College of Science University of Misan
Date: / /2025
(The Dean)

Dedication

I dedicate this work

To

The spirit of my cherished father.

To my mother, who has consistently supported me and surrounded me with love.

To

my beloved children, brothers, sisters, and friends.

To

my dear parents in law for their kind support.

To

my beloved partner, my husband, whose belief in my ability and constant encouragement made this achievement possible.

Duaa Mohammed

Acknowledgements

Praise be to ***Allah***, lord of the whole creation and peace be on his Messenger ***Mohammed***.

I would like to express my deepest thanks and gratitude to my supervisor ***Prof. Dr. Zahraa Abd-Alhussein*** for her invaluable guidance, advice, and continuous support throughout this research. Besides, I am deeply thankful to the Dean of the College of Science, the Head of the Physics Department, and all my professors in the department for enriching my academic experience with their knowledge and wisdom.

My sincere thanks also go to ***Prof. Dr. Fidaa Al-Mawla*** for her encouragement and guidance during my academic journey.

I am very grateful to ***Dr.Yousif Raad*** and ***Dr.Jalal Ibrahim*** for their generous assistance.

My appreciation is also extended to the Ministry of Environment–Misan Environment Directorate, especially ***Dr. Basim Mohammed*** and ***Eng. Saif Saleh***, for providing the necessary equipment for this study.

I also thank the Ministry of Health, National Authority for Nuclear, Radiological, Chemical and Biological Regulatory Authority, particularly ***Dr.Sabah Al-Hassani*** and ***Mr. Mazen Mohammed***, for their collaboration and assistance in analyzing the collected samples with professionalism and care.

Special thanks are due to Iraqi Ministry of Defense, whose protection ensured my safety during the fieldwork and sample collection phases. Their service made this research possible.

I owe heartfelt thanks to my family for their unwavering support.

Finally, this work stands as a testament to the combined efforts of all who believed in the power of knowledge and service. Thank you.

Duaa Mohammed

Table of Contents

List of Tables

List of Figures

List of symbols

No.	Symbol	Description
1	Bq	Becquerel
2	Ci	Curie
3	Sv	Sievert
4	nGy	Nano Gray
5	α	Alpha particles
6	β	Beta particles
7	γ	Gama radiation
8	$T_{1/2}$	Physical half-life of the radionuclide
9	I_{γ}	Gamma radiation level index
10	H_{in}	Internal hazard index
11	H_{ex}	External hazard index
12	D_{γ}	Air absorbed dose rate for gamma
13	$\varepsilon(E\gamma)$	Detector efficiency at energy (E_{γ})
14	λ	Decay constant
15	KeV	Kilo electron volt
16	MeV	Mega electron volt
17	°K	Degree kelvin
18	°C	Degree centigrade

List of Abbreviations

No.	Symbols	Description
1	ARS	Acute radiation syndrome
2	B. D. L	Below detection limit
3	ICRP	International committee on radiation protection
4	HPGe	High purity germanium
5	IAEA	International atomic energy agency
6	Ra_{eq}	Radium equivalent activity
7	H_{in}	Internal hazard index
8	H_{ex}	External hazard index
9	I_{γ}	Gamma Index
10	D_{in}	Absorbed dose rate indoor
11	D_{out}	Absorbed dose rate outdoor
12	D_{tot}	Absorbed dose rate total
13	$AEDE_{in}$	Annual effective dose equivalent indoor
14	$AEDE_{out}$	Annual effective dose equivalent outdoor
15	$AEDE_{tot}$	Annual effective dose equivalent total
16	$ELCR_{in}$	Excess lifetime cancer risk indoor
17	$ELCR_{out}$	Excess lifetime cancer risk outdoor
18	$ELCR_{tot}$	Excess lifetime cancer risk total
19	AGDE	Annual gonadal dose equivalent
20	DL	Duration of life
21	DNA	Deoxyribonucleic acid
22	UNSCEAR	United nations scientific committee on the effects of atomic radiation
23	FWHM	Full width at half maximum
24	Dis	Disintegration
25	CNF	Calibration nuclear factor
26	B. G	Radiation background
27	GPS	Geological position system
28	ISO	International organization for standardization
29	PCA	personal computer spectrum analyzer
30	MCA	Multichannel analyzer
31	MDA	Minimum detection activity
32	S. A	Specific activity

No.	Symbols	Description
33	D.L.	Detection limit
34	Uk	United Kingdom
35	N_{BG}	Net peak area
36	SI	International system of units
37	IEC	International electro technical commission

Summary

Natural radionuclides (^{226}Ra, ^{232}Th, and ^{40}K) and artificial radionuclide (^{137}Cs) were measured in soils of Al-Majar and Kalaat Saleh, in Misan province, Iraq. A total of fifty soil samples were collected and analyzed using high-purity germanium (HPGe) detector.

The average activity concentrations of ^{226}Ra, ^{232}Th, ^{40}K, and ^{137}Cs in Al-Majar were14.012 ± 4.650 Bq/kg, 14.589 ± 2.521 Bq/kg, 176.791 ± 9.827 Bq/kg, and 1.626 ± 0.963 Bq/kg, respectively. In Kalaat Saleh, the corresponding values were 16.072 ± 5.455 Bq/kg, 20.752 ± 3.650 Bq/kg, 187.813 ± 11.011 Bq/kg, and 2.480 ± 1.023 Bq/kg, respectively.

The hazard indices has been calculated in the present thesis, which include radium equivalent activity (Ra_{eq}), internal and external hazard indices (H_{in} and H_{ex}), gamma level index (I_{γ}), absorbed gamma dose rates (D_{in}, D_{out}, and D_{tot}), annual effective dose equivalents ($AEDE_{in}$), external annual effective dose equivalents ($AEDE_{in}$, $AEDE_{out}$, and $AEDE_{tot}$), excess lifetime cancer risks ($ELCR_{in}$, $ELCR_{out}$, $ELCR_{tot}$), and annual gonadal dose equivalent (AGDE), and the average values were found to be (48.488 ± 5.749 Bq/kg), (0.1688 ± 0.026 and 0.130 ± 0.015), (0.178 ± 0.019), (43.260 ± 4.916 nGy/h, 22.658 ± 2.542 nGy/h, and 65.918 ± 7.457 nGy/h), (0.212 ± 0.024 mSv/y, 0.027 ± 0.003 mSv/y, and 0.240 ± 0.027 mSv/y), ((0.742 ± 0.084)×10^{-3}, (0.097 ± 0.010)×10^{-3}, and (0.840 ± 0.095)×10^{-3}), (159.795 ± 17.088 μSv/y), respectively in Al-Majar. While in Kalaat Saleh the corresponding value were (60.209 ± 9.223 Bq/kg), (0.206 ± 0.037, and 0.162 ± 0.024), (0.219 ± 0.031), (52.826 ± 7.844 nGy/h, 27.791 ± 11.945 nGy/h, and 80.618 ± 11.945 nGy/h), (0.259 ± 0.038 mSv/y, 0.034 ± 0.005 mSv/y, and 0.293 ± 0.0435 mSv/y), ((0.907± 0.134)×10^{-3}, (0.119 ± 0.017)×10^{-3}, and (1.026 ± 0.152)×10^{-3}), (195.381 ± 27.988 μSv/y), respectively.

The results showed that the activity concentrations of ^{226}Ra, ^{232}Th, ^{40}K, and ^{137}Cs were below the recommended value by United nations scientific committee on the effects of atomic radiation (UNSCEAR). Moreover, all estimated radiation hazard parameters for natural radionuclides in both cities were below the recommended limits, suggestion no health risk from radioactivity in the study areas.

Introduction and Literature Review

Chapter One

Introduction and Literature Review

1.1. Introduction

In 1898, Marie Curie discovered that uranium and thorium undergo radioactivity. Before the end of 1898, Marie Curie discovered two radioactive elements, one of which she called polonium and the other radium [1]. The experiments of the scientist Ernest Rutherford in 1898 showed the existence of two types of particles, the first of which has the ability to be easily absorbed by matter and the other of which has the ability to penetrate. He called these alpha and beta particles. In 1900, the French scientist Villard discovered rays with greater penetrating power, which he called gamma rays [2]. Later it was found that particles such as neutrons and positrons are also emitted from some decaying nuclei [3].

Radiation is defined as the energy released by unstable atomic nuclei and can travel as particles (neutrons, beta, or alpha) or electromagnetic waves (gamma or X-rays). Radioactivity refers to the spontaneous decay of these atoms, with the excess energy released resulting in ionizing radiation [4]. The two primary sources of ionizing radiation that all living things are constantly exposed to are natural and man-made radionuclides. Natural radiation, which includes both cosmic and terrestrial radiation, makes up about 85% of the dose absorbed [5]. Many radionuclides of artificial origin have been released to the environment by different processes. Cesium isotopes are the most important ones that may be deposited by fallout over soil and plants as they are produced anthropogenically by several types of nuclear activities including past testing of nuclear weapons and nuclear accidents[6]. Transuranic (plutonium isotopes) and long - lived fission products (^{137}Cs, ^{90}Sr) are examples of manufactured radionuclides[7].

Numerous geological formations, including earth's crust, rocks, soils, plants, water, and air exhibit natural radioactivity. The concentration of this radioactivity varies depending on geographical factors and is observed at different levels in soils across various geological regions [8].

Soil is the upper part of the earth's crust, formed as a result of rock deformation driven by complex physicochemical processes such as weathering, decomposition, and water movement Consequently, soil represents the outcome of both weathering and human activities affecting crustal rocks. Due to its mineral composition, soil is inherently radioactive, and the level of natural radioactivity can vary substantially between different soil types [9].

One of the major sources of natural background radiation is soil radionuclide activity. Natural radionuclides such as ^{238}U, ^{232}Th, and ^{40}K can be found in granite and salt. Rain fall and water movement bring these radionuclides to the soil, and human activity also affects soil radioactivity [10].

These long radionuclides mostly originate from two sources: cosmogenic radioisotopes (^{3}H,^{7}Be,^{14}C, and ^{22}Na), and natural radionuclides, which are radionuclides from the three natural decay chains (^{238}U,^{235}U,^{232}Th). After being discharged into the atmosphere, radionuclides are quickly deposited on the surface of the earth through either wet or dry deposition. The top surface of the soil is where radionuclides are first deposited, but they quickly move into the first centimeter of soil, particularly if they are deposited by rainfall. The mineral composition of rocks and sediments is closely linked to the levels of Thorium, Uranium, and Potassium [11, 12].

1.2. Radionuclides Behavior in the Soil

The earth's surface layer known as soil, is composed of roughly 45% mineral materials, 5% organic materials which are represented by plant and animal waste accumulations, 25% air, which is represented by gases like Co_2, N_2, and O_2, and 25% water. The natural, chemical, and biological makeup of these elements determines the soil's fertility and yield [13]. So, it's a complex physicochemical system. Soil is made up of several different elements that can affect radionuclide mobility. The four distinct layers, known as horizons, these horizons divided into [14].

1.2.1. The first upper horizon: known as surface soil layer, approximately 30 cm deep, and contains the majority of biological activity. The uppermost layer contains loose leaves and organic fragments most of which have not yet degraded.

1.2.2. The second horizon: known as the subsoil layer, is located around one meter below the soil's surface. The surface soil layer's suspended material builds up in this layer. In this layer comprises partially decomposed organic material, and organic compounds are combined with mineral material.

1.2.3. The third horizon: which reaches a depth of 1.5 meters, is made up of layers of loose stones that have been partially shattered into small pieces, as well as weathered rocks that serve as the soils' parent materials.

1.2.4. The fourth horizon: it consists of layers that were not the soil's parent material but has a significant influence on the underlying ground [15].

There are several mechanisms responsible for radionuclide movement in soil, including convection and diffusion. Radionuclides may return to the atmosphere through volatilization, wind, or upper migration from the surface soil layers. The vertical migration rate in soil depends on depth and is not constant [16]. Diffusion plays a significant role only under extremely dry soil conditions. Since the study

area is characterized by long, hot, dry summers and cold, rainy winters, these climatic conditions strongly influence radionuclide concentrations in soil. These mechanisms highlight how environmental factors control radionuclide behavior and create the basis for their potential transfer to plants [17].

Long-lived radionuclides such as ^{40}K, ^{238}U decay series, ^{232}Th decay series, and ^{137}Cs when present in soil, are absorbed by plants and subsequently transferred into the food chain. They reach humans indirectly through animal products such as meat and milk. Due to their high biological mobility, these radionuclides pose serious health risks once internally deposited, as they emit radiation that can cause biological damage [18].

The environment is one of the most critical determinates of human health and life. Soil, air, water, and plants serve as essential resources, but may also act as carriers of radiation exposure. Understanding this environmental pathway is therefore essential to assess for evaluating risks and ensuring public health protection. Monitoring these levels is vital for protecting community health and safety, as increased exposure is associated with adverse somatic and genetic effects. Furthermore, elevated radiation levels contribute to radioactive pollution, which is a form of environmental pollution [19].

Radioactive contamination refers to the presence of dispersed radioactive material that poses either a potential or an actual risk to human health.[20].

Thus, it is imperative to investigate the effects of radiation, assess radionuclides concentrations, and evaluate their potential risks to human health and the

1.3. Biological Impacts of Ionizing Radiation

Humans can be exposed to radioactive nuclides through three main routes: ingestion, contact, and inhalation. Lung cancer risk will rise as a result of the inhaled radioactive particles passing via lungs. When consumed, these particles may accumulate in the bone, increasing the risk of leukemia in the red bone marrow or bone cancer. Also they inhabit soft tissues, such as the gonads, raising the risk of genetic health effects, including as birth abnormalities [22].

Ionizing radiation can disrupt a molecule's structure by transferring energy into body tissue. This energy transfers in living things and can alter the genetic mutation of cells (hereditary effect), disrupt or destroy cellular activities (somatic effect, which includes both deadly and nonfatal cancer) [23]. wherefore, two categories are commonly used to classify the biological consequences of radiation: In the first category, there are short-term or acute effects from high doses of radiation exposure, and in the second category, there are long-term or chronic effects from low doses of radiation exposure over a longer period of time (Stochastic) [24]. Whereas low dosages tend to change or harm cells, big quantities tend to kill them. Excessive dosages have the potential to destroy a large number of cells, harming organs and tissues [25]. The rapid whole-body reaction known as Acute Radiation Syndrome (ARS) may ensue from this [26].

To measure soil radioactivity and build the pictures of risk distribution is an effective solution to determine natural background radiation[27].

Despite its drawbacks although ionizing radiation has many beneficial applications in industry, research, medicine, and agriculture, if it is used or handled poorly, it can pose health hazards [28].

1.4. Literature Review

Many earlier studies International, Arabic and the Local on measuring the concentrations of natural and artificial radionuclides in soils are done using a high purity germanium (HPGe) detector.

The following are the most important researches:

1.4.1. The International Studies

- Selvasekarapandian and et al. (2000) measured the radioactivity of the nuclides ^{238}U, ^{232}Th, ^{40}K in samples of surface soils from different locations Gudalore Taluk in the Udagamandalam district, India. They have found that the growth rate and radioactivity concentrations of these nuclides were (75.3±44.1) Bq/kg, (37.7±10.1) Bq/kg, and (195.2±85.1) Bq/kg, respectively [29].
- Chikasawa and et al. (2001) measured the radioactivity of the ^{40}K, ^{208}TI, ^{214}Bi, and ^{137}Cs nuclides in soil samples collected from Kochi Prefecture, Japan. The concentration of the radionuclides ranged are (1300-16.6) Bq/kg, (82.8−1.3) Bq/kg, (100- B.D.L) Bq/kg, and (150-1.4) Bq/kg, respectively [30].
- Kannan and et al. (2002) measured the radioactivity of ^{238}U, ^{232}Th, and ^{40}K in soil samples collected from Kalpakkam, India. They found that the concentrations of the radionuclides ranged are (71–5) Bq/kg, (776–15) Bq/kg, and (854–200) Bq/kg, respectively [31].
- Hannan and Hanson (2006) measured the radioactivity of ^{238}U, ^{235}U, ^{226}Ra, ^{40}K, and ^{137}Cs in soil samples collected from Mission, Texas, USA. The concentrations of radionuclides for ^{238}U: (3.11±0.47) Bq/kg – (42.5±5) Bq/kg, ^{235}U: (2.14±0.43) Bq/kg – (8.75±1.14) Bq/kg, ^{226}Ra: (35±4) Bq/kg – (248±25) Bq/kg, ^{40}K: (75±11.3) Bq/kg – (178±22) Bq/kg, and ^{137}Cs: (3.11±0.44) Bq/kg – (13.2±1.85) Bq/kg, respectively [32].

- Akhtar and et al. (2004) studied and measured the radioactivity of the ^{40}K, ^{226}Ra, ^{232}Th, and ^{137}Cs nuclides in soil samples collected from the city of Lahore in Pakistan. The concentrations of the radionuclides ranged between (524.84-601.62) Bq/kg,(28.17-24.73)Bq/kg, (52.61-45.46) Bq/kg, and (B.D.L.), respectively [22].
- Yordanova and et al. (2005) measured the radioactivity of the radionuclides ^{137}Cs, ^{238}U, ^{235}U, ^{226}Ra, and ^{232}Th in soil samples collected from different locations along the Danube River in Bulgaria. They found that the concentrations of the radionuclides ranged from (76±2-2±0.5) Bq/kg, (23±5-50±10) Bq/kg, (1±0.3 - 2±0.5) Bq/kg, (40±5-9±2) Bq/kg, and (50±8-12±2)Bq/kg, respectively [33].
- Júnior and et al. (2005) measured the radioactivity of the ^{40}K nuclide in soil samples collected from western Pernambuco State, Brazil, and found that the concentrations of the radionuclide ranged from (3572-541) Bq/kg [34].
- Adrovic and et al. (2007) measured the radioactivity of the ^{226}Ra, ^{232}Th, ^{40}K, ^{238}U, and ^{235}U isotopes in soil samples collected from some areas in Kosovo (Serbia). They found that the concentrations of the radionuclides ranged from (55-19)Bq/kg, (66-11)Bq/kg, (648-83)Bq/kg, (95-26)Bq/kg, and (4.6-1.2)Bq/kg, respectively [35].
- Alias and et al. (2008) measured the radioactivity of ^{40}K, ^{226}Ra and ^{228}Ra in soil samples collected from different locations in Malaysia. They found that the concentrations of radionuclides ranged between (383.8±41.4-11.3±1.3) Bq/kg, (42±1.5-10.5±0.7) Bq/kg, and (44.9±3.7-11.4±1.2) Bq/kg, respectively [36].
- Mehra and et al. (2009) measured the radioactivity of ^{238}Ra, ^{232}Th and ^{40}K isotopes of soil samples collected from different locations in Faridkot and Mansa districts of Punjab, India. They found that the concentrations of the radionuclides ranged from (40.23-21.42)Bq/kg, (61.01-142.34)Bq/kg, and (227.11-357.13) Bq/kg, respectively [37].

- Śleziak and et al. (2010) measured the radioactivity of the ^{226}Ra, ^{232}Th, ^{40}k, and ^{137}Cs radionuclides in soil samples collected from an industrial area in Poland. They found that the concentrations of the radionuclides ranged between (155±2-35±1) Bq/kg, (83±1-53±1) Bq/kg, (580±11-428±10)Bq/kg, and (146±4-1.8±0.2) Bq/kg, respectively [38].
- Sahoo and et al. (2011) measured the radioactivity of the ^{226}Ra, ^{232}Th, and ^{40}K radionuclides in soil samples collected from different locations in Japan. They found that the concentration of the radionuclides ranged from (35.6±0.6- 6.7± 0.4) Bq/kg, (59.1±1.1-8.6±0.4) Bq/kg, and (852.8±6.5-136.2±2.7) Bq/kg, respectively [39].
- Ramola and et al. (2011) measured the radioactivity of the nuclides ^{40}K, ^{238}U, ^{235}U, ^{226}Ra, ^{232}Th, ^{230}Th, ^{210}Pb, and ^{137}Cs in soil samples collected from the eastern part of the Himalayas in India. They found that the concentrations of the radionuclides ranged from (1758-124.6) Bq/kg, (1305.5-32.6) Bq/kg, (18.2-1.2) Bq/kg, (186.9-2.4) Bq/kg, (16.3-136.3) Bq/kg, (11.5-0.2) Bq/kg, (260.6-0.1) Bq/kg, and (8.2-0.4) Bq/kg, respectively [40].
- Pallavicini (2011) measured the radioactivity of the nuclides ^{210}Pb, ^{232}Th, ^{238}U, ^{226}Ra, ^{40}K and ^{137}Cs in soil samples collected from different areas in Sweden. They found that the concentrations of the radionuclides ranged from (899-B.D.L.), (66-25) and (985-B.D.L.) Bq/kg, (658-27), (1060-76), and (1300-4) Bq/kg, respectively [41].
- Ferdous and et al. (2015) measured the radioactivity of the nuclides ^{238}U, ^{232}Th, ^{40}K isotopes of soil samples collected from Habiganj District of Bangladesh, and they found that the activity concentration levels were found to be in the range of (5 to 19) Bq/kg, (7 to 38) Bq/kg, and (93 to 392) Bq/kg, with mean values of (11, 22) and (227) Bq/kg, respectively. No ^{137}Cs was found in this study [42].

- Dizman and et al. (2019) measured the average activity concentrations (range) of ^{226}Ra, ^{232}Th, 40K, and ^{137}Cs in Bolu province, Turkey and found to be 18.2 (3.8–49.9) Bq/kg, 17.3 (4.1–37.9) Bq/kg, 258.3 (64.6–518.9) Bq/kg, and 7.5 (0.6–43.6) Bq/kg, respectively [43].
- Jananee and et al. (2021) measured the activity concentration of natural radionuclides and the associated radiation hazards in soils of Elephant hills, Tamil Nadu, India using gamma-ray spectrometry. They found that The average activity concentrations of ^{226}Ra, ^{232}Th and ^{40}K are (52, 48, and 840) Bq/kg, respectively [44].
- Kebede and Gebeyehu (2021) measured the Natural Radioactive Elements and Hazardous Indexes in soil samples using High Pure Germanium Gamma Ray Spectroscopy in Ethiopia. the result has found that Radium equivalent activity, external hazard index and representative gamma index of the sample were (56.19, 0.1515, 0.804, 0.408, 0.0001) Bq/kg, respectively [45].
- Ozden and et al. (2023) measured the natural and artificial radioactivity concentrations and Health Risks due to radionuclides in the Soil in Nevsehir Cappadocia, Turkey. The Activity concentrations of ^{226}Ra, ^{232}Th, and ^{40}K were range from (58.31 to 77.40) Bq/kg, (60.56 to 90.97) Bq/kg, and (796.42 to 1142.8) Bq/kg, respectively [46].

1.4.2. The Arabic Studies

- Mahjoubi and et al. (2006) in Tunisia measured the radioactivity of ^{238}U, ^{232}Th,^{40}K and ^{137}C in soil samples. The determination of radionuclide specific concentrations in the soil samples (0–5 cm) by gamma ray spectrometry showed the following ranges: (5–50) Bq/kg, (5–30) Bq/kg, (93–319) Bq/kg, and (1–19) Bq/kg, respectively [47].

- Mowafi and et al. (2009) measured the radioactivity of the ^{226}Ra, ^{232}Th and ^{40}K nuclides in soil samples collected from the northeastern Nile Delta in Egypt. It was found that the concentrations of radionuclides in the soil samples ranged from (49.5- 4.2) Bq/kg, (71.5-4.1) Bq/kg, and (404-95.5) Bq/kg, respectively [48].
- Saleh (2012) measured the radioactivity of the ^{238}U, ^{232}Th, and ^{137}Cs nuclides in soil samples collected from the Musandam Peninsula in the Sultanate of Oman. They found that the concentrations of the radionuclides ranged from (25.70-1.5) Bq/kg, (20.1-0.7) Bq/kg, and (15350-52.5) Bq/kg, respectively [49].
- Attia and et al. (2014) measured the radioactivity of the ^{226}Ra, ^{232}Th, and ^{40}K isotopes of soil samples collected from the city of Port Said in Egypt. They found that the concentrations of the radionuclides ranged from (398.66-18.03) Bq/kg, (75.7-5.28) Bq/kg, and (3237.88-583.12) Bq/kg, respectively [50].
- Al-Harmali (2020) evaluated the natural radioactivity in soil samples in northern regions of Oman. The results showed that ^{238}U radionuclide was presented in concentrations of the range (4.5–24.0) Bq/kg while ^{232}Th was found in the range (2.4-20.6) Bq/kg. Ranges of ^{235}U and ^{40}K were reported as (0.6-2.5) Bq/kg and (47-296) Bq/kg, respectively. Artificial radionuclide ^{137}Cs was found in all soil samples in the range (2.8- 11.9) Bq/kg [51].
- Al-Azri and et al. (2022) measured the natural and artificial radioactivity of soil samples in Dakhiliya Governorate-Sultanate of Oman. The result of the activity concentrations of ^{137}Cs, ^{226}Ra, ^{40}K, ^{235}U and ^{228}Ac were found as (0.82 ± 0.04, 29.01 ±1.37, 290.14±2.79, 5.88±0.65, and 39.57± 3.85) Bq/Kg, respectively. Radium-equivalent activity Ra_{eq} was obtained and varied in the range from (340 to 43) Bq/Kg with a mean value of (108.3) Bq/Kg [52].

- Alfull and et al. (2023) measured the natural radioactivity in soil samples in Saudi Arabia. The results of this work showed that the values of the activity for ^{226}Ra, ^{232}Th, and ^{40}K were found to be (19.9, 19.08, and 370.14) Bq/Kg, respectively [53].

- Maglas and et al. (2024) measured the natural activity of ^{40}K, ^{232}Th and ^{226}Ra, in surface soil samples from the phosphate region in Al-Ruseifa, Zarqa, Jordan. Which were (147.13, 14.79, and 322.51) Bq/kg, respectively. The average value of radium equivalent activity was (355.05) Bq/kg, while the absorbed dose rate in air was (164.07) nGy/h and the annual effective radiation dose attributed to natural radioactivity was found to be(0.20) mSv/year [54].

1.4.3. The Local Studies

- Abather and et al. (2016) measured the specific activity concentration of the natural radioactive isotopes ^{40}K, ^{212}Pb, ^{214}Pb, ^{214}Bi, ^{228}Ac, in soils and sediments for selected areas for Marshes of Southern Iraq-Basra province and northern Arabian Gulf. They found that the specific activity measurement results were around (320.1-1310.9) Bq/kg for ^{40}K, (0–12.1) Bq/kg^{212}Pb, (0–6.3) Bq/kg for ^{214}Pb, (3.2-10.2) Bq/Kg for ^{214}Bi, and (0–4.4) Bq/Kg for ^{228}Ac [55].
- Najam and et al. (2016) measured the activity concentration of ^{232}Th, ^{40}K, and ^{137}Cs in soil surface of Thi-Qar governorate, Iraq by using high purity germanium (HPGe) detecto and they foud that the activities were (22.7, 304.6, and 3.15) Bq/kg, respectively [56].
- Al-Sudani. (2016) measured the radionuclide Concentrations soils sample in Misan province, Iraq. For ^{232}Th, ^{40}K, ^{137}Cs, respectively, found to be (15.271±0.091) Bq/kg, (354.812±0.006) Bq/kg, (0.797±0.568) Bq/kg [57]

- Reza and Shahroodi (2018) measured the radionuclide Concentrations in soils sample in Karbala. They found that specific activities of ^{226}Ra, ^{232}Th, ^{40}K, and ^{137}Cs in the soil samples varied within the ranges of ((29.37-38.86), (23.24-45.70), (291.15-549.78), and (1.25-10.82)) Bq/kg, respectively. The excess lifetime cancer risk due to the ingestion of wheat and barley were calculated as (0.013×10^{-3}) and (0.006×10^{-3}), respectively, which are lower than the maximum acceptable value (10^{-3}) [58].
- Taqi and et al. (2018) measured the natural radioactivity of soil samples in Kirkuk city. they have found that the specific activity ranged from (27.4 to 57.0) Bq/kg for ^{226}Ra, from (11.0 to 25.4) Bq/kg for ^{232}Th, and from (207.4 to 516.0) Bq/kg for ^{40}K. The results have been compared with the average values worldwide. The hazard indices have also been calculated [59].
- Al-Wasiti (2010) measured the radioactivity of the nuclides ^{214}Bi, ^{228}Ac, ^{212}Pb, ^{40}K, and ^{137}Cs for soil samples collected from different areas in Wasit Governorate, Iraq. He found that the concentration of radionuclides ranged from (19.2 - 8.8) Bq/Kg, (14.5- 6.9) Bq/kg, (10.7-B.D.L) Bq/kg, (266.5-164.9) Bq/Kg, and (4.6-B.D.L) Bq/kg, respectively [60].
- Jahfer and et al. (2022) measured the activity concentrations of ^{226}Ra, ^{232}Th, ^{40}K and ^{137}Cs in the surface soil along the Little Zab River-Iraq. They found that the activity were in ranges of (4.4–34.7) Bq/kg, (1.5–13.3) Bq/kg, (42.1–583.9) Bq/kg, and (0.5–31.5) Bq/kg, respectively[61].
- Hussian and Ali (2024) measured the natural and artificial radionuclides distribution in surface soil in Baghdad international airport region. The result showed that the average activities of ^{226}Ra, ^{232}Th, and ^{40}K in the study area were (36.9, 29.1, and 362.7) Bq/kg, respectively. While the average activity of ^{137}Cs ranged between below detection limit (BDL) and (19.4) Bq/kg [62].

- Al-Sudani, and et al. (2025) measured the average activity concentrations of radionuclides radium-226, thorium-232, and potassium-40, in Ali Al-Sharqi and Kumait, Misan province, Iraq were found to be (15.1±2.5) Bq/kg, (14.7±2.4) Bq/kg, and (180.8±7.9) Bq/kg, respectively, for Ali Al-Sharqi. In Kumait, the corresponding values were (13.6±2.1) Bq/kg, (17.2±2.4) Bq/kg, and (193.6±8.6) Bq/kg, respectively [63].
- Al-sudani. (2025) measured the natural and artificial concentrations in Ali Al-Gharbi in Misan province, Iraq for ^{226}Ra,^{232}Th, ^{40}K, and ^{137}Cs were found to be (32.676±3.684) Bq/kg, (18.150±1.562) Bq/kg, (377.376±15.266) Bq/kg, and (1.906±0.422) Bq/kg, respectively. The findings showed that the ^{226}Ra, ^{232}Th, ^{40}K, and ^{137}Cs were below the recommended value by the UNSCEAR[64].

1.5. The aim of the study

1. Measure the activity concentrations of both natural radionuclides (^{226}Ra, ^{232}Th, and ^{40}K) and artificial radionuclide (^{137}Cs) in soil samples of Al-Majar and Kalaat Saleh using high-purity germanium (HPGe
2. Determined radiological hazard parameters including radium equivalent activity (Ra_{eq}), internal and external hazard indices (H_{in} and H_{ex}), gamma level index (Iγ), absorbed gamma dose rates (D_{in}, D_{out}, and D_{tot}), annual effective dose equivalents ($AEDE_{in}$, $AEDE_{out}$, and $AEDE_{tot}$), excess lifetime cancer risks ($ELCR_{in}$, $ELCR_{out}$, and $ELCR_{tot}$), and annual gonadal dose equivalent (AGDE).
3. Comparison of radioactivity results between Al-Majar and Kalaat Saleh.

Theoretical Considerations

Chapter Two

Theoretical Considerations

2.1. Radioactivity

Radioactivity is characterized by a transformation of an unstable nucleus into a more stable entity that may be unstable and will decay further through a chain of decays until a stable nuclear configuration is reached [65]. Three radioactive chains now exist in nature, namely, Thorium chain (starting with ^{232}Th), Actinium chain (starting with ^{235}U), and Uranium chain (parent nucleus ^{238}U) in which heavy nuclides lost mass and changed their atomic number in successive steps, the decays ending at the stable isotope of lead (^{208}Pb, ^{207}Pb, and ^{206}Pb) respectively. In all of these spontaneous changes, generally, three types of nuclear radiation were recognized, namely, α-particles (energetic helium nuclei), β-particles (electrons or positrons) , and γ-rays (electromagnetic waves) [66]. The amount of radioactivity present is traditionally determined by estimating the number of curies (Ci) present. The more curies present, the greater amount of radioactivity and emitted radiation. In the System International of units (SI system) the unit of Becquerel (Bq) is used as its unit of radioactivity, and one disintegration per second equals one Becquerel. The relation between Curie and Becquerel is [2, 67].

1 Curie (Ci) = 3.7 x 10^{10} Bq (dis/s)

Most of the nuclei found on earth are stable because all short-lived radioactive nuclei have decayed. There are approximately 270 stable isotopes and 50 radioactive isotopes can be make a thousands of radioisotopes in laboratory [68].

2.2. Law of Radioactivity

Radioactive decay is a random process that has been shown to follow the Poisson distribution. This effectively implies that the rate of decay of radioactive nuclei in a large sample depends only on the quantity of decaying nuclei in the sample [3]. Frederic Soddy and Ernest Rutherford in 1902 described their theory of radioactivity and formulated the first exponential laws that govern the decay and growth of radioactive substances [69]. Mathematically this can be written as:

$$A = -\left|\frac{dN}{dt}\right| = \lambda N \qquad \text{.....(2-1)}$$

When we integrate above equation, we get the number of atoms at any time.

$$\int \frac{dN}{N} = -\int \lambda dt \qquad \text{.....(2-2)}$$

$$\ln \frac{N_t}{N_0} = -\lambda t \qquad \text{.....(2-3)}$$

$$N_t = N_0 e^{-\lambda t} \qquad \text{.....(2-4)}$$

Equation (2-4) describes the number of radionuclides (N_t) remaining at time (t) from the original number of atoms (N_0) present at time (t = 0). This is the basic equation describing all radioactive decay processes, and (λ) is the decay constant which is defined as the probability of a nucleus decaying per unit time [70].

The half-life ($t_{1/2}$) is related to the decay constant (λ) by the following relationship:

$$t_{1/2} = \frac{\ln 2}{\lambda} \qquad \text{.....(2-5)}$$

The half-life varies greatly between different types of atoms and ranges from less than a second to billions of years. The quantity that characterizes the rate of radioactive decay is called the activity. The activity is defined as the number of nuclei decaying per unit time[71].

By substituting equations (2-4) and (2-5) into equation (2-1), we get:

$$A_t = A_0 e^{\left[-\frac{\ln 2 \times t}{t_{1/2}}\right]} \quad \ldots\ldots\ldots (2\text{-}6)$$

Since A_0 is the activity at t = 0, while A_t is the efficiency at time t, and the negative sign indicates the fact that the activity decreases with time.

2.3. Sources of Radioactivity

There are several ways that ionizing radiation may enter our life. It results from both industrial operations, like the use of x-rays in medicine, and natural processes, such the decay of uranium in the earth. There are two major sources of environmental radiation exposure: natural and artificial sources. Numbers of different radionuclides present naturally in food and water, as well as decay products in the air from natural sources such cosmic rays, gamma rays, and radon. Artificial sources include radioactive waste from the nuclear industry, fallout from nuclear weapons in the atmosphere, industrial gamma rays, medical x-rays, and other items like consumer goods [72].

2.3.1. Natural Radioactivity

Ionizing radiation exposure from natural sources is a constant and unavoidable aspect of life on Earth. Natural radiation exposures are primarily caused by two sources: high-energy cosmic ray particles from the earth's atmosphere and

radioactive nuclides from the earth's crust that are found throughout the environment, including the human body [73].

2.3.1.1. Cosmic Radiation

Cosmic radiation is divided into different types according to the origin, its energy and type and the flux density [74]. There are two main sources of such cosmic radiation:

1. ***Cosmic Rays***

Through ionization and nuclear processes, cosmic rays lose energy when they enter the earth's atmosphere. Cosmic radiation is prevented by the thickness of the earth's atmosphere before reaches the surface is made up of muons and neutrinos from the decay of pions created in these interactions with a trace quantity of nuclear material reaching and being absorbed by the crust [75]. At sea level in the mid-latitudes, the ionizing component of cosmic rays generates an average absorbed dose rate in air of 31 $nGy.h^{-1}$, which translates to an effective dose rate of 31 $nSv.h^{-1}$. The population-weighted average annual effective dosage from cosmic rays is 340 μSv, taking into account shielding by buildings for the ionizing component and the distribution of the world's population with altitude [73]. High-energy particles with a mean energy of roughly 10^4 MeV make up cosmic rays. These include light atomic nuclei, high-energy electrons, alpha particles, and protons [76].

2. ***Cosmogenic Radionuclides***

The interactions of the atmosphere with cosmic rays produce radionuclides like ^{3}H, ^{7}Be, ^{14}C, and ^{22}Na [73]. ^{14}C is the most common radioactive production in the atmosphere, which is a secondary product of the ^{14}N (n, p) ^{14}C reaction. The most common absorption process is the exothermic (n, p) reaction on abundant atmospheric nitrogen:

$n + {}^{14}N \rightarrow {}^{14}C + p$, $t_{1/2}({}^{14}C) = 5730$ year.

The produced ^{14}C enters the food chain through CO_2 ingesting plants. The ^{14}C abundance in organic living matter is 10^{-12} relative neutral carbon and has activity of 250 $Bq.kg^{-1}$ [77]. The neutrons emitted can be combined with ^{16}O to produce tritium as follows:

$n + {}^{16}O \rightarrow {}^{3}H + {}^{14}N$, $t_{1/2}({}^{3}H) = 12.34$ year.

And this tritium combines with oxygen to form water rains, which fall down on the earth, and this was the primary source of naturally occurring tritium because of its short half-life. Some other cosmogenic radionuclides are ^{10}Be, ^{26}Al, ^{36}Cl, ^{80}Kr, ^{14}C, ^{32}Si, ^{39}Ar, ^{22}Na, ^{35}S, ^{37}Ar, ^{33}P, ^{32}P, ^{38}Mg, ^{24}Na, ^{38}S, ^{31}Si, ^{18}F, ^{39}Cl, ^{38}Cl, ^{34}mCl [75].

2.3.1.2. Terrestrial Radiation (Primordial Radionuclides)

The natural terrestrial radiation that humans are exposed to outside comes primarily from the top 30 cm of the soil. Half-lived radionuclides can be compared to the earth's age or to the decay products of terrestrial stuff [78]. The most significant chains of naturally occurring radionuclides are:

2.3.1.2.1. Uranium Series ($^{238}_{92}U$)

The first isotope in this series is Uranium-238, which has a half-life of 4.5×10^{9} years, as Figure (2.1) illustrates [79] [80]. In nature, uranium is found as ^{234}U, ^{235}U, and ^{238}U. Since all of their daughters after ^{238}U have shorter half-lives than the parent nuclide ^{238}U, this series is said to be in secular equilibrium [81]. The ^{226}Ra, which has half-lives of 1600 years and chemical characteristics that are obviously distinct from those of uranium, is part of this decay series. When ^{226}Ra decays, it produces ^{222}Rn, an inert noble gas that can enter the atmosphere and

quickly attack dust and aerosol particles that have been deposited there. It also does not establish any chemical interactions. The lungs may sustain injury from the radiation released during the breakdown of these compounds.

This chain is still in existence today. An alpha particle is released when the radionuclide ^{238}U decays into ^{234}Th, the newly created nuclide is likewise unstable and continues to decay as shown in Figure (2-1). Stable lead is eventually created following a total of 14 such processes, which release 8 alpha and 6 beta particles along with gamma radiation.

2.3.1.2.2. Thorium Series ($^{232}_{90}Th$)

In Figure (2-2), the degradation series is displayed. There are six alpha particles released throughout the course of ten decay stages. The four nuclides ^{228}Ac, ^{212}Pb, ^{212}Bi, and ^{208}Tl are easily detected using gamma spectrometry. ^{212}Bi decay is branched, only 35.94% of decays result in ^{208}Tl through alpha decay. ^{212}Po is produced via the beta decay branch. The branching must be corrected by dividing the ^{208}Tl measurement by 0.3594 if the thorium activity is to be estimated [82]. The body of an adult human has roughly 0.8 Bq of ^{232}Th. Nearly all of natural thorium is composed of ^{232}Th, with very trace amounts of ^{234}Th, ^{230}Th, ^{231}Th, and ^{227}Th, and 1.35×10^{-8} percent of ^{228}Th [13].

2.3.1.2.3. Actinium Series ($^{235}_{92}U$)

It is sometimes referred to as the Uranium-235 series and it begins with ^{235}U before evolving into the stable lead ^{207}Pb through a sequence of changes. Its natural uranium content is 0.72%. Despite being a very minor fraction of the element, its shorter half-life means that it has spectrometric significance comparable to ^{238}U in terms of radiations released. (Ignoring a number of minor decay branches), the decay sequence, depicted in Figure (2-3), involves 12

nuclides in 11 decay stages and the emission of 7 alpha particles. It is not included in the measurements due to its extremely low abundance [82].

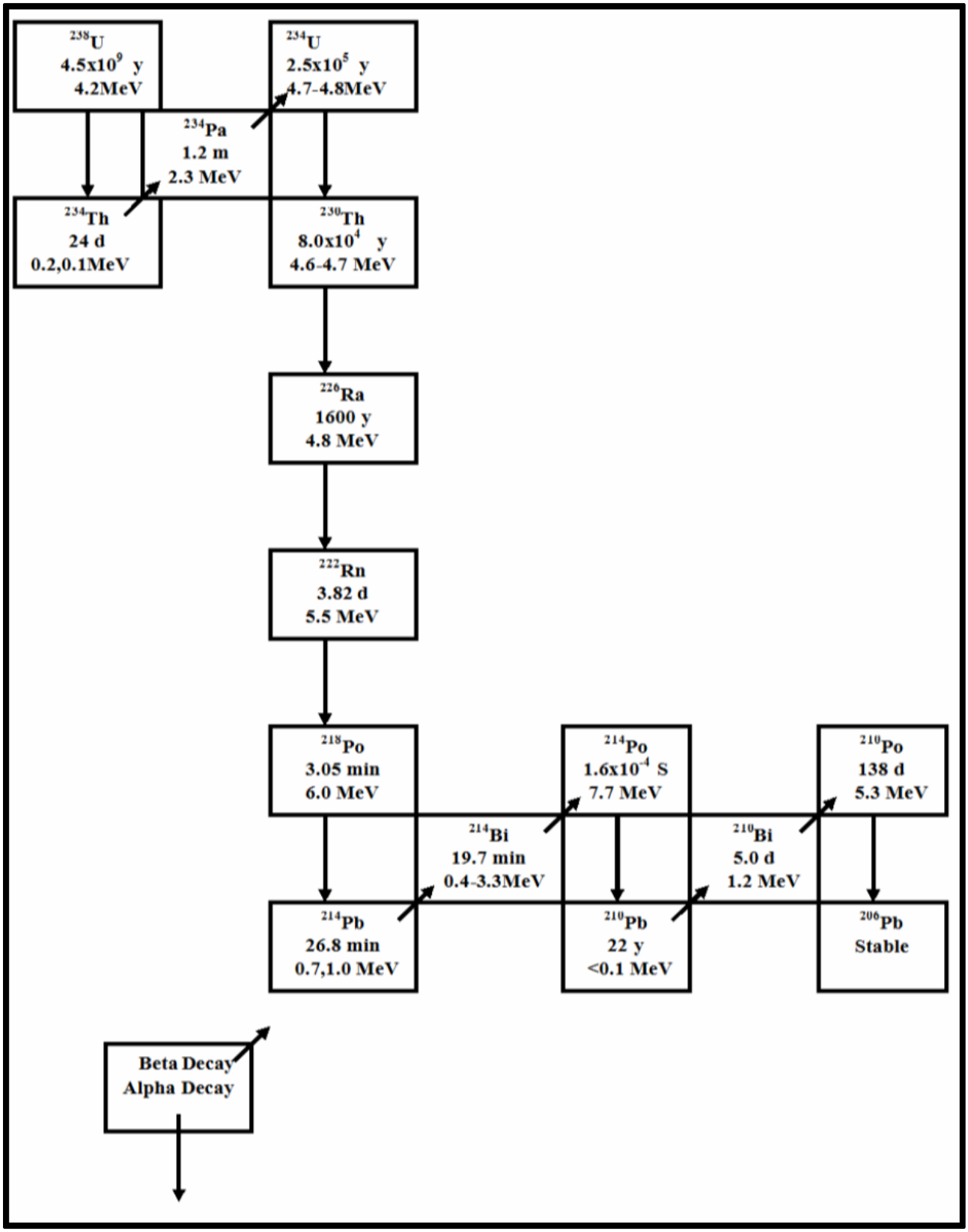

Figure (2-1): Decay Diagram of The Uranium Series $^{238}_{92}U$ [41].

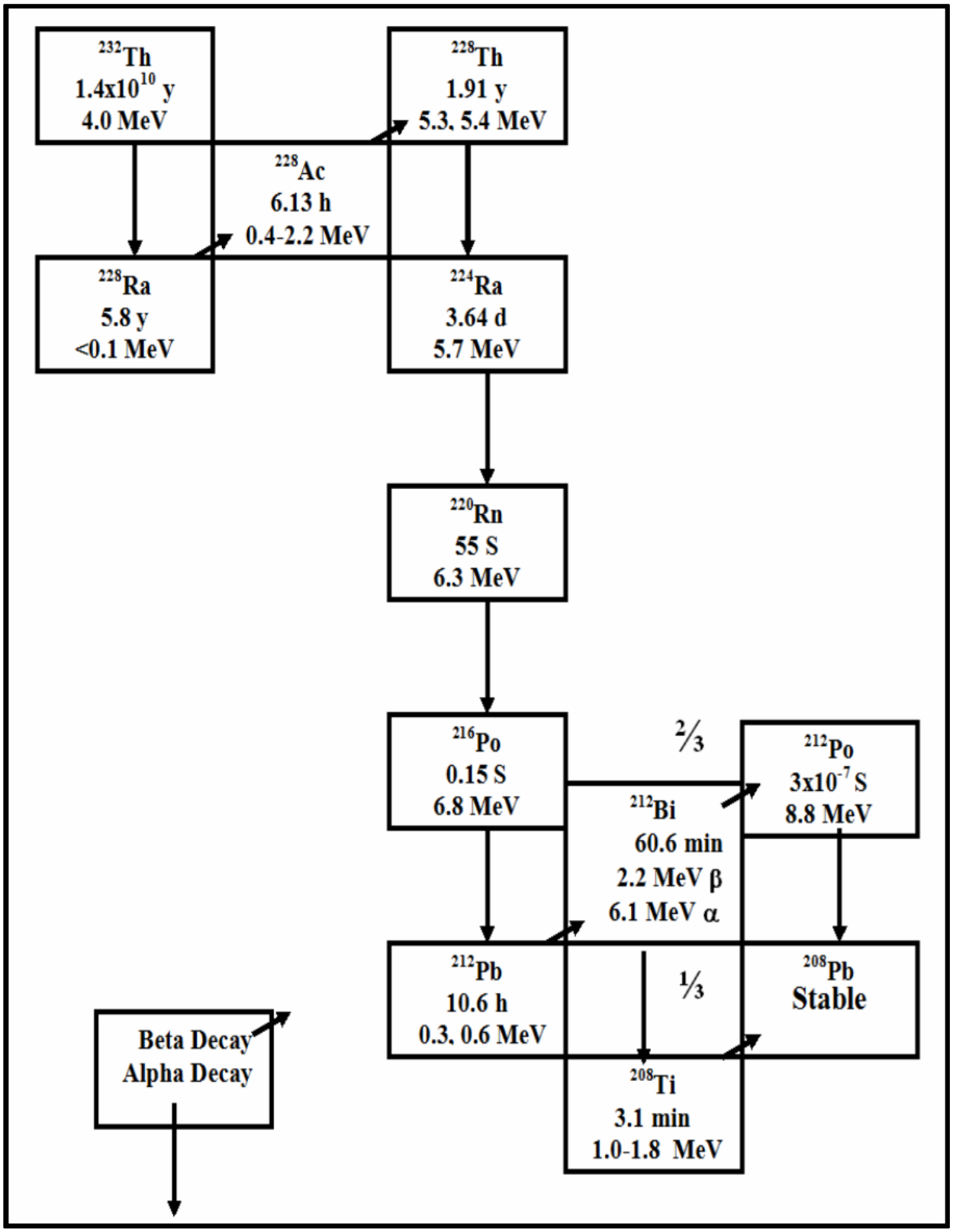

Figure (2.3): Decay Diagram of The Thorium Series $^{232}_{90}Th$ [41].

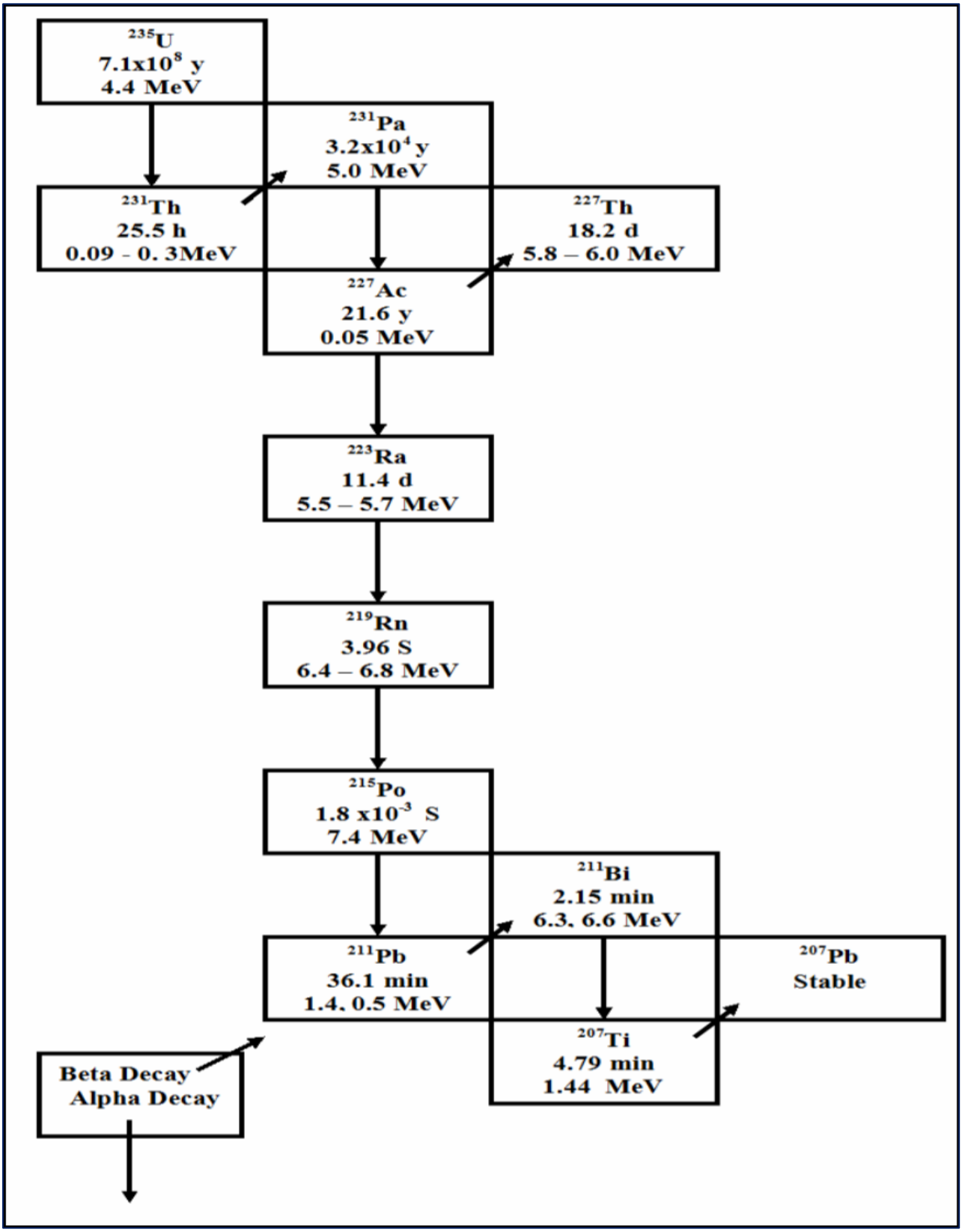

Figure (2-3): Decay Diagram of The Actinium Series $^{235}_{92}$U [41].

2.3.1.2.4. Potassium-40

Possibly the most significant terrestrial radionuclide, at least from a biological perspective is potassium-40 as shown in Figure (4-2), a primordial radioisotope of potassium. Only ^{40}K, one of the three isotopes of potassium with mass numbers 39, 40, and 41, is radioactive and has a half-life of 1.3 x 10^9 years. All living and extinct things have ^{40}K since potassium is necessary for life. According to the bioenvironmental perspective, ^{40}K is the most important radionuclide (half-life = 1.28x10^9 years, isotopic abundance = 0.0118%). The potassium content of a 70 kg man is around 140 g, primarily in the muscles, which is equivalent to 4.4 KBq of ^{40}K in the body [83].

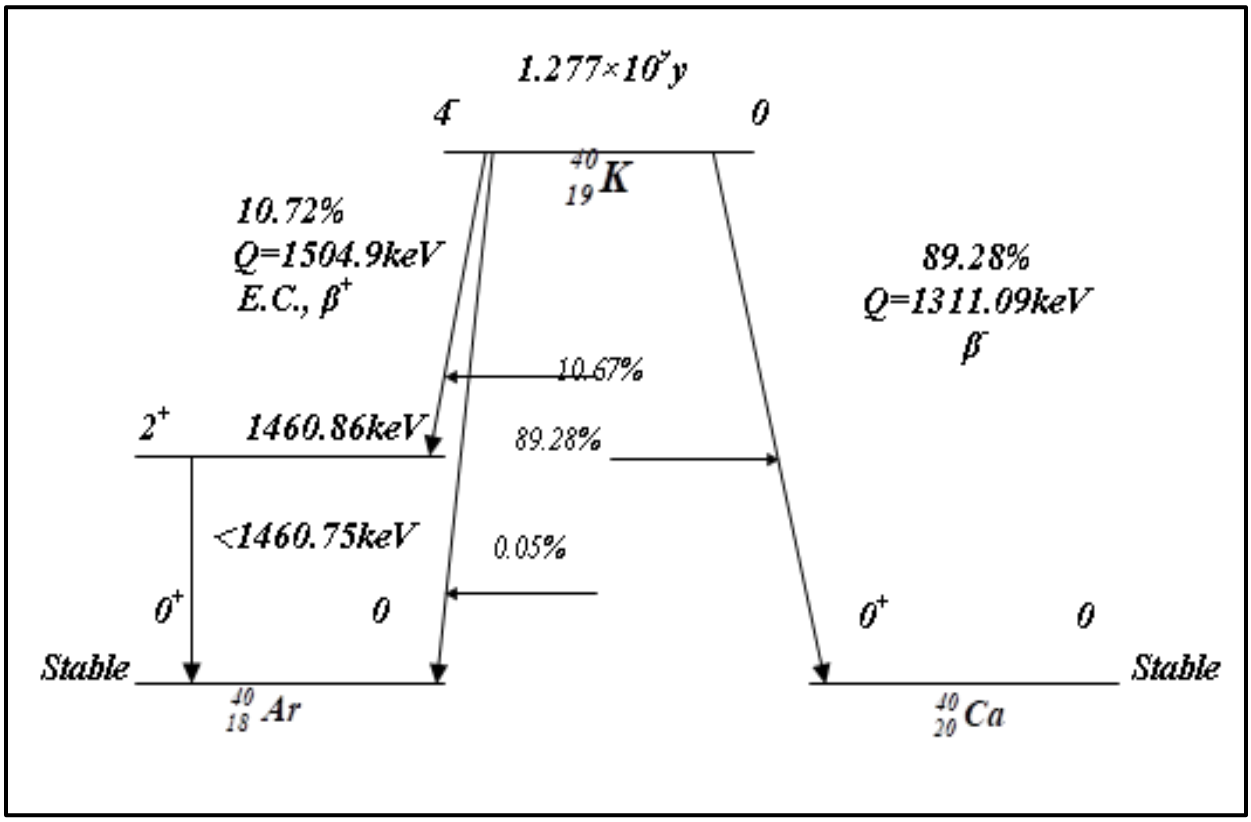

Figure (2-4): Decay Diagram of The Potassium ^{40}K [41].

2.3.2. Artificial Radioactivity

In the early days of the 20th Century human abilities to create artificial radioactive sources were limited to chemical isolation and the concentration of natural radionuclides. Later in this century linear accelerators were developed for producing beams of particles that could be used to artificially transmute nuclei. With the application of nuclear fission, for both peaceful and military purposes in the 1940, the ability of humans to produce large quantities of artificial radionuclides was greatly expanded [84].

The fission process itself, and the high neutron flux densities achieved in nuclear weapons explosions and fission reactor cores, led to the production of large quantities of fission and activation products. Fission products are the isotopes with mass number in the range about 70-170, formed by thermal fission of ^{235}U and other heavy fissile nuclei (e.g., ^{239}Pu). High-yield fission products include ^{89}Sr, ^{90}Sr, ^{91}Y, ^{95}Zr, ^{95}Nb, ^{99}Mo, ^{103}Ru, ^{131}I, ^{133}Xe, ^{137}Cs, ^{140}Ba, ^{140}La, ^{141}Ce, ^{144}Ce, ^{143}Pr and ^{147}Nd [84].

However, in most situations, the most radiologically important fission products in the short term are ^{89}Sr, ^{90}Sr, and ^{131}I, and in the long term, ^{90}Sr and ^{137}Cs, because of their yields half-lives and chemical properties. Activation products are the isotopes formed principally by the capture of neutrons by stable isotopes in high neutron flux environments. Typical activation products formed in the structure of nuclear reactors include ^{51}Cr, ^{54}Mn, ^{55}Fe, ^{59}Fe, ^{60}Co, ^{63}Ni, ^{65}Ni, ^{64}Cu, ^{65}Zn, ^{69}Zn,^{110}Ag, ^{109}Cd, ^{134}Cs, ^{236}U and ^{239}U [84].

The most significant contribution to this comes from the medical application of ionizing radiation in diagnostic radiology and radiotherapy. There are very wide variations in the dose an individual receives. The dose from a chest x- ray

is about 0.2 mSv; while someone given a computed tomography scan might receive 10 mSv [85].

The average dose due to the radioactive fallout from nuclear weapons testing in the atmosphere in 1999 was 0.004 mSv per year in the UK, compared with a peak of 0.014 mSv per year in 1963. The average dose due to the Chernobyl reactor accident in 1986 has declined to 0.001 mSv per year average over the UK, though there are considerable regional variations. In normal operation the nuclear power industry does not add appreciably to the average dose. The average dose from all stages of the nuclear fuel cycle averages to 0.0002 mSv per year. Again there are wide variations it has been estimated that people living near some nuclear facilities receive annual doses of 0.5 mSv [85].

Nuclear facilities, nuclear explosions, radiation sources utilized in business, medicine, and agricultural, as well as different kind of electronic gadgets, are example of man-made radiation sources. Radionuclide, or artificial sources of radiation, can be produced artificially as a result of physical procedures involving neutron activation, nuclear fusion, and nuclear fission [86].

2.4. Decay Equilibrium

Depending on the difference between the decay constants of the mother nucleus and the daughter nucleus, it is possible that after some time their activity will reach a state of equilibrium. This equilibrium has several states, namely, Secular equilibrium, transition equilibrium, and the state of disequilibrium [87].

2.4.1. Secular Equilibrium

Secular equilibrium is achieved when the radioactivity of the mother nucleus and the daughter nucleus are equal. This occurs when the half-life of the mother

nucleus is much greater than the half-life of the daughter nucleus (($t_{P\ 1/2} >> t_{D\ 1/2}$ or $\lambda_P << \lambda_D$))[88].

This is done through the following equation of equal activity:

$$A_D = \frac{\lambda_D}{\lambda_D - \lambda_P} A_{oP}(e^{-\lambda_P t} - e^{-\lambda_D t}) \qquad \text{.....(2-7)}$$

It is clear that if ($\lambda_P > \lambda_D$) this leads to $t \rightarrow \infty$ and so we can neglect the second term of the right-hand side of Equation (2-7). Thus the radioactivity of the daughter nucleus is given by the relations [88]:

$$A_D = \frac{\lambda_D}{\lambda_D - \lambda_P} A_{oP} e^{-\lambda_P t} = \frac{\lambda_D}{\lambda_D - \lambda_P} A_P \qquad \text{.....(2-8)}$$

$$\frac{A_P}{A_D} \approx 1 - \frac{\lambda_P}{\lambda_D} \qquad \text{..... (2-9)}$$

Also, ($\lambda_P << \lambda_D$) we can neglect the second term on the right side of the equation above and thus we get:

$$A_P \approx A_D \qquad \text{.....(2-10)}$$

This indicates that if the half-life of the mother nucleus is much greater than the half-life of the daughter nucleus then the nuclei eventually reach a state of secular equilibrium in which the radioactivity of the mother and daughter nuclei is equal [87].

2.4.2. Transient Equilibrium

Transient equilibrium occurs when the radioactivity of the parent and daughter nuclei is not equal but differs by a small fraction. This occurs when the half-life of

the parent nucleus is slightly higher than the half-life of the daughter nucleus, i.e. ($t^{P}_{1/2} > t^{D}_{1/2}$ or $\lambda_P < \lambda_D$) [87].

2.4.3. Non-Equilibrium

If the half-life of parent is less than the half-life of daughter, i.e. $\boldsymbol{t^{p}_{1/2}} < \boldsymbol{t^{D}_{1/2}}$ or $\boldsymbol{\lambda_{dP}} > \boldsymbol{\lambda_{dD}}$. Then the activity due to parent nuclide will diminish quickly as it decays into the daughter. Consequently the net activity will be solely determined [3].

2.5. High Purity Germanium (HPGe) Detector

Germanium semiconductor detectors were first introduced in 1962 which are now the detectors of choice for high energy-resolution γ-ray studies. These detectors directly collect the charges produced by the ionization of the semiconductor material [89].

The production of high-purity germanium (HPGe) with an impurity concentration of 10^{16} atoms/cm^3 or less has made possible the construction of detectors without lithium drifting. The sensitive depth of the detector depends on the impurity concentration and the voltage applied. Germanium detectors are fabricated in many different geometries, thus offering devices that can be connected to the specific needs of the measurement [90]. There are widely uses for (HPGe) in many applications such as that in nuclear and industrial products because of its sensitivity and good efficiency and ease of spectrum analysis. The drawback to using these detectors, is its need to cool them to near cryogenic temperatures[91]. Cooling the detector, when it uses is necessary because germanium has a relatively narrow energy gap, and at room and in higher temperatures a leakage current due to thermally generated charge carriers induces such noise that the energy resolution

of the device is destroyed. The (HPGe) detectors operate at a temperature range of (85-105 K), so we need the cooling material which used with a cryostat and Dewar combination designed to provide the cooling path. The liquid nitrogen, which has a temperature of (77 K or (–196 °C)), is the common cooling medium for such detectors. The liquid nitrogen is kept in a large cryostat that can contain sufficient quantity of the liquid to last at least a week [92, 93].

2.6. The Activity Concentration

The activity concentration is calculated by placing the sample (soil) in a Marnelli container, which is fixed around a high-purity germanium detector, and recording the gamma-ray spectrum for (3600 sec). The program (Genie-2000) in the computer draws the spectrum and produces a report that includes the channel numbers and their corresponding energies and the net area under the peak of the spectrum curve. Then, the specific effectiveness of each sample is calculated by using of the following Equation [94].

$$A\left(\frac{Bq}{kg}\right) = \frac{A_n}{\varepsilon\, p_\gamma\, M\, t} \qquad \ldots\ldots\ldots (2-11)$$

Where A represents the specific activity, A_n represents the net count under the full energy peaks, Ɛ is the detector efficiency at the specified energy, P_γ is the absolute transition probability, M is the sample mass (kg), and t the counting time (second).

2.7. Evaluation of Radiation Health Risk Parameters

Radiation risk parameters were evaluated to obtain relevant information on the radiation health status of the research areas as follows:

2.7.1. Radium Equivalent Activity (Ra_{eq})

The radium equivalent activity is a very useful guideline in organizing the safety standards in radiation protection for humans and it was calculated using Equation (2-12) [95]. Its limited values were 370 Bq/kg of ^{226}Ra, 259 Bq/kg of ^{232}Th, and 4810 Bq/ kg of ^{40}K produce the same gamma-ray dose rate.

$$Ra_{eq} = A_{Ra} + (1.43 \times A_{Th}) + (0.077 \times A_k) \quad \ldots\ldots\ldots (2-12)$$

where A_{Ra}, A_{Th}, and A_K are the activity concentrations of ^{226}Ra,^{232}Th, and ^{40}K in Bq/kg, respectively.

2.7.2. Hazard Index (H)

To account for the hazards associated with the external and internal exposure of the radiation emanating from ^{226}Ra,^{232}Th, and ^{40}K in the studied soil samples, the internal hazard index (H_{in}) and external hazard index (H_{ex}) were determined using Equations (2-13) and (2-14) [95].

$$H_{in} = \frac{A_{Ra}}{185} + \frac{A_{Th}}{259} + \frac{A_K}{4810} \quad \ldots\ldots\ldots (2-13)$$

$$H_{ex} = \frac{A_{Ra}}{370} + \frac{A_{Th}}{259} + \frac{A_K}{4810} \quad \ldots\ldots\ldots (2-14)$$

The prime objective of H_{in} and H_{ex} is to limit the radiation dose to dose equivalent limit of 1 mSv/year. Thus, their values must be less than unity (i.e. ≤ 1) for the radiation hazards to be considered negligible.

2.7.3. Gamma Index (Iγ)

The radioactivity level index (Iγ) can be used to estimate the gamma-radiation hazard levels typically those associated with the natural radionuclides and it was evaluated using Equation (2-15) [96].

$$I_\gamma = \frac{A_{Ra}}{300} + \frac{A_{Th}}{200} + \frac{A_K}{3000} \quad \ldots\ldots\ldots (2-15)$$

The value of Iγ must be less than unity in order to keep the radiation hazard insignificant.

2.7.4. Absorbed Dose Rate (D)

The absorbed dose rate in air in one meter above the ground surface is an express the received dose the outdoor. This factor is an important quantity to evaluate when considering radiation risk. The indoor, outdoor, and total absorbed gamma dose rates (D_{in}, D_{out}, and D_{tot}) were computed using Equations (2-16) - (2-18) [97].

$$D_{in}\left(\frac{nGy}{h}\right) = (0.92 \times A_{Ra}) + (1.1 \times A_{Th}) + (0.081 \times A_K) \quad \ldots\ldots\ldots (2-16)$$

$$D_{out}\left(\frac{nGy}{h}\right) = (0.462 \times A_{Ra}) + (0.604 \times A_{Th}) + (0.0417 \times A_K). \ldots\ldots (2-17)$$

$$D_{tot}\left(\frac{nGy}{h}\right) = D_{in} + D_{out} \quad \ldots\ldots\ldots (2-18)$$

2.7.5. Annual Effective Dose Equivalent (AEDE)

In order to estimate the annual effective doses, one has to take into account the conversion coefficient 0.7 (Sv/Gy), which is used to convert the absorbed rate in air to human effective dose equivalent with indoor and outdoor occupancy of 80 and 20%, respectively. The indoor, outdoor, and total annual effective dose rates ($AEDE_{in}$, $AEDE_{out}$, and $AEDE_{tot}$) were determined using Equations (2-19)-(2-21) [98].

$$AEDE_{in}\left(\frac{mSv}{y}\right) = D_{in}\left(\frac{nGy}{h}\right) \times 0.7\left(\frac{Sv}{Gy}\right) \times 0.8 \times 8760\frac{h}{y} \times 10^{-6} \quad \ldots\ldots\ldots (2-19)$$

$$AEDE_{out}\left(\frac{mSv}{y}\right) = D_{out}\left(\frac{nGy}{h}\right) \times 0.7\left(\frac{Sv}{Gy}\right) \times 0.2 \times 8760\frac{h}{y} \times 10^{-6} \ldots\ldots\ldots (2-20)$$

$$AEDE_{tot}\left(\frac{mSv}{y}\right) = AEDE_{in} + AEDE_{out} \quad \ldots\ldots\ldots (2-21)$$

2.7.6. Excess Lifetime Cancer Risk (ELCR)

Excess Lifetime Cancer Risk (ELCR) is used in radiation protection assessment to predict the probability of cancer development by individual over a lifetime due to low radiation exposure level. Based upon the calculated values of annual effective dose rates, the indoor, outdoor, and total lifetime cancer risks ($ELCR_{in}$, $ELCR_{out}$, and $ELCR_{tot}$) have been calculated using the Equations (2-22)-(2-24) [99].

$$ELCR_{in} = AEDE_{in}\left(\frac{mSv}{y}\right) \times DL \times RF \quad \ldots\ldots\ldots (2-22)$$

$$ELCR_{out} = AEDE_{out}\left(\frac{mSv}{y}\right) \times DL \times RF \quad \ldots\ldots\ldots (2-23)$$

$$ELCR_{tot} = ELCR_{in} + ELCR_{out} \quad \ldots\ldots\ldots (2-24)$$

where DL is the duration of life (70 years) and RF is the risk factor (ICRP 60 uses values of 0.05 Sv^{-1} for the public).

2.7.7. Annual Gonadal Dose Equivalent (AGDE)

Radiation has many different effects on all living things. These effects might kill the cell or cause it to change, but they might not have any effect on DNA. The main focus of the tissues is on the gonads, the active bone marrow, and the cells on the bone surface. Because of this, Equation (2-25) was used to figure out the AGDE that came from the actions of ^{226}Ra, ^{232}Th, and ^{40}K [100].

$$AGDE\left(\frac{\mu Sv}{y}\right) = (3.09 \times A_{Ra}) + (4.18 \times A_{Th}) + (0.314 \times A_{K}) \quad \ldots\ldots\ldots (2-25)$$

Chapter Three

Experimental Part

Chapter Three

Experimental Part

3.1. Introduction

This chapter provides a brief overview of the materials, laboratory equipment, and sample collection procedures employed in this study. Along with the practical procedures for preparing environmental soil samples, it also covers the high-purity germanium (HPGe) analysis technique.

3.2. Analysis using gamma-ray spectroscopy

This process includes figuring out how many and what kind of radionuclides are present. After defining the radionuclides using the energy calibration method, their quantities are ascertained by comparing them to stander sources using the relative approach. The following is description for completing this process:

3.2.1. Samples Collection

In the present study, fifty samples of soil were collected during the months of August and September in the year 2024 from the study area (35 samples were from Al-Majar and 15 samples were from Kalaat Saleh). Each sample was taken from a depth of 0–5 cm. The geographical coordinates of the sampling sites were recorded using a Garmin eTrex Vista HCX GPS device (Part No. 20233, Garmin, USA), as listed in Tables (3-1) and (3-2), and as shown in Figures (3-1) and (3-2). The collected samples were placed in clean zip-lock bags and labeled with unique identification codes.

Table (3-1): Sample code, Location and the Coordinates of the Soil Samples in Al-Majar.

sample code	Sample location	Location coordinate	
		Latitude	Longitude
S_1	Sudur Al-Majar	13.67227	47.17301
S_2	Al-Waraq	13.64078	47.18503
S_3	Al-Saeida	31.60145	47.17977
S_4	Eidawiya	31.59854	47.16349
S_5	Al-Easkari	31.58770	47.15581
S_6	Yarmouk	31.58755	47.16563
S_7	Al-Jameiaat	31.58498	47.16350
S_8	Al-Shurta	31.58605	47.15740
S_9	Al-Shuhada'	31.58368	74.14985
S_{10}	Al-Rahma	31.57590	47.16106
S_{11}	14 –Ramadan	31.57668	47.16528
S_{12}	Al-Sinaea	31.57582	47.15800
S_{13}	Al-Liwa'	31.56034	47.15597
S_{14}	Al-Hasharia	31.61756	47.16464
S_{15}	AL-Aadel	31.50652	47.12622
S_{16}	Al-Khayr	31.46443	47.09426
S_{17}	First field	31.59904	47.17292
S_{18}	Second field	31.60026	47.17216
S_{19}	Third field	31.60163	47.17168
S_{20}	Fourth field	31.60385	47.16765
S_{21}	Fifth field	31.60677	47.16677
S_{22}	Eastern Sugar dwar	31.59028	47.18138
S_{23}	Western Sugar dwar	31.59402	47.17164
S_{24}	Al-Sadrayn	31.58786	47.16856
S_{25}	Old Hussein (Al-Rifaq)	31.58236	47.17883
S_{26}	New Hussein	31.58553	47.17089
S_{27}	Al-Jumhuria	31.57792	47.17702
S_{28}	Imam Al-Hassan	31.57735	47.18190
S_{29}	Al-Saray	31.57250	47.17105
S_{30}	Al- Kashashiya (First Al-Rahma)	31.57465	47.17663
S_{31}	Al- Kashashiya (Second Al-Rahma)	31.57233	47.17444
S_{32}	Al-Badrawi	31.57022	47.16860
S_{33}	Al-Akhilas	31.56883	47.16639
S_{34}	Knikil	31.56183	47.16580
S_{35}	Al-Wadia	31.49549	47.19170

Table (3-2): Sample code, Location and the Coordinates of the Soil Samples in Kalaat Saleh.

Sample code	Sample location	Location coordinate	
		Latitude	Longitude
S_1	Al-Amir (Al-Easkari)	31.53406	47.29151
S_2	Al-Ghadir	31.52985	47.29638
S_3	First Karama	31.52499	47.30359
S_4	Second Karama	31.52683	47.30088
S_5	Third Karama	31.53161	47.30147
S_6	Al-Husaynia (Al-Shibisha)	31.52160	47.29754
S_7	Al-Zahraa (Al-Baeth)	31.52419	47.29177
S_8	Al-Sadr	31.52215	47.29104
S_9	Al-Huriya	31.52063	47.28979
S_{10}	Al-Euruba	31.51593	47.28893
S_{11}	Abu Samej (Al-Firqa)	31.50208	47.28234
S_{12}	Al-Eizz River	31.37316	47.35526
S_{13}	Al-Majaria	31.53964	47.29093
S_{14}	Sulaymaniyah	31.39828	47.38855
S_{15}	Al-Bayda and Al-Sawda	31.32790	47.42663

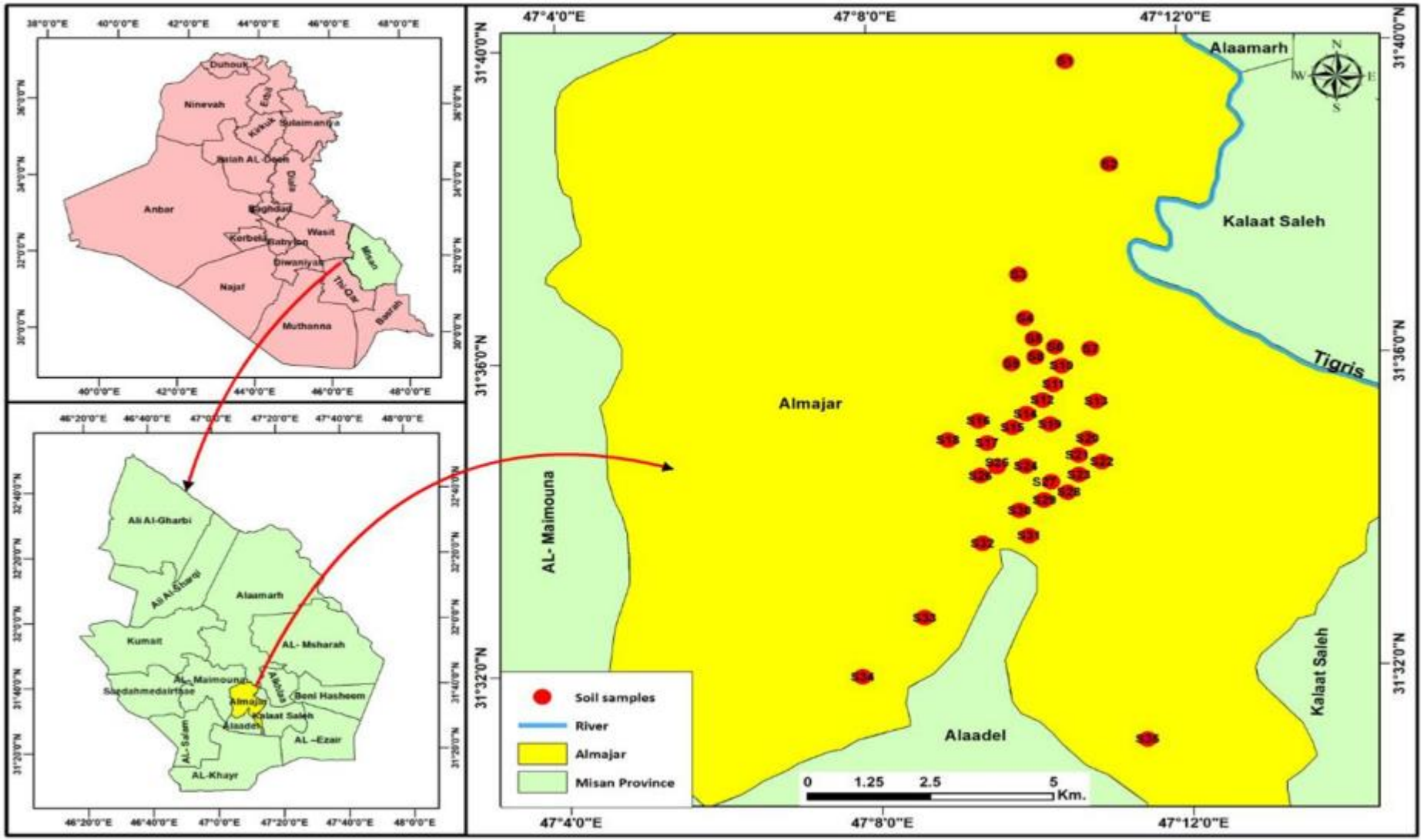

Figure (3-1): The study area (Al-Majar) depicts soil sample locations.

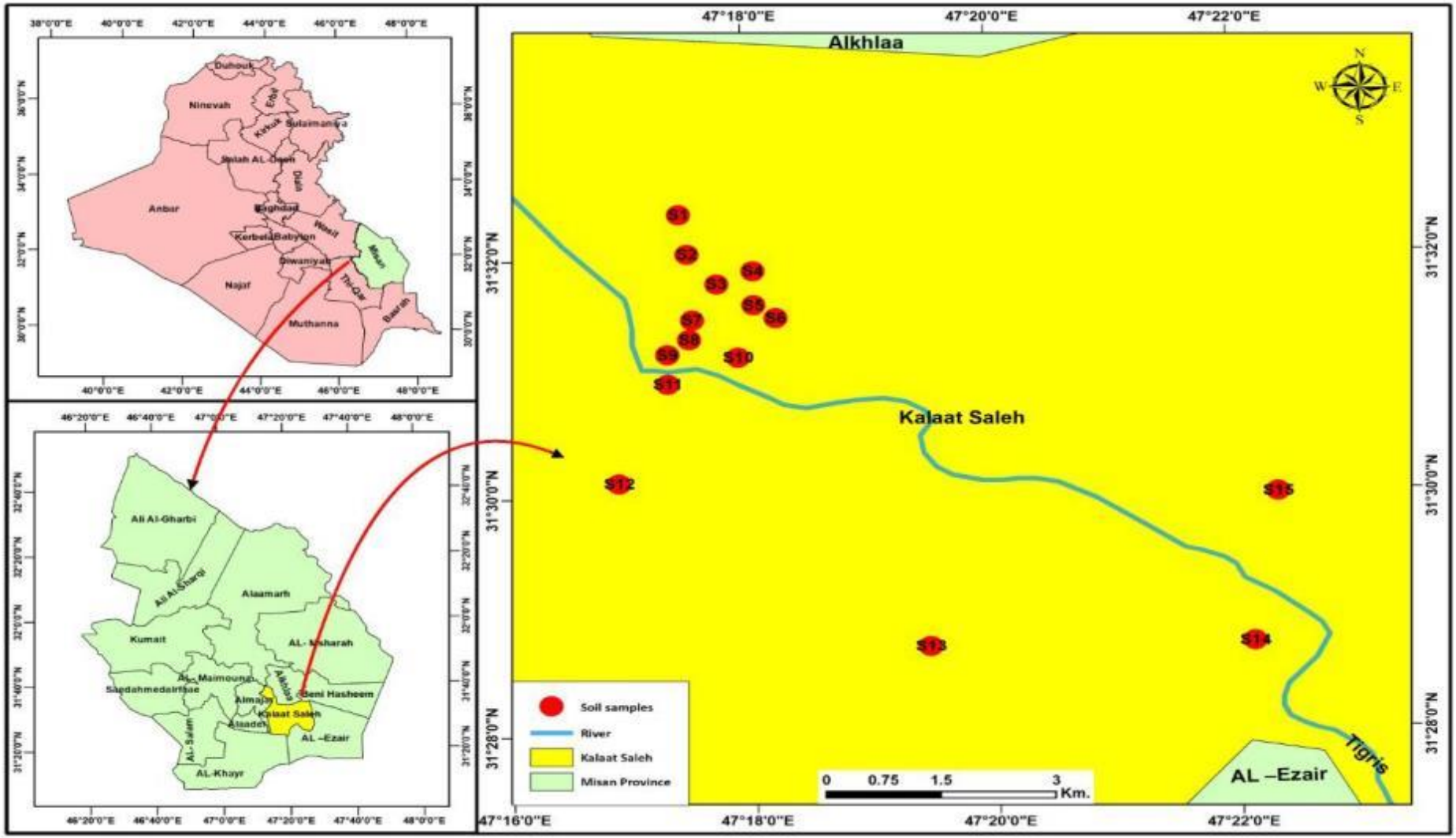

Figure (3-2): The study area (Kalaat Saleh) depicts soil sample locations.

3.2.2. Samples Preparation

In the laboratory, the samples were sieved using a 75 µm mesh sieve (200 mm × 50 mm, Part No. 60132000075, Serial No. 03008399, Retsch, Germany). They were then dried in an electric oven (Electrolux, Sweden) at 80°C for 2 hours to remove moisture. After drying, each sample was weighed to exactly 500 gm. Subsequently, the samples were transferred into 500 mL Marinelli polyethylene beakers (GA-MA, USA), sealed tightly with plastic tape to avoid the leakage of airborne radionuclides, and stored for four weeks. This storage period allowed the decay products to reach radioactive secular equilibrium with their parent radionuclides (^{226}Ra and ^{222}Rn) before gamma spectrometric analysis [101, 102]. The samples were analyzed at the laboratories of the National Authority for Nuclear, Radiological, Chemical, and Biological/Directorate of Instruments and Laboratories, Baghdad-Iraq, which are accredited according to ISO/IEC 17025.

3.2.3. Gamma Spectroscopy System

For the purpose of measuring natural and artificial radionuclides in soil samples, a gamma spectroscopy system was used, as shown in Figures (3-3) and (3-4), this system consists of the following equipment's:

3.2.3.1. High Purity Germanium Detector (HPGe)

The natural and artificial radionuclides in soil samples have been measured utilizing a gamma spectrometer system consisting of a P-type HPGe coaxial detector, Model GC4020 and Number 10025 (Canberra Company, USA), which has a constant relative efficiency of 40% as well as a resolution at full-width half maximum (FWHM) of 2 keV at the 1332 keV gamma line at ^{60}Co. A crystal diameter of 62.2 mm was operated under high voltage with a bias of +3000 V (DC) (Appendix (A)) [103].

3.2.3.2. High–Voltage Power Supply

The high power supply is connected to the detector to supply the photomultiplier base with voltage in the range (+3000 volts) (Appendix (A))[104].

3.2.3.3. Preamplifier

The main purpose of the preamplifier is to optimize coupling between the counting system and the output of the detector, and to reduce the noise. The preamplifier which is used in this system is connecting with detector issued from (CNABERA-model 2002CSL- serial number 13001333) (Appendix(A)) [104].

3.2.3.4. Main amplifier

The main amplification unit is the linear amplifier. It increases the signal by 1000 times or more. The main amplifier which was used exists in the multi- channel card analyzer [104].

3.2.3.5. Multichannel Analyzer (MCA)

Recorded and stores pulses according to their height. At the end of a counting period, the spectrum that was recorded may be displayed on the screen [105].

3.2.3.6. Computer and Software

A personal computer spectrum analyzer (PCA) was used, which is a personal computer equipped with electronic units that receive and classify the pulse coming from the main amplifier according to its amplitude and then store it in locations based on the amplitude, displayed as a visual image on the computer screen. The program (Genie -2000, version 3.1), which is an integrated program for qualitative and quantitative analysis of the gamma spectrum was used to find the radioactivity of the gamma-ray-emitting nuclides from the sample, and the data is printed using the printer attached to the computer [104].

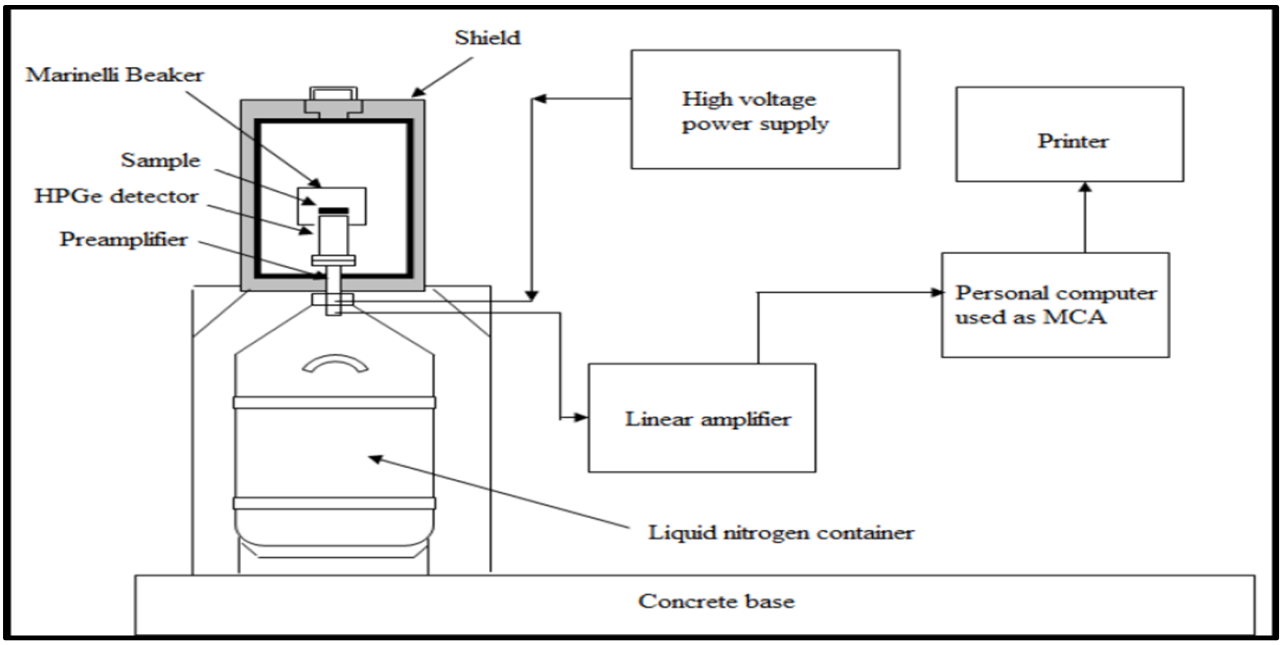

Figure (3-3): Measurement System Diagram [57].

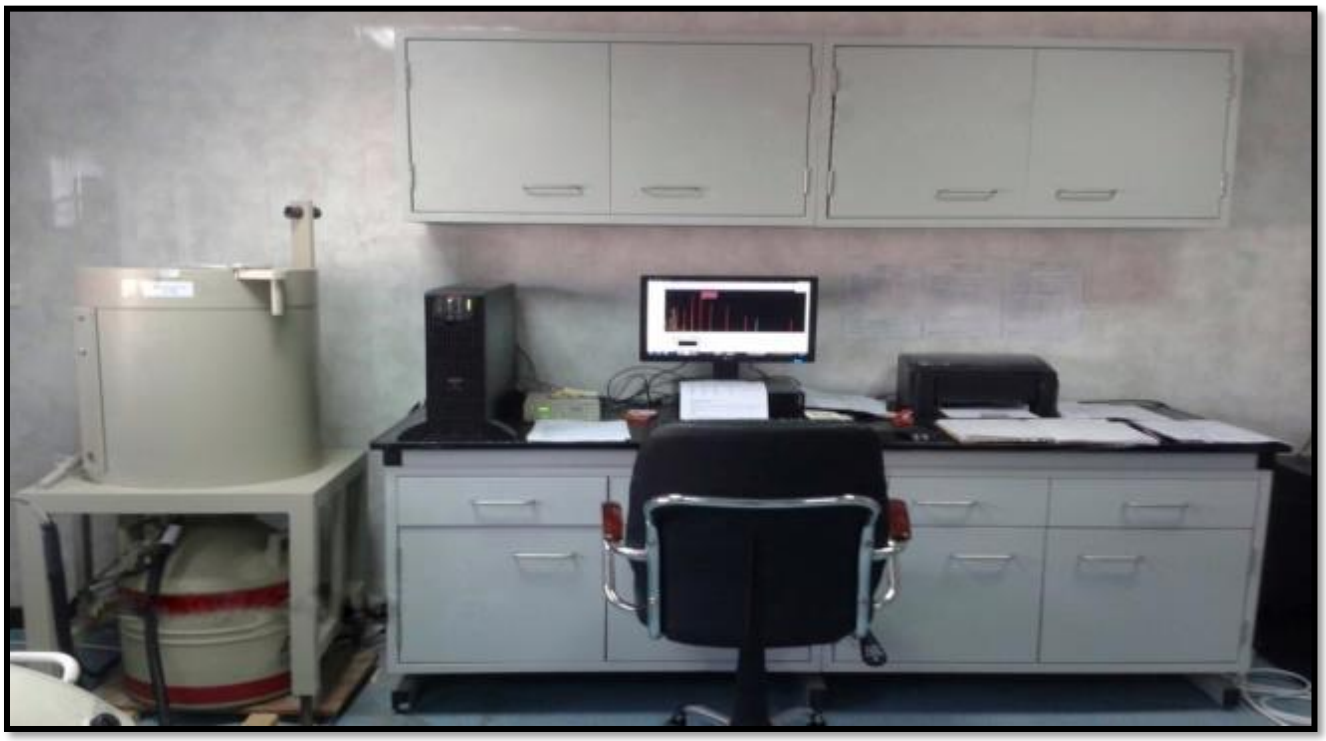

Figure (3-4): External Measurement System.

3.2.4. Energy and Efficiency Calibration

The energy and relative efficiency calibrations were performed using a standard source multi-gamma with certificate number 1035-SE-40524-16, Type CBSS 2, serial number 280616-1597016, and certificate issue date of July 18, 2016 (Czech Metrology Institute, Czech Republic). Containing 12 radionuclides, including ^{241}Am (59.54 keV), ^{109}Cd (88.3 keV), ^{139}Ce (165.85 keV),^{57}Co (122.06 and 136.47 keV),^{60}Co (1173.24 and 1332.5 keV), ^{137}Cs (662 keV), ^{113}Sn (391.69 keV),^{85}Sr (514 keV), ^{88}Y(898.02 and 1836.08 keV), ^{51}Cr (320 keV), ^{54}Mn (834.8 keV), and ^{65}Zn (1116 keV) in the energy range of 59.54 keV to 1836.08 keV with a mass of 441.0 gm, a density of 0.98±0.01 g/cm^3, and a volume of 450.0±4.5 cm^3 (Appendix (B)) [103] [106]. The calibration curves of the energy and efficiency are shown in Figures (3-5) and (3-6).

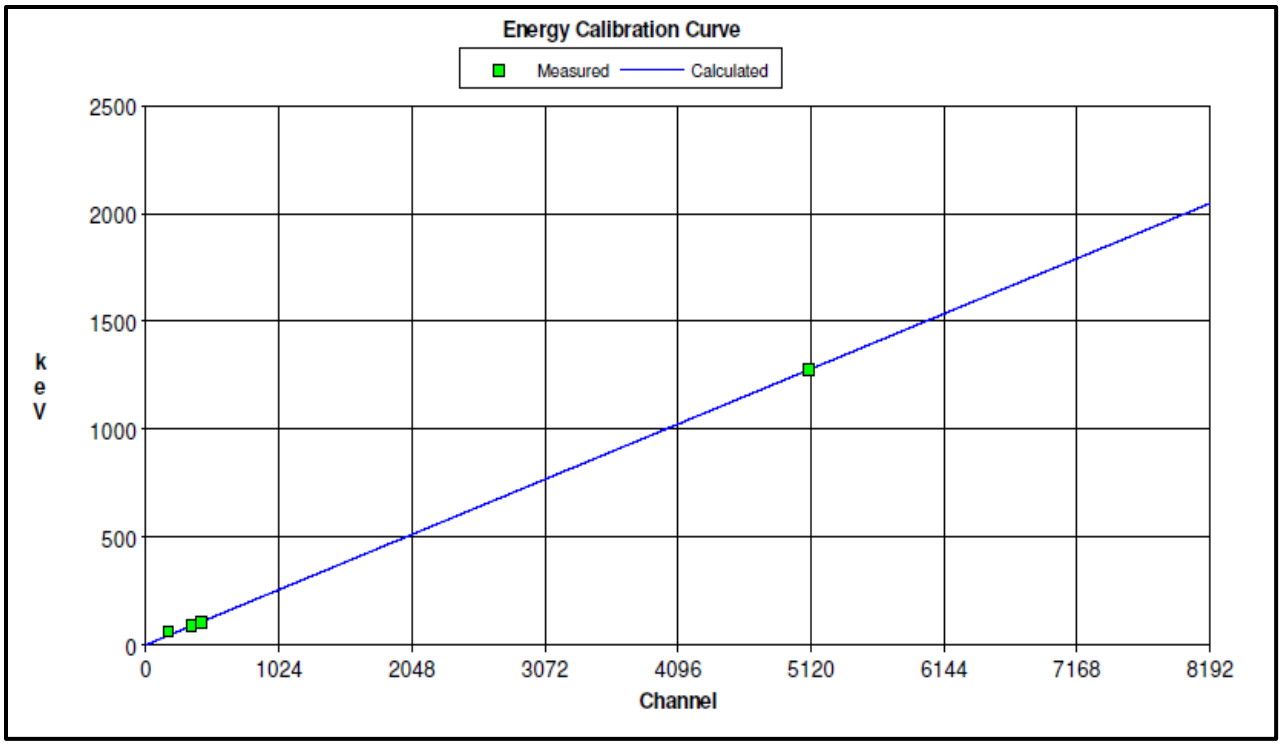

Figure (3-5): Energy Calibration Using a Standard Source Multi-Gamma.

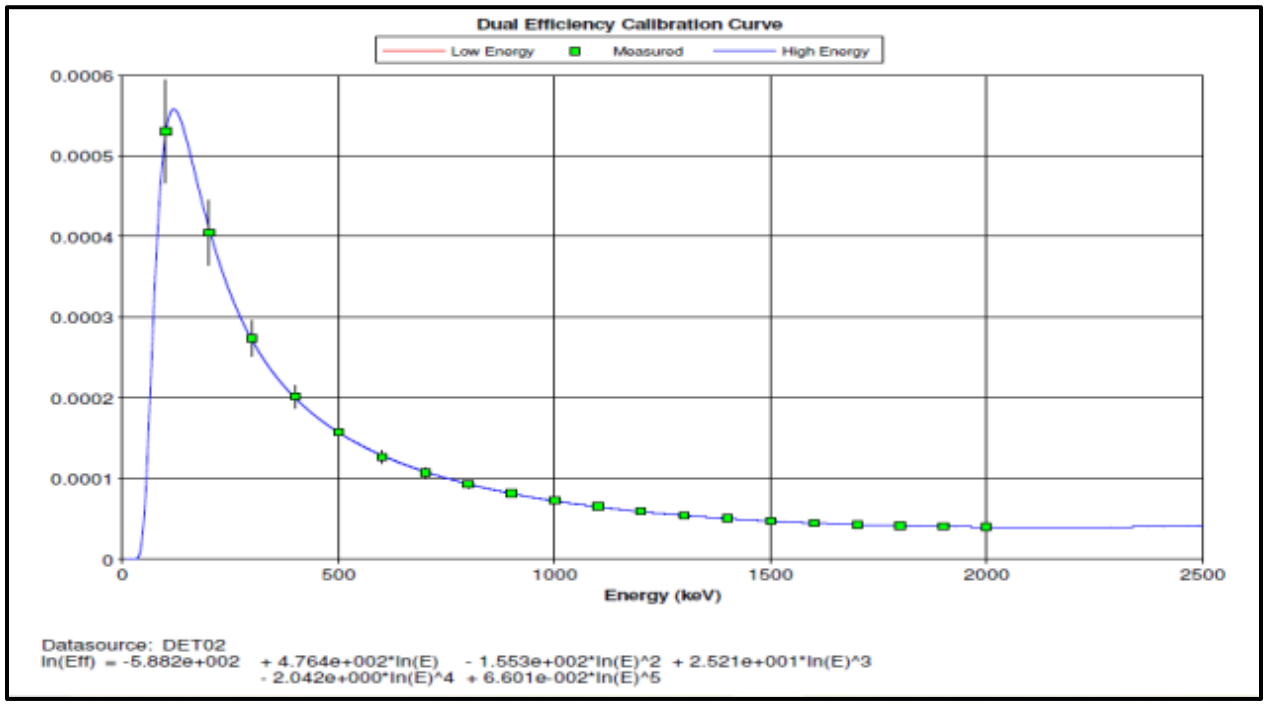

Figure (3-6): Efficiency Calibration Curve of HPGe Detector Using a Standard Source Multi-Gamma.

3.2.5. Background Radiation

In this research, the background radiation was measured by placing an empty Marinelli container, the same container used to measure the radioactivity of the models on the neck of the detector for the same period of time required for the measurements to collect the gamma ray spectrum on the computer screen and determine the energies that could fall on the detector, as well as to determine the area under the curve of the peaks for the purpose of subtracting this number from the recorded readings of the models and the same energies. To reduce the background radiation a cylindrical lead shield 12 cm thick is used because it has properties that qualify it to be one of the best materials for making barriers that protect against gamma rays (Appendix A). The background radiation is calculated using the following Equation [104].

$$A_{BG} = \frac{N_{BG}}{I_{\gamma}(E_{\gamma}) \times \varepsilon(E_{\gamma}) \times t} \quad \ldots\ldots\ldots (3-1)$$

Where A_{BG} represents the background radiation in units of (Bq/kg), N_{BG} is the area under the peaks, $I_{\gamma}(E_{\gamma})$ represents the gamma ray energy intensity, $\varepsilon(E_{\gamma})$ is the detector efficiency, and t represents the measurement time, which is 3600 sec, as shown in Figure (3-7).

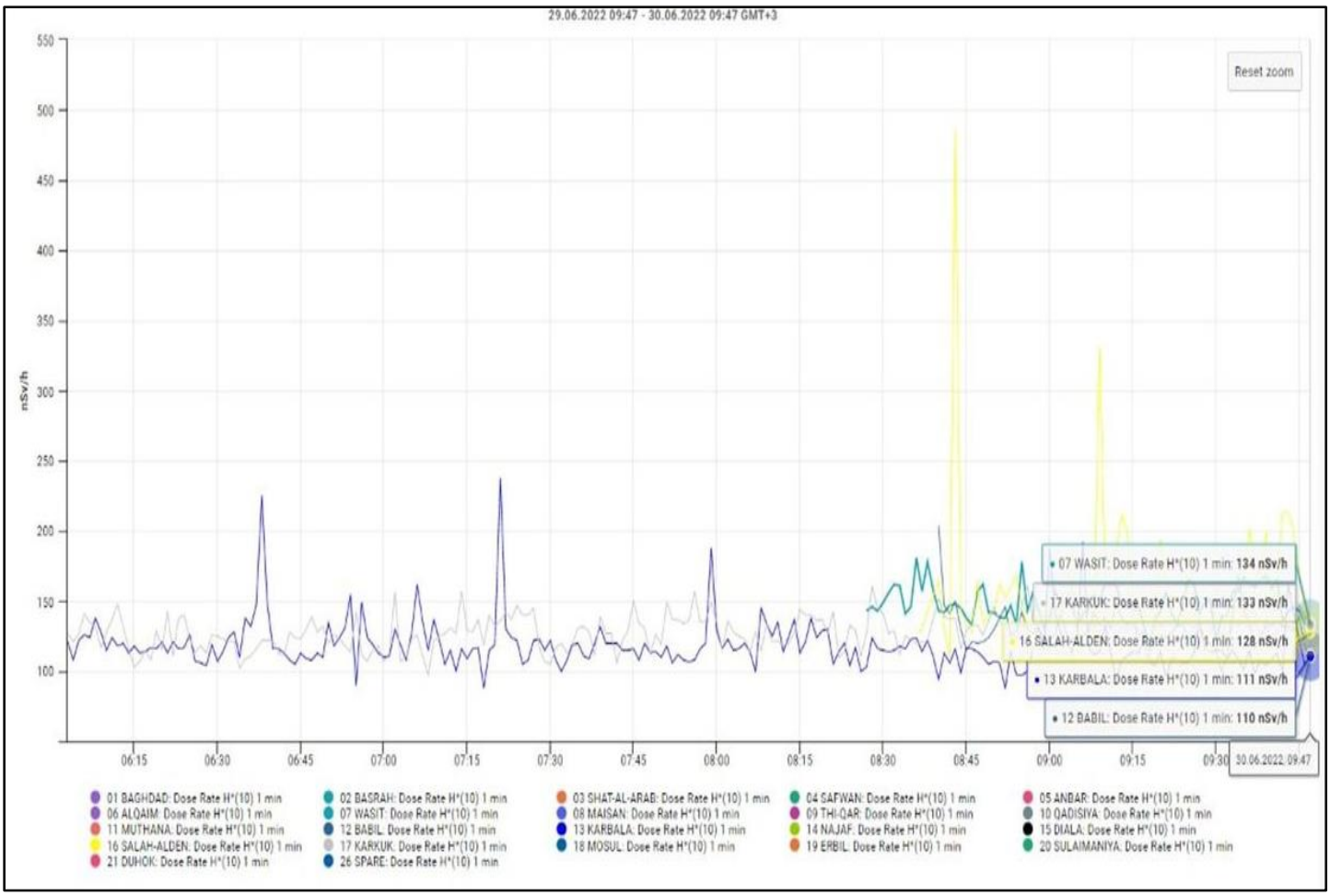

Figure (3-7): Background Radiation.

3.2.6. Minimum Detection Activity

The minimum detection limit (MDA) is known as the smallest amount of radionuclides that can be reliably identified for a given measurement. The MDA can be calculated using the following equation [107]:

$$\mathrm{MDA} = \frac{\mathrm{D.L.}}{\varepsilon_f \times p_\gamma \times T} \qquad \ldots\ldots\ldots (3-2)$$

Where MDA represents the minimum detection activity, D.L. is the detection limit (lowest radioactivity of a radionuclide that can be detected at the time of

measurement), ε_f is the detector efficiency, p_γ represents the probability of gamma ray emission, and T represents the counting time.

The D.L. can be calculated by using the following equation:

$$D.L. = \left(2.77 + 3.29\sqrt{B.G}\right) \times \frac{S.A.}{NetArea} \quad \ldots\ldots\ldots (3-3)$$

Where S.A. represents the specific activity (Bq/kg) or (Bq/L), Net Area represents the net area under the peaks, and B.G. represents the background radiation which can be calculated by Equation [88] (3-4).

$$B.G = Gross(Integral) - NetArea\ (A) \quad \ldots\ldots\ldots (3-4)$$

The minimum detection activity of natural and artificial radionuclides shown in table (3-3).

Table (3-3): The Efficiency and the Minimum Detectable Activity (MDA) for ^{226}Ra, ^{232}Th, ^{40}K, and ^{137}Cs.

Nuclide	Efficiency	MDA (Bq/kg)
^{226}Ra	0.06103	1.831
^{232}Th	0.01142	2.632
^{40}K	0.0113	2.79
^{137}Cs	0.0206	0.853

Results and Discussion

Chapter Four

Results and Discussion

4.1. Gamma Spectroscopy Technique

The quantitative and qualitative examination of the surface soil samples was carried using a high-purity germanium detector (HPGe). The ^{226}Ra activity was calculated by taking the mean activity of ^{214}Pb gamma-ray energy peaks at 295.2 and 351.9 keV, the ^{214}Bi peaks at 609.3, 1120.3, and 1764.5 keV under equilibrium conditions. On the other hand, the gamma-ray energy peaks used for the determination of the ^{232}Th activities were the ^{212}Pb gamma-ray energy peak at 238.6 keV, the ^{228}Ac energy peaks at 338.4, 463, 911.2, 964.6 and 969.0 keV, and the ^{208}Tl energy peaks at 583.2 and 860.6 keV, the ^{40}K energy peak at 1460.80 keV. Also, the peak energy of (661.66 keV) was utilized to determine the concentration of ^{137}Cs [108].

4.1.1. Measurement of Activity Concentrations for Soil Samples

The results of activity concentrations of (^{226}Ra, ^{232}Th, ^{40}K, and ^{137}Cs) in soils of Al-Majar and Kalaat Saleh are presented in Tables (4-1) and (4-2). Also shown in Figures from (4-1) to (4-16).

The activity concentrations of ^{226}Ra,^{232}Th,^{40}K and ^{137}Cs in Al-Majar varied from 5.724±1.684 Bq/kg (S_{12}) to 33.911±3.424 Bq/kg (S_1), 8.314±2.343 Bq/kg (S_2) to 18.536±2.517 Bq/kg (S_{26}), 158.324±7.251 Bq/kg (S_{14}) to 193.625±8.518 Bq/kg (S_{18}), and 0.327±0.0104 Bq/kg (S_{11}) to 2.917±0.771 Bq/kg (S_6), with an average value of 14.012±4.650 Bq/kg, 14.589±2.521 Bq/kg, 176.791±9.827 Bq/kg, and

1.626±0.963 Bq/kg, respectively, as listed in Table (4-1), shown in Figures from (4-1) to (4-4) and (4-9) to (4-12) (contour maps). Whereas in Kalaat Saleh the activity concentrations of related radionuclides were varied from 7.426±1.354 Bq/kg (S_{15}) to 27.624±2.617 Bq/kg (S_{11}), 16.709±2.864 Bq/kg (S_2) to 29.562±2.761 Bq/kg (S_{11}), 167.232±8.116 Bq/kg (S_6) to 211.424±9.454 Bq/kg (S_7), and 0.384±0.008 Bq/kg (S_3) to 3.823±1.014Bq/kg (S_7), with an average value of 16.072±5.455 Bq/kg, 20.752±3.650 Bq/kg, 187.813±11.011 Bq/kg, and 2.480±1.023 Bq/kg respectively for ^{226}Ra,^{232}Th,^{40}K, and ^{137}Cs as listed in Table (4-2), shown in Figures from (4-5) to (4-8) and (4-13) to (4-16) (contour maps).The contour map illustrates the spatial distribution of radiological concentrations of natural radionuclides (^{238}U, ^{232}Th, and ^{40}K) and artificial radionuclide (^{137}Cs) within the study area (Al-Majar, Kalaat Saleh). The map was generated using ArcGIS software (version 10.8). The activity concentration levels of both natural and artificial radionuclides were compared in Al-Majar and Kalaat Saleh cities. The activity concentrations of radionuclides in Kalat Saleh were higher than in Al-Majar which can be attributed to geological differences of the two regions. In addition, Kalaat Saleh is an agricultural area where various types of fertilizers are extensively used for soil enrichment. These fertilizers contain certain amounts of radionuclides, which contributes to an increase in the radiation levels in the soil. The findings indicate that average values of ^{226}Ra, ^{232}Th, and ^{40}K in soil samples of Al-Majar and Kalaat Saleh are below the global average values of 35 Bq/kg, 30 Bq/kg, and 400 Bq/kg, respectively [109]. The artificial radionuclide ^{137}Cs is not naturally present in samples. It is rather a byproduct of fallout radioactivity. The probable introduction of these isotopes into the study area's soil could be attributed to incidents like the Chernobyl nuclear power plant disaster on April 26, 1986, and nuclear weapons testing [43].

Table (4-1): Natural and Artificial Radioactivity in Soil Samples of Al-Majar.

Sample Code	Sample location	Radionuclide activity concentrations (Bq/kg)			
		^{226}Ra±S. D	^{232}Th±S. D	^{40}K±S. D	^{137}Cs±S. D
S_1	Sudur Al-Majar	33.911±3.424	17.422±2.715	163.431±8.434	0.523±0.011
S_2	Al-Waraq	21.543±2.511	8.314±2.343	172.824±8.715	0.372±0.009
S_3	Al-Hasharia	11.932±1.416	16.342±2.821	184.227±7.722	0.482±0.019
S_4	Fifth field	8.912±1.746	17.223±2.526	187.424±8.836	2.136±1.162
S_5	Fourth field	17.153±3.431	15.522±2.173	167.714±6.121	2.615±0.663
S_6	Third field	14.426±2.952	13.432±2.652	167.826±5.336	2.917±0.771
S_7	Al-Saeida	18.652±2.143	13.132±1.867	169.434±8.752	0.471±0.0105
S_8	Second field	13.153±2.446	11.846±2.426	186.225±7.502	2.716±1.161
S_9	Eidawiya	14.541±2.647	14.843±1.762	167.753±8.662	2.311±0.513
S_{10}	First field	10.912±3.232	14.425±2.442	178.524±7.511	2.662±0.471
S_{11}	Western Sugar dwar	13.222±2.454	14.262±2.654	169.874±6.815	0.327±0.0104
S_{12}	Al-Sadrayn	5.724±1.684	8.604±1.295	189.164±8.149	2.321±1.383
S_{13}	Eastern Sugar dwar	13.125±2.321	14.223±2.362	183.432±7.932	2.764±0.692
S_{14}	Yarmouk	14.418±3.534	16.427±2.321	158.324±7.251	0.524±0.011
S_{15}	Al-Jameiaat	15.225±1.817	17.321±1.853	161.519±5.921	0.394±0.0067
S_{16}	Al-Easkari	15.912±1.843	13.452±2.45	165.824±7.973	0.382±0.0075
S_{17}	Al-Shurta	14.225±2.651	16.881±2.174	169.625±7.312	2.181±0.553
S_{18}	Al-Shuhada'	14.352±2.152	10.812±1.295	193.625±8.518	0.463±0.014
S_{19}	New Hussein	15.573±2.391	17.635±2.812	175.735±8.686	2.114±1.353
S_{20}	Old Hussein (Al-Rifaq)	9.639±1.738	9.625±1.265	193.411±7.257	0.493±0.013
S_{21}	Al-Jumhuria	13.651±2.782	15.335±2.262	167.534±6.363	0.521±0.011
S_{22}	Imam Al-Hassan	11.274±1.372	16.624±2.291	188.746±8.522	2.204±0.741
S_{23}	Al- Kashashiya (First Al-Rahma)	13.478±1.252	16.622±2.163	179.426±6.282	2.142±0.364
S_{24}	14 –Ramadan	12.533±2.152	14.216±2.562	175.635±9.411	2.621±0.455
S_{25}	Al-Rahma	12.253±2.761	15.126±2.421	188.312±8.176	1.701±0.463
S_{26}	Al-Sinaea	12.716±2.235	18.536±2.517	177.925±7.732	1.964±0.241
S_{27}	Al-Saray	13.522±2.361	13.532±1.815	167.536±7.313	1.717±0.834
S_{28}	Al- Kashashiya (Second Al-Rahma)	10.953±1.873	16.714±2.231	166.264±5.976	0.561±0.012
S_{29}	Al-Badrawi	13.551±1.746	13.712±1.832	178.741±6.243	2.154±0.4825
S_{30}	Al-Akhilas	7.624±1.367	14.723±2.192	177.464±7.325	1.706±0.542
S_{31}	Knikil	19.232±2.673	12.215±1.565	187.725±9.515	1.715±0.584
S_{32}	Al-Liwa'	10.912±2.572	14.432±2.382	179.821±6.532	0.471±0.016
S_{33}	AL-Aadel	11.922±1.863	17.327±2.191	175.821±6.834	2.725±1.104
S_{34}	Al-Khayr	13.734±2.272	15.452±2.252	193.431±8.501	2.721±0.874
S_{35}	Al-Wadia	16.535±2.912	14.323±1.883	177.412±6.134	2.843±1.033
Average± Stander Division		**14.012±4.650**	**14.589±2.521**	**176.791±9.827**	**1.626±0.963**
World average UNSCEAR-2000 [109]		**35**	**30**	**400**	**-**

Table (4-2):Natural and Artificial Radioactivity in Soil Specimens of Kalaat Saleh.

Sample Code	Sample location	Radionuclide activity concentrations (Bq/kg)			
		^{226}Ra±S. D	^{232}Th±S. D	^{40}K±S. D	^{137}Cs±S. D
S_1	Al-Ghadir	21.564±2.891	20.472±2.775	198.435±9.492	3.253±1.127
S_2	First Karama	8.616±1.237	17.224±2.441	177.427±7.583	2.464±0.472
S_3	Al-Husaynia (Al-Shibisha)	13.474±2.715	21.717±2.493	195.515±11.683	0.384±0.008
S_4	Third Karama	18.814±1.746	18.521±2.363	176.421±7.244	3.822±1.0337
S_5	Second Karama	19.821±1.393	16.709±2.864	183.527±8.214	1.853±0.562
S_6	Al-Euruba	19.523±2.745	19.754±2.894	167.232±8.116	2.813±1.225
S_7	Al-Zahraa (Al-Baeth)	15.814±2.793	26.603±3.692	211.424±9.454	3.823±1.014
S_8	Al-Sadr	11.754±2.113	17.314±1.815	194.541±11.219	2.198±0.881
S_9	Al-Huriya	12.832±2.126	16.925±2.493	179.413±6.954	2.134±0.821
S_{10}	Abu Samej (Al-Firqa)	14.424±2.293	23.723±3.143	189.831±8.273	3.284±1.012
S_{11}	Al-Eizz River	27.624±2.617	29.562±2.761	189.202±8.732	2.426±1.252
S_{12}	Al-Majaria	21.428±2.286	19.763±3.178	178.843±7.211	2.272±1.041
S_{13}	Al-Amir (Al-Easkari)	16.546±2.473	21.542±2.718	190.311±9.764	2.72±1.031
S_{14}	Sulaymaniyah	11.424±2.133	21.735±3.211	188.356±8.221	3.273±1.226
S_{15}	Al-Bayda and Al-Sawda	7.426±1.354	19.721±3.385	196.721±11.403	0.483±0.0104
Average± Stander Division		**16.072±5.455**	**20.752±3.650**	**187.813±11.011**	**2.480±1.023**
World average UNSCEAR-2000 [109]		**35**	**30**	**400**	**-**

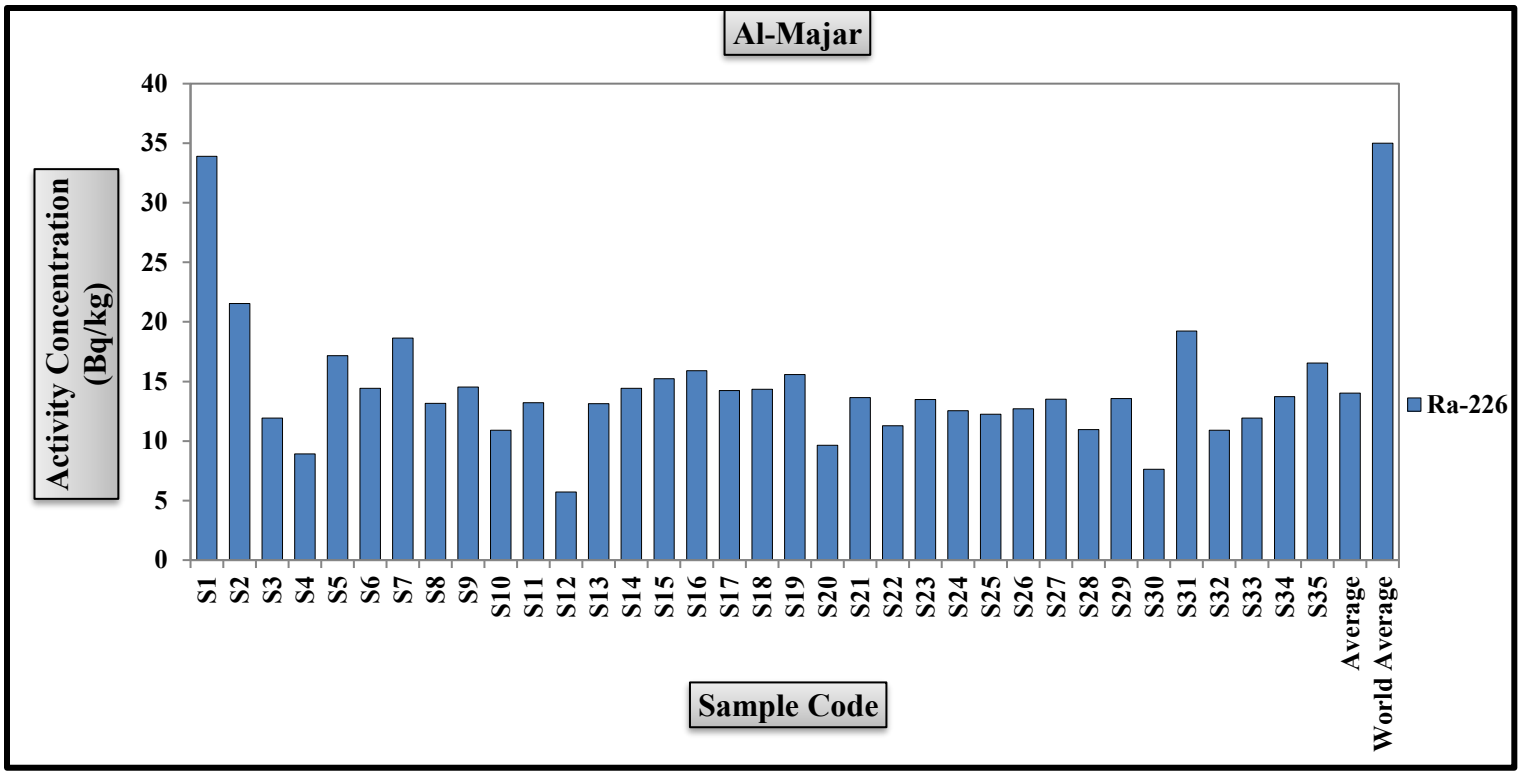

Figure (4-1): Activity concentrations of ^{226}Ra in surface soil samples in Al-Majar.

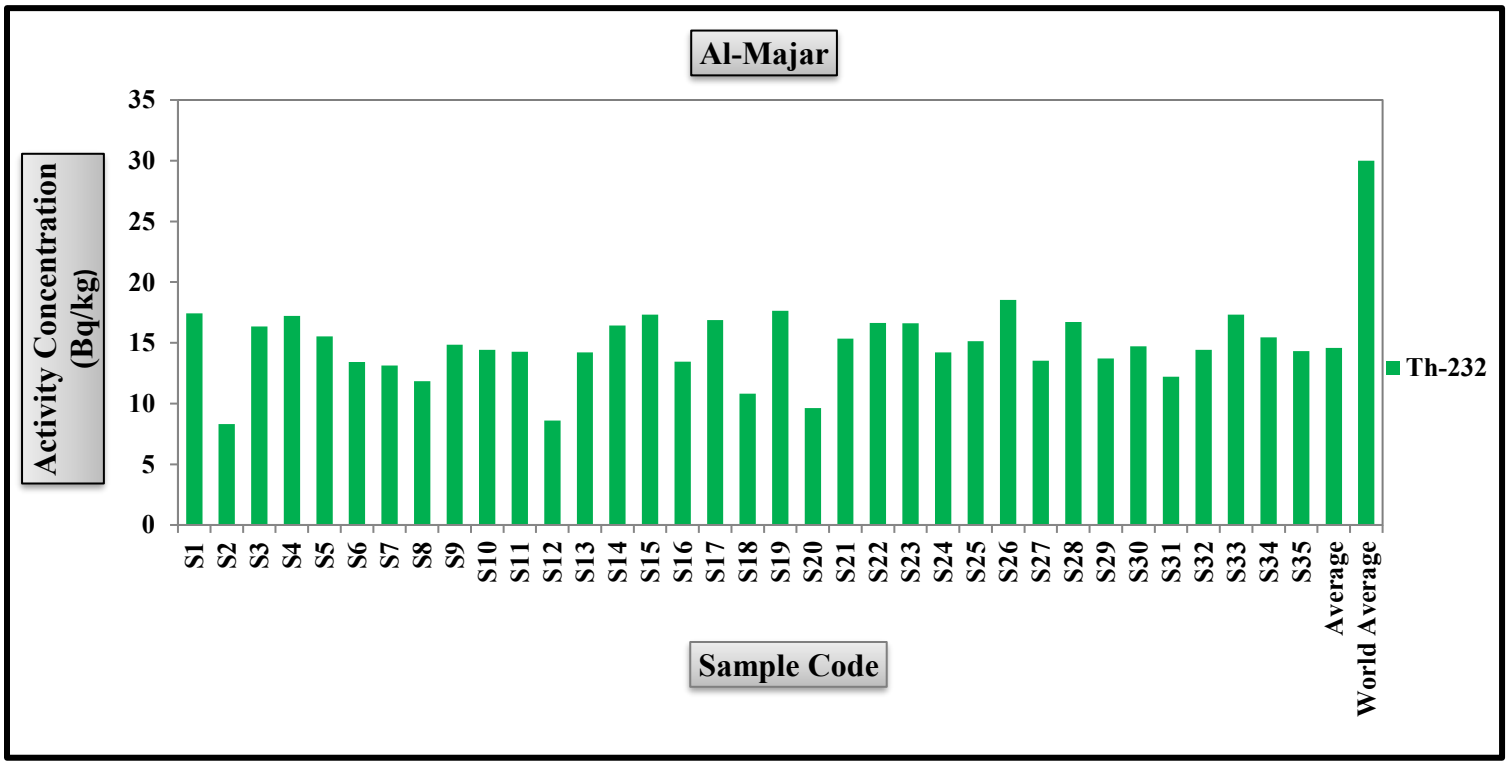

Figure (4-2): Activity concentrations of ^{232}Th in surface soil samples in Al-Majar.

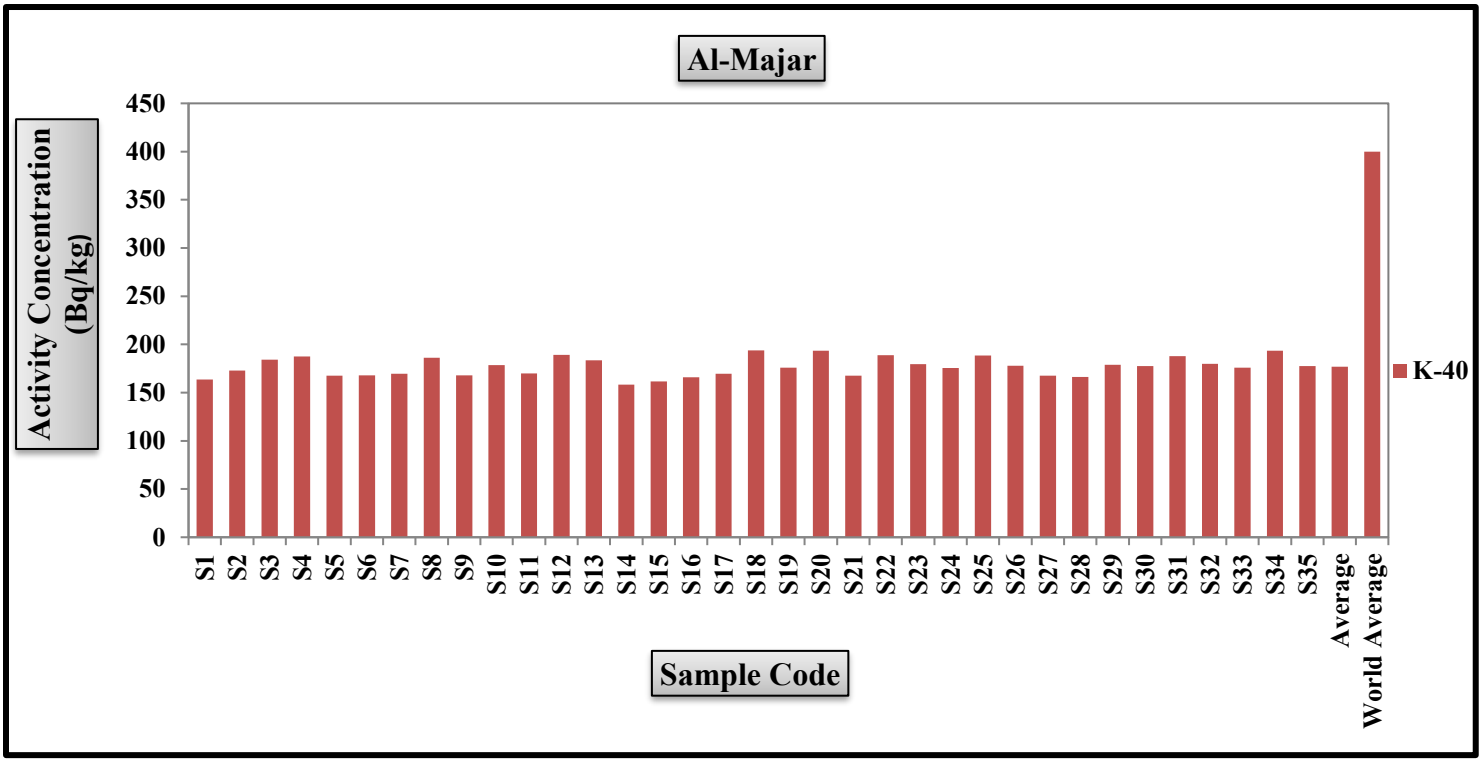

Figure (4-3): Activity concentrations of ^{40}K in surface soil samples in Al-Majar.

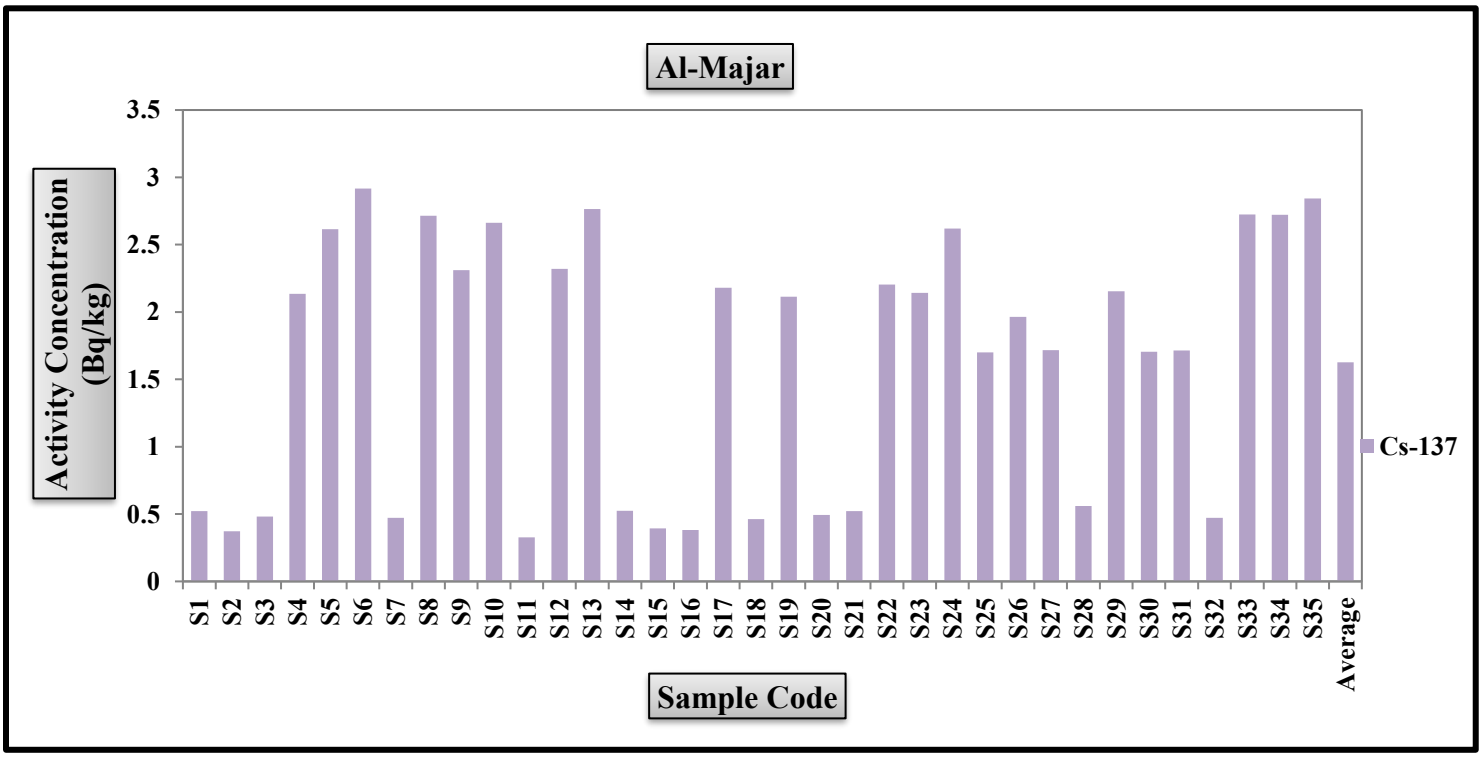

Figure (4-4): Activity concentrations of ^{137}Cs in surface soil samples in Al- Majar.

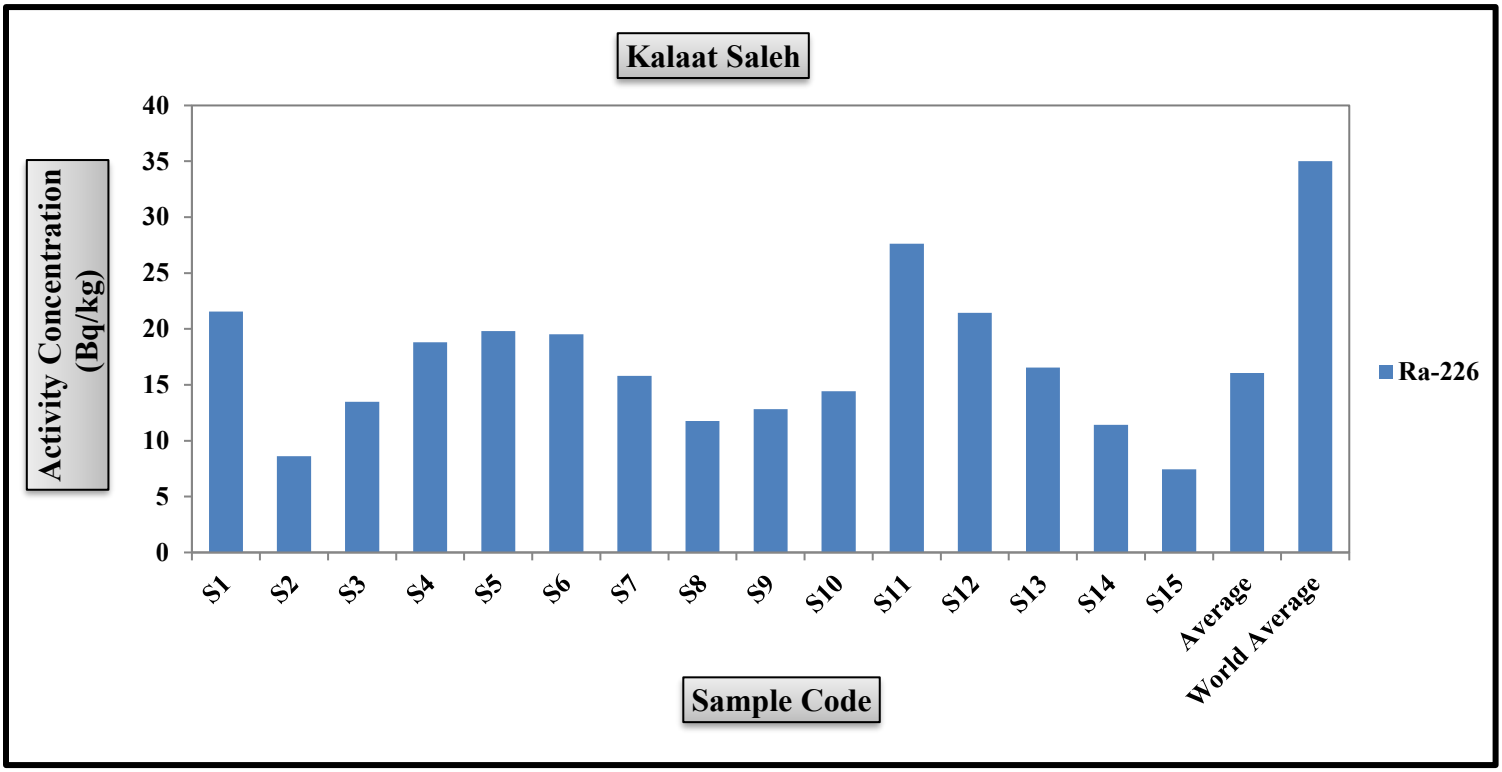

Figure (4-5): Activity concentrations of ^{226}Ra in surface soil samples Kalaat Saleh.

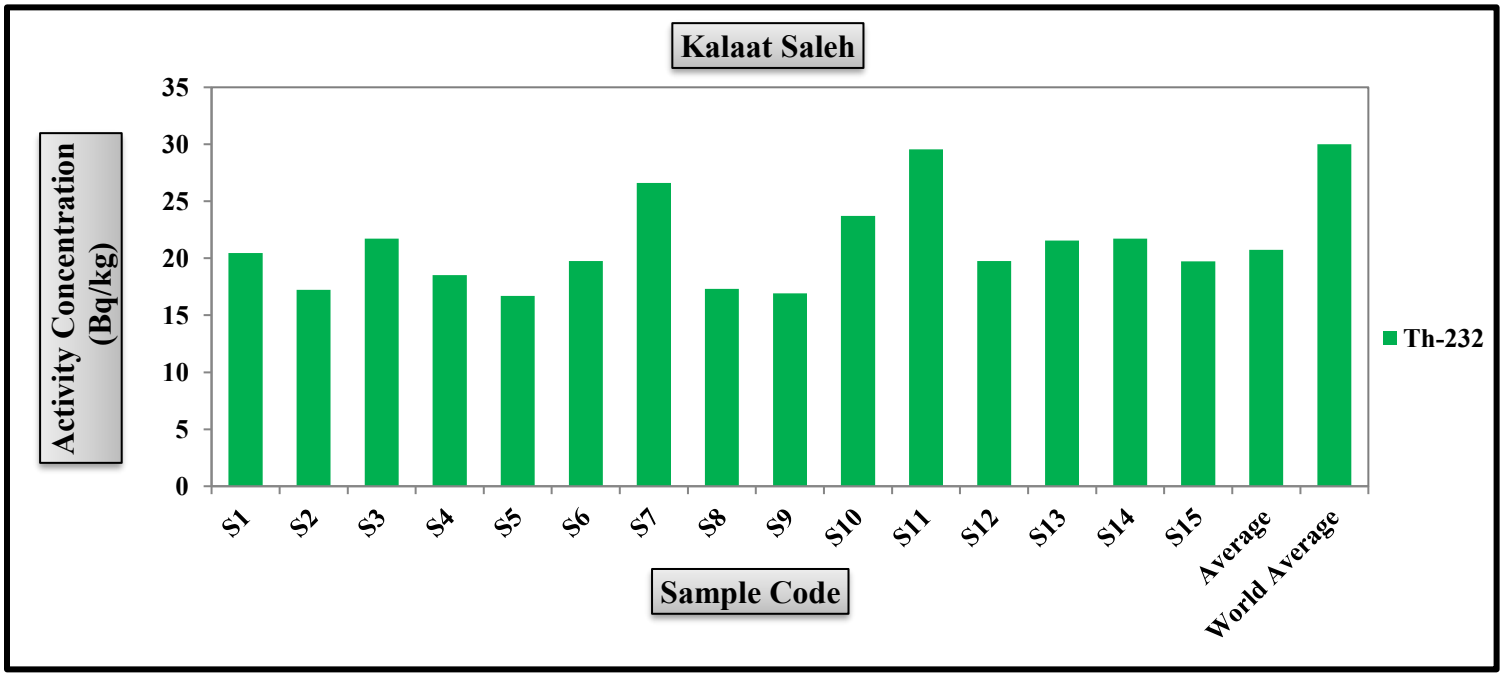

Figure (4-6): Activity concentrations of ^{232} Th in surface soil samples in Kalaat Saleh.

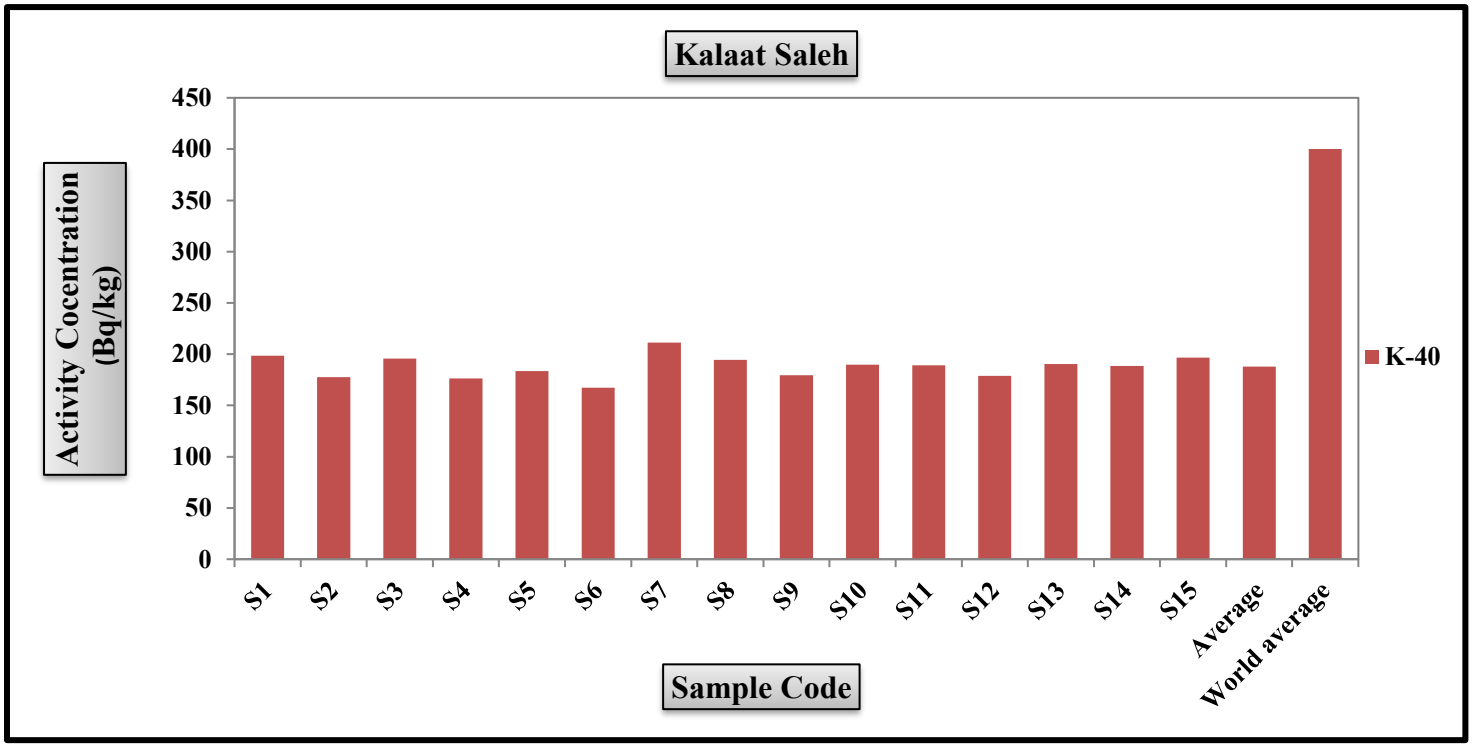

Figure (4-7): Activity concentrations of ^{40}K in surface soil samples in Kalaat Saleh.

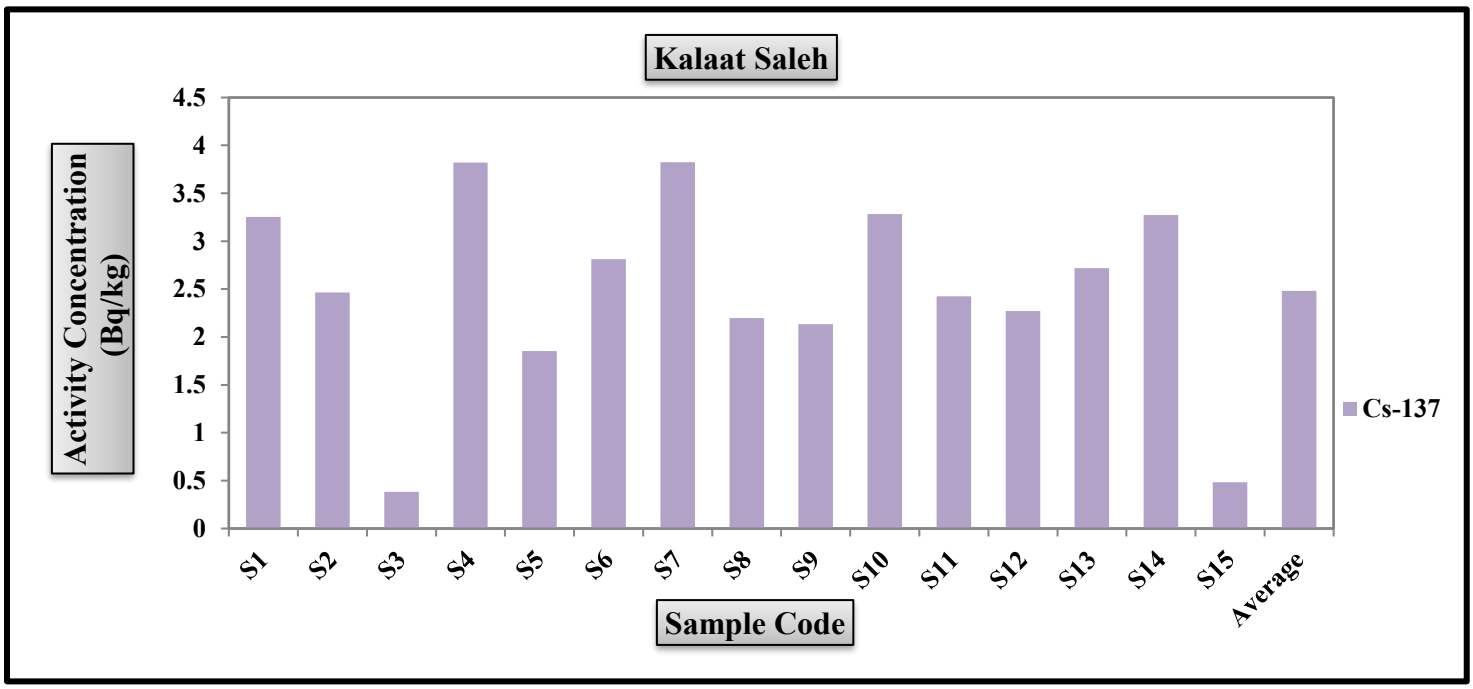

Figure (4-8): Activity concentrations of ^{137}Cs in surface soil samples in Kalaat Saleh.

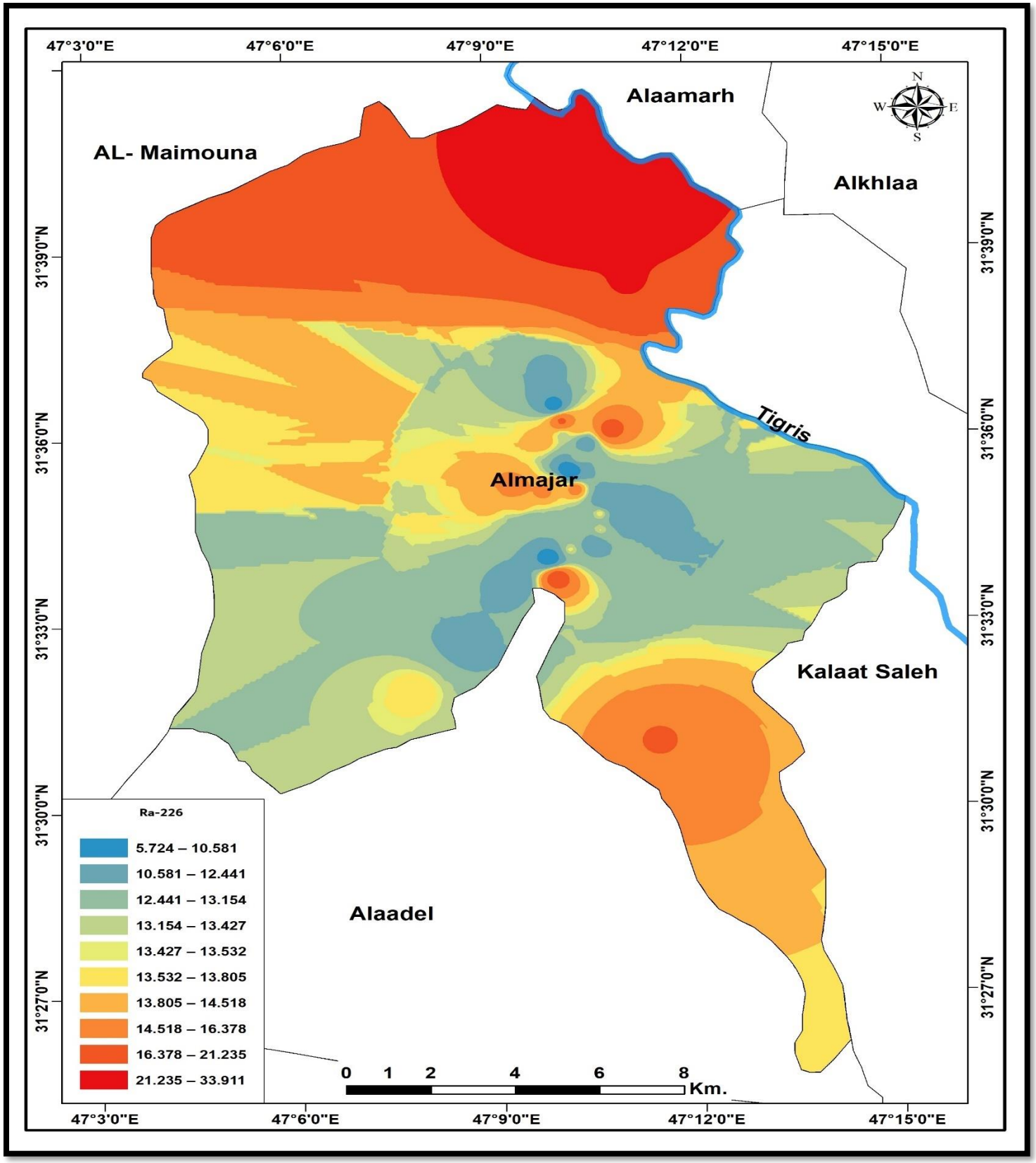

Figure (4-9): Contour map of the activity concentrations of ^{226}Ra in surface soil samples in Al-Majar.

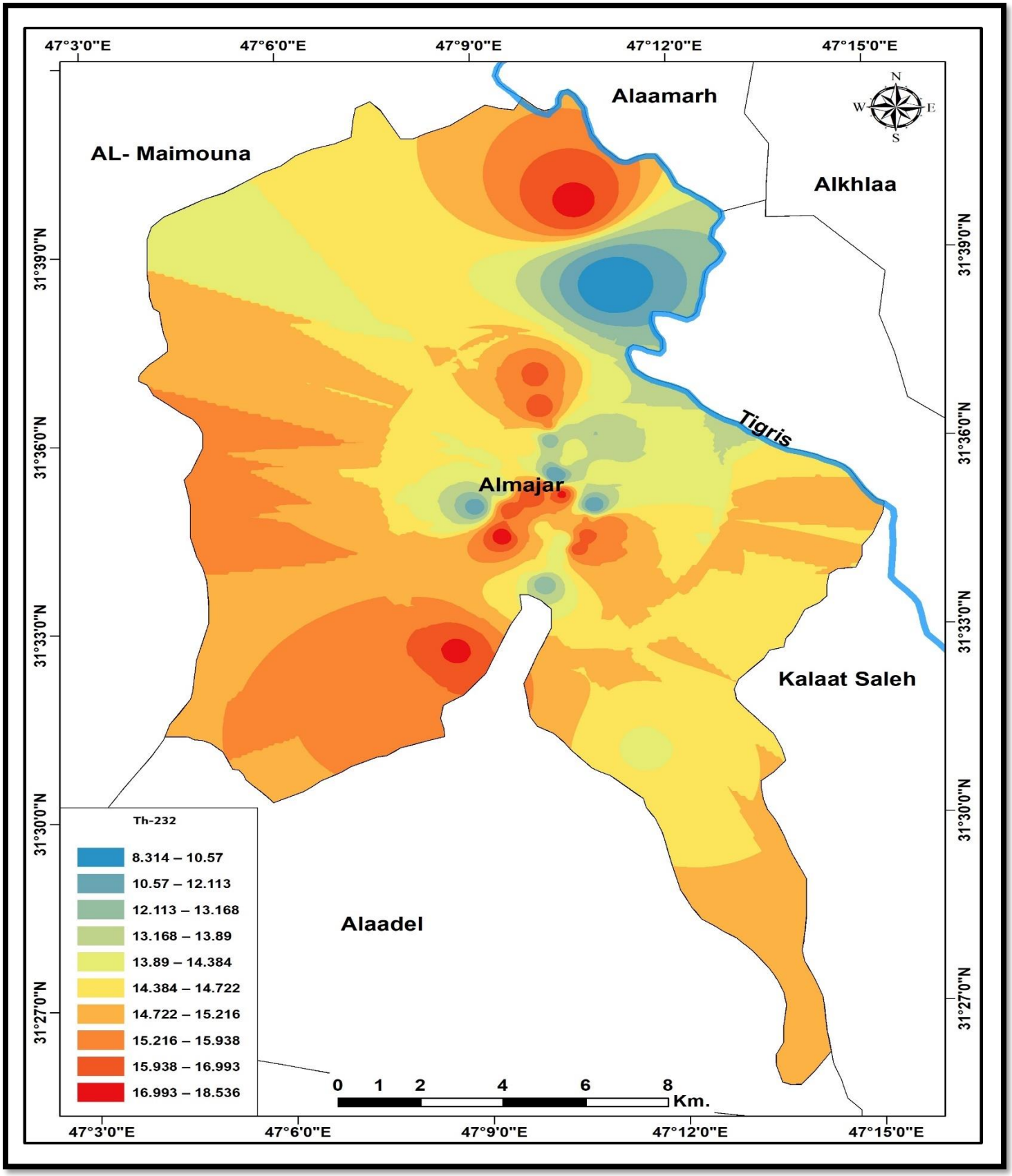

Figure (4-10): Contour map of the activity concentration of ^{232}Th in surface soil samples in Al-Majar.

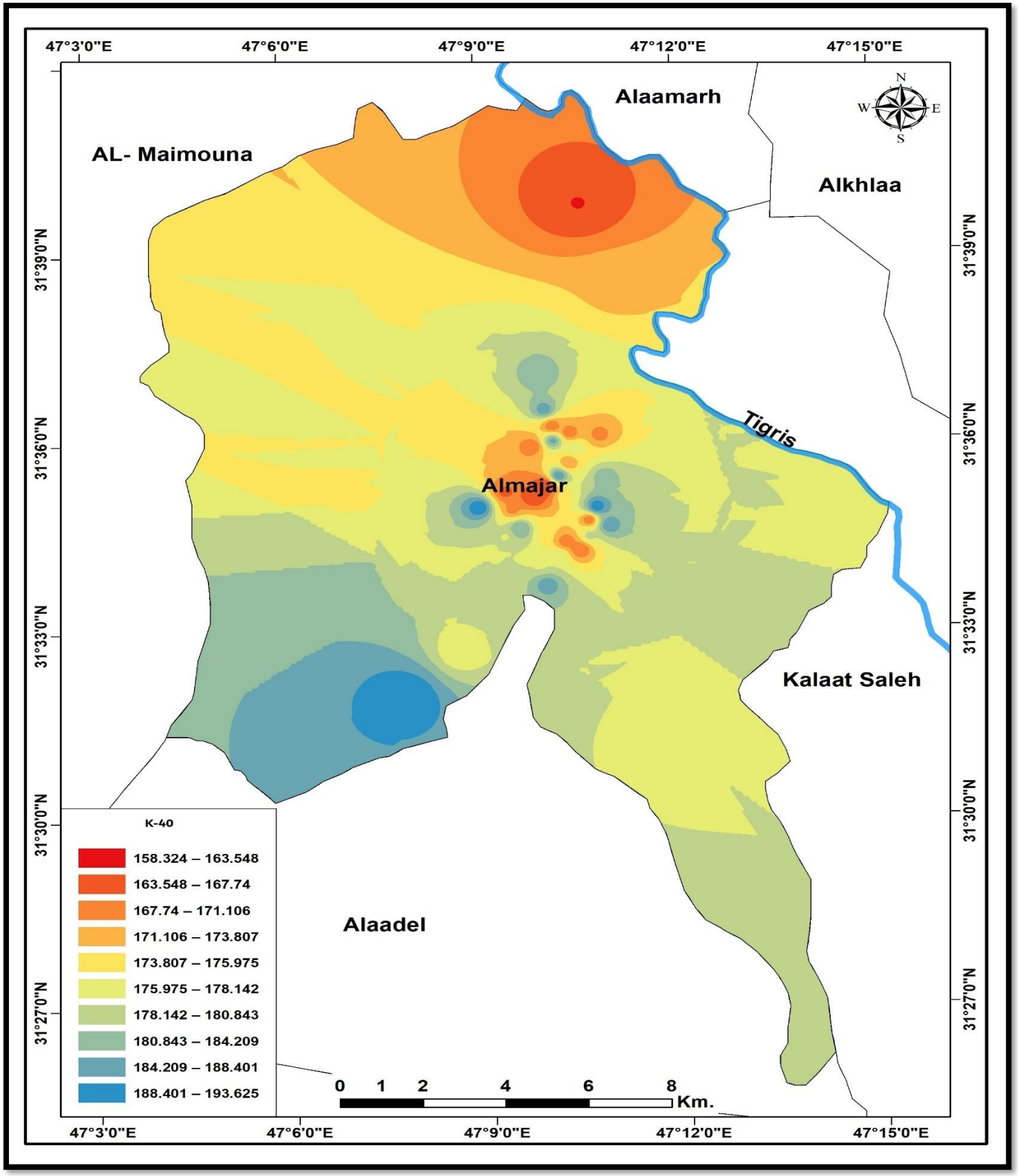

Figure (4-11): Contour map of the activity concentrations of ^{40}K in surface soil samples in Al-Majar.

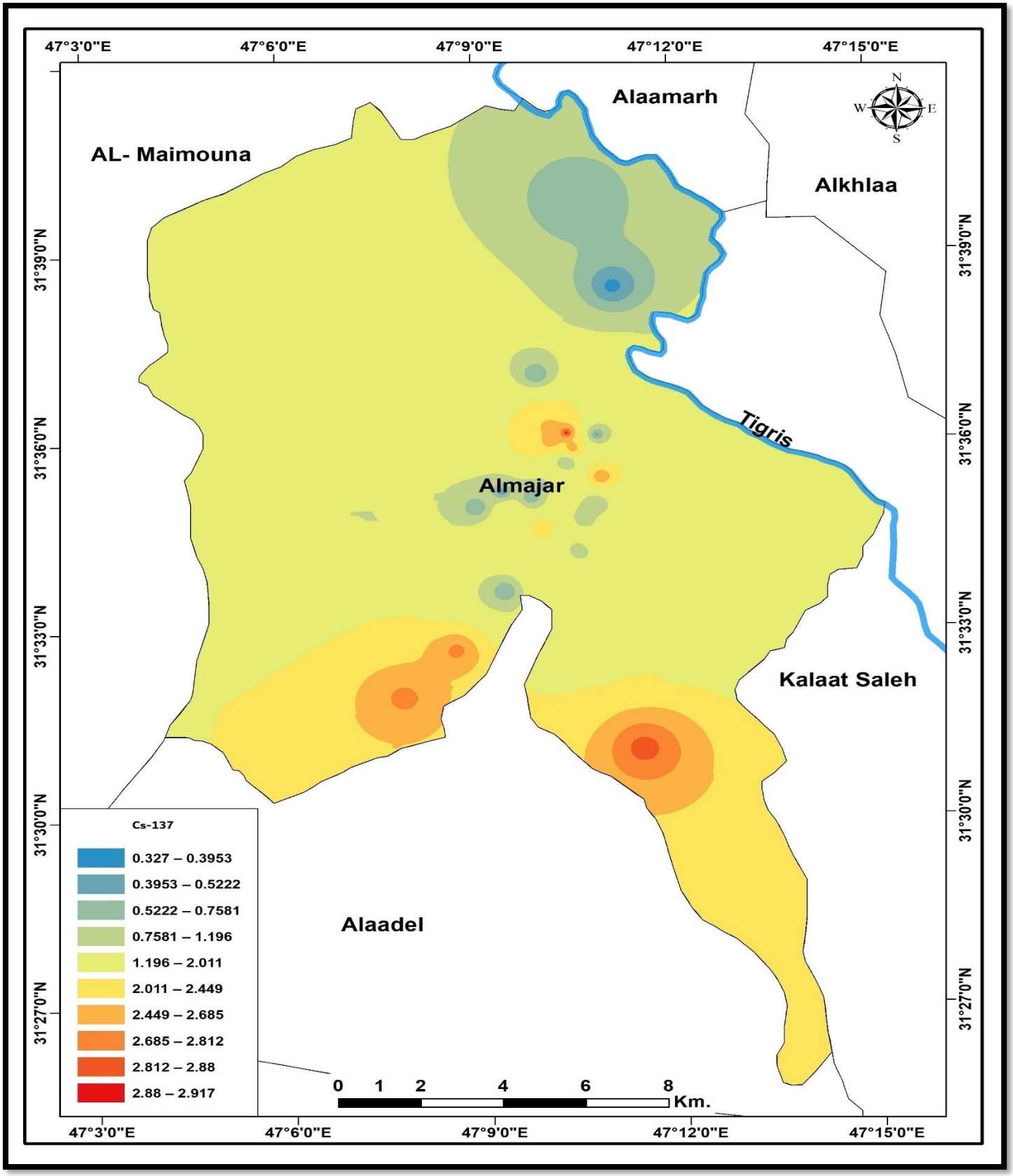

Figure (4-12): Contour map of the activity concentrations levels of ^{137}Cs in surface soil samples in Al-Majar.

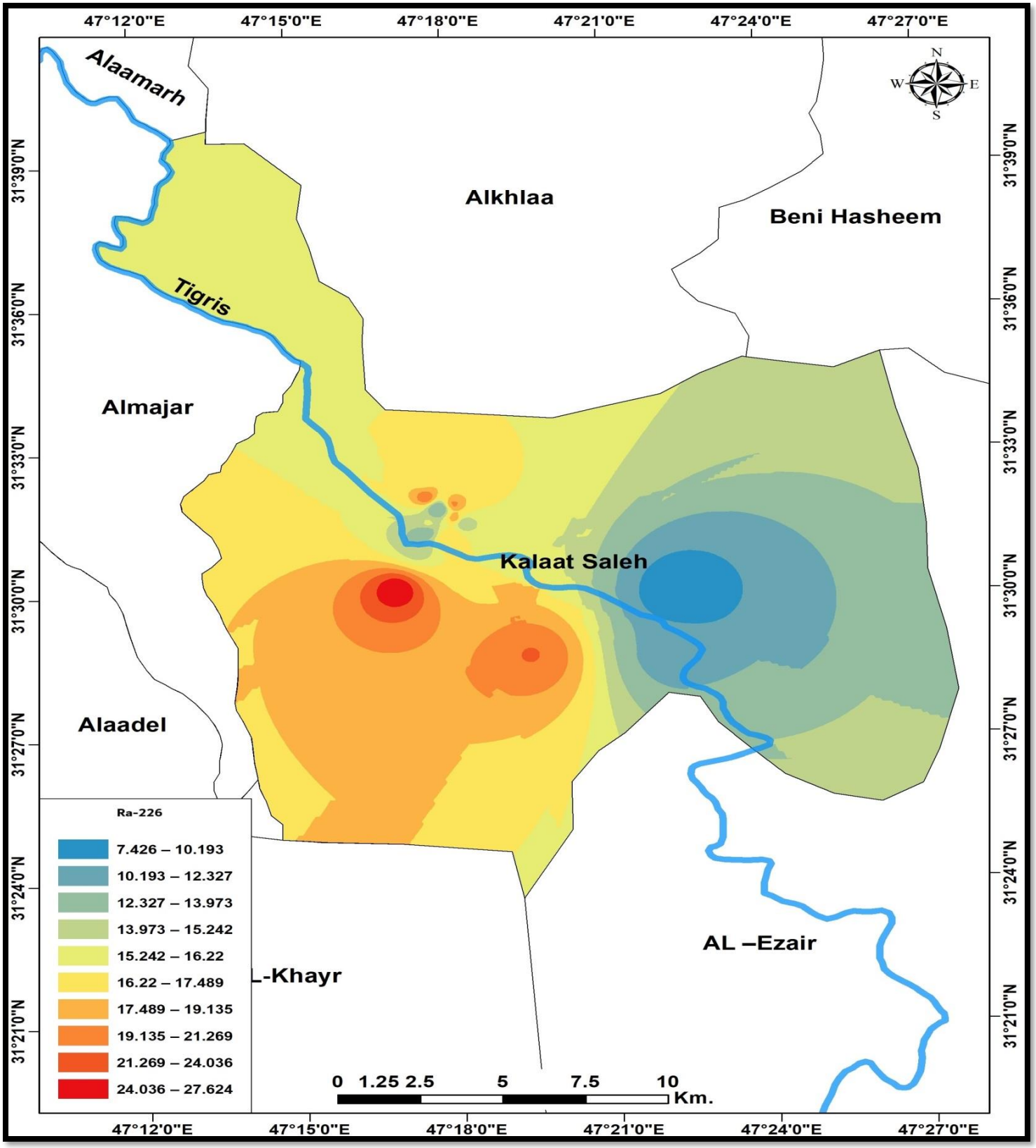

Figure (4-13): Contour map of the activity concentrations of ^{226}Ra in surface soil samples in Kalaat Saleh.

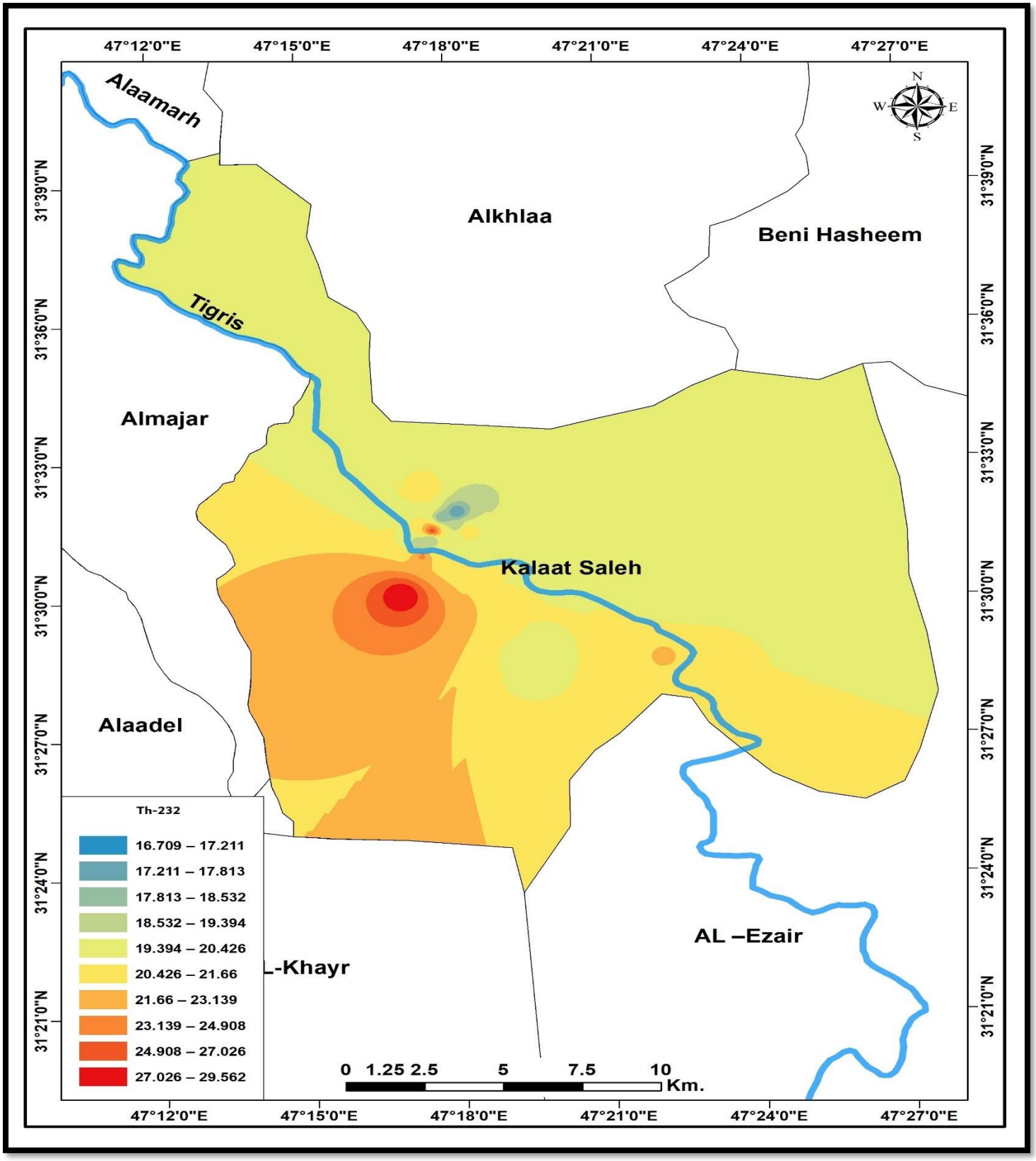

Figure (4-14): Contour map of the activity concentrations of ^{232}Th in surface soil samples in Kalaat Saleh.

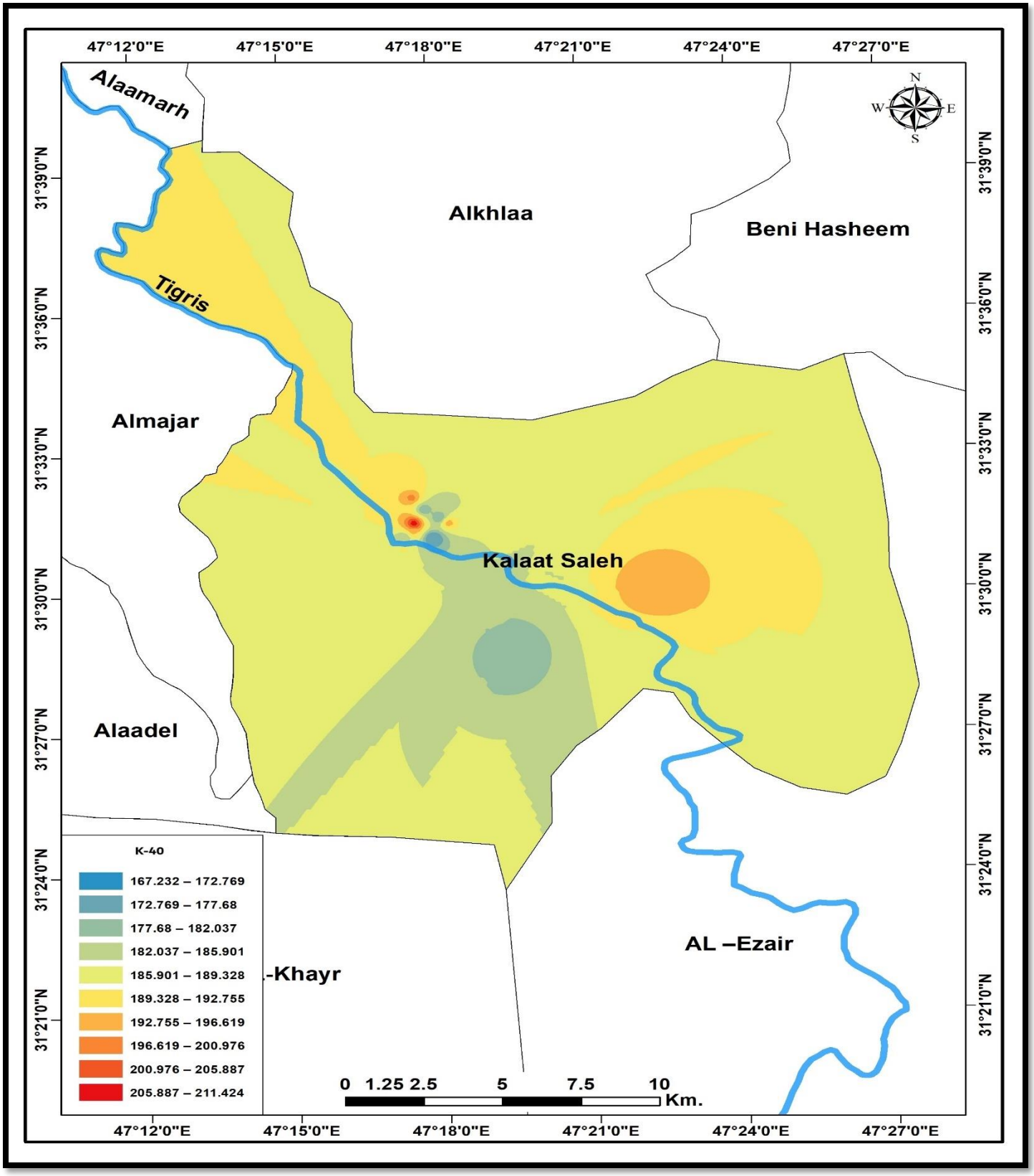

Figure (4-15): Contour map of the activity concentrations of ^{40}K in surface soil samples in Kalaat Saleh.

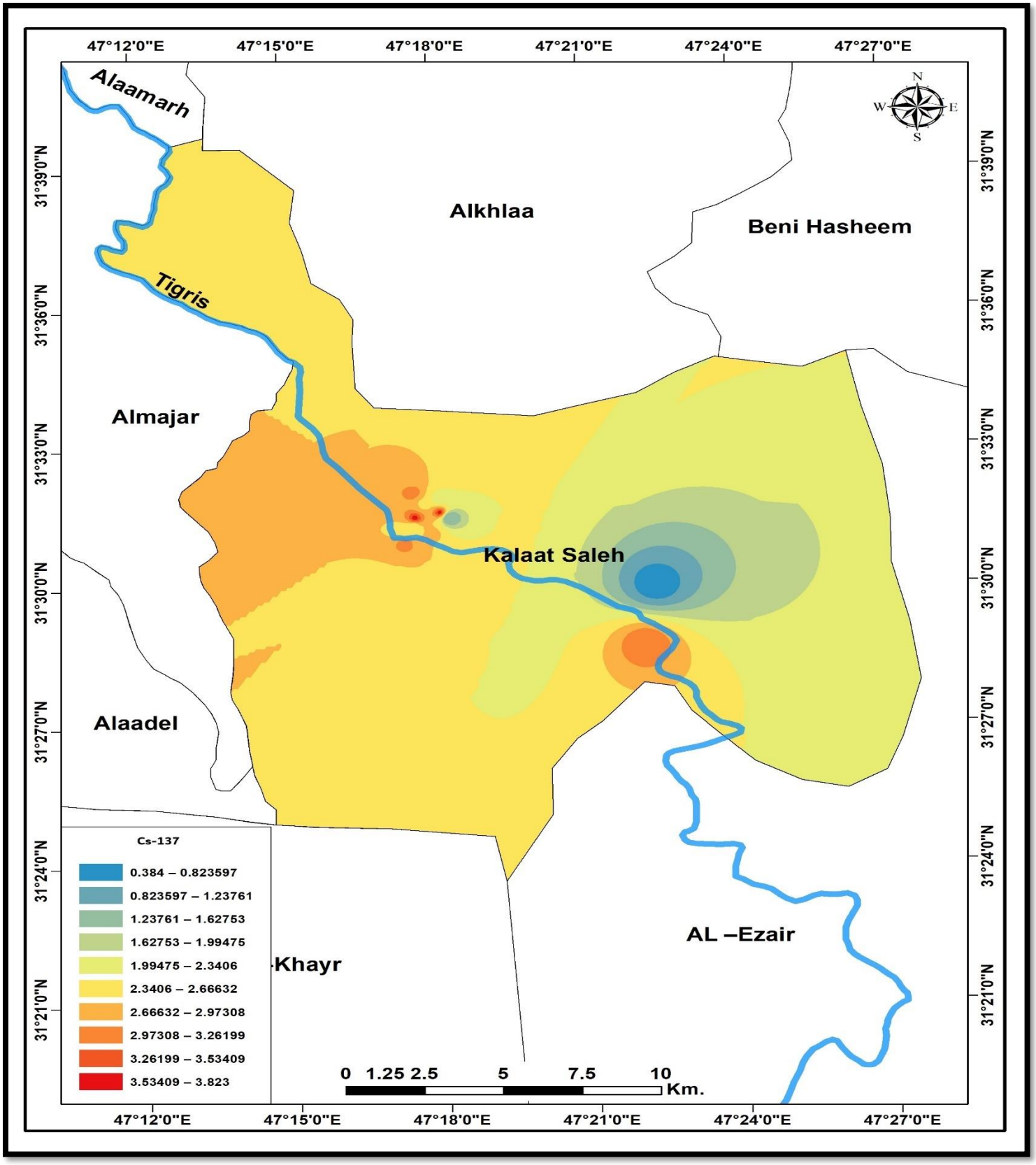

Figure (4-16): Contour map of the activity concentrations of ^{137}Cs in surface soil samples in Kalaat Saleh.

4.1.2. Comparison of Results of the Activity Concentrations in the Present Study with Literature Values

The average activity concentrations of natural and artificial radionuclides in soil samples of the research areas (Al-Majar and Kalaat Saleh) were compared with identical measurements conducted in the world and Iraq, as demonstrated in Table (4-3). The mean concentration of ^{226}Ra, ^{232}Th, ^{40}K, and ^{137}Cs of the present study is lower than the corresponding values reported in all the cited studies.

Table (4-3): Mean Activity Concentrations of ^{226}Ra,^{232}Th, ^{40}K and ^{137}Cs in the Present Study Compared with Literature Values.

Country	Mean activity concentration (Bq/kg)				Reference
	^{226}Ra	^{232}Th	^{40}K	^{137}Cs	
South East Europe	40	47.8	522	35	[110]
Setif, Algeria	47	33	329	Not measured	[111]
southwestern region, Nigeria	54.5	91.1	286.5	Not measured	[112]
Malaysian Peninsula, Malaysia	57	68	427	Not measured	[113]
Uttara Kannada, India	36.13	48.47	415.76	Not measured	[114]
Waziristan, Pakistan	69.5	123.68	453.60	Not measured	[115]
Inani Beach,Bangladesh	44.39	69.79	1007.25	Not measured	[116]
West Bank,Palestine	68.7	48	630	Not measured	[117]
Sana'a, Yemen	48.2	41.7	939.1	Not measured	[118]
Anzali wetland, Iran	24.66	31.94	506.38	11.66	[119]
Kastamonu, Turkey	37.4	27.2	431.4	8.0	[120]
Jordan	42.5	26.7	291.1	Not measured	[121]
Nineveh, Iraq	33.55	21.52	326.74	Not measured	[122]
Al-Tuwaitha, Iraq	-	25.29	363.47	8.72	[105]
Baghdad, Iraq	21.74	25.81	434.67	Not measured	[123]
Thi-Qar, Iraq	29.2	22.7	304.6	Not measured	[56]
World average UNSCEAR-2000	35	30	400	Not measured	[124]
Al-Majar	**14.012**	**1.912**	**176.791**	**1.626**	**Present study**
Kalaat Saleh	**16.072**	**20.752**	**187.813**	**2.480**	

4.1.3. Evaluation of Radiological Hazard Effects for Soil Samples

Tables (4-4) and (4-5) show the radiological risk parameters obtained from soil samples in the study areas.

The levels of Ra_{eq} ranged from 32.593 (S_{12}) to 71.408 (S_1) Bq/kg with an average of 48.488 ± 5.749 Bq/kg in Al-Majar, as shown in Figure (4-17), and from 46.908 (S_2) to 84.466 (S_{11}) Bq/kg with an average of 60.209 ± 9.223 Bq/kg in Kalaat Saleh, as shown in Figure (4-24). All values of Ra_{eq} were lower than the worldwide average value of 370 Bq/kg [109, 125].

The values of H_{in} varied from 0.103(S_{12}) to 0.284 (S_1) with an average of 0.1688± 0.026 in Al-Majar, and from 0.1499 (S_2) to 0.302 (S_{11}) with an average of 0.206 ± 0.037 in Kalaat Saleh. Whereas values of H_{ex} varied from 0.088 (S_{12}) to 0.192(S_1) with an average of 0.130± 0.015 in Al-Majar, and from 0.126 (S_2) to 0.228 (S_{11}) with an average of 0.162 ± 0.024 in Kalaat Saleh. All these values of H_{in} and H_{ex} were less than the value of (1). As shown in Figure (4-18) for Al-Majar and Figure (4-25) for Kalaat Saleh [125].

The levels of Iγ varied from 0.125 (S_{12}) to 0.254 (S_1) with an average of 0.178 ± 0.019 in Al-Majar, as shown in Figure (4-19), and from 0.173 (S_2) to 0.302 (S_{11}) with an average of 0.219 ± 0.031 in Kalaat Saleh, as shown in Figure (4-26). The determined values of Iγ were below the value of (1) [109, 125].

The levels of D_{in} ranged from 30.052 (S_{12}) to 63.600 (S_1) nGy/h with an average of 43.260 ± 4.916 nGy/h in Al-Majar, and from 41.244 (S_2) to 73.257 (S_{11}) nGy/h with an average of 52.826 ± 7.844 nGy/h in Kalaat Saleh. D_{out} values ranged from 15.729 (S_{12}) to 33.004 (S_1) nGy/h with an average of 22.658± 2.542 nGy/h in Al-Majar, and from 21.782 (S_2) to 38.507 (S_{11}) nGy/h with an average of 27.791± 11.945 nGy/h in Kalaat Saleh. Furthermore, the values of D_{tot} ranged from 45.782(S_{12}) to 96.605(S_1) nGy/h with an average of 65.918± 7.457 nGy/h in Al-Majar, and from 63.027 (S_2) to 111.765 (S_{11}) nGy/h with an average of

80.618 ± 11.945 nGy/h in Kalaat Saleh. These computed values of air absorbed dose rates were below the world average values of 84 nGy/h, 59 nGy/h, and 143 nGy/h, for D_{in}, D_{out}, and $D_{tot,}$ respectively [109]. As shown in Figure (4-20) for Al-Majar and Figure (4-27) for Kalaat Saleh [125].

The $AEDE_{in}$ values varied from 0.147 (S_{12}) to 0.311 (S_1) mSv/y with a mean of 0.212±0.024 mSv/y in Al-Majar, and from 0.202 (S_2) to 0.359 (S_{11}) mSv/y with a mean value of 0.259 ± 0.038 mSv/y in Kalaat Saleh. $AEDE_{out}$ values varied from 0.019 (S_{12}) to 0.040 (S_1) mSv/y with a mean value of 0.027 ± 0.003 mSv/y in Al-Majar, and from 0.026 (S_2) to 0.047 (S_{11}) mSv/y with a mean value of 0.034 ± 0.005 mSv/y in Kalaat Saleh. In addition, $AEDE_{tot}$ values varied from 0.166 (S_{12}) to 0.352 (S_1) mSv/y with a mean value of 0.240±0.027 mSv/y in Al-Majar, and from 0.229 (S_2) to 0.406 (S_{11}) mSv/y with a mean value of 0.293 ± 0.0435 mSv/y in Kalaat Saleh. The estimated values of annual effective dose equivalents were lower than the worldwide average values of 0.41 mSv/y, 0.07 mSv/y, and 0.48 mSv/y, for $AEDE_{in}$, $AEDE_{out}$, and $AEDE_{tot}$, respectively [109].

The levels of $ELCR_{in}$ ranged from 0.515×10^{-3} (S_{12}) to 1.091×10^{-3}(S_1) with an average of $(0.742\pm 0.084)\times10^{-3}$ in Al-Majar, and from 0.708×10^{-3}(S_2) to 1.257×10^{-3} (S_{11}) with an average of $(0.907\pm 0.134)\times10^{-3}$ in Kalaat Saleh, as shown in Figure (4-21) for Al-Majar and Figure (4-28) for Kalaat Saleh [125]. While $ELCR_{out}$ values ranged from 0.067 $\times10^{-3}$ (S_{12}) to 0.141×10^{-3} (S_1) with an average of $(0.097\pm0.010)\times10^{-3}$ in Al-Majar, and from 0.093×10^{-3} (S_2) to 0.165×10^{-3} (S_{11}) with an average of $(0.119\pm 0.017)\times10^{-3}$ in Kalaat Saleh. Moreover, $ELCR_{tot}$ values varied from 0.583×10^{-3} (S_{12}) to 1.233×10^{-3} (S_1) with an average of $(0.840\pm 0.095)\times10^{-3}$ in Al-Majar, and from 0.801×10^{-3} (S_2) to 1.423×10^{-3} (S_{11}) with an average of $(1.026\pm 0.152)\times10^{-3}$ in Kalaat Saleh. The evaluated values of excess lifetime cancer risks were below the worldwide average values of 1.16×10^{-3}, 0.29×10^{-3}, and

1.45×10^{-3}, for $ELCR_{in}$, $ELCR_{out}$, and $ELCR_{tot}$, respectively [109]. As shown in Figure (4-22) for Al-Majar and Figure (4-29) for Kalaat Saleh [125].

The levels of AGDE varied from 113.049 (S_{12}) to 228.926 (S_1) μSv/y with a mean value of 159.795 ± 17.088 μSv/y in Al-Majar (column 15 of Table (4-4)), as shown in Figure (4-23)), and from 154.331 (S_2) to 268.336 (S_{11}) μSv/y with a mean value of 195.381± 27.988 μSv/y in Kalaat Saleh, as shown in Figure (4-30). These AGDE values were less than the worldwide average value of 300 μSv/y [109, 125].

According to the outcomes above, the results clearly indicate that the mean values of the radiological risk parameters in the soil of the research areas were below the globally recommended levels, and therefore, there are no potential health risks to the general public health in the cities of Al-Majar and Kalaat Saleh, and the radiation levels therein remain in normal ranges.

Table (4-4): Radiological Risk Indices in Al-Majar Soils.

Sample Code	Radiation Hazard Indices													
	Ra_{eq} (Bq/kg)	H_{in}	H_{ex}	$I\gamma$	D_{in} (nGy/h)	D_{out} (nGy/h)	D_{tot} (nGy/h)	$AEDE_{in}$ (mSv/y)	$AEDE_{out}$ (mSv/y)	$AEDE_{tot}$ (mSv/y)	$ELCR_{in}$ ($\times10^{-3}$)	$ELCR_{out}$ ($\times10^{-3}$)	$ELCR_{tot}$ ($\times10^{-3}$)	AGDE (µSv/y)
S_1	71.408	0.284	0.192	0.254	63.600	33.004	96.605	0.311	0.040	0.352	1.091	0.141	1.233	228.926
S_2	46.739	0.184	0.126	0.170	42.963	22.181	65.144	0.210	0.027	0.237	0.737	0.095	0.832	155.587
S_3	49.486	0.165	0.133	0.182	43.876	23.065	66.941	0.215	0.028	0.243	0.753	0.099	0.852	163.026
S_4	47.972	0.153	0.129	0.178	42.325	22.335	64.661	0.207	0.027	0.235	0.726	0.095	0.822	158.381
S_5	52.263	0.187	0.141	0.190	46.439	24.293	70.733	0.227	0.029	0.257	0.797	0.104	0.901	170.546
S_6	46.556	0.164	0.125	0.171	41.641	21.776	63.417	0.204	0.026	0.230	0.714	0.093	0.808	153.419
S_7	50.477	0.186	0.136	0.184	45.329	23.614	68.943	0.222	0.028	0.251	0.778	0.101	0.879	165.728
S_8	44.432	0.155	0.120	0.165	40.215	20.997	61.212	0.197	0.025	0.223	0.690	0.090	0.780	148.633
S_9	48.683	0.170	0.131	0.178	43.293	22.678	65.971	0.212	0.027	0.240	0.743	0.097	0.840	159.649
S_{10}	45.286	0.151	0.122	0.168	40.366	21.198	61.565	0.198	0.025	0.224	0.693	0.090	0.784	150.071
S_{11}	46.696	0.161	0.126	0.172	41.612	21.806	63.418	0.204	0.026	0.230	0.714	0.093	0.808	153.811
S_{12}	32.593	0.103	0.088	0.125	30.052	15.729	45.782	0.147	0.019	0.166	0.515	0.067	0.583	113.049
S_{13}	47.588	0.163	0.128	0.176	42.578	22.303	64.881	0.208	0.027	0.236	0.731	0.095	0.826	157.606
S_{14}	50.099	0.174	0.135	0.182	44.158	23.185	67.343	0.216	0.028	0.245	0.758	0.099	0.857	162.930
S_{15}	52.430	0.182	0.141	0.191	46.143	24.231	70.374	0.226	0.029	0.256	0.792	0.104	0.896	170.163
S_{16}	47.916	0.172	0.129	0.175	42.867	22.391	65.259	0.210	0.027	0.237	0.736	0.096	0.832	157.466
S_{17}	51.425	0.177	0.138	0.188	45.395	23.841	69.237	0.222	0.029	0.251	0.779	0.102	0.881	167.780
S_{18}	44.722	0.159	0.120	0.166	40.780	21.235	62.015	0.200	0.026	0.226	0.700	0.091	0.791	150.340
S_{19}	54.322	0.188	0.146	0.198	47.960	25.174	73.134	0.235	0.030	0.266	0.823	0.108	0.931	177.015
S_{20}	38.295	0.129	0.103	0.144	35.121	18.331	53.453	0.172	0.022	0.194	0.603	0.078	0.681	130.748
S_{21}	48.480	0.167	0.130	0.178	42.997	22.555	65.552	0.210	0.027	0.238	0.738	0.096	0.835	158.887
S_{22}	49.579	0.164	0.133	0.183	43.946	23.120	67.067	0.215	0.028	0.243	0.754	0.099	0.853	163.591

S_{23}	51.063	0.174	0.137	0.187	45.217	23.748	68.966	0.221	0.029	0.250	0.776	0.101	0.878	167.466
S_{24}	46.385	0.159	0.125	0.171	41.394	21.700	63.095	0.203	0.026	0.229	0.710	0.093	0.803	153.299
S_{25}	48.383	0.163	0.130	0.179	43.164	22.649	65.814	0.211	0.027	0.239	0.741	0.097	0.838	160.218
S_{26}	52.922	0.177	0.142	0.194	46.500	24.490	70.990	0.228	0.030	0.258	0.798	0.105	0.903	172.641
S_{27}	45.773	0.160	0.123	0.168	40.895	21.406	62.302	0.200	0.026	0.226	0.702	0.091	0.794	150.953
S_{28}	47.656	0.158	0.128	0.175	41.929	22.088	64.018	0.205	0.027	0.232	0.719	0.094	0.814	155.916
S_{29}	46.922	0.163	0.126	0.173	42.028	21.996	64.024	0.206	0.026	0.233	0.721	0.094	0.816	155.313
S_{30}	42.342	0.134	0.114	0.158	37.583	19.815	57.399	0.184	0.024	0.208	0.645	0.085	0.730	140.823
S_{31}	51.154	0.190	0.138	0.187	46.335	24.091	70.426	0.227	0.029	0.256	0.795	0.103	0.898	169.431
S_{32}	45.395	0.152	0.122	0.168	40.479	21.256	61.736	0.198	0.026	0.224	0.695	0.091	0.786	150.507
S_{33}	50.237	0.167	0.135	0.184	44.269	23.305	67.574	0.217	0.028	0.245	0.760	0.100	0.860	164.473
S_{34}	50.724	0.174	0.136	0.187	45.300	23.744	69.044	0.222	0.029	0.251	0.777	0.101	0.879	167.764
S_{35}	50.677	0.181	0.136	0.185	45.337	23.688	69.026	0.222	0.029	0.251	0.778	0.101	0.880	166.670
Average ± Standard Deviation	**48.488 ± 5.749**	**0.168 ± 0.026**	**0.130 ± 0.015**	**0.178 ± 0.019**	**43.260 ± 4.916**	**22.658 ± 2.542**	**65.918 ± 7.457**	**0.212 ± 0.024**	**0.027 ± 0.003**	**0.240 ± 0.027**	**0.742 ± 0.084**	**0.097 ± 0.0109**	**0.840 ± 0.095**	**159.795 ± 17.088**
World Average UNSCEAR [109]	**370**	**≤1**	**≤1**	**≤1**	**84**	**59**	**143**	**0.41**	**0.07**	**0.48**	**1.16**	**0.29**	**1.45**	**300**

Table (4-5): Radiological Risk indices in Kalaat Saleh Soils.

Sample Code	Radiation Hazard Indices													
	Ra_{eq} (Bq/kg)	H_{in}	H_{ex}	Iγ	D_{in} (nGy/h)	D_{out} (nGy/h)	D_{tot} (nGy/h)	$AEDE_{in}$ (mSv/y)	$AEDE_{out}$ (mSv/y)	$AEDE_{tot}$ (mSv/y)	$ELCR_{in}$ ($\times10^{-3}$)	$ELCR_{out}$ ($\times10^{-3}$)	$ELCR_{tot}$ ($\times10^{-3}$)	AGDE (µSv/y)
S_1	66.118	0.236	0.178	0.240	58.431	30.602	89.033	0.286	0.037	0.324	1.003	0.131	1.134	214.514
S_2	46.908	0.149	0.126	0.173	41.244	21.782	63.027	0.202	0.026	0.229	0.708	0.093	0.801	154.331
S_3	59.583	0.197	0.160	0.218	52.121	27.495	79.616	0.255	0.033	0.289	0.894	0.118	1.012	193.803
S_4	58.883	0.209	0.159	0.214	51.972	27.235	79.207	0.254	0.033	0.288	0.892	0.116	1.009	190.949
S_5	57.846	0.209	0.156	0.210	51.480	26.902	78.383	0.252	0.032	0.285	0.883	0.115	0.999	188.717
S_6	60.648	0.216	0.163	0.219	53.236	27.924	81.160	0.261	0.034	0.295	0.914	0.119	1.033	195.408
S_7	70.135	0.232	0.189	0.256	60.937	32.190	93.128	0.298	0.039	0.338	1.046	0.138	1.184	226.452
S_8	51.492	0.170	0.139	0.190	45.616	24.000	69.617	0.223	0.029	0.253	0.783	0.103	0.886	169.778
S_9	50.849	0.172	0.137	0.187	44.955	23.632	68.587	0.220	0.028	0.249	0.771	0.101	0.873	166.733
S_{10}	62.964	0.209	0.170	0.229	54.741	28.908	83.650	0.268	0.035	0.303	0.939	0.124	1.063	203.339
S_{11}	84.466	0.302	0.228	0.302	73.257	38.507	111.765	0.359	0.047	0.406	1.257	0.165	1.423	268.336
S_{12}	63.460	0.229	0.171	0.229	55.939	29.294	85.233	0.274	0.035	0.310	0.960	0.125	1.086	204.978
S_{13}	62.005	0.212	0.167	0.226	54.333	28.591	82.925	0.266	0.035	0.301	0.932	0.122	1.055	200.930
S_{14}	57.008	0.184	0.153	0.209	49.675	26.260	75.935	0.243	0.032	0.275	0.852	0.112	0.965	185.296
S_{15}	50.774	0.157	0.137	0.188	44.459	23.545	68.004	0.218	0.028	0.246	0.763	0.101	0.864	167.150
Average ± Standard Deviation	**60.209** ± 9.223	**0.206** ± 0.037	**0.162** ± 0.024	**0.219** ± 0.031	**52.826** ± 7.844	**27.791** ± 11.945	**80.618** ± 11.945	**0.259** ± 0.038	**0.034** ± 0.005	**0.293** ± 0.043	**0.907** ± 0.134	**0.119** ± 0.017	**1.026** ± 0.152	**195.381** ± 27.988
World Average UNSCEAR [109]	**370**	**≤1**	**≤1**	**≤1**	**84**	**59**	**143**	**0.41**	**0.07**	**0.48**	**1.16**	**0.29**	**1.45**	**300**

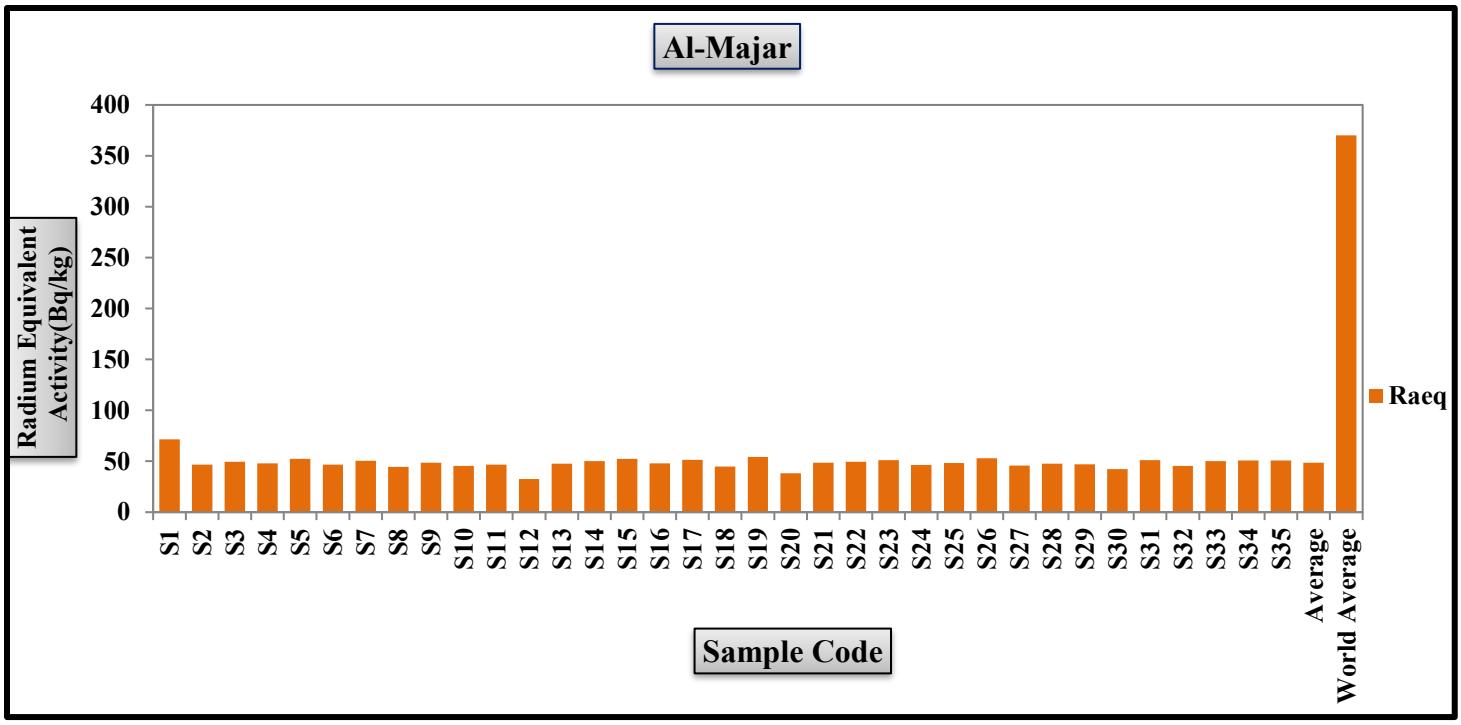

Figure (4-17): Radium equivalent activity levels (Ra_{eq}) in surface soil samples in Al-Majar.

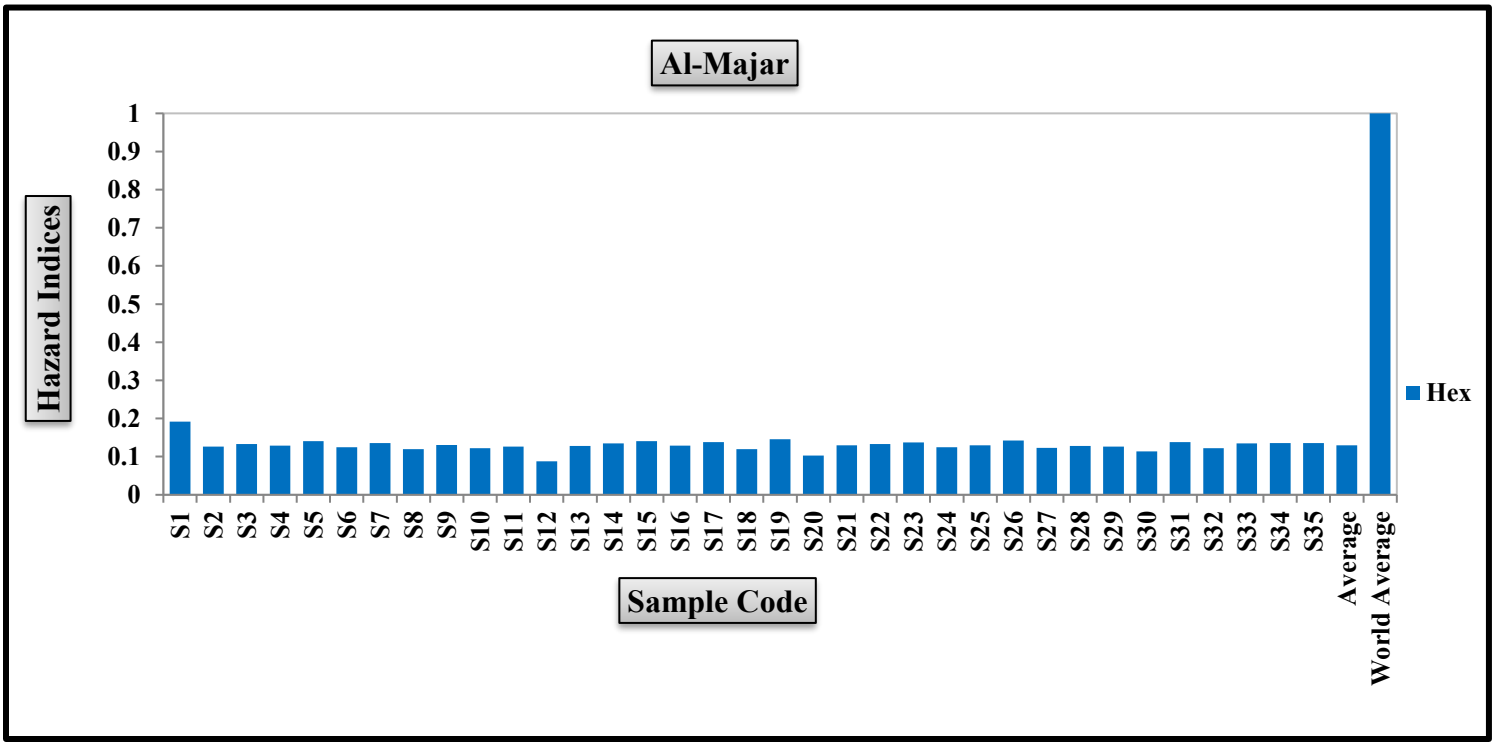

Figure (4-18): Internal (H_{in}) and external (H_{out}) hazard index levels in surface soil samples in Al-Majar.

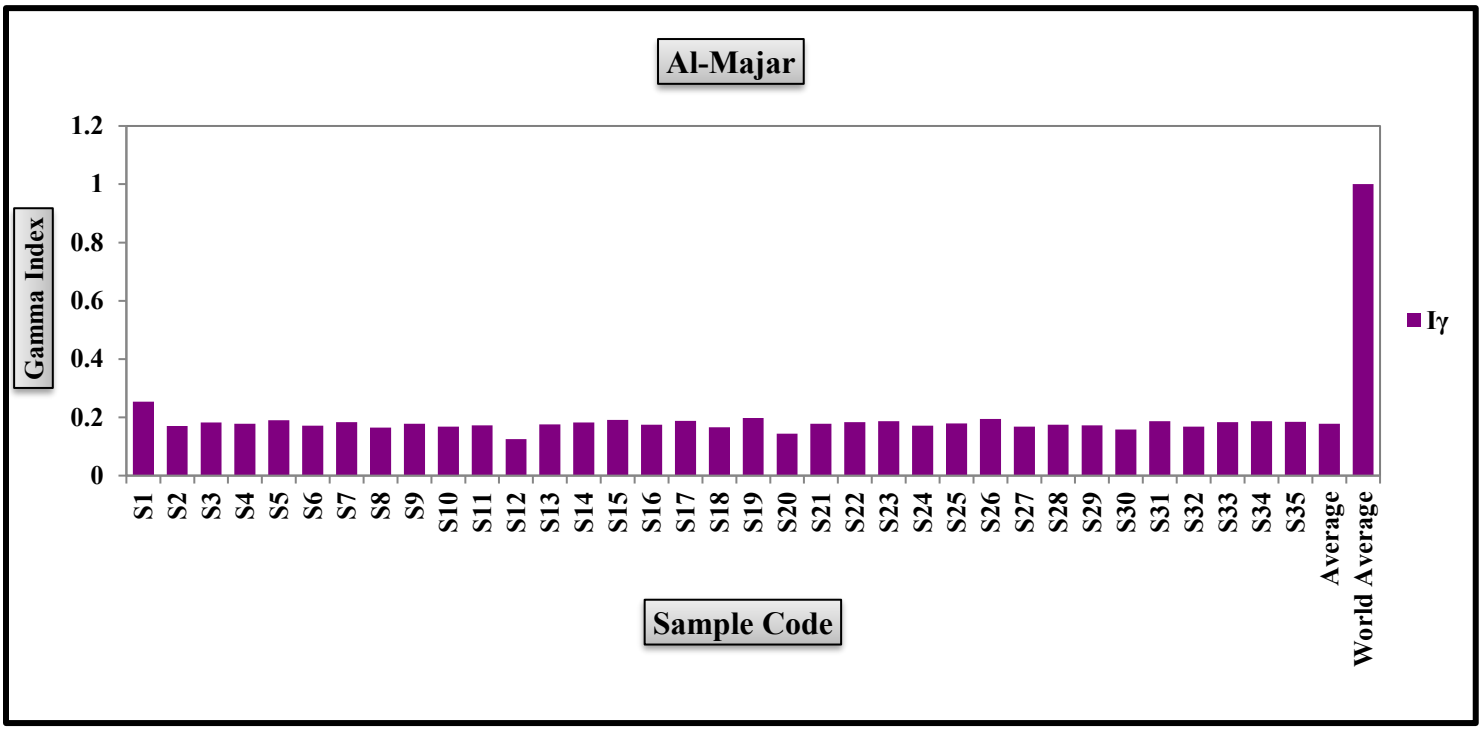

Figure (4-19): Hazard index levels of gamma radiation (Iγ) in surface soil samples in Al-Majar.

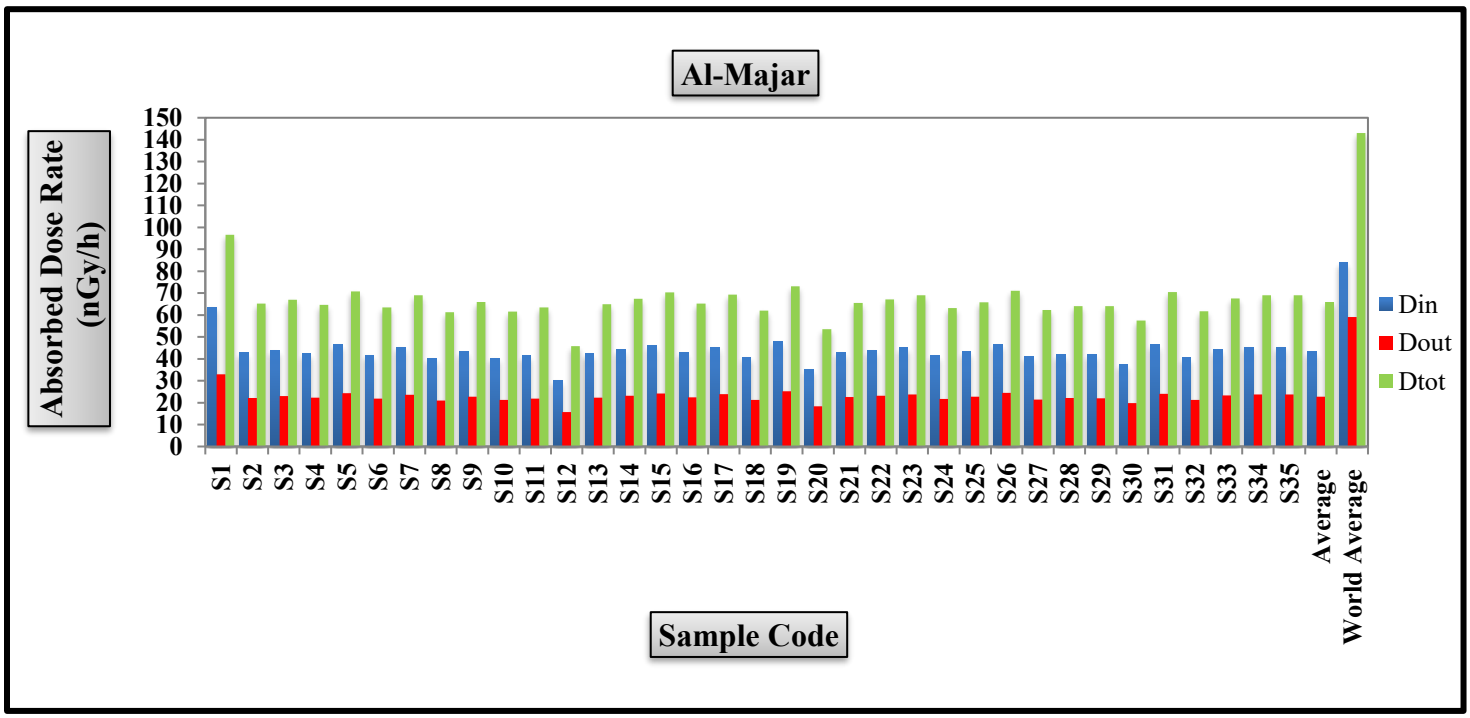

Figure (4-20): Absorbed dose rate (D) in surface soil samples in Al-Majar.

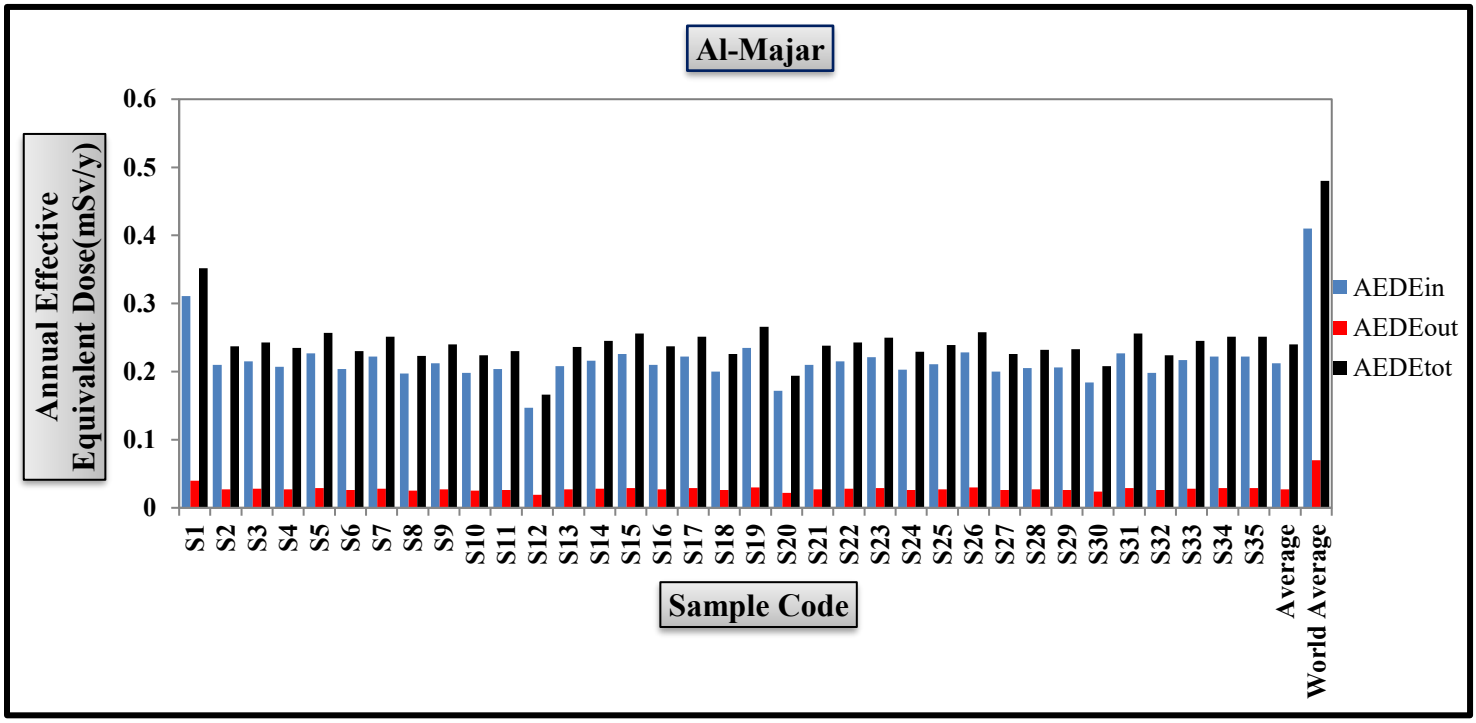

Figure (4-21): Annual effective dose equivalent (AEDE) in surface soil samples in Al-Majar.

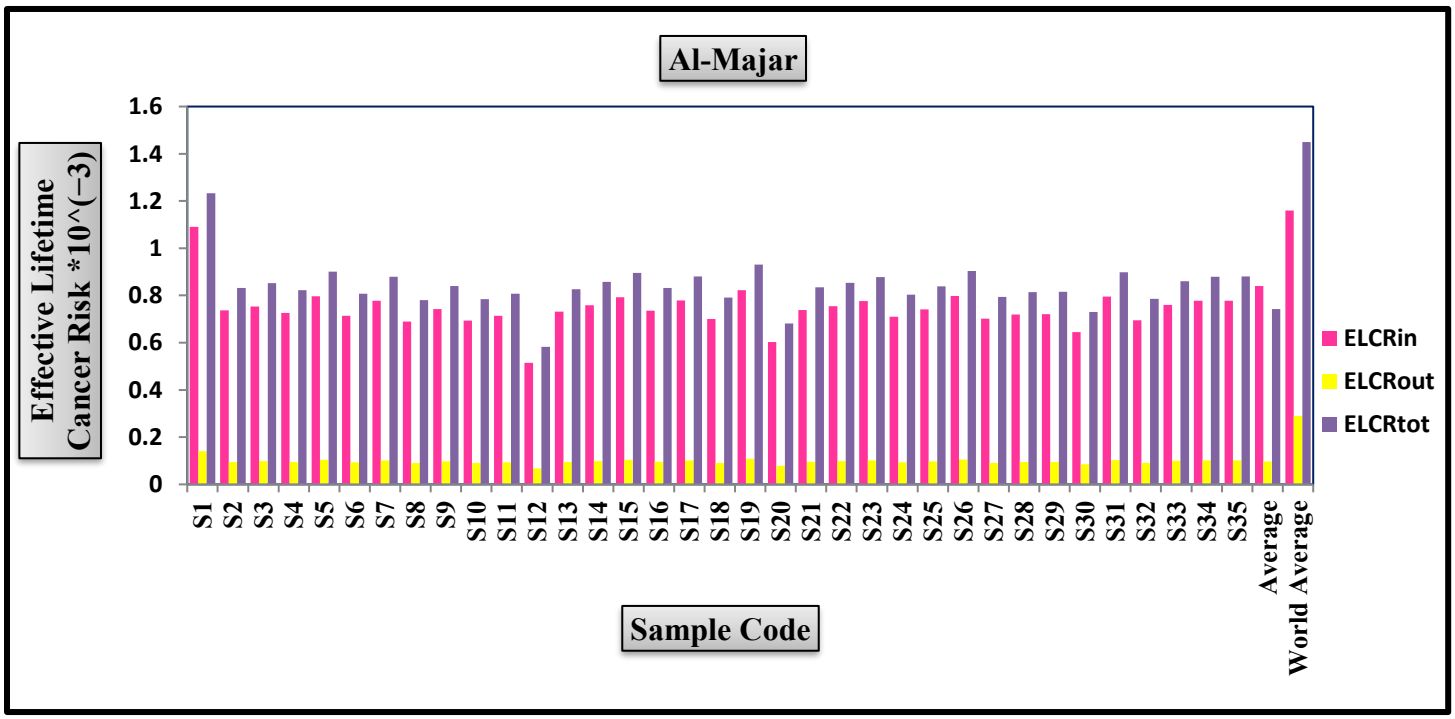

Figure (4-22): Effective lifetime cancer risk levels (ELCR) in surface soil samples in Al-Majar.

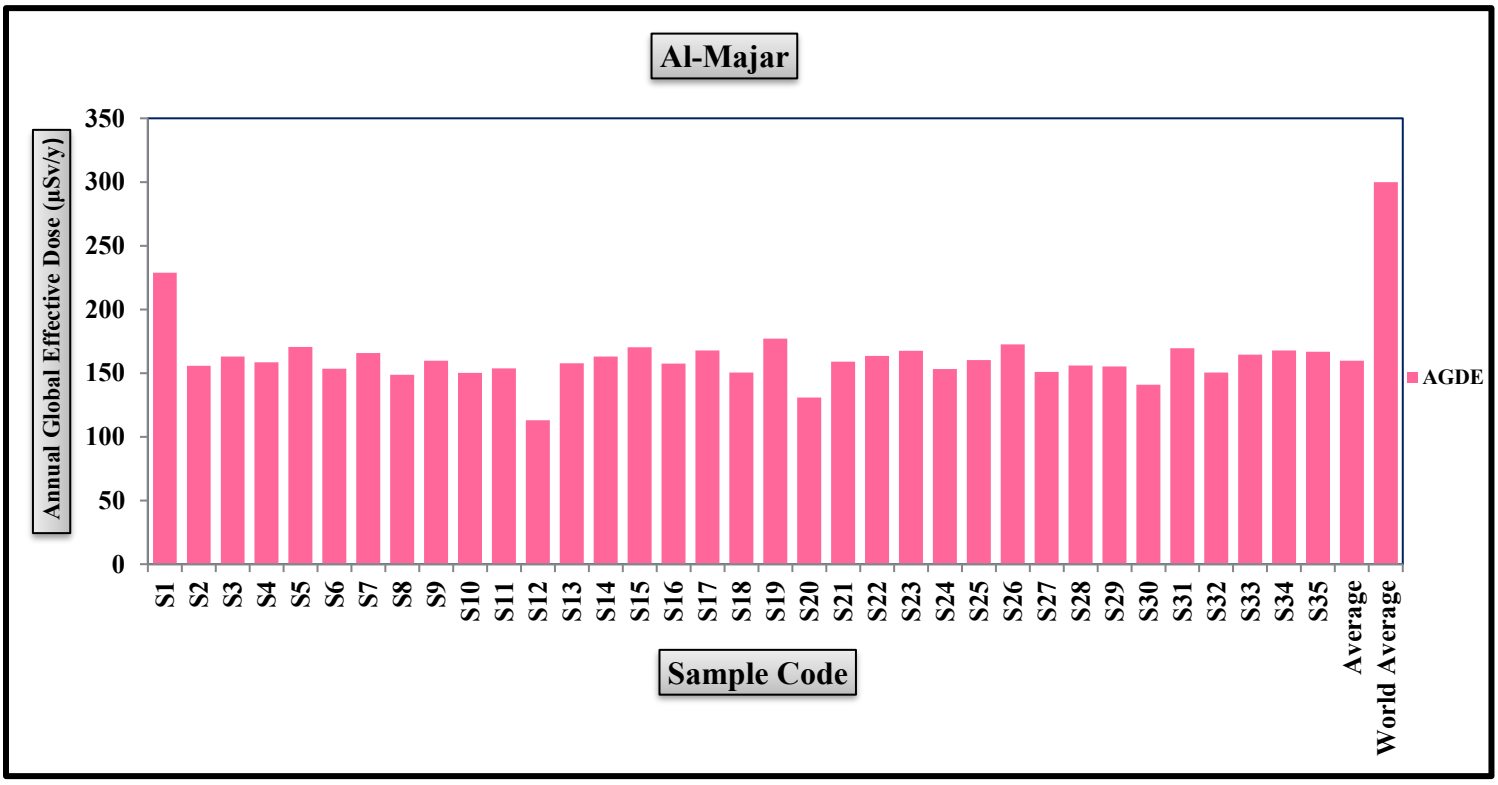

Figure (4-23): Annual global effective dose (AGED) in surface soil samples in Al-Majar.

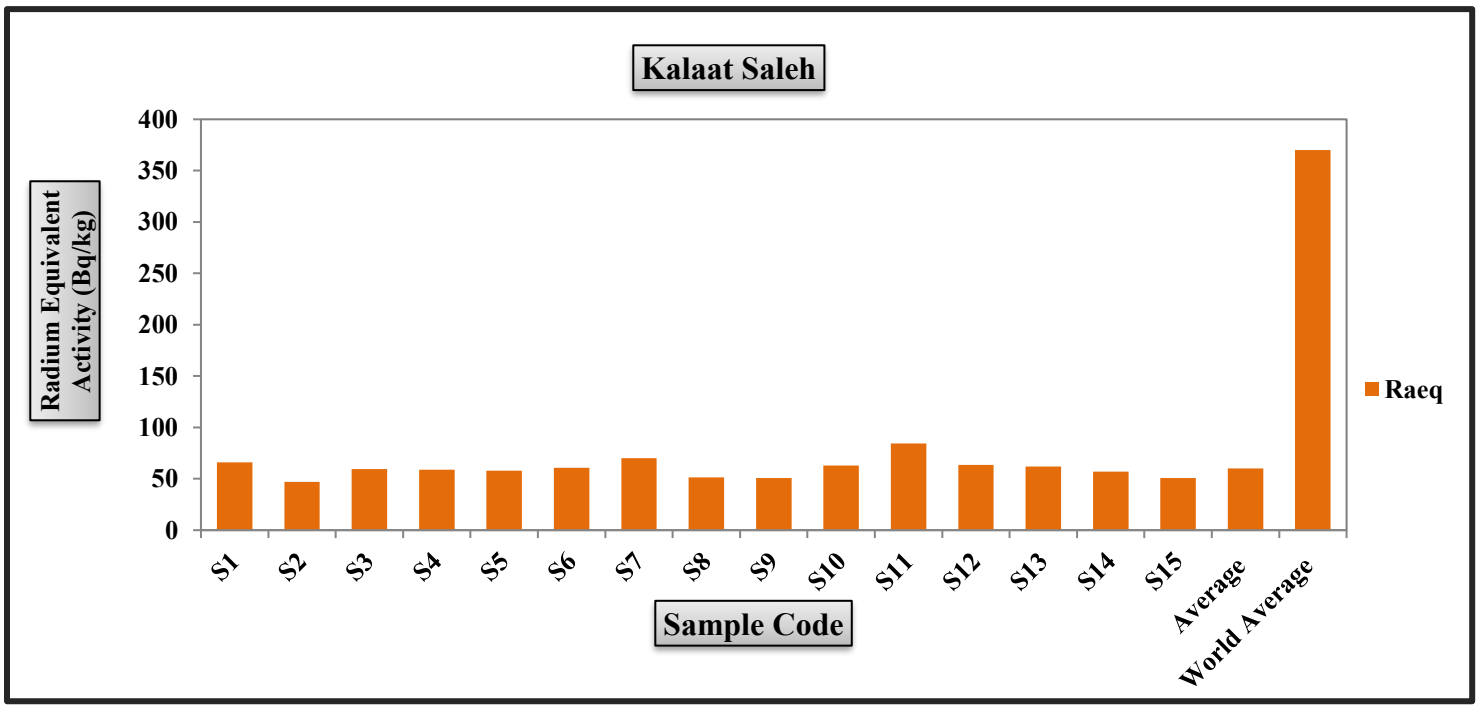

Figure (4-24): Radium equivalent activity levels (Ra_{eq}) in surface soil samples in Kalaat Saleh.

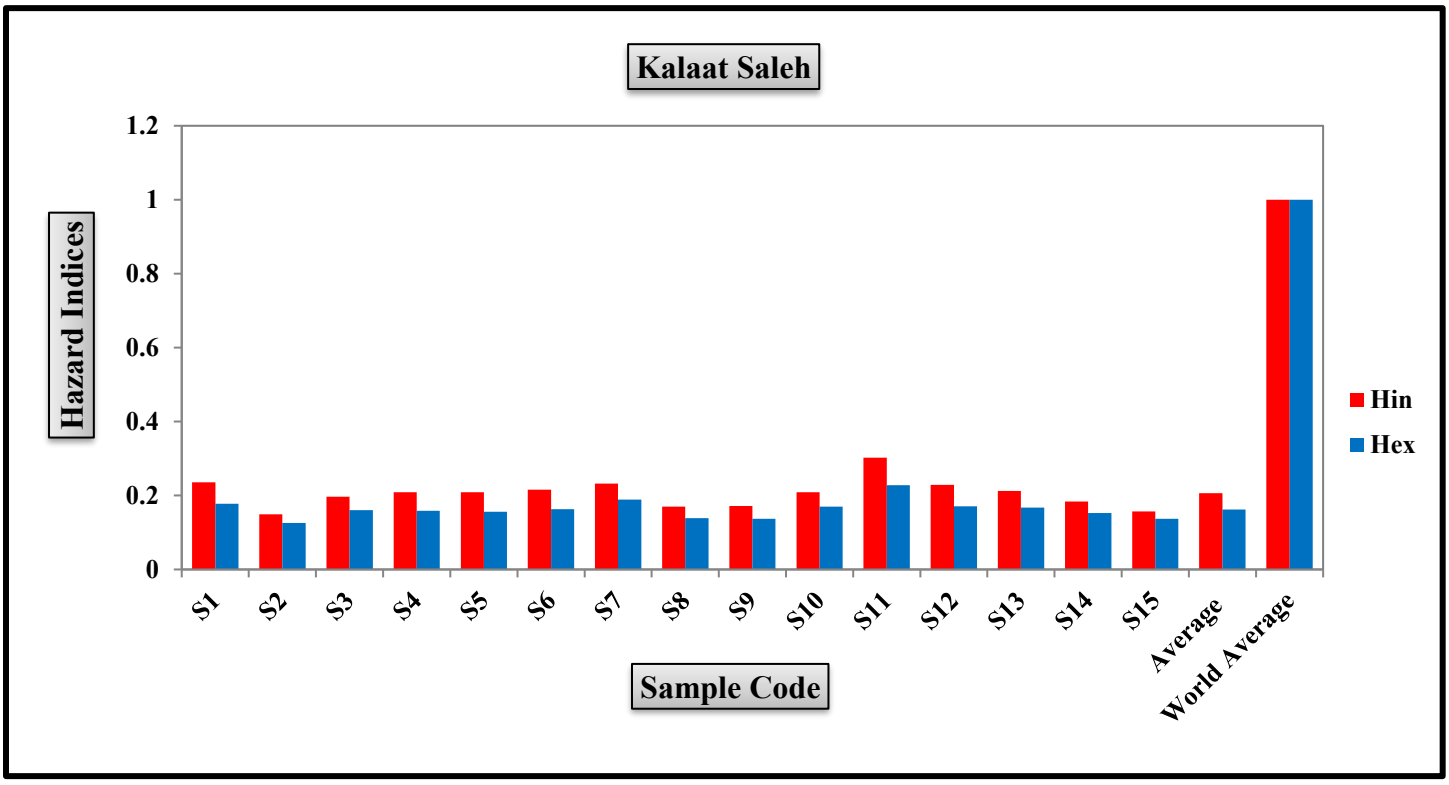

Figure (4-25): Internal (H_{in})and external (H_{ex}) hazard index levelsin surface soil samples in Kalaat Saleh.

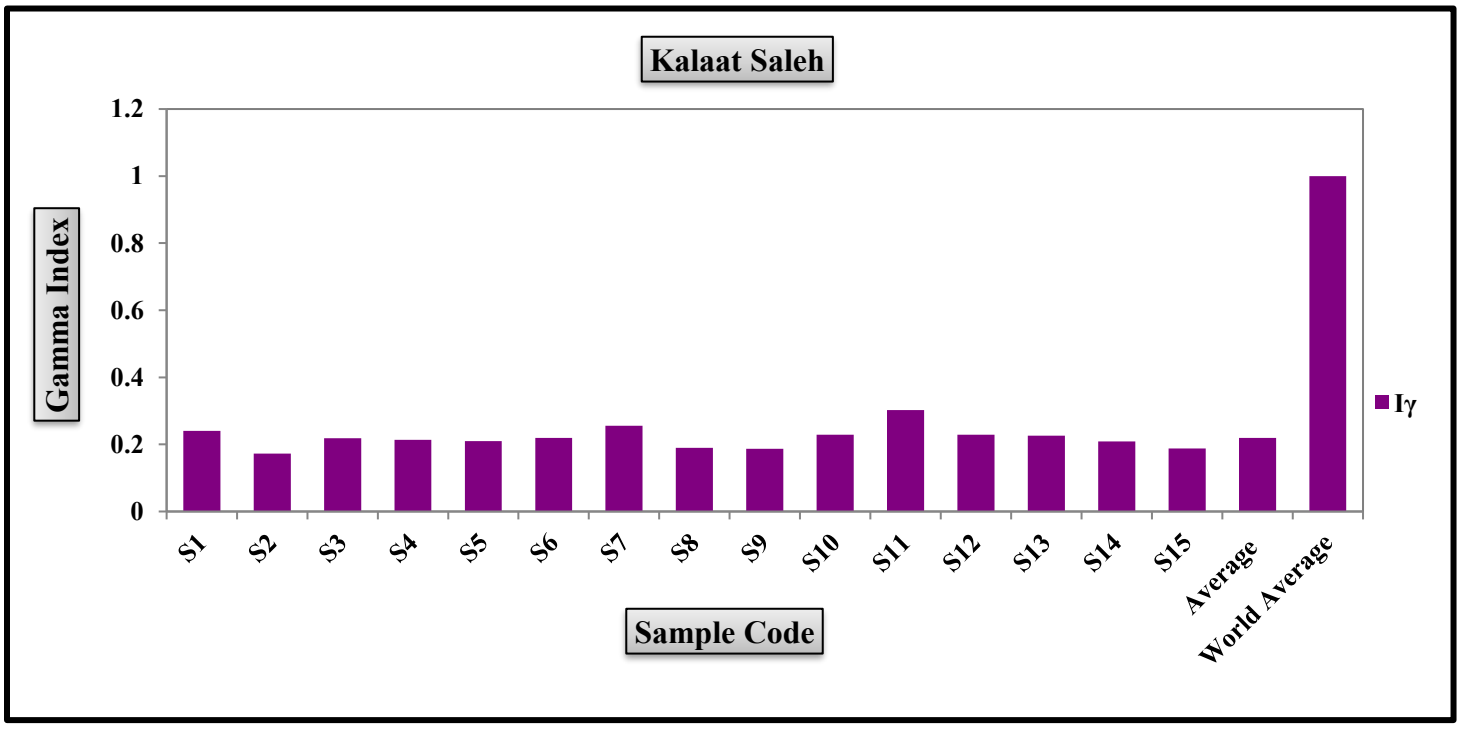

Figure (4-26): Hazard index levels of gamma radiation (Iγ) in surface soil samples in Kalaat Saleh.

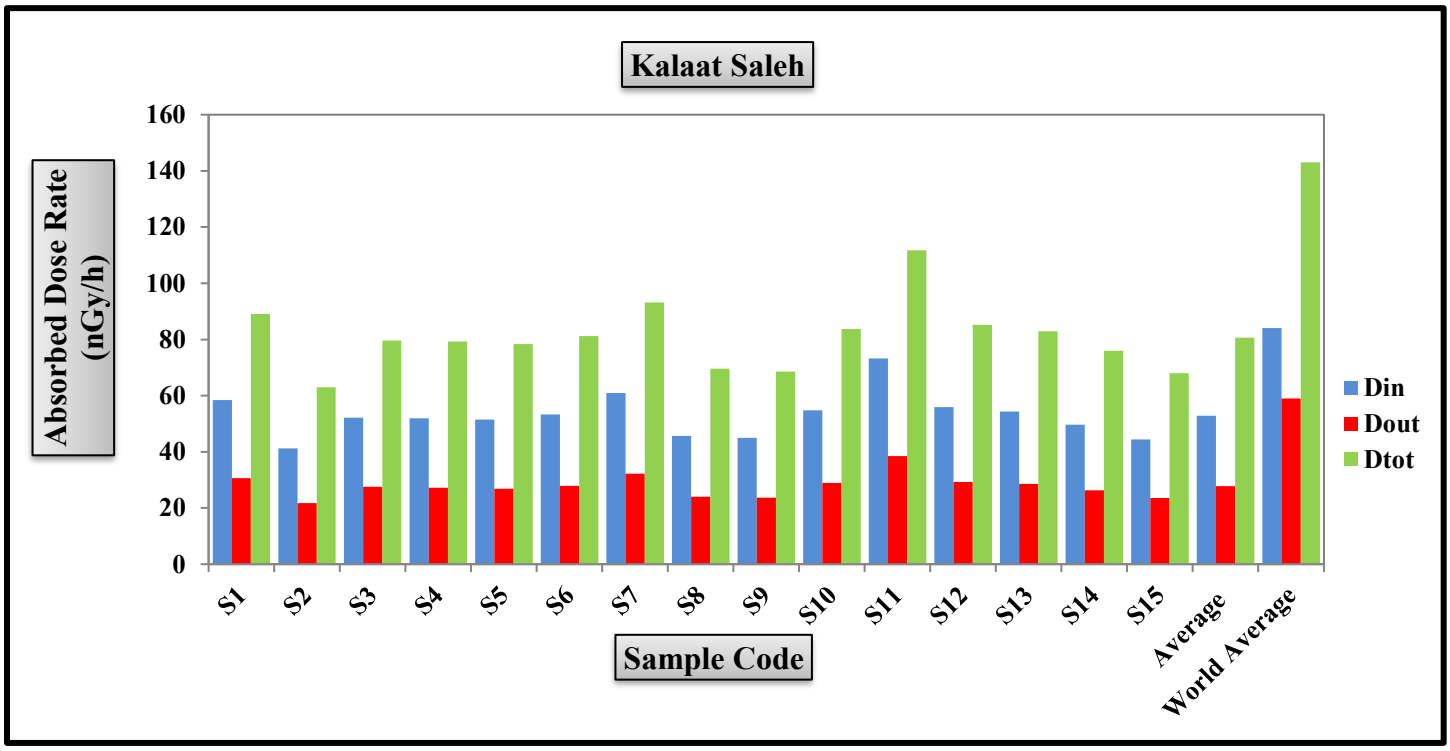

Figure (4-27): Absorbed dose rate (D) in surface soil samples in Kalaat Saleh.

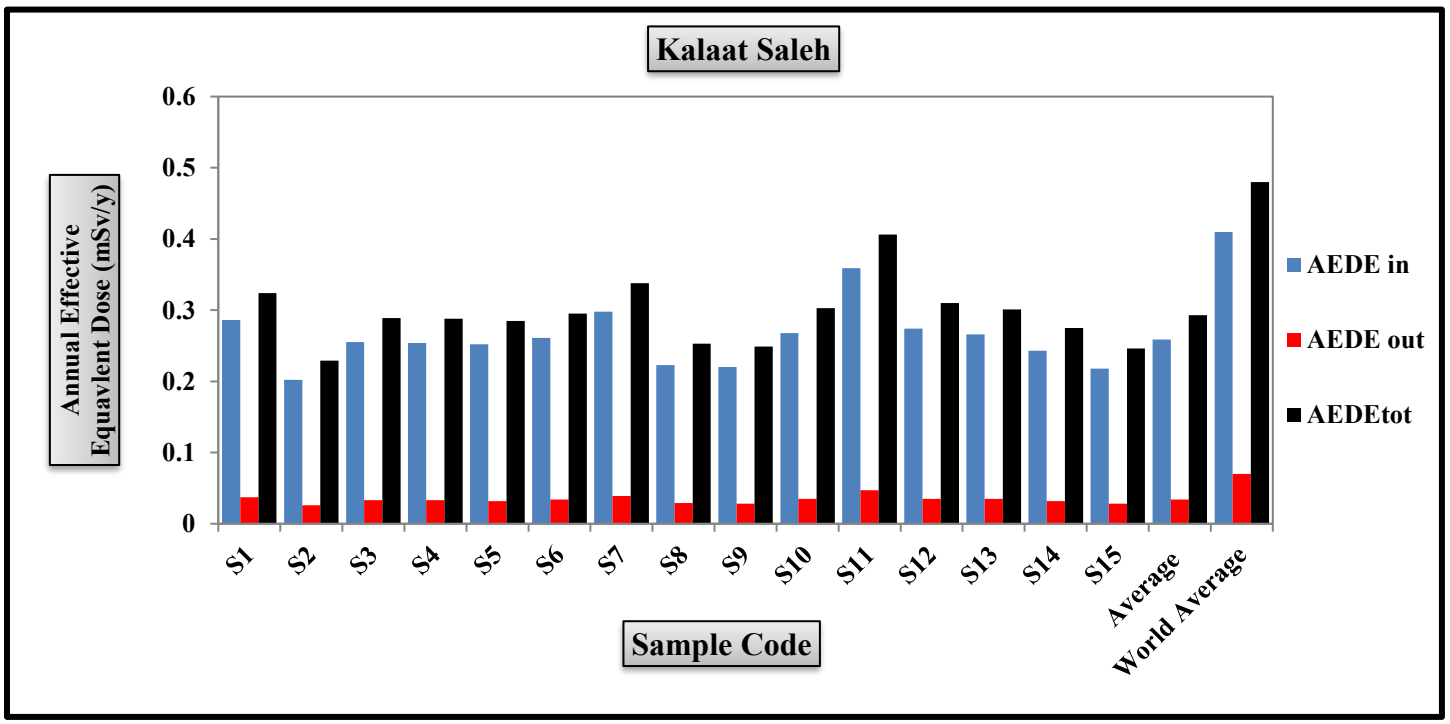

Figure (4-28): Annual effective dose equivalent (AEDE) in surface soil samples in Kalaat Saleh.

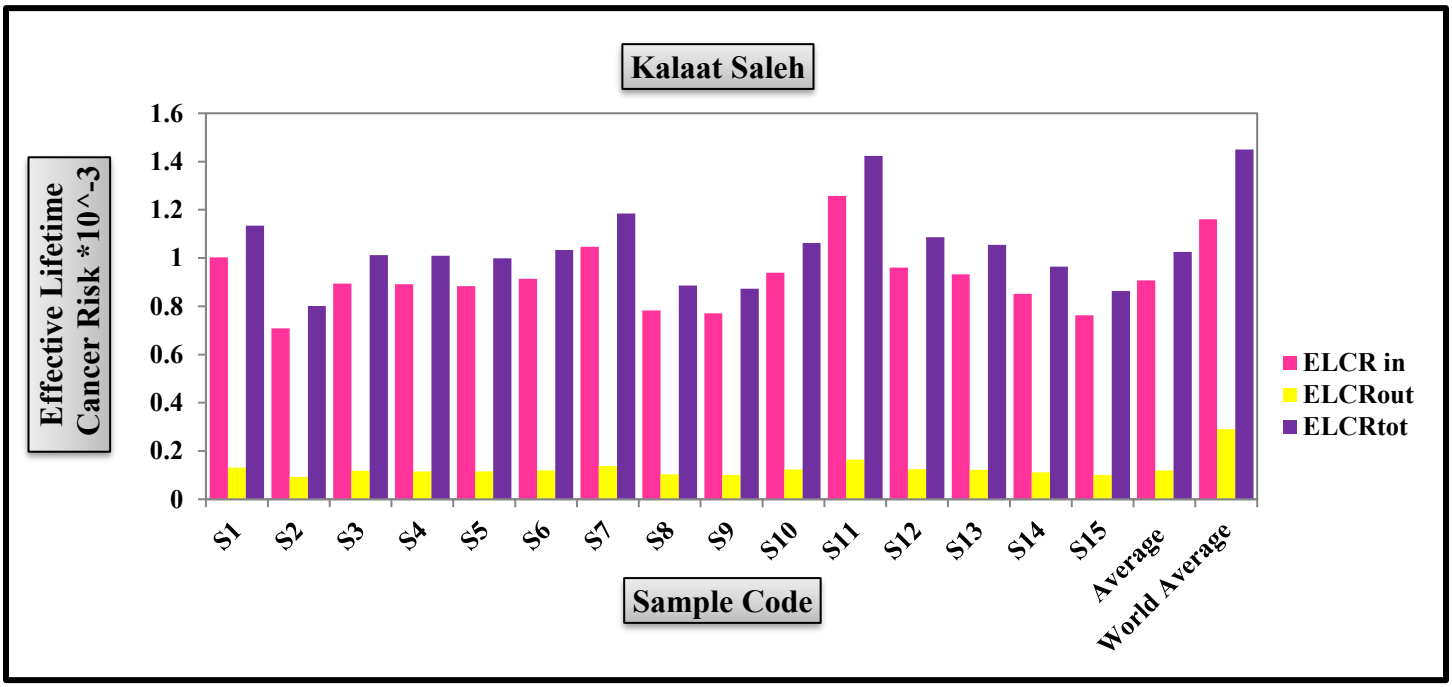

Figure (4-29): Effective lifetime cancer risk levels (ELCR) in surface soil samples in Kalaat Saleh.

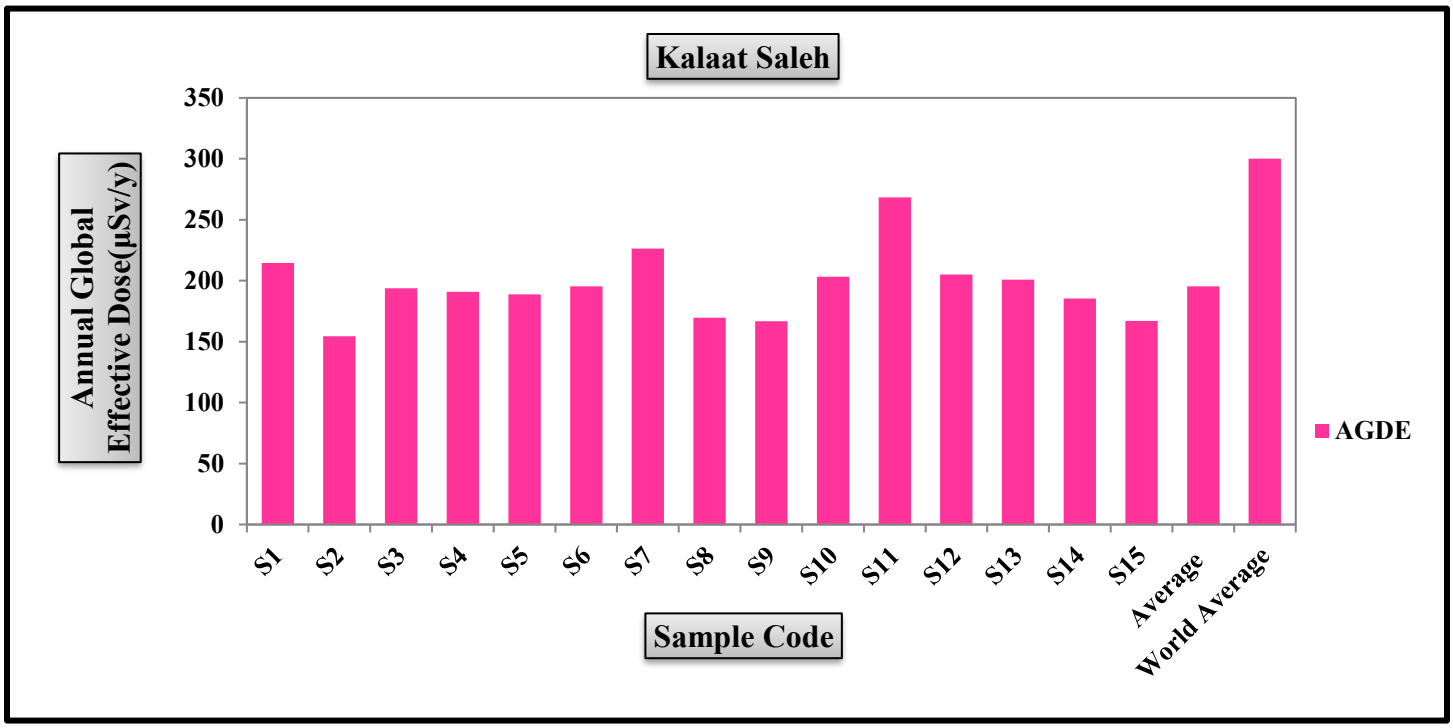

Figure (4-30): Annual global effective dose (AGED)in surface soil samples in Kalaat Saleh.

4.1.4. Comparison of Radiological Hazard Indices of the Soil of the Current Study with Identical Research

The average radiological risk indices obtained from the soils of the research areas were compared with those obtained from other regions in the world and Iraq, as shown in Table (4-6).

The mean values for Ra_{eq}, H_{in}, H_{ex}, I_{γ}, D_{in}, D_{out}, $AEDE_{in}$, $AEDE_{out}$, $ELCR_{in}$, $ELCR_{out}$, and AGDE in the present study are generally lower compared to these studies.

Table (4-6): Radiological Hazard Indices in the Investigated Soil Samples Compared to Literature Values.

Country	Radiological Hazard Indices											Reference
	Ra_{eq} (Bq/kg)	H_{in}	H_{ex}	Iγ	D_{in} (nGy/h)	D_{out} (nGy/h)	$AEDE_{in}$ (mSv/y)	$AEDE_{out}$ (mSv/y)	$ELCR_{in}$ ($\times10^{-3}$)	$ELCR_{out}$ ($\times10^{-3}$)	AGDE (μSv/y)	
Sicily, Italy	72	-	-	-	-	34	0.32	0.04	-	-	-	[126]
Mounana, Gabon	2928.75	15.51	7.92	-	-	1352.76	9.30	1.66	-	-	-	[127]
Uttara Kannada, India	140.74	0.48	0.38	0.51	-	64.84	0.32	0.08	-	1.59	478.8	[128]
Punjab, Pakistan	179.26	0.642	0.482	-	-	85.045	0.417	0.105	-	-	-	[129]
Taghdoua, Saudi Arabia	-	-	-	-	70	37	0.3	0.1	1.3	0.2	-	[43]
Bolu, Turkey	62.8	-	0.2	0.2	-	29.9	-	36.6	-	1.3	209.7	[130]
Ma'an, Jordan	94.21	0.41	0.25	-	-	37.15	-	0.045	-	-	-	[131]
Tulkarem, Palestine	72	0.3	0.21	0.55	-	35.5	-	0.044	-	-	-	[132]
Pshdar, Iraq	69.83	0.227	0.200	-	-	33.26	-	0.040	-	-	-	[133]
Kirkuk, Iraq	81.182	0.286	0.210	0.603	-	38.618	0.189	0.048	-	-	-	[59]
Al-Sadr, Iraq	61.434	0.208	0.166	-	57.974	29.535	0.285	0.037	0.997	0.128	-	[134]
Al Dayr, Iraq	-	-	-	-	91.72	46.16	0.45	0.06	1.48	0.19	-	[135]
World Average (UNSCEAR)	370	≤1	≤1	≤1	84	59	0.41	0.07	1.16	0.29	300	[109]
Al Majar	**48.488**	**0.168**	**0.130**	**0.178**	**43.260**	**22.658**	**0.212**	**0.0277**	**0.742**	**0.097**	**159.795**	**Present study**
kalaat Saleh	**60.209**	**0.206**	**0.162**	**0.219**	**52.826**	**27.791**	**0.259**	**0.0340**	**0.907**	**0.119**	**195.381**	

Conclusions and Recommendations

Chapter Five

Conclusions and Recommendations

5.1. Conclusions

1. The study revealed that the mean activity levels in the soils of Al-Majar and Kalaat Saleh were below the recommended standards.
2. And from the activity concentrations values, radiological hazard indices were calculated. It was found that the mean values of these indices in the soils were below the international average.
3. The results obtained in this research indicate that the soils of Al-Majar and Kalaat Saleh are considered radiologically safe with no associated health risk to the area's inhabitants.
4. The activity concentration levels of the natural radionuclides (Ra-226, Th-232, and K-40) and the anthropogenic radionuclide (Cs-137) were compared in Al-Majar and Kalaat Saleh cities. The results showed that the activity concentrations of these radionuclides in Kalaat Saleh were higher than in Al-Majar. This difference is mainly attributed to variations in geological characteristics and agricultural practices, particularly the extensive use of fertilizers in Kalaat Saleh.
5. This data may be crucial in developing a radioactivity map of the area for

5.2. Recommendations

1. It is necessary to do more studies and continually to all environment elements (air, water, soil and plant) in the others areas in Misan province, Iraq.
2. It is necessary to use other techniques in addition to gamma spectroscopy like neutron activation analysis technique or x-ray fluorescence technique (XRF) to measure the environmental radioactivity.
3. It is necessary to use detectors of beta particles to measure radionuclides, which emit beta particles.
4. Measurement of the environmental radioactivity in agricultural soils, marshlands, and oil field soils in Misan province.
5. The use of the theoretical programs to investigate the level of environmental radioactivity and concentrations of radionuclides before and after pollution operation.
6. Strongly recommended, periodic monitoring and dose estimation for these important regions in order to assess the risk on the public health arising from the radiation hazards.
7. Promote environmental awareness within the community through media campaigns and the integration of environmental issues into educational curricula.

References

References

1. L'Annunziata, M.F., *Introduction: radioactivity and our well-being.* Radioactivity, 2007: p. 1-45.
2. L'Annunziata, M.F., *Handbook of radioactivity analysis*. 2012: Academic press.
3. Ahmed, S.N., *Physics and engineering of radiation detection*. 2007: Academic Press.
4. Ji, Z., D. Pons, and J. Pearse, *Measuring industrial health using a diminished quality of life instrument.* Safety, 2018. **4**(4): p. 55.
5. Dołhańczuk-Śródka, A., *Estimation of external gamma radiation dose in the area of Bory Stobrawskie forests (PL).* Environmental monitoring and assessment, 2012. **184**: p. 5773-5779.
6. Celik, N., et al., *Natural and artificial radioactivity measurements in Eastern Black Sea region of Turkey.* Journal of hazardous materials, 2009. **162**(1): p. 146-153.
7. Poluianov, S., et al., *Production of cosmogenic isotopes 7Be, 10Be, 14C, 22Na, and 36Cl in the atmosphere: Altitudinal profiles of yield functions.* Journal of Geophysical Research: Atmospheres, 2016. **121**(13): p. 8125-8136.
8. Ramasamy, V., et al., *Evaluation of natural radionuclide content in river sediments and excess lifetime cancer risk due to gamma radioactivity.* Research Journal of Environmental and Earth Sciences, 2009. **1**(1): p. 6-10.
9. White, R.E., *Principles and practice of soil science: the soil as a natural resource*. 2005: John Wiley & Sons.
10. Taskin, H., et al., *Radionuclide concentrations in soil and lifetime cancer risk due to gamma radioactivity in Kirklareli, Turkey.* Journal of environmental radioactivity, 2009. **100**(1): p. 49-53.
11. Whitfield, J.M., J. Rogers, and J. Adams, *The relationship between the petrology and the thorium and uranium contents of some granitic rocks.* Geochimica et Cosmochimica Acta, 1959. **17**(3-4): p. 248-271.
12. Rogers, J.J. and P.C. Ragland, *Variation of thorium and uranium in selected granitic rocks.* Geochimica et Cosmochimica Acta, 1961. **25**(2): p. 99-109.
13. Sparks, D.L., *1.4 bioavailability of soil potassium.* Handbook Of Soil. CRC Press, New York, 2000.
14. Eisenbud, D., *Linear sections of determinantal varieties.* American Journal of Mathematics, 1988. **110**(3): p. 541-575.
15. Richard, P., N. Shimizu, and C. Allegre, *143Nd/146Nd, a natural tracer: an application to oceanic basalts.* Earth and Planetary Science Letters, 1976. **31**(2): p. 269-278.

16. Bunzl, K., et al., *Migration of fallout 239+ 240Pu, 241Am and 137Cs in the various horizons of a forest soil under pine.* Journal of Environmental Radioactivity, 1995. **28**(1): p. 17-34.
17. Liu, H.Q. and A. Huete, *A feedback based modification of the NDVI to minimize canopy background and atmospheric noise.* IEEE transactions on geoscience and remote sensing, 1995. **33**(2): p. 457-465.
18. El-Shershaby, A., et al., *Assessment of natural and man-made radioactivity levels of the plant leaves samples as bio-indicators of pollution in Hebron District.* Arab J Nucl Sci Appl, 2006. **39**(2): p. 231-242.
19. Ridha, A.A. and T. IMAN, *Determination of radionuclides concentrations in construction materials used in Iraq.* Unpublished Ph. D Thesis, Republic of Iraq Ministry of Higher Education and Scientific Research University of Al-Mustansiriyah College of Science, 2013.
20. Severa, J. and J. Bár, *Handbook of radioactive contamination and decontamination*. Vol. 47. 1991: Newnes.
21. Al-Ubaidi, A., *Environmental Radioactivity of Al-Rashidiyah Site–Baghdad*. 2015, Ph. D. Thesis, University of Baghdad, College of Science for Women.
22. Akhtar, N., et al., *Estimation of radiation exposure associated with the saline soil of Lahore, Pakistan.* J. Res. Sci, 2004. **15**: p. 59-65.
23. Organization, W.H.O, *International basic safety standards for protection against ionizing radiation and for the safety of radiation sources.* 1997.
24. Martin, D. and W. Jacobi, *Diffusion deposition of small-sized particles in the bronchial tree.* Health Physics, 1972. **23**(1): p. 23-29.
25. Desouky, O., N. Ding, and G. Zhou, *Targeted and non-targeted effects of ionizing radiation.* Journal of Radiation Research and Applied Sciences, 2015. **8**(2): p. 247-254.
26. Donnelly, E.H., et al., *Acute radiation syndrome: assessment and management.* Southern medical journal, 2010. **103**(6): p. 541.
27. Belyaeva, O., et al., *Natural radioactivity in urban soils of mining centers in Armenia: dose rate and risk assessment.* Chemosphere, 2019. **225**: p. 859-870.
28. Zakariya, N.I. and M. Kahn, *Benefits and biological effects of ionizing radiation.* Sch. Acad. J. Biosci, 2014. **2**(9): p. 583-591.
29. Selvasekarapandian, S., et al., *Natural radionuclide distribution in soils of Gudalore, India.* Applied radiation and isotopes, 2000. **52**(2): p. 299-306.
30. Chikasawa, K., T. Ishii, and H. Sugiyama, *Terrestrial gamma radiation in Kochi prefecture, Japan.* Journal of Health Science, 2001. **47**(4): p. 362-372.
31. Kannan, V., et al., *Distribution of natural and anthropogenic radionuclides in soil and beach sand samples of Kalpakkam (India) using hyper pure germanium (HPGe) gamma ray spectrometry.* Applied Radiation and isotopes, 2002. **57**(1): p. 109-119.

32. Hannan, M. and G. Hanson. *Measurement of active concentrations of radio nuclides (238U, 235U, 226Ra, 40K, and 137Cs) in Mission (Texas) soils using the high purity germanium gamma-ray spectrometry*. in *Pacific Basin Nuclear Conference (15th: 2006: Sydney, Australia)*. 2006. Australian Nuclear Association Sydney, NSW.
33. Yordanova, I., D. Staneva, and T. Bineva, *Natural and artificial radioactivity in Bulgarian soils along the Danube river.* Journal of Central European Agriculture, 2005.
34. Santos Júnior, J.A.d., et al., *Analysis of the 40K levels in soil using gamma spectrometry.* Brazilian Archives of Biology and technology, 2005. **48**: p. 221-228.
35. Adrovic, F., et al., *Survey of natural and artificial radionuclide contents in soil samples from some areas of the AP Kosovo (Serbia).* 2010.
36. Alias, M., et al., *An assessment of absorbed dose and radiation hazard index from natural radioactivity.* Malaysian Journal of Analytical Sciences, 2008. **12**(1): p. 195-204.
37. Mehra, R., S. Singh, and K. Singh, *Analysis of 226 Ra, 232 Th and 40 K in soil samples for the assessment of the average effective dose.* Indian Journal of Physics, 2009. **83**: p. 1031-1037.
38. Śleziak, M., L. Petryka, and M. Zych, *Natural radioactivity of soil and sediment samples collected from postindustrial area.* Polish J. of Envir. Studies, 2010. **19**(5): p. 1095-99.
39. Sahoo, S.K., et al., *Thorium, uranium and rare earth elements concentration in weathered Japanese soil samples.* Progress in Nuclear Science and Technology, 2011. **1**: p. 416-419.
40. Ramola, R., et al., *Radionuclide analysis in the soil of Kumaun Himalaya, India, using gamma ray spectrometry.* Current Science, 2011: p. 906-914.
41. Pallavicini, N., *Activity concentration and transfer factors of natural and artificial radionuclides in the Swedish counties of Uppsala and Jämtland.* 2011.
42. Ferdous, J., et al., *Radioactivity distributions in soils from Habiganj District, Bangladesh and their radiological implications.* 2015.
43. Dizman, S., et al., *The assessment of radioactivity and radiological hazards in soils of Bolu province, Turkey.* Environmental forensics, 2019. **20**(3): p. 211-218.
44. Jananee, B., et al., *Natural radioactivity in soils of Elephant hills, Tamilnadu, India.* Journal of Radioanalytical and Nuclear Chemistry, 2021. **329**: p. 1261-1268.
45. Kebede, B.Z. and T. Gebeyehu, *Evaluation of Natural Radioactive Elements and Hazardous Indexes Using High Pure Germanium Gamma Ray Spectroscopy in Sekota, Waghimra, Zone, Ethiopia.* American Journal of Physics and Applications, 2021. **9**(2): p. 48-52.

46. Özden, S. and S.l.A. Pehlivanoğlu, *Natural and Artificial Radioactivity Concentrations and Health Risks due to Radionuclides in the Soil of Nevşehir (Cappadocia).* International Journal on Applied Physics and Engineering, 2023. **2**: p. 144-151.
47. Mahjoubi, H., et al., *Survey of natural and artificial radioactivity in Tunisian soils.* International Journal of Low Radiation, 2006. **2**(1-2): p. 60-70.
48. Moafy, W. and M. El-Tahawy, *Radiological Study Investigation of the Black Sand Region of the North-East of the Nile Delta.* 2009.
49. Saleh, I.H., *Radioactivity of 238U, 232Th, 40K, and 137Cs and assessment of depleted uranium in soil of the Musandam Peninsula, Sultanate of Oman.* Turkish J. Eng. Env. Sci, 2012. **36**(3): p. 236-248.
50. Attia, T., E. Shendi, and M. Shehata, *Assessment of natural and artificial radioactivity levels and radiation hazards and their relation to heavy metals in the industrial area of Port Said city, Egypt.* Environmental Science and Pollution Research, 2015. **22**: p. 3082-3097.
51. Al-Harmali, A. *Evaluation of natural radioactivity in selected soil samples collected from northern regions of Oman*. in *IOP Conference Series: Materials Science and Engineering*. 2020. IOP Publishing.
52. Al-Azri, H., et al. *Measuring of natural and artificial radioactivity in Al-Dakhiliya governorate, Sultanate of Oman*. in *IOP Conference Series: Earth and Environmental Science*. 2022. IOP Publishing.
53. Alfull, Z.Z., et al., *Review Study of Natural Radioactivity in the Soil of the Kingdom of Saudi Arabia.* 2023.
54. Maglas, N., et al., *Measurement of Natural Radioactive Activity and Estimation of Radiation Doses in Surface Soil Samples in the Phosphate-Rich Area of Al-Ruseifa Hpge.* Available at SSRN 4789165.
55. Bashar, A.J., et al., *Determination of the Specific Activity for the natural radioactive isotopes (40K, 212Pb, 214Pb, 214Bi, 228Ac) in soils and sediments for selected areas of the marshes southern Iraq, Basra province and the northern Arabian Gulf.* Marsh Bulletin, 2016. **11**(1): p. 1-10.
56. Najam, L.A., et al., *Measurement of radioactivity in soil samples for selected regions in Thi-Qar Governorate-Iraq.* Journal of Radiation and Nuclear Applications, 2016. **1**(1): p. 25-30.
57. AL-Sudani, Z., *Natural and Artificial radionuclide concentrations for different environmental samples in AL-Amara city, Missan governorate*. 2016, Ph. D. Thesis, College of Science for Women, Baghdad University.
58. Pourimani, R. and S.M.M. Shahroodi, *Radiological assessment of the artificial and natural radionuclide concentrations of wheat and barley samples in Karbala, Iraq.* Iranian Journal of Medical Physics, 2018. **15**(2): p. 126-31.

59. Taqi, A., A. Shaker, and A. Battawy, *Natural radioactivity assessment in soil samples from Kirkuk city of Iraq using HPGe detector.* International Journal of Radiation Research, 2018. **16**(4): p. 455-463.
60. Al-Wasity, A., *A Study of concentration measurement of alpha and gamma-emitting radionuclides in the soil of Wasit governorate*. 2010, M. Sc. Thesis, University of Baghdad, Iraq.
61. Smail, J.M., S.T. Ahmad, and H.H. Mansour, *Estimation of the natural radioactivity levels in the soil along the Little Zab River, Kurdistan Region in Iraq.* Journal of Radioanalytical and Nuclear Chemistry, 2022. **331**(1): p. 119-128.
62. Hussian, H.A. and K.K. Ali, *Natural and Artificial Radionuclides Distribution in Surface Soil in Baghdad International Airport Region.* The Iraqi Geological Journal, 2024: p. 214-228.
63. AL-Sudani, Z., S. Sherif, and M. Mohammed, *Natural radioactivity and radiation risks of soils in Ali Al-Sharqi and Kumait, Iraq.* Asian Journal of Water Environment and Pollution, 2025. **22**(2): p. 125.
64. AL-Sudani, Z.A.I., *Radioactive Levels and Radiological Hazards in Ali Al-Gharbi City Soil.* The International Journal of Radiation Research, 2025. **23**(3): p. 690-683.
65. Izewska, J., G. Rajan, and E. Podgorsak, *Radiation Oncology Physics: A Handbook for Teachers and Stu dents.* Ed. EB Podgorsak, IAEA, Vienna, 2005: p. 71-99.
66. Borrelli, R.A., *A characterization of radioactivity in the environment*. 1999, Worcester Polytechnic Institute.
67. Michael, F. and E. Annuziata, *Radioactivity: Introduction and History.* Elsevier, 2007.
68. Aubrecht, G., *A teachers guide to the nuclear science wall chart.* Contemporary Physics Education Project, 2003: p. 1-4.
69. Hughes, E.A. and A. Zalts, *Radioactivity in the Classroom.* Journal of Chemical Education, 2000. **77**(5): p. 613.
70. Jevremovic, T., *Nuclear principles in engineering*. 2005: Springer.
71. Poschl, M. and L.M. Nollet, *Radionuclide concentrations in food and the environment*. 2006: CRC Press.
72. ElBaradei, M., *Statement to the Forty-eighth Regular Session of the IAEA General Conference 2004. 20 September 2004, Vienna, Austria*. 2004, International Atomic Energy Agency, Vienna (Austria).
73. Annex, D. and U.N.S.C.o.t.E.o.A. Radiation, *Sources and effects of ionizing radiation.* Investigation of I, 2000. **125**.
74. United Nation Scientific Committee on the *Effects of atomic radiation.* UNSCEAR. Scientific Annexes E, 2008: p. 203-204.

75. Basdevant, J.-L., J. Rich, and M. Spiro, *Fundamentals in nuclear physics: From nuclear structure to cosmology*. 2005: Springer Science & Business Media.
76. Khudir, R. and A.H. Al-Mashhadani, *Estimation of the Annual Absorbed Dose of Protons Produced from 12C (Alpha, P) 15N Reaction.* Library of Progress-Library Science, Information Technology & Computer, 2024. **44**.
77. Ehsanpour, E., et al., *226 Ra, 232 Th and 40 K contents in water samples in part of central deserts in Iran and their potential radiological risk to human population.* Journal of Environmental Health Science and Engineering, 2014. **12**: p. 1-7.
78. Anekwe, U. and S. Ibe, *Estimation of radiation risk due to exposure to terrestrial radiation.* Archives of Current Research International, 2017. **9**(4): p. 1-10.
79. Semat, H., *Introduction to atomic and nuclear physics*. 2012: Springer Science & Business Media.
80. Abojassim, A.A., R.J. Dosh, and A.K. Abdulzahar, *Radioactivity in Soil.* Current Research in Soil Science, 2022. **89**: p. 150-166.
81. Benenson, W., *Hand book of physics. Spriger–Velarg, New York*. 2002, INC.
82. Harb, S.R.M., *On the human radiation exposure as derived from the analysis of natural and man-made radionuclides in soils.* 2004.
83. Kathren, R.L., *NORM sources and their origins.* Applied radiation and isotopes, 1998. **49**.
84. Arctic Monitoring and Assessment Programme (AMAP), *assessment report: Arctic pollution issues*. 1998.
85. Cottingham, W.N. and D.A. Greenwood, *An introduction to nuclear physics*. 2001: Cambridge University Press.
86. Watson, S., et al., *Ionising radiation exposure of the UK population: 2005 review*. 2005: Health Protection Agency Chilton, Oxon.
87. Xhixha, G., *Advanced gamma-ray spectrometry for environmental radioactivity monitoring.* 2012.
88. Gilmore, G., *Practical Gamma-Ray Spectrometry*. 2008, John Wiley & Sons Ltd.
89. Khandaker, M.U., *High purity germanium detector in gamma-ray spectrometry.* International journal of Fundamental physical sciences, 2011. **1**(2): p. 42-46.
90. Tsoulfanidis, N. *Measurement and detection of radiation*. in *Fuel and Energy Abstracts*. 1995.
91. Valkovic, V., *Radioactivity in the environment: physicochemical aspects and applications*. 2000: Elsevier.

92. Upp, D., R. Keyser, and T. Twomey, *New cooling methods for HPGE detectors and associated electronics.* Journal of radioanalytical and nuclear chemistry, 2005. **264**(1): p. 121-126.
93. Broerman, E., et al. *Performance of a new type of electrical cooler for HPGe detector systems*. in *Institute of Nuclear Materials Management Conference, Indian Wells, CA*. 2001.
94. Ehsanpour, E., et al., *226Ra, 232Th and 40K contents in water samples in part of central deserts in Iran and their potential radiological risk to human population.* Journal of Environmental Health Science and Engineering, 2014. **12**(1): p. 80.
95. Beretka, J. and P. Mathew, *Natural radioactivity of Australian building materials, industrial wastes and by-products.* Health physics, 1985. **48**(1): p. 87-95.
96. Valentin, J., *The 2007 recommendations of the international commission on radiological protection*. Vol. 37. 2007: Elsevier Oxford.
97. Trevisi, R., et al., *Radioactivity in building materials: a first overview of the European scenario*. 2008, International Radiation Protection Association (IRPA), Fontenay-aux-Roses ….
98. Asaduzzaman, K., et al., *Natural radioactivity levels and radiological assessment of decorative building materials in Bangladesh.* Indoor and Built Environment, 2016. **25**(3): p. 541-550.
99. Ugbede, F.O., et al., *Baseline radioactivity in the soil of evangel take-off campus, Evangel University, Nigeria, and its associated health risks.* Chemistry Africa, 2021. **4**(3): p. 703-713.
100. Agar, O., et al., *Measurement of radioactivity levels and assessment of radioactivity hazards of soil samples in Karaman, Turkey.* Radiation Protection Dosimetry, 2014. **162**(4): p. 630-637.
101. Begy, R., H. Simon, and C. Cosma, *Radiological assessment of stream sediments between Băiţa-Plai and Beiuş.* Faculty of Environmental Sciences and Engineering, Babeș-Bolyai University, Fântânele Str, 2012. **30**.
102. Adrovic, F., et al., *Survey of natural and artificial radionuclide contents in soil samples from some areas of the AP Kosovo (Serbia)*. 2008, International Radiation Protection Association (IRPA), Fontenay-aux-Roses ….
103. Fajgelj, A., et al., *Intended Use of the IAEA Reference Materials-Part I: Examples on Reference Materials for the Determination of Radionuclides or Trace Elements.* Special Publications of the Royal Society of Chemistry, 1999. **238**: p. 65-80.
104. Martinčič, R., *Generic procedures for monitoring in a nuclear or radiological emergency*. 1999: IAEA.
105. Al-Bayati, A., *Determination of the concentrations for radioactive elements around AL-Tuwaitha center using gamma-ray spectroscopy and CR-39*

detectors. 2017, Ph. D. Thesis, College of Education for Pure Science Ibn Al-Haitham ….
106. May, K., *Calibration of a modified Andersen bacterial aerosol sampler.* Applied microbiology, 1964. **12**(1): p. 37-43.
107. Zhang, Y., et al., *Research on minimum detectable activity (MDA) of underwater gamma spectrometer for radioactivity measurement in the marine environment.* Applied Radiation and Isotopes, 2020. **155**: p. 108917.
108. Knoll, G.F., *Radiation detection and measurement*. 2010: John Wiley & Sons.
109. U.N.S.C.E.A.R, *Sources and Effects of Ionizing Radiation, United Nations Scientific Committee on the Effects of Atomic Radiation (UNSCEAR) 2000 report, volume I: report to the general assembly, with scientific annexes-sources*. 2000: United Nations.
110. Džoljić, J.A., et al., *Natural and artificial radioactivity in some protected areas of south east Europe.* Nuclear technology and radiation protection, 2017. **32**(4): p. 334-341.
111. Boukhenfouf, W. and A. Boucenna, *The radioactivity measurements in soils and fertilizers using gamma spectrometry technique.* Journal of environmental radioactivity, 2011. **102**(4): p. 336-339.
112. Ajayi, O.S.J.R. *Measurement of activity concentrations of 40 K, 226 Ra and 232 Th for assessment of radiation hazards from soils of the southwestern region of Nigeria.* 2009. **48**: p. 323-332.
113. Almayahi, B., et al., *Radiation hazard indices of soil and water samples in Northern Malaysian Peninsula.* 2012. **70**(11): p. 2652-2660.
114. Suresh, S., et al., *Estimation of natural radioactivity and assessment of radiation hazard indices in soil samples of Uttara Kannada district, Karnataka, India.* Journal of Radioanalytical and Nuclear Chemistry, 2022. **331**(4): p. 1869-1879.
115. Khan, I., et al., *Evaluation of health hazards from radionuclides in soil and rocks of North Waziristan, Pakistan.* 2020. **18**(2): p. 243-253.
116. Ahmed, M., et al., *Study of natural radioactivity and radiological hazard of sand, sediment, and soil samples from Inani Beach, Cox's Bazar, Bangladesh.* Journal of Nuclear and Particle Physics, 2014. **4**(2): p. 69-78.
117. Dabayneh, K.M., L. Mashal, and F. Hasan, *Radioactivity concentration in soil samples in the southern part of the West Bank, Palestine.* Radiation protection dosimetry, 2008. **131**(2): p. 265-271.
118. Harb, S., et al., *Specific activities of natural rocks and soils at quaternary intraplate volcanism north of Sana'a, Yemen.* 2012. **37**(1): p. 54-60.
119. Darabi-Golestan, F., A. Hezarkhani, and M. Zare, *Geospatial analysis and assessment of 226Ra, 235U, 232Th, 137Cs, and 40K at Anzali wetland, north of Iran.* Environmental Monitoring and Assessment, 2019. **191**(6): p. 390.

120. Kam, E. and A. Bozkurt, *Environmental radioactivity measurements in Kastamonu region of northern Turkey.* Applied Radiation and Isotopes, 2007. **65**(4): p. 440-444.
121. Al-Hamarneh, I.F. and M.I.J.R.m. Awadallah, *Soil radioactivity levels and radiation hazard assessment in the highlands of northern Jordan.* 2009. **44**(1): p. 102-110.
122. Elsaman, R., et al., *Natural radioactivity levels and radiological hazards in soil samples around Abu Karqas Sugar Factory.* 2018.
123. Najam, L.A. and S.A. Younis, *Assessment of natural radioactivity level in soil samples for selected regions in Nineveh Province (Iraq).* International Journal of Novel Research in Physics Chemistry & Mathematics, 2015. **2**(2): p. 1-9.
124. Unscear, S.J.U.N., New York, *effects of Ionizing Radiation.* 2000: p. 453-487.
125. Tawfiq, N.F., H. Mansour, and M. Karim, *Natural radioactivity in soil samples for selected regions in Baghdad governorate.* International Journal of Recent Research and Review, 2015. **8**(1): p. 1-7.
126. Lanzo, G., S. Rizzo, and E. Tomarchio, *A radiometric and petrographic interpretation of discrepancies on uranium content in samples collected at Alte Madonie Mounts region (Sicily, Italy).* Journal of environmental radioactivity, 2014. **129**: p. 73-79.
127. Mouandza, S.L., et al., *Study of natural radioactivity to Assess of radiation hazards from soil samples collected from Mounana in south-east of Gabon.* International Journal of Radiation Research, 2018. **16**(4): p. 443-453.
128. Suresh, S., et al., *Estimation of natural radioactivity and assessment of radiation hazard indices in soil samples of Uttara Kannada district, Karnataka, India.* 2022. **331**(4): p. 1869-1879.
129. Rahman, S., et al., *Measurement of naturally occurring/fallout radioactive elements and assessment of annual effective dose in soil samples collected from four districts of the Punjab Province, Pakistan.* Journal of radioanalytical and nuclear chemistry, 2011. **287**(2): p. 647-655.
130. Dizman, S., F.K. Görür, and R. Keser, *Determination of radioactivity levels of soil samples and the excess of lifetime cancer risk in Rize province, Turkey.* International Journal of Radiation Research, 2016. **14**(3): p. 237.
131. Saleh, H. and M.A. Shayeb, *Natural radioactivity distribution of southern part of Jordan (Ma' an) Soil.* Annals of Nuclear Energy, 2014. **65**: p. 184-189.
132. Thabayneh, K., *Natural radioactivity levels and estimation of radiation exposure in environmental soil samples from Tulkarem Province–Palestine.* 2012.

133. Muhammed, M.I. and P.H. Mangur, *The Investigation of Terrestrial Radioactivity in Soil Samples around Pshdar Region in Iraqi-Kurdistan.* ZANCO Journal of Pure and Applied Sciences, 2016. **28**(6): p. 13-20.
134. Al-Alawy, I., W. Taher, and O. Mzher, *Soil radioactivity levels, radiation hazard assessment and cancer risk in Al-Sadr City, Baghdad Governorate, Iraq.* International Journal of Radiation Research, 2023. **21**(2): p. 293-298.
135. Mohammed, R. and R. Ahmed, *Estimation of excess lifetime cancer risk and radiation hazard indices in southern Iraq*. *Environ Earth Sci 76: 303*. 2017.

CANBERRA

Detector Specification and Performance Data

Doc. No.: DPF-009
Rev: E
Date: 12/6/2010

Specifications

Detector Model	GC4020	Detector Serial Number	10025
Preamplifier Model	2002CSL	Preamp Serial Number	13001333
Cryostat Model	7500SL	Order Number	26963

The purchase specifications, and therefore the warranted performance, of this detector are as follows:

Relative Efficiency	≥ 40	%	Active Volume	---	cc
Resolution	≤ 2.0	keV (FWHM) @ 1.33 MeV			
	---	keV (FWTM) @ 1.33 MeV			
	---	keV (FWHM) @ 122 keV			
	---	keV (FWHM) @ 5.9 keV			
Peak/Compton	≥ 54	:1			
Well Diameter	---	mm	Well Depth	---	mm

Cryostat Description (if special): 3.0" Ø End Cap

Physical Characteristics

Active Diameter	62.2	mm	Active Area	---	mm^2
Length/Thickness	59.5	mm	Well Diameter	---	mm
Distance from Window	5.48	mm	Well Depth	---	mm
Window Thickness	---	mm	Active Volume	---	cc
Window Material	---				

Electrical Characteristics

Depletion Voltage	(+)2200	V dc
Recommended Bias Voltage	(+)3000	V dc
Test Point voltage at recommended bias	(-)1.01	V dc (RC preamp only)
Reset interval at recommended bias	---	sec. (Reset preamp only)
Capacitance at recommended bias	~ 27	pF

Measured Performance

With amp time constant of 4 µS

Isotope	^{57}Co	^{60}Co	^{55}Fe	^{57}Co	^{109}Cd	^{109}Cd	^{109}Cd
Energy (keV)	122	1332	5.9	6.4*	22	88	22
FWHM (keV)	0.89	1.77	---	---	---	---	
FWTM (keV)	1.61	3.30	---	---	---	---	
Peak/Compton/Bkgd	---	67.6:1	---	---	---	---	
Efficiency %	---	45.3	---	---	---	---	

* Substitutes for ^{55}Fe in some cases where ^{55}Fe peaks are not well separated

Cool Down Time 6 Hrs LN_2 Loss Rate <1.8 l/h PRTD 41.9 Ω (c

Tested by: [signature] Date: 10/14/2011

Appendix A : Measurement System Specifications.

Czech Metrology Institute
Okružní 31, 638 00 Brno, Czech Republic
phone +420 545 555 111
www.cmi.cz

Workplace: **Regional Branch Prague, Radiová 1136/3, 102 00 Praha 10**
Ionizing Radiation Building, Radiová 1288/1a
Phone: +420 266 020 497

CERTIFICATE

Certificate No.: 1035 - SE - 40524-16 Type: CBSS 2 Serial No.: 280616-1597016

Radionuclide	Half life, days	Activity, kBq	Combined standard uncertainty, %
Am-241	158004	4,057	1,1
Cd-109	461,9	13,93	1,6
Ce-139	137,64	3,196	1,2
Co-57	271,8	0,9577	1,2
Co-60	1925,2	2,338	1,2
Cs-137	10976	1,991	1,4
Sn-113	115,09	2,929	2,2
Sr-85	64,85	3,987	1,2
Y-88	106,63	4,949	1,5
Cr-51	27,704	19,98	1,9
Mn-54	312,19	1,672	1,3
Zn-65	244,01	3,980	1,2

Mass: 441,0 g Density: 0,98 ± 0,01 g/cm^3 Volume: 450,0 ± 4,5 cm^3
Radionuclide impurities: gamma < 0,1 %
Reference date: 8.8.2016 Homogeneity better than: 1 %

Description:
Radioactive material is homogeneously dispersed in silicone resin. Composition of the matrix: C - 0,324 H - 0,0816 O - 0,216 Si - 0,379 (mass ratio).

Measuring method:
Preparation issues from standard ER solutions whose activities were determined by suitable absolute method. Final control is based on gamma spectrometry on HPGe detector.

Note:
As the criterion of homogeneity standard deviation of the activity value of 1 cm^3 element was chosen (n=10). The volume is calculated from the mass and the density.

Date of the certificate issue: 18.7.2016 Certificate validity:
(6 months f

Customer:
Ministry of Environment, Radiation Protection Centre Baghdad
Iraq Baghdad

Vlasta Zdychova
Head of Department
Production of Standard Radionuclide Sources
RB Prague

Ing. Jiří Šurán, MBA
Deputy Director of RB Prague

Control: Ing. Vlasta Zdychová, RNDr. Pavel Dryák, CSc.

Appendix B: Certificate Stander Source Multi-Gamma.

Appendix c

Spectral Analysis of Samples for Al-Majar.

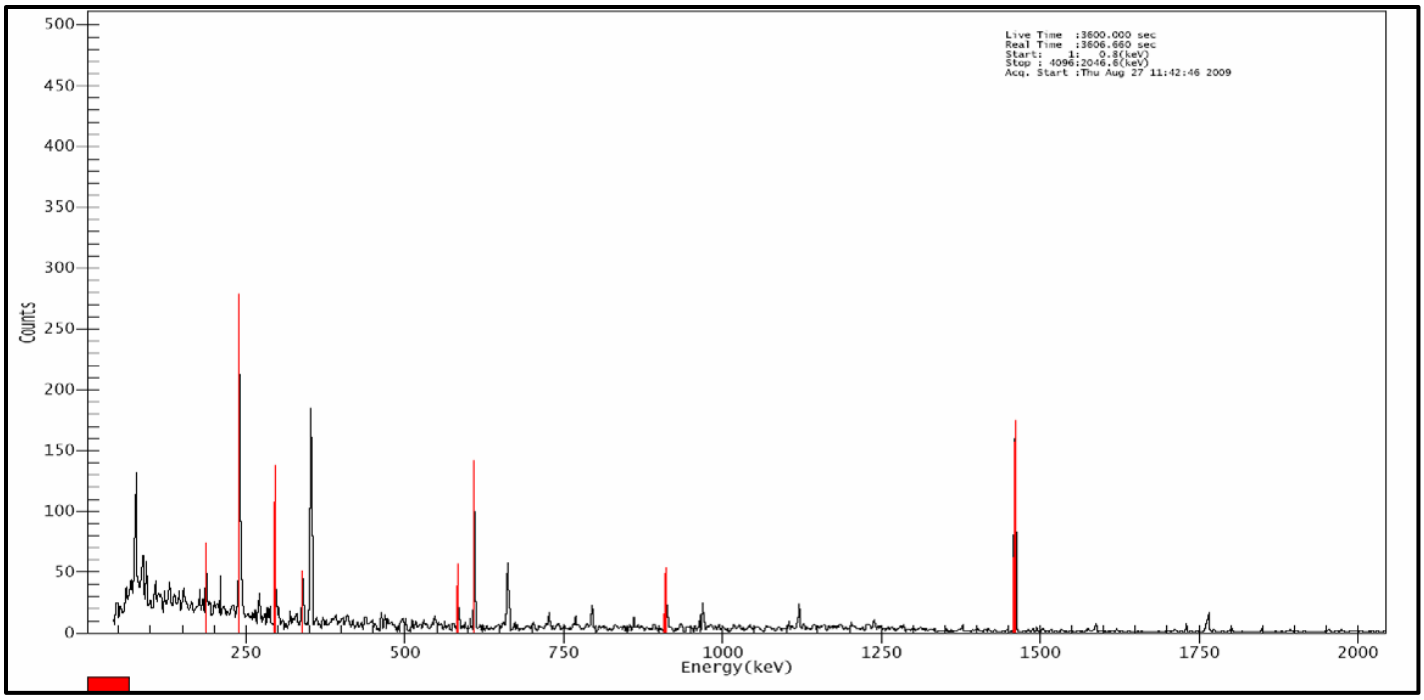

Sample (1): Sudur Al-Majar.

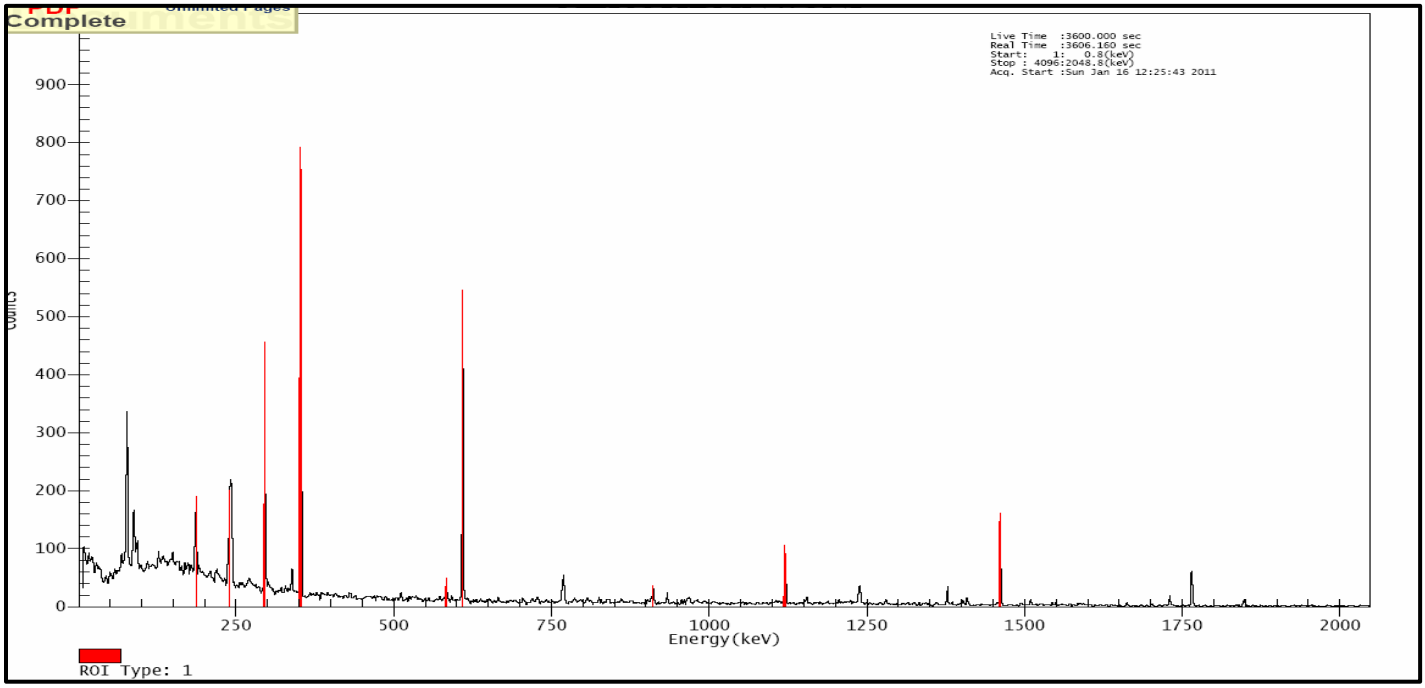

Sample (2): Al-Waraq.

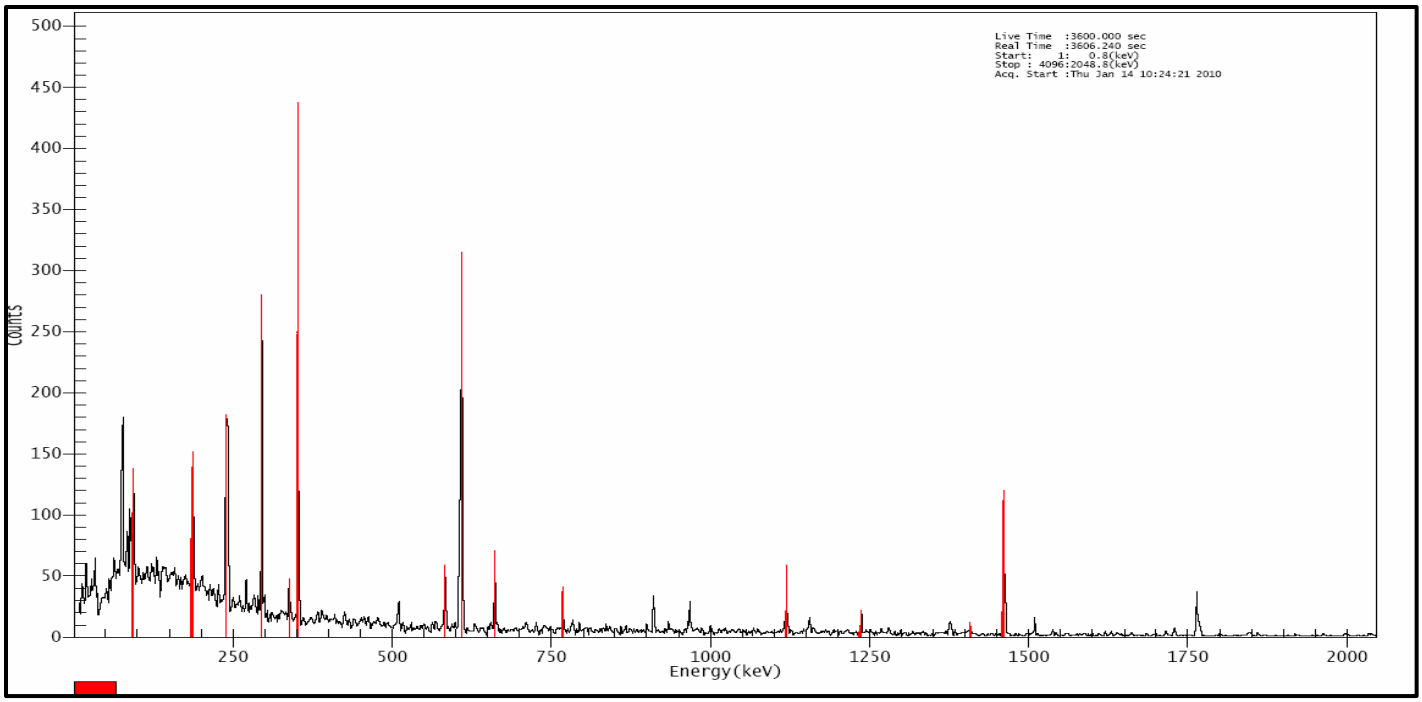

Sample (3): Al-Hasharia.

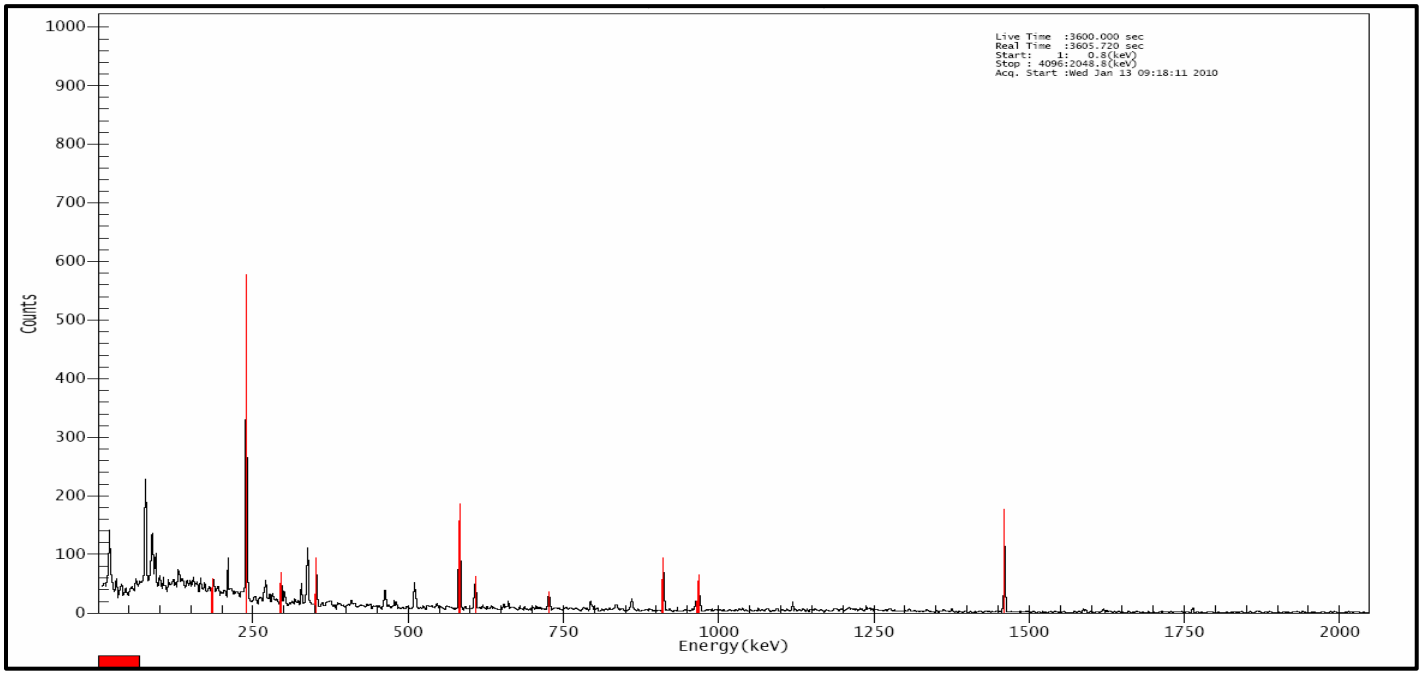

Sample (4): Fifth field.

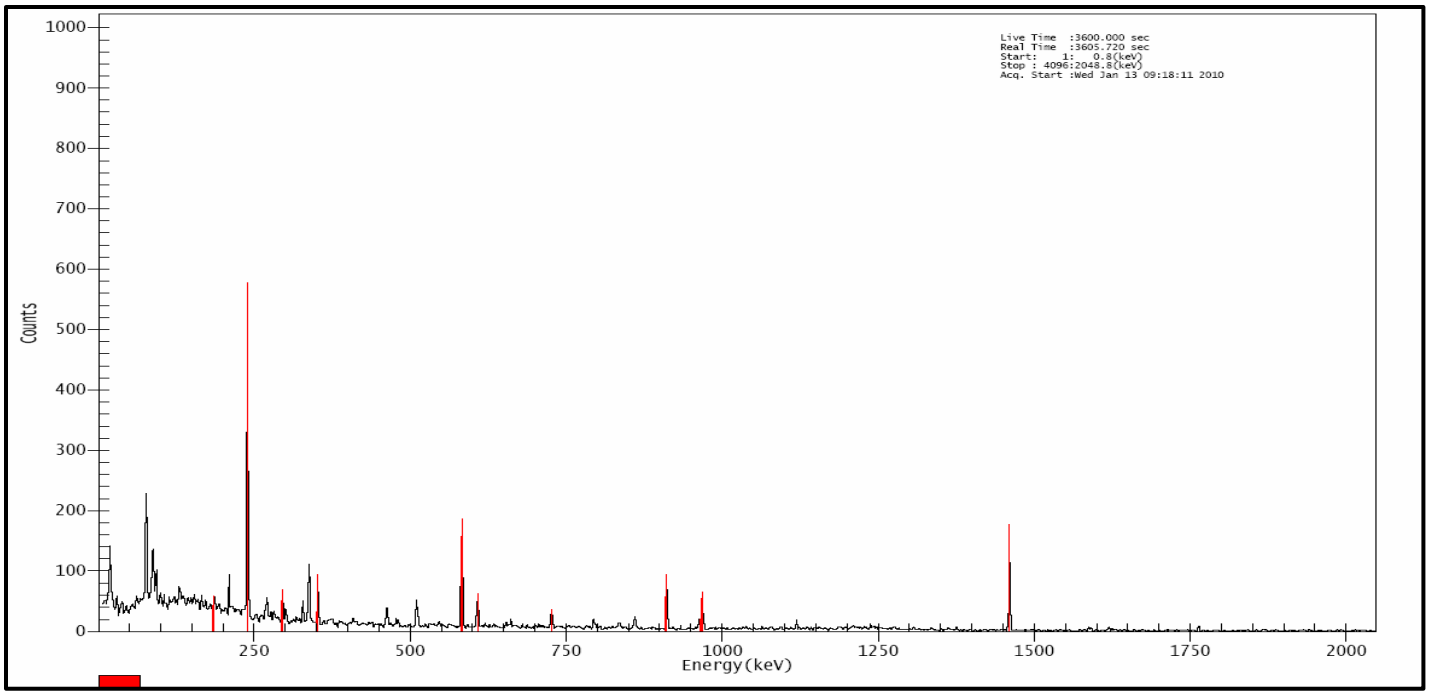

Sample (5): Fourth field.

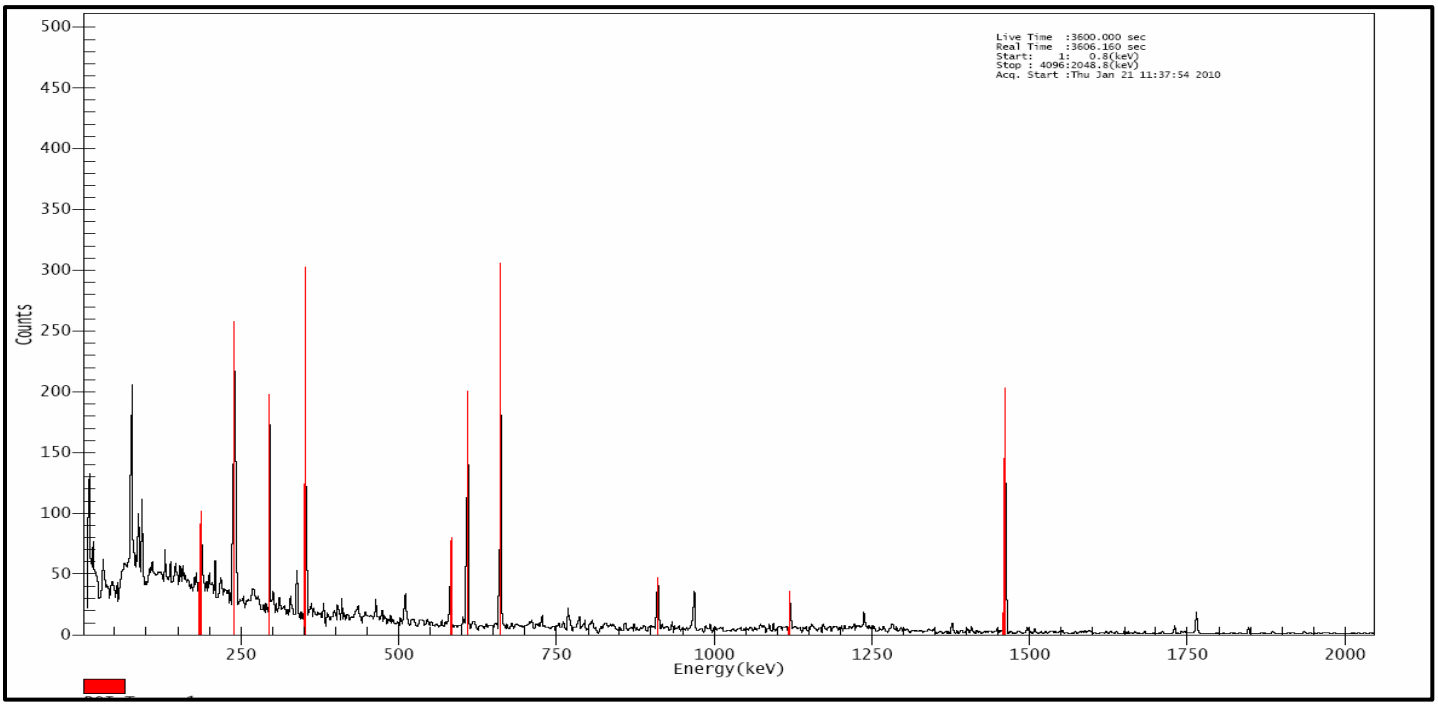

Sample (6): Third field.

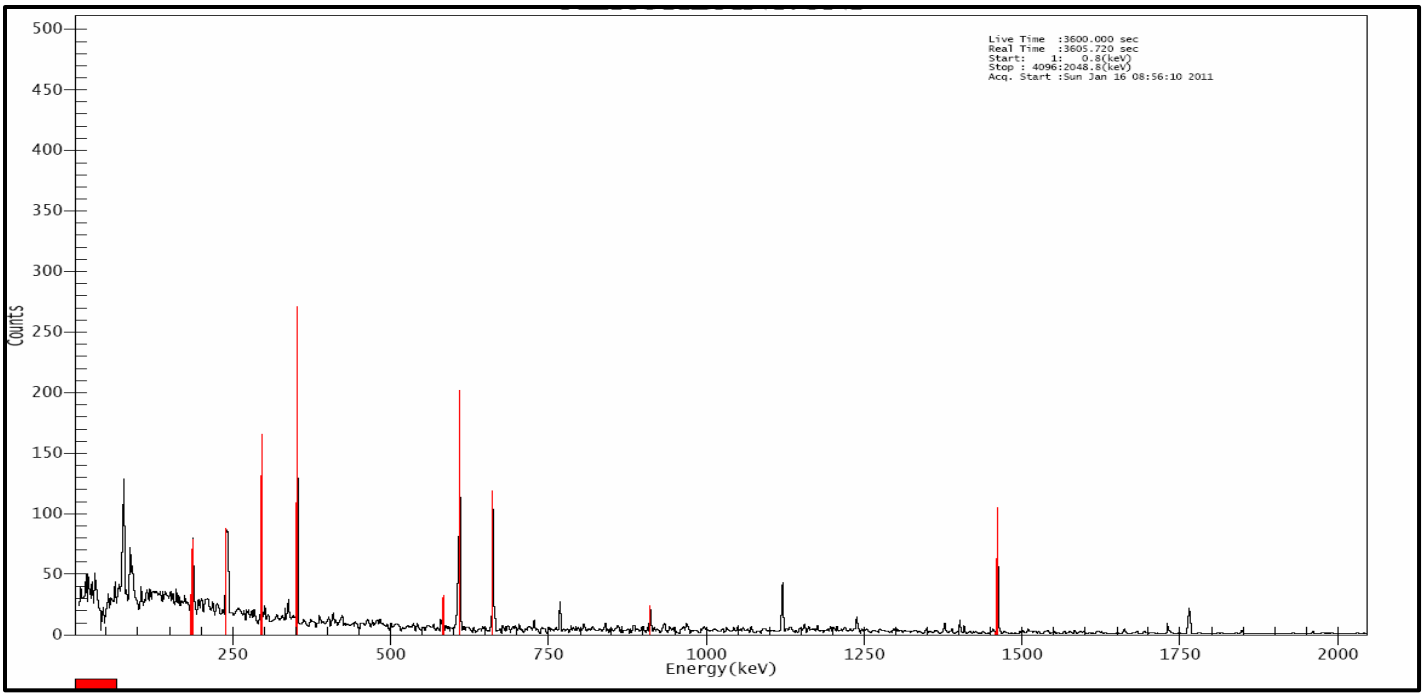

Sample (7): Al-Saeida.

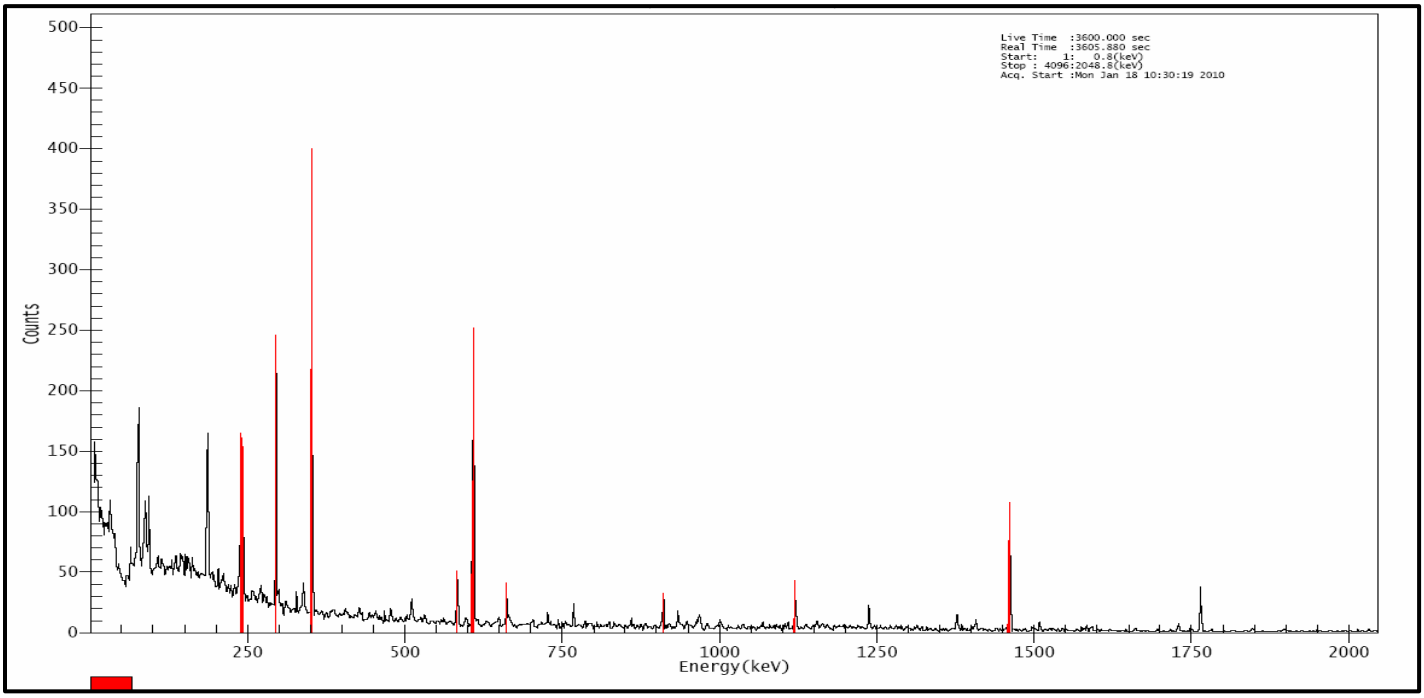

Sample (8): Second field.

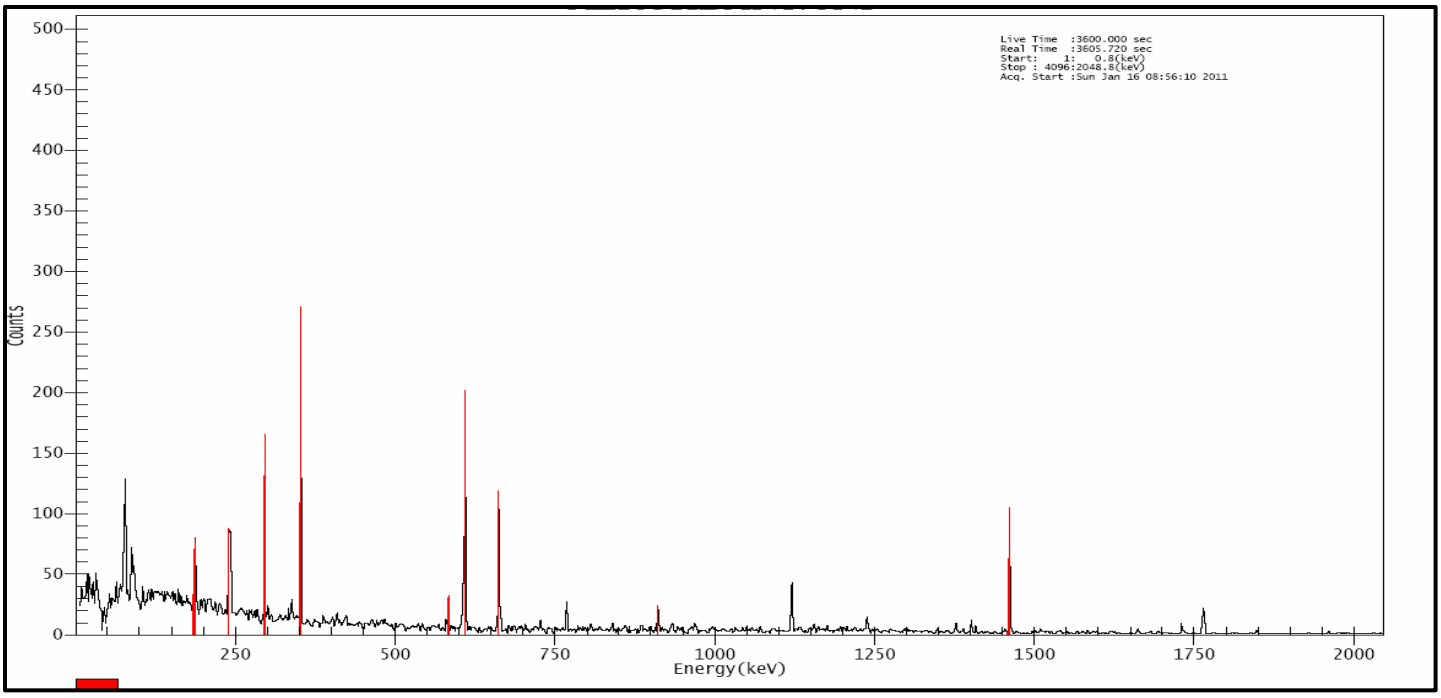

Sample (9): Eidawiya.

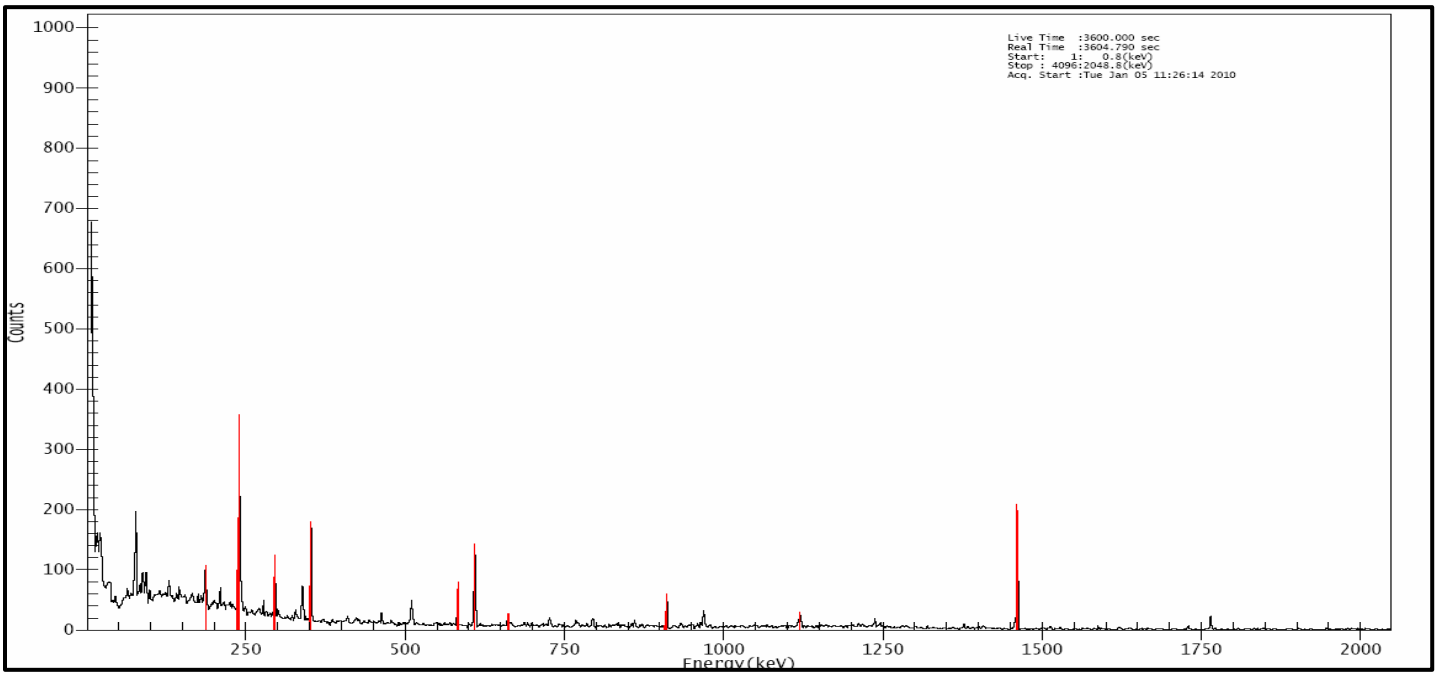

Sample (10): First field.

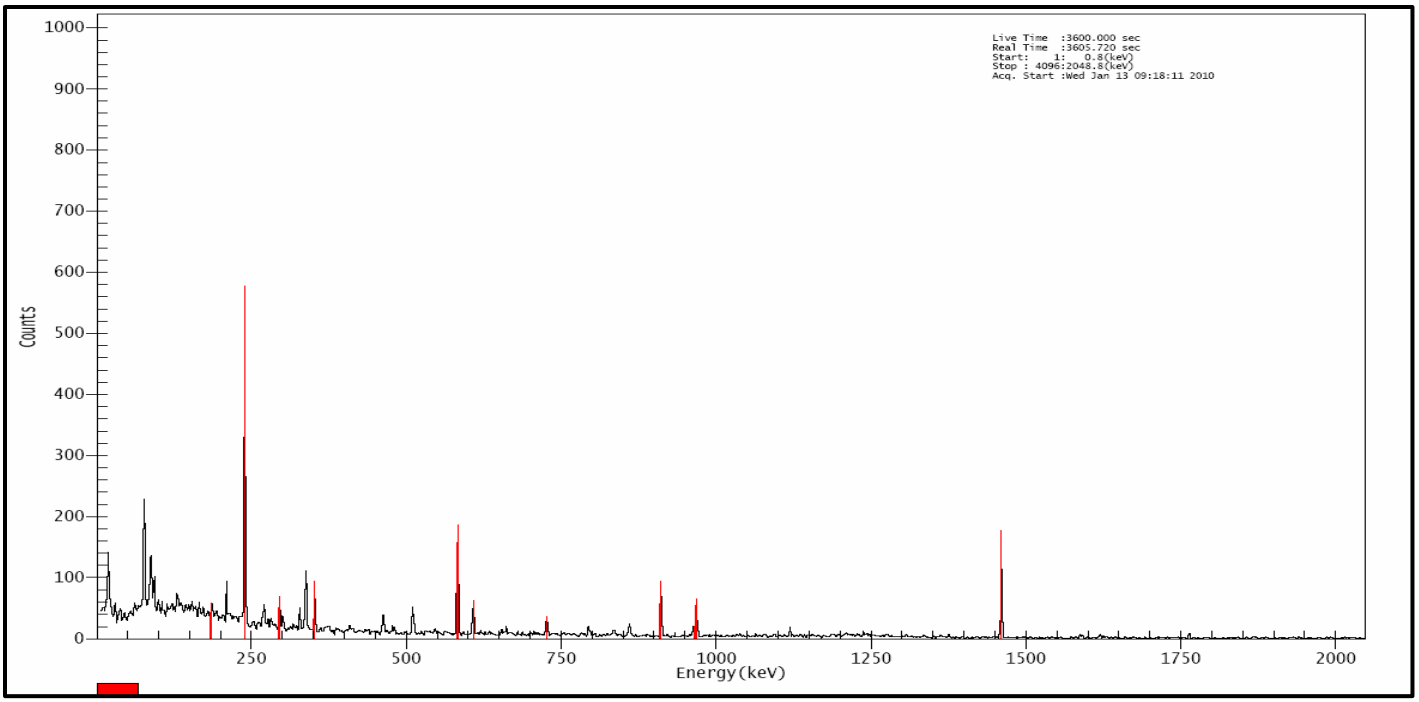

Sample (11) : Western Sugar dwar.

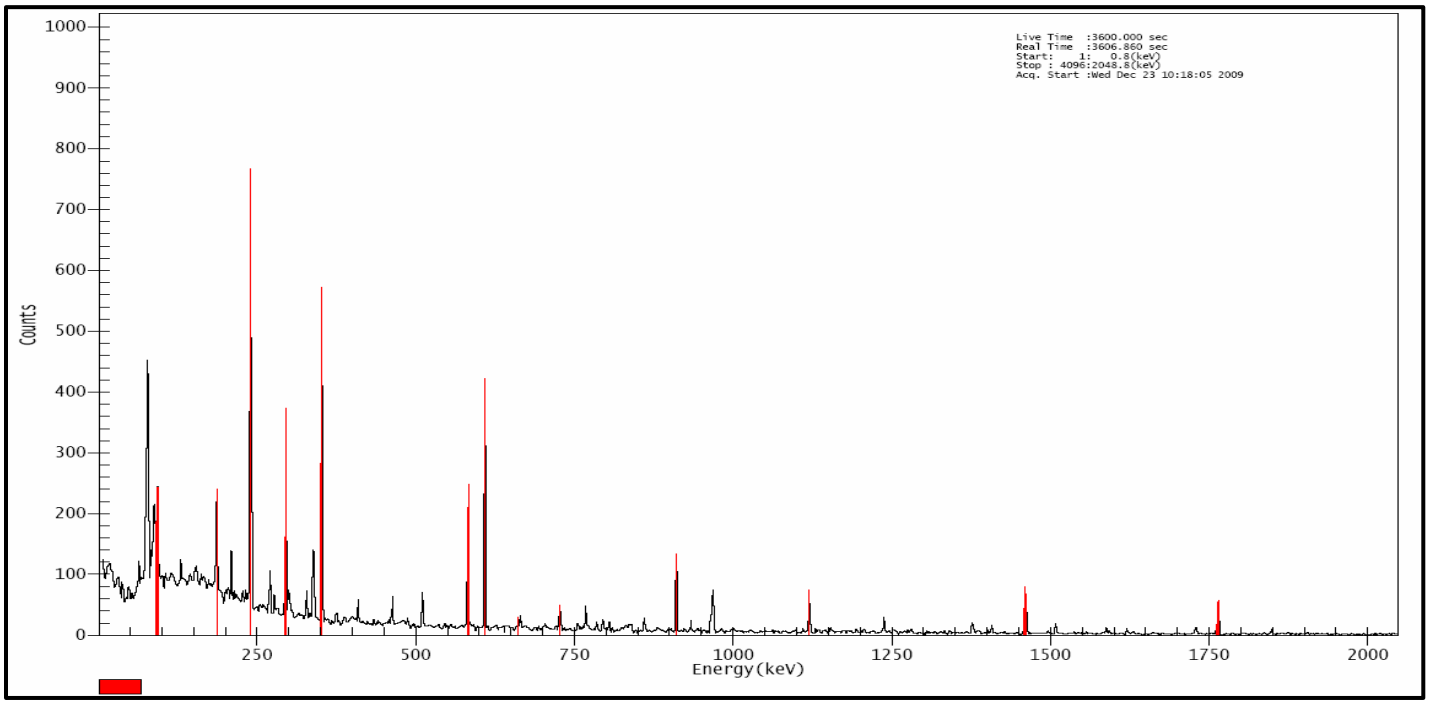

Sample (12) : Al-Sadrayn.

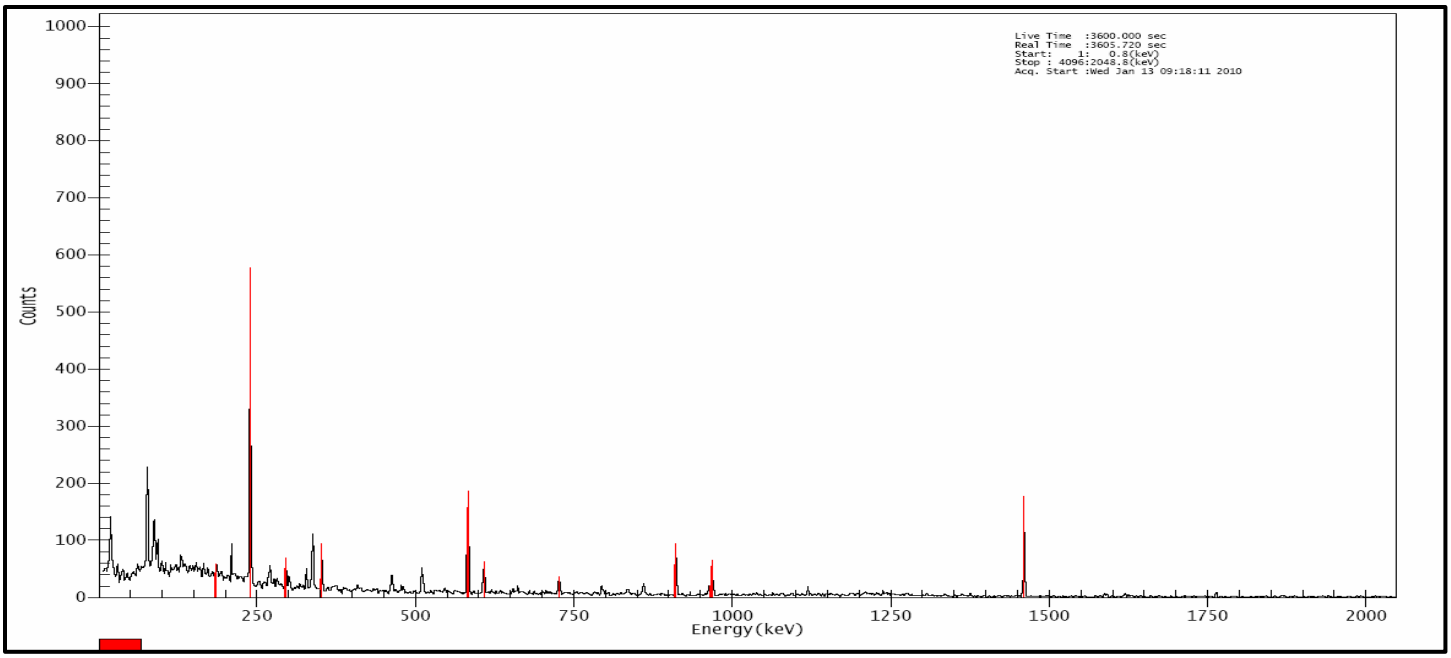

Sample (13): Eastern Sugar dwar.

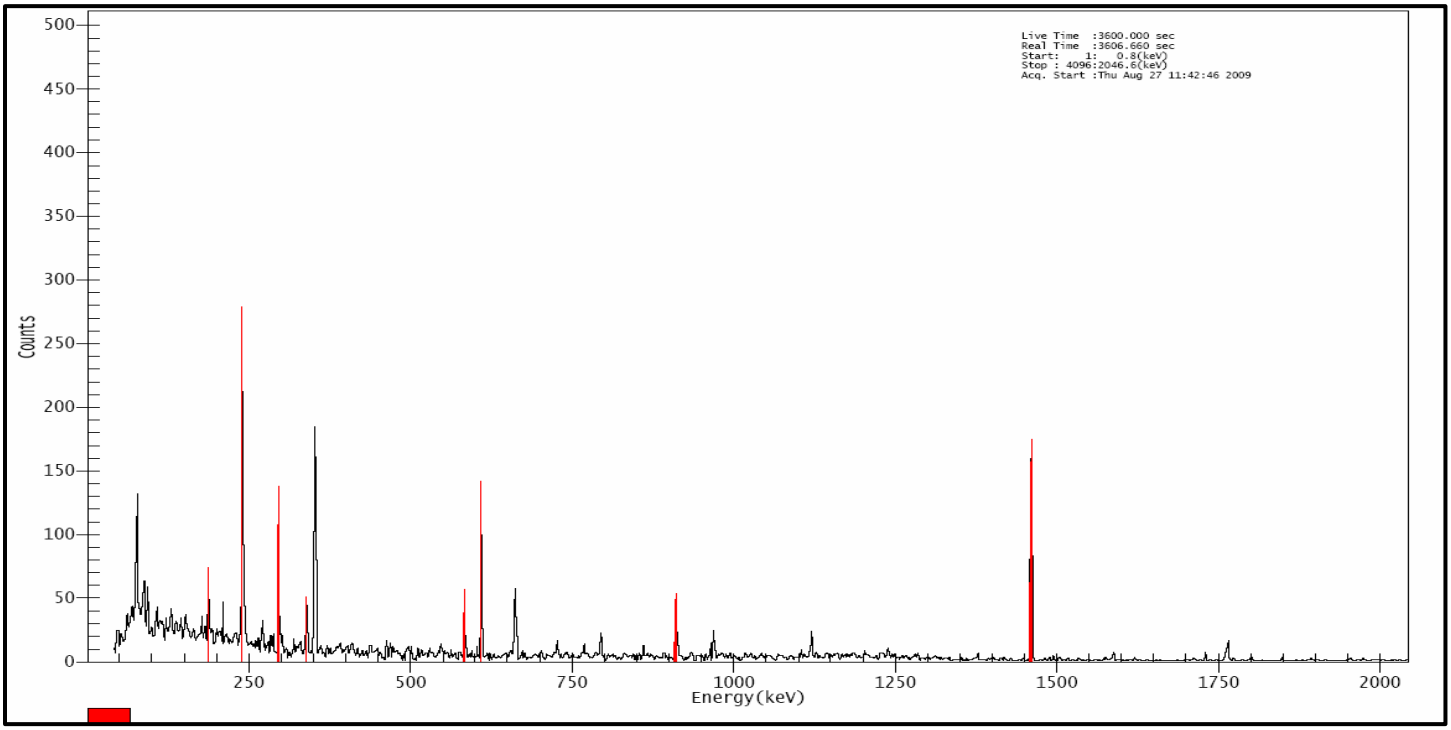

Sample (14): Yarmouk.

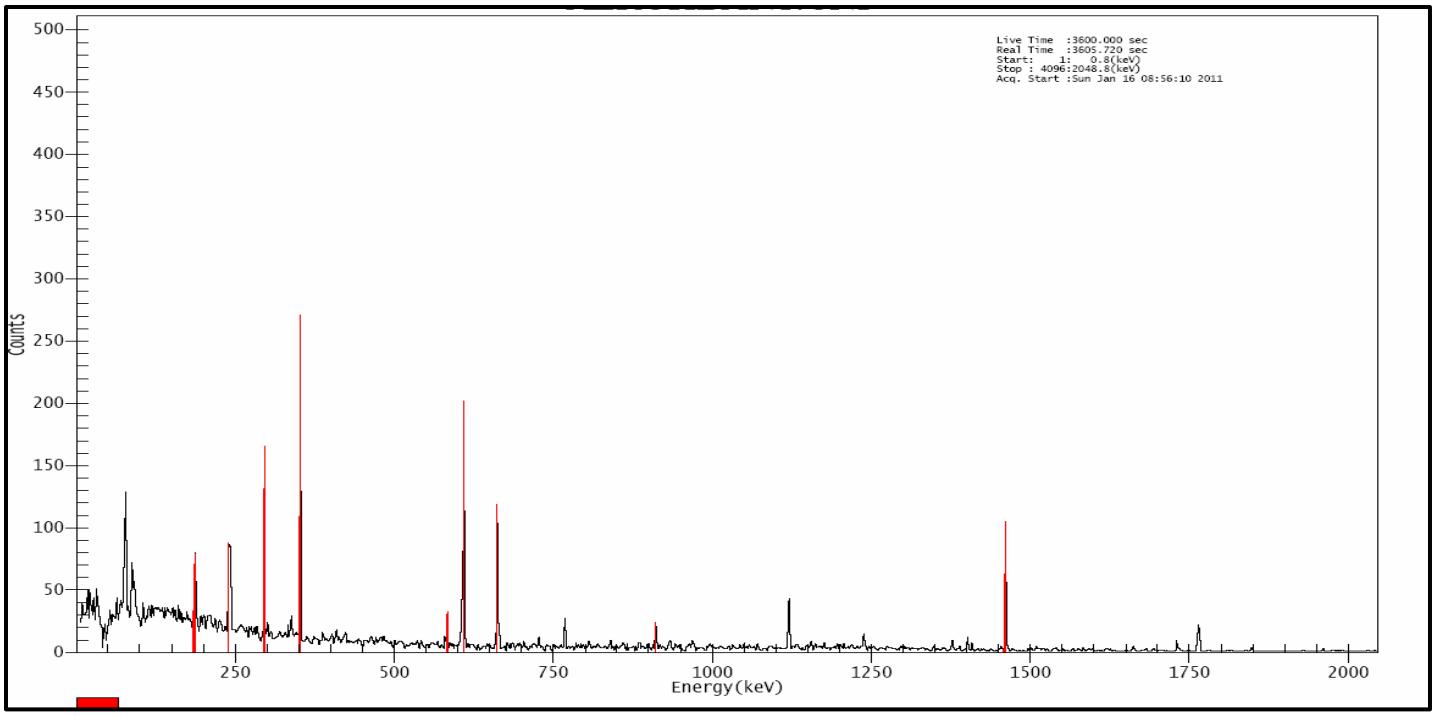

Sample (15): Al-Jameiaat.

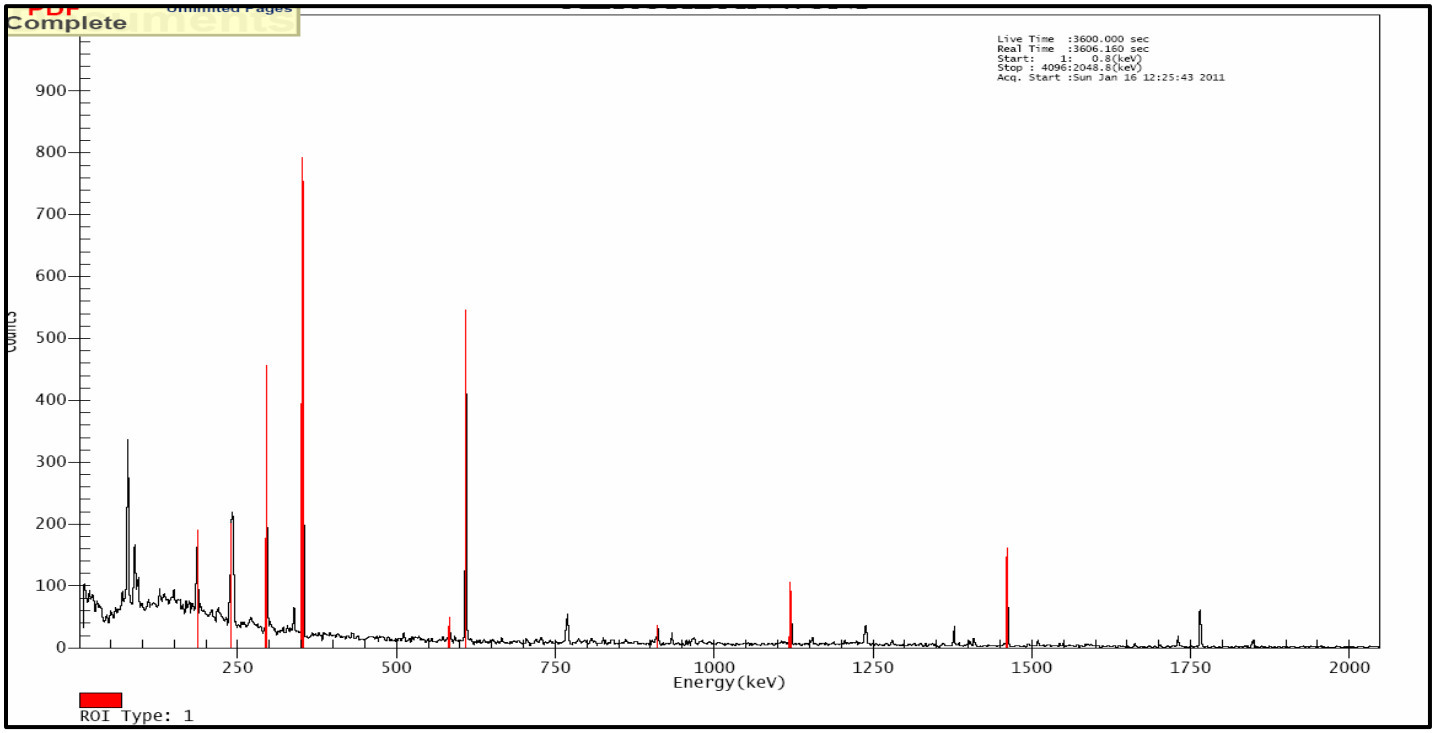

Sample (16): Al-Easkari.

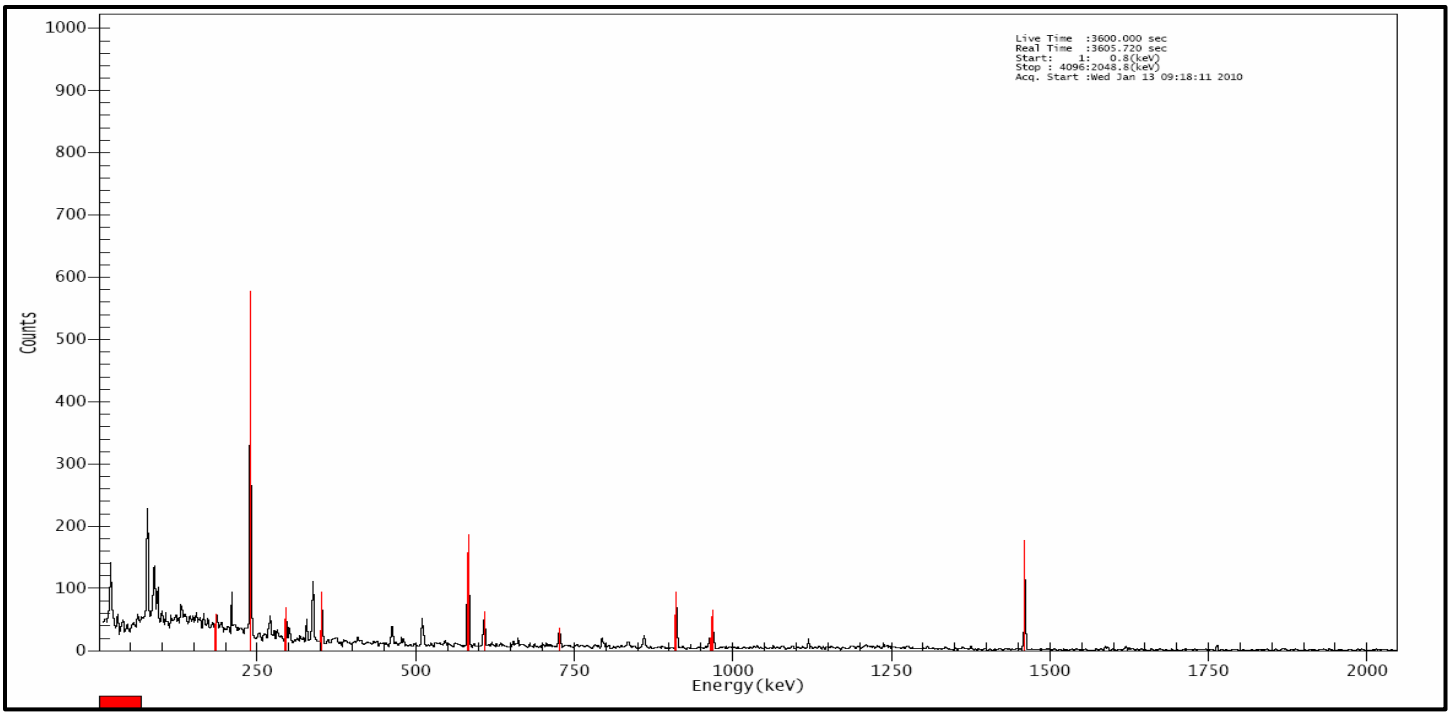

Sample (17): Al-Shurta.

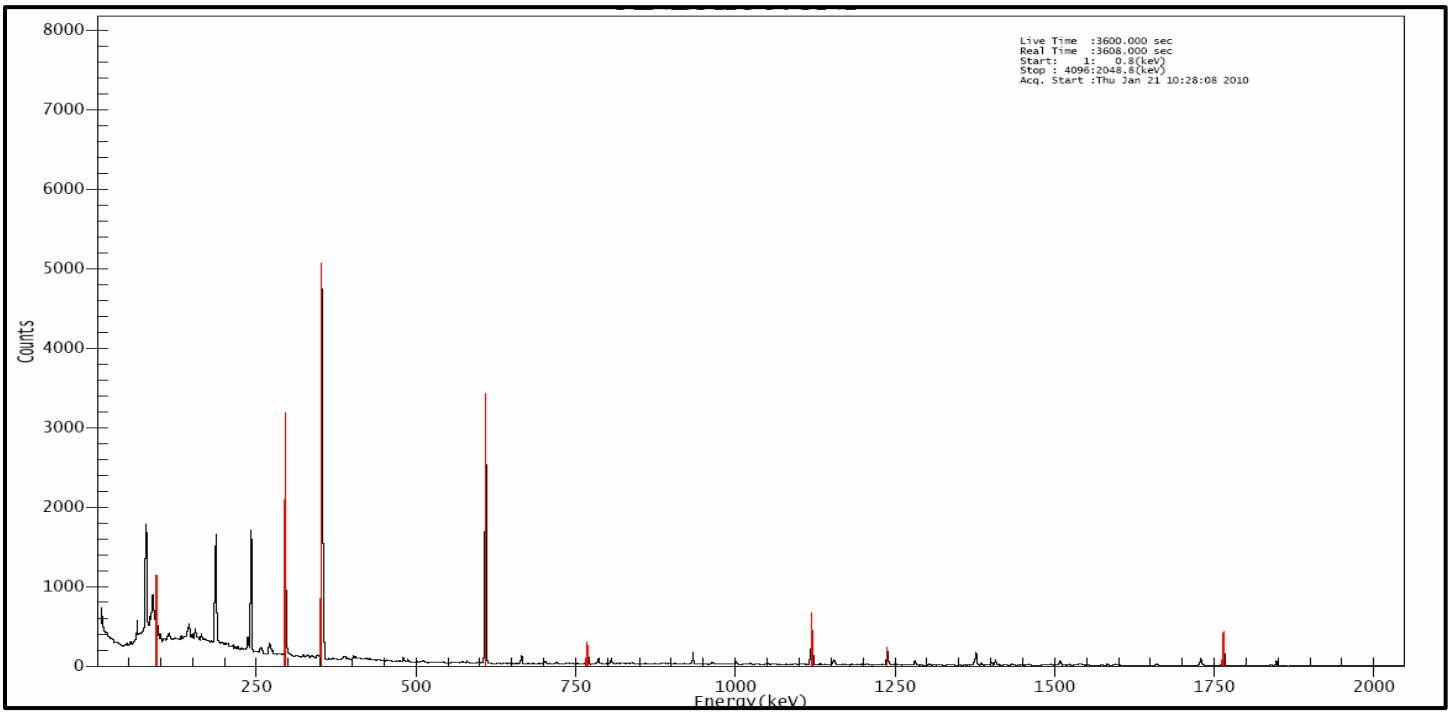

Sample (18): Al-Shuhada'.

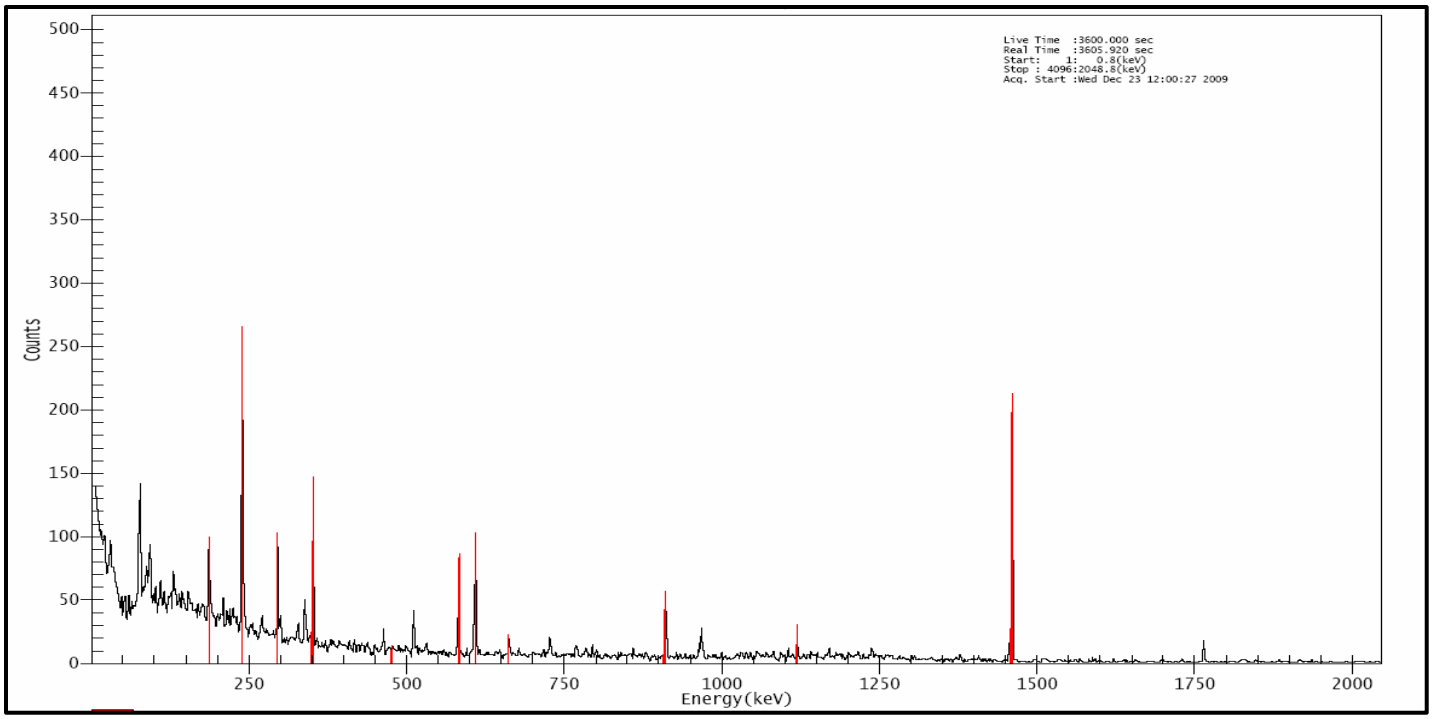

Sample (19): New Hussein.

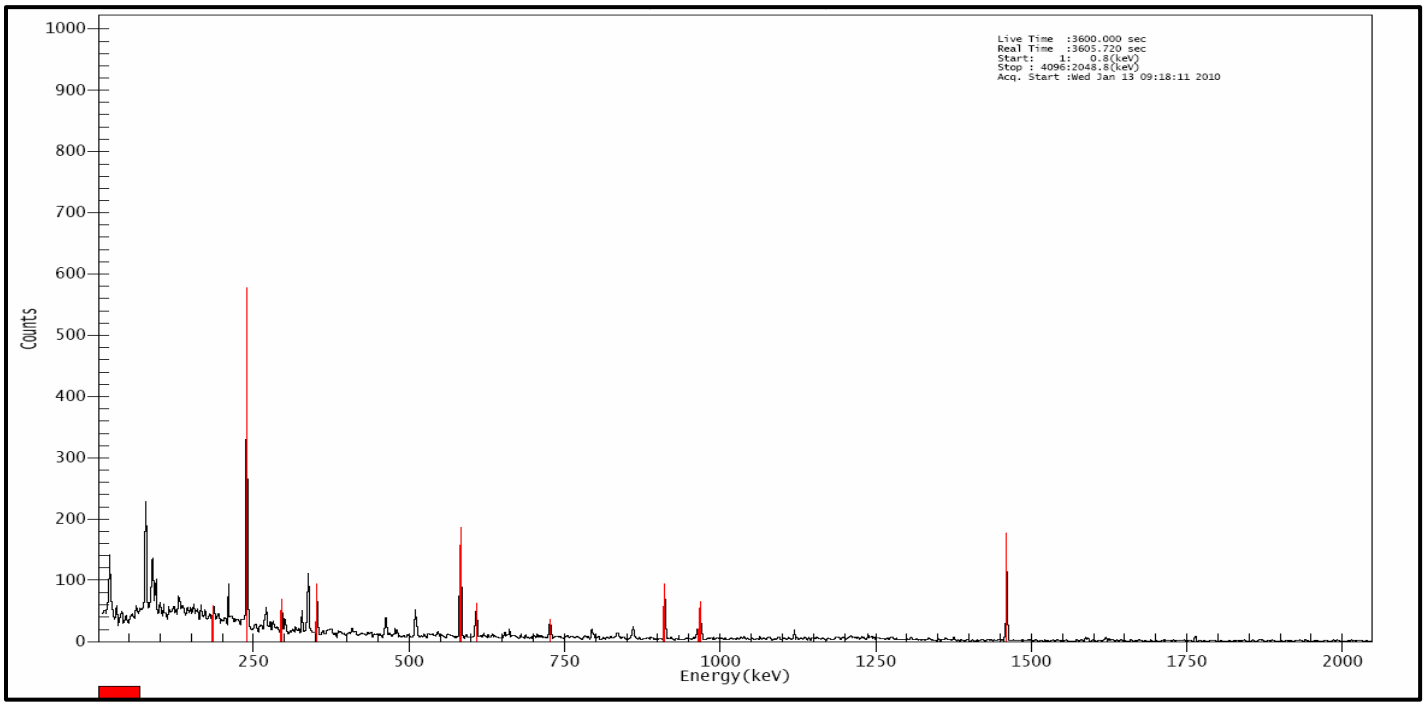

Sample (20): Old Hussein (Al-Rifaq).

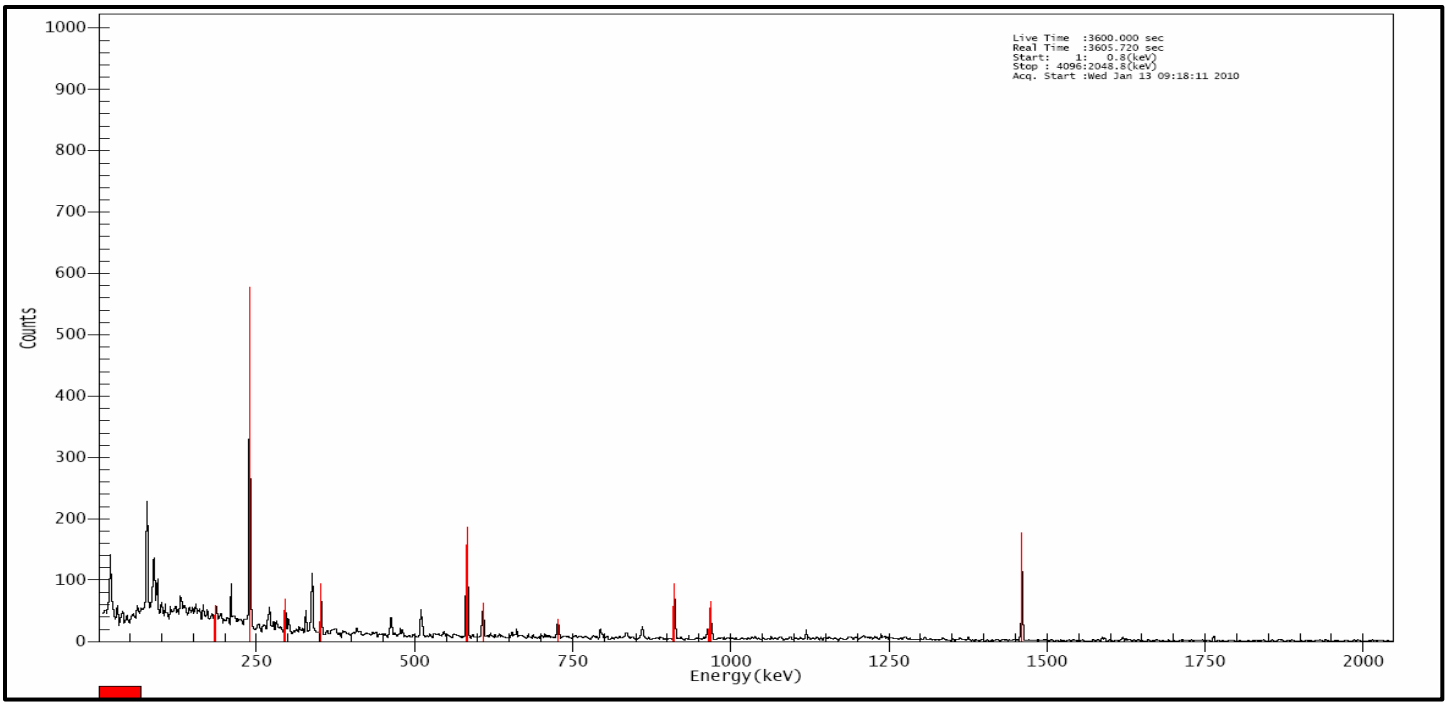

Sample (21): Al-Jumhuria.

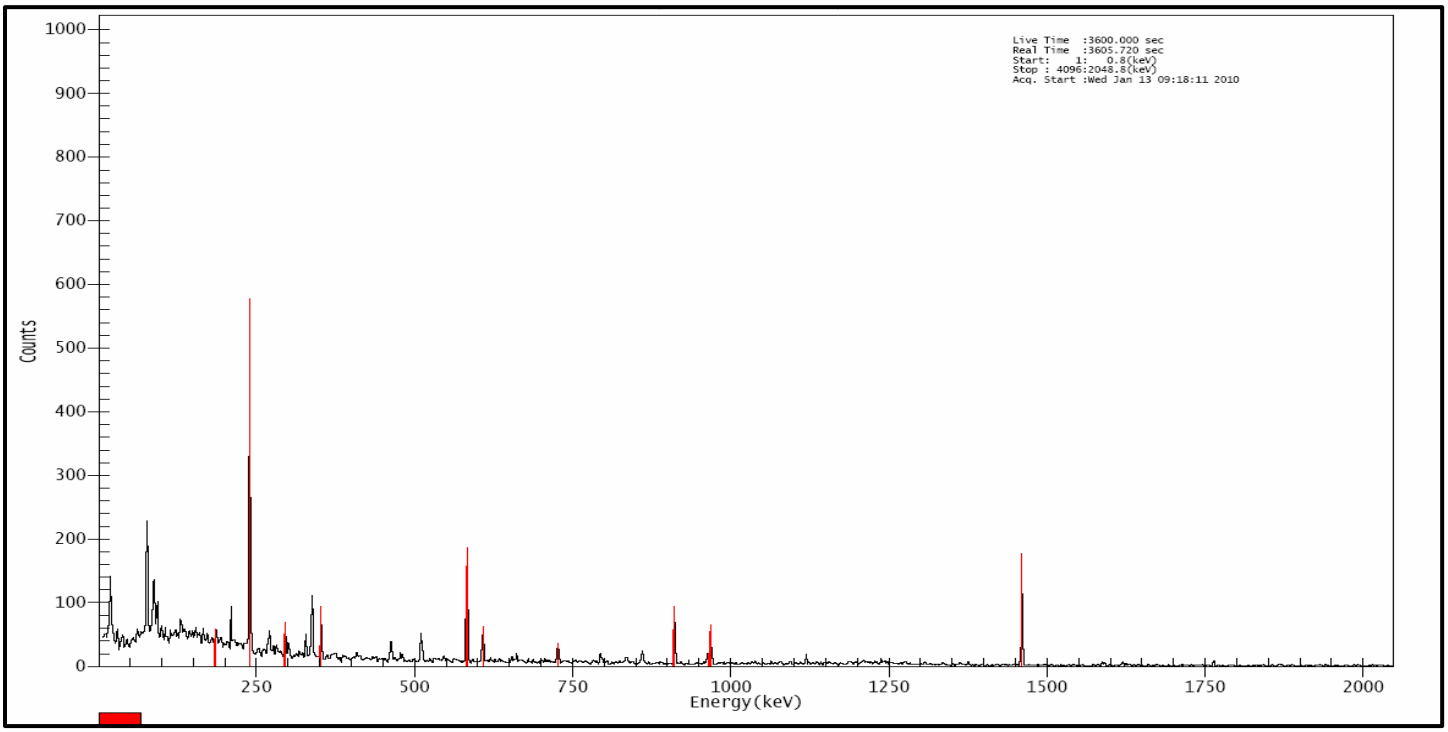

Sample (22): Imam Al-Hassan.

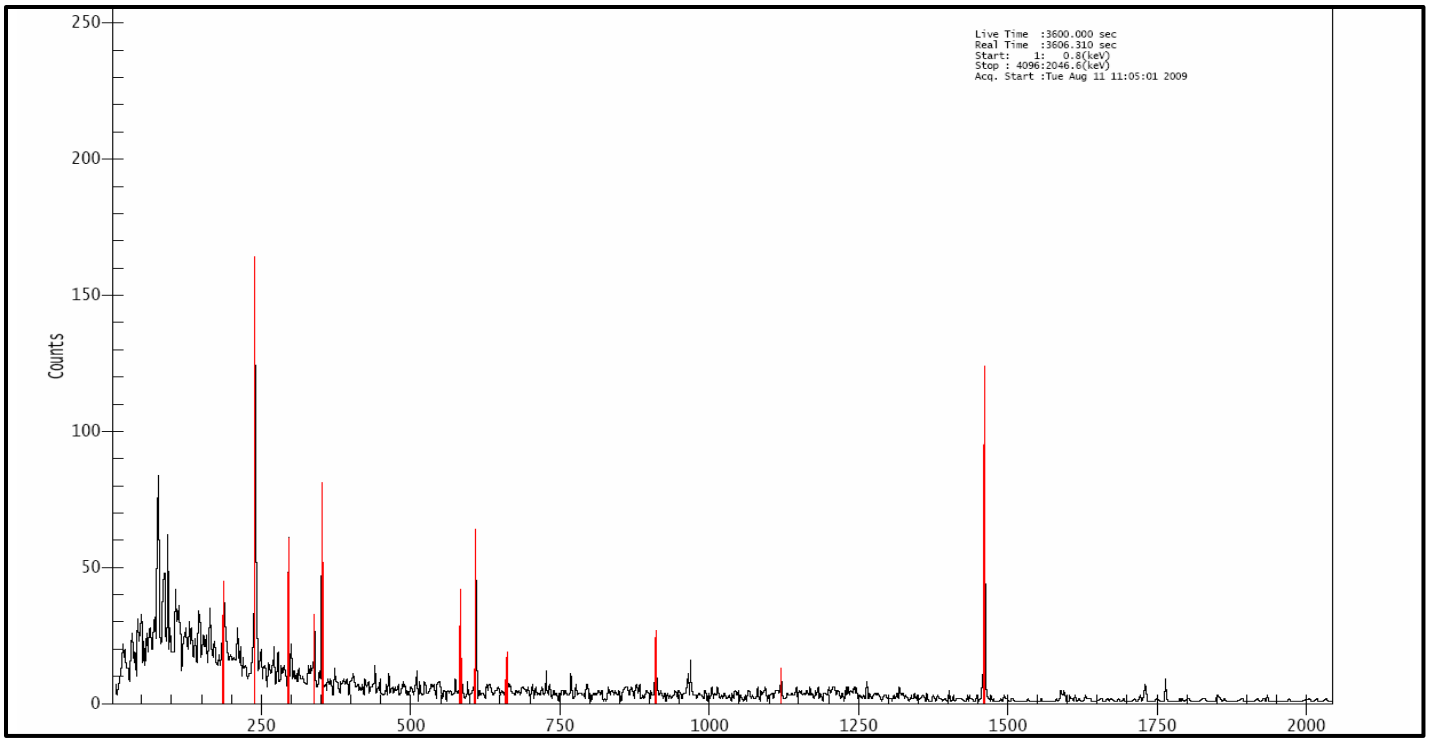

Sample (23): Al- Kashashiya (First Al-Rahma).

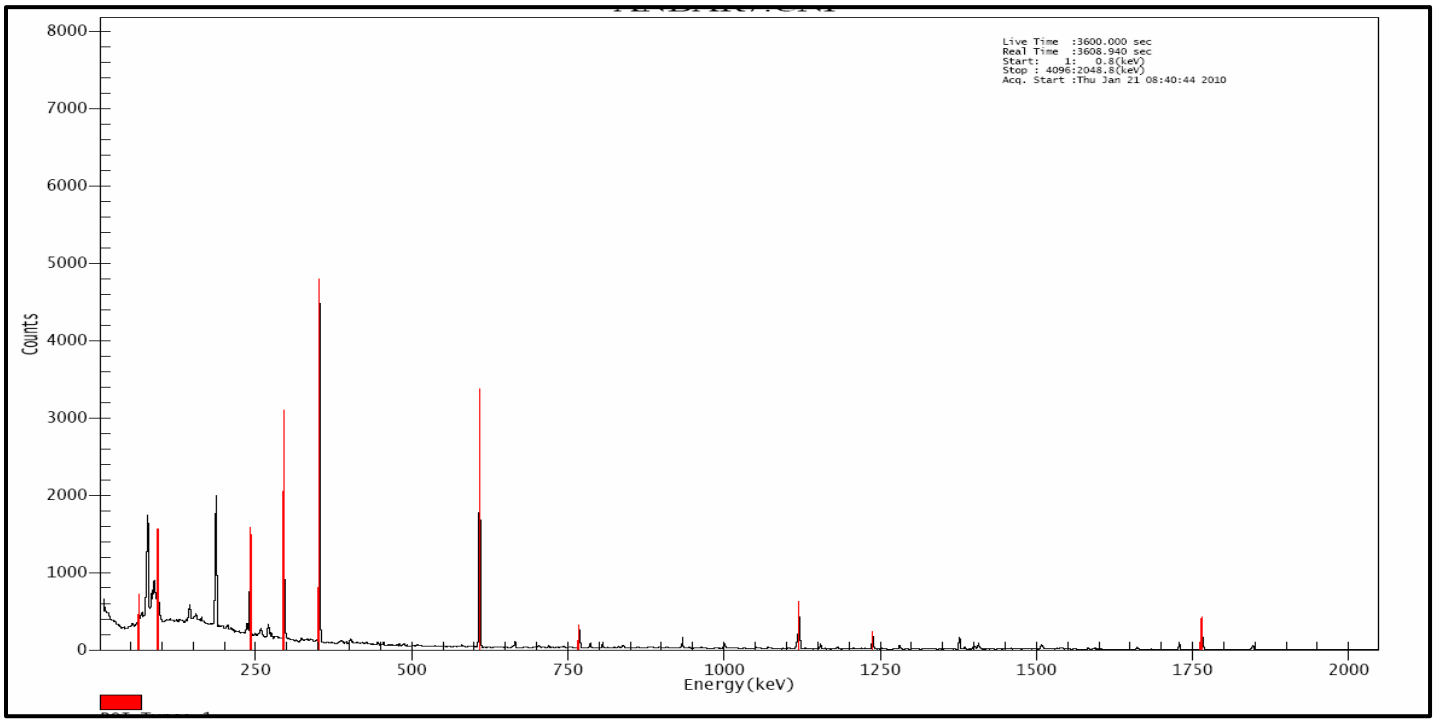

Sample (24): 14 –Ramadan.

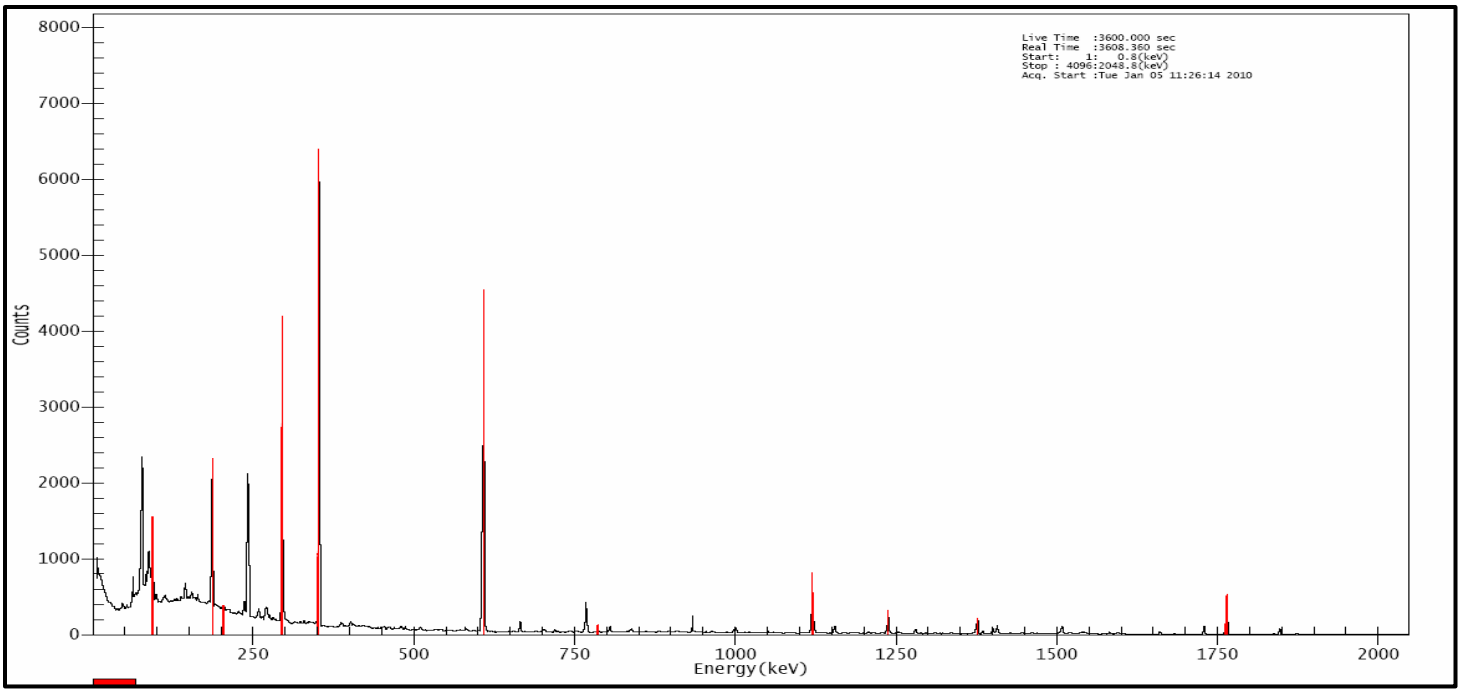

Sample (25): Al-Rahma.

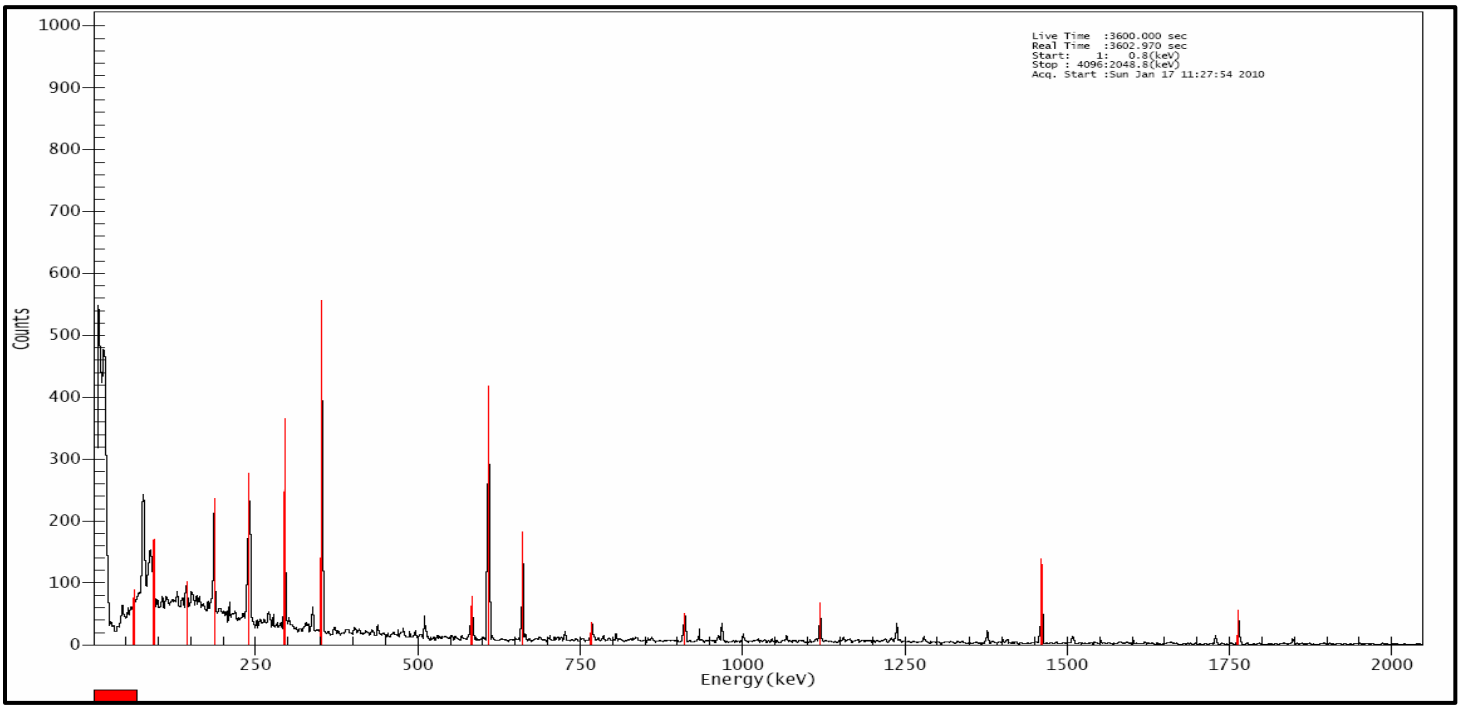

Sample (26): Al-Sinaea.

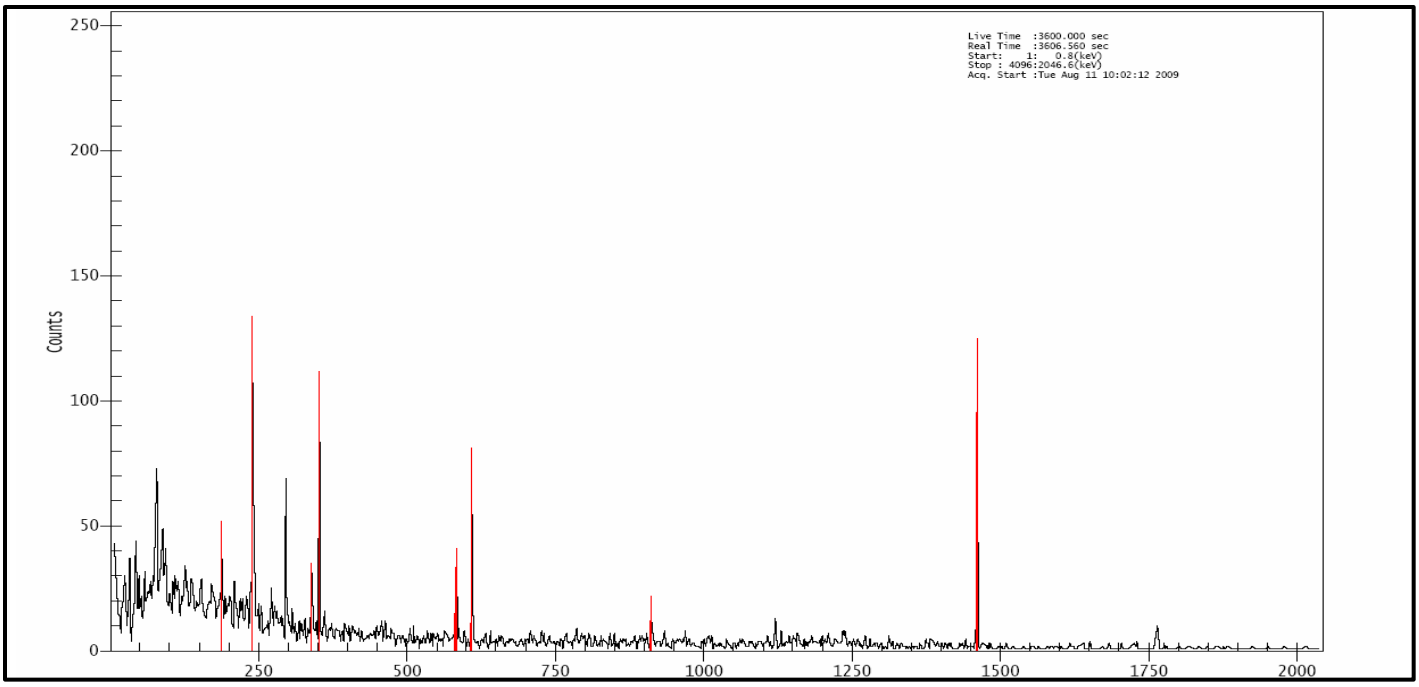

Sample (27) : Al-Saray.

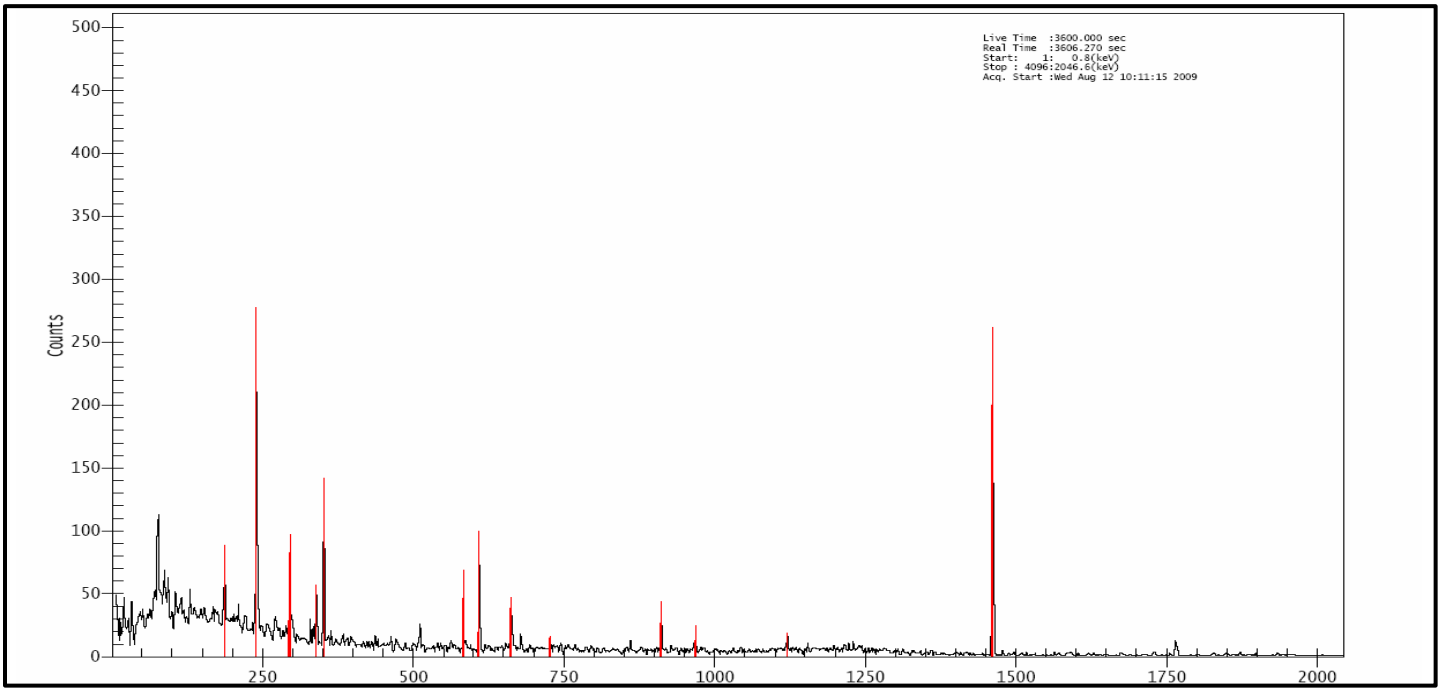

Sample (28): Al- Kashashiya (Second Al-Rahma).

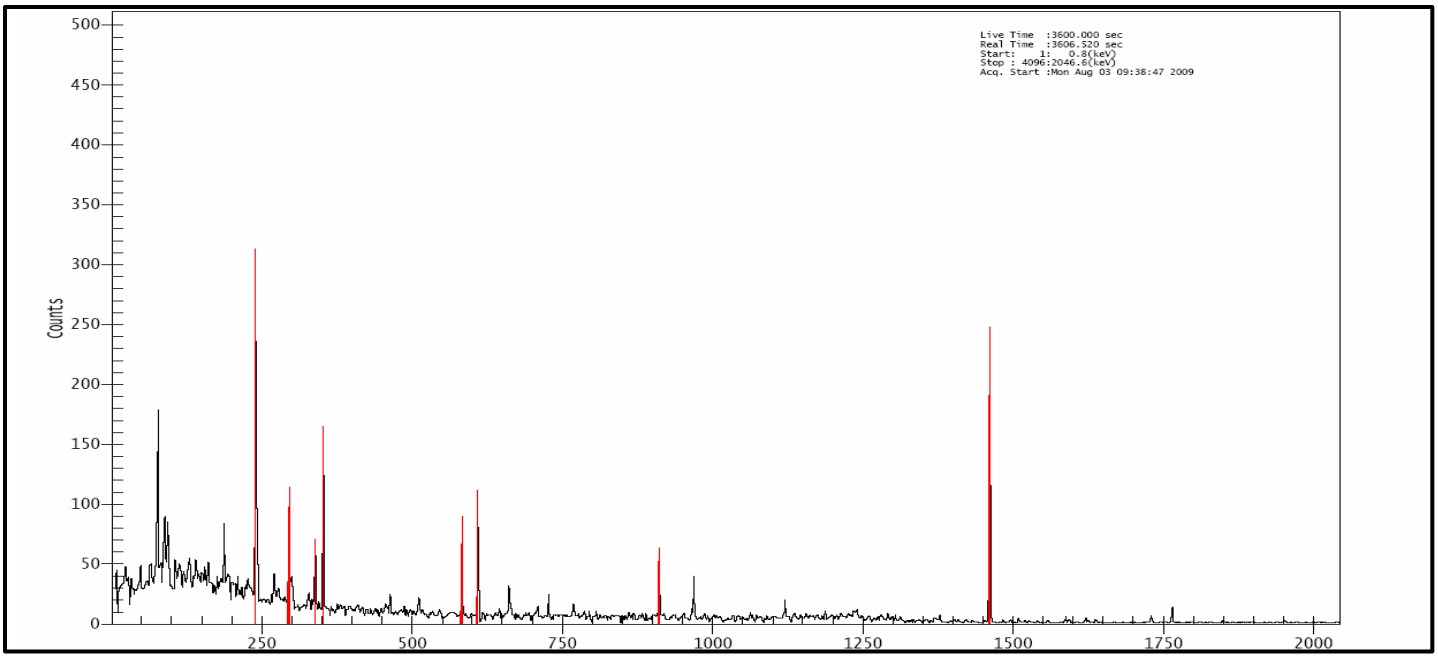

Sample (29): Al-Badrawi.

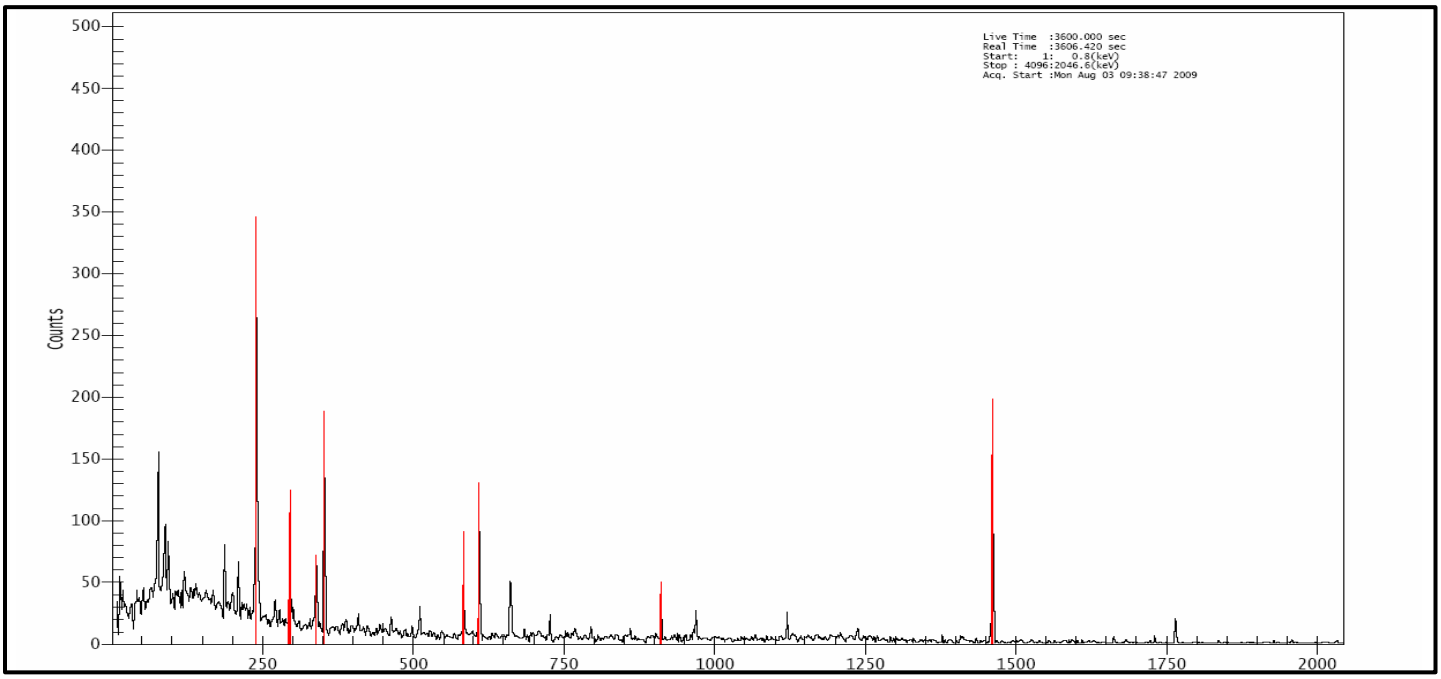

Sample (30) : Al-Akhilas.

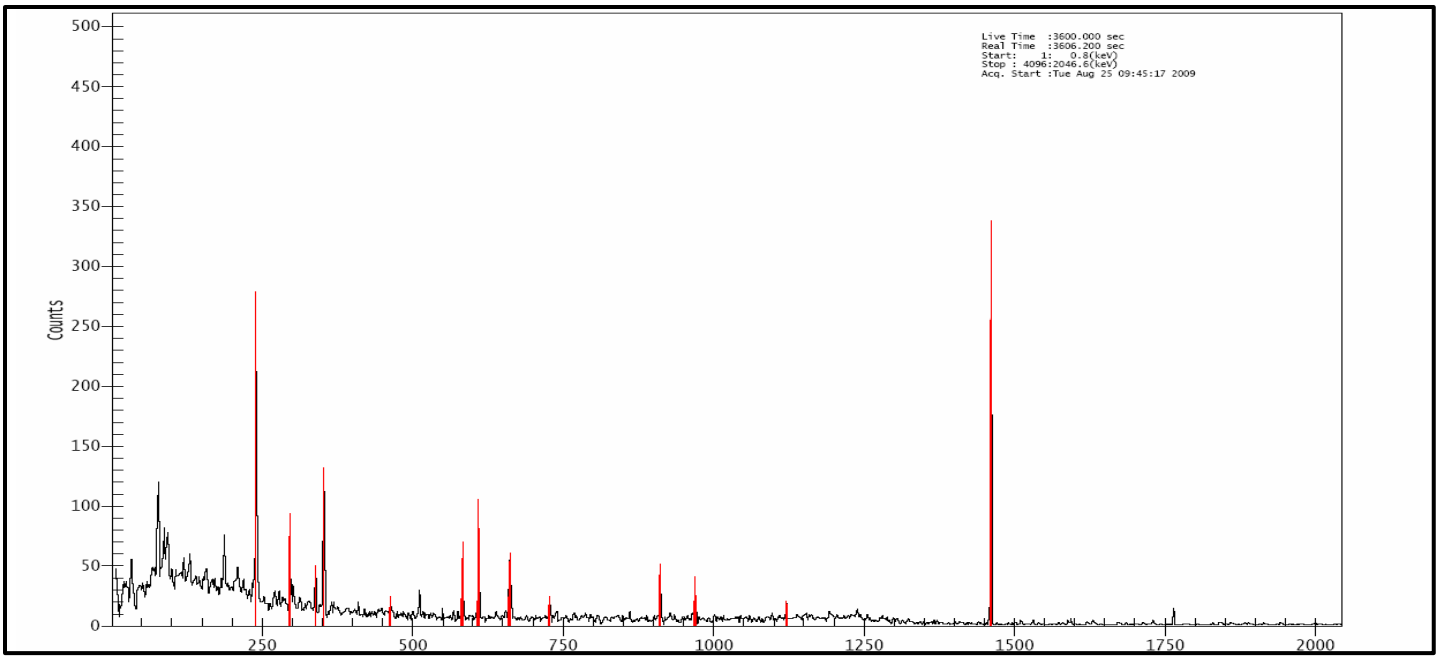

Sample (31): Knikil.

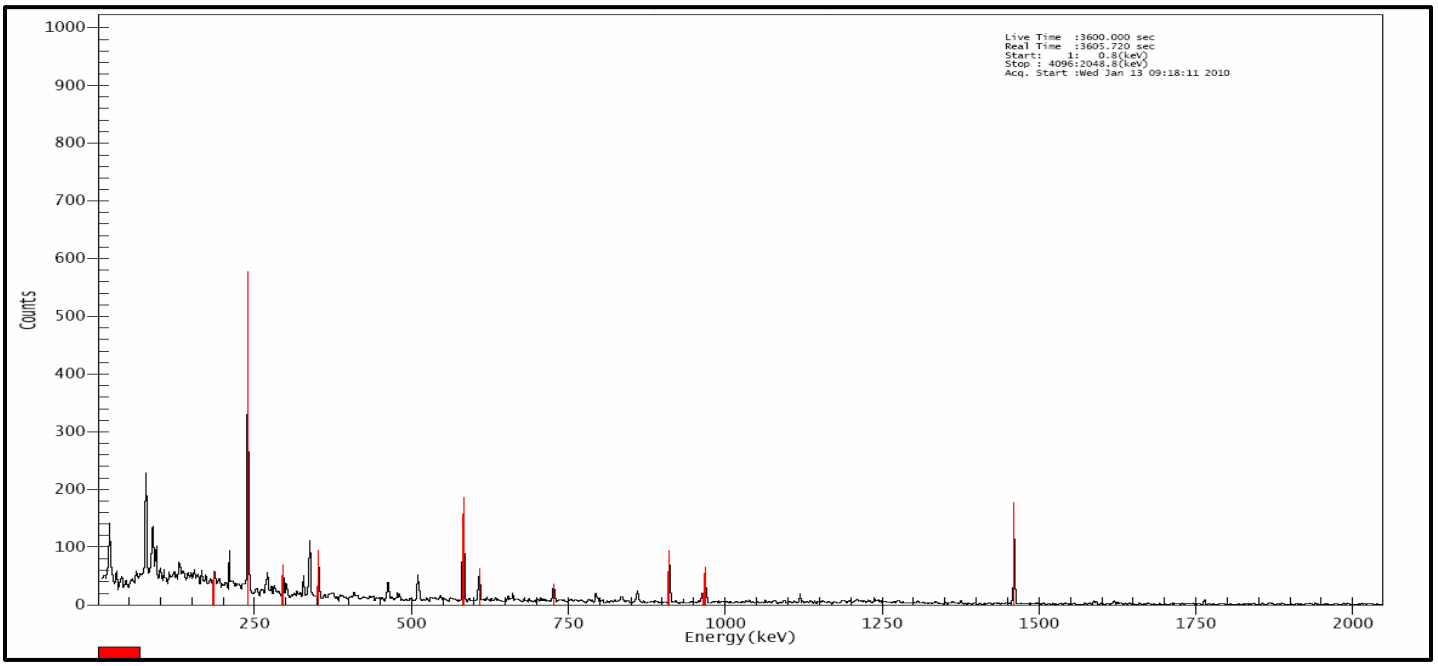

Sample (32): Al-Liwa'.

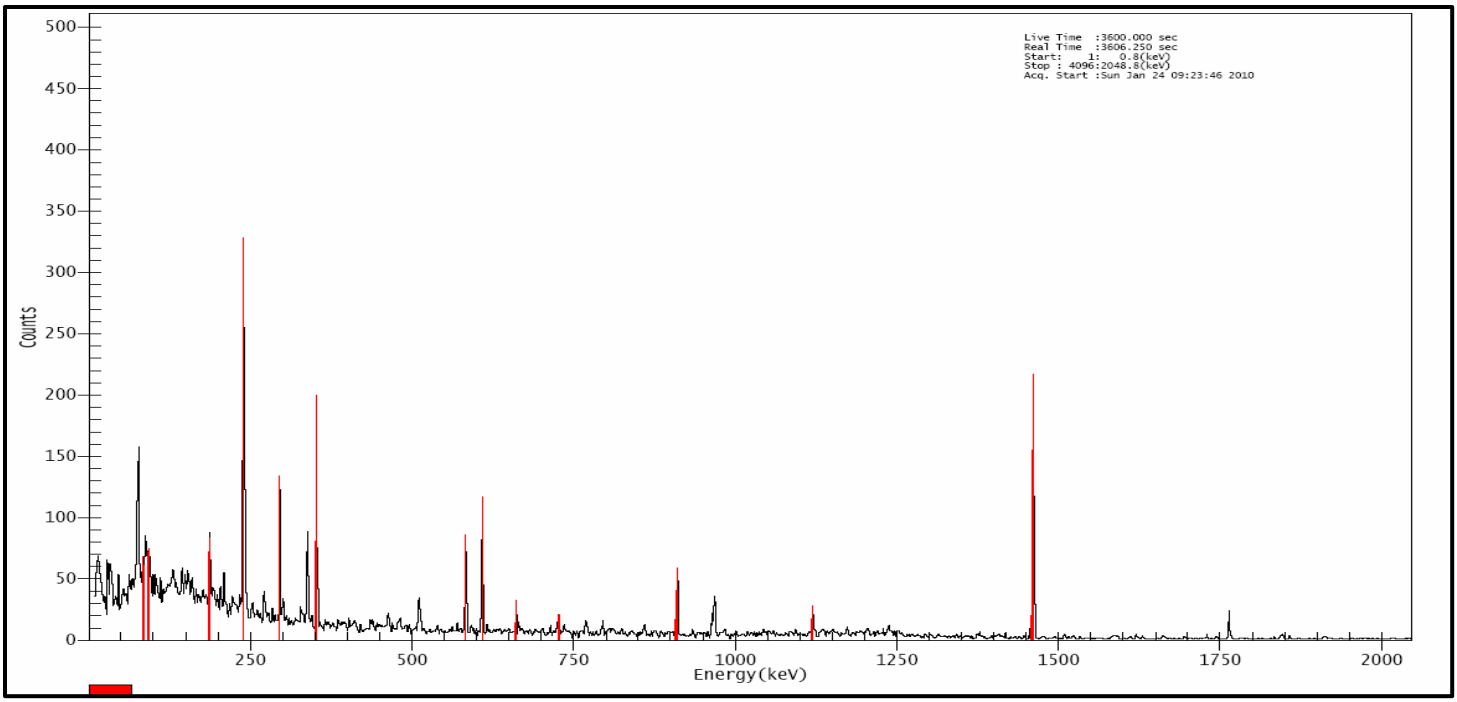

Sample (33): AL-Aadel.

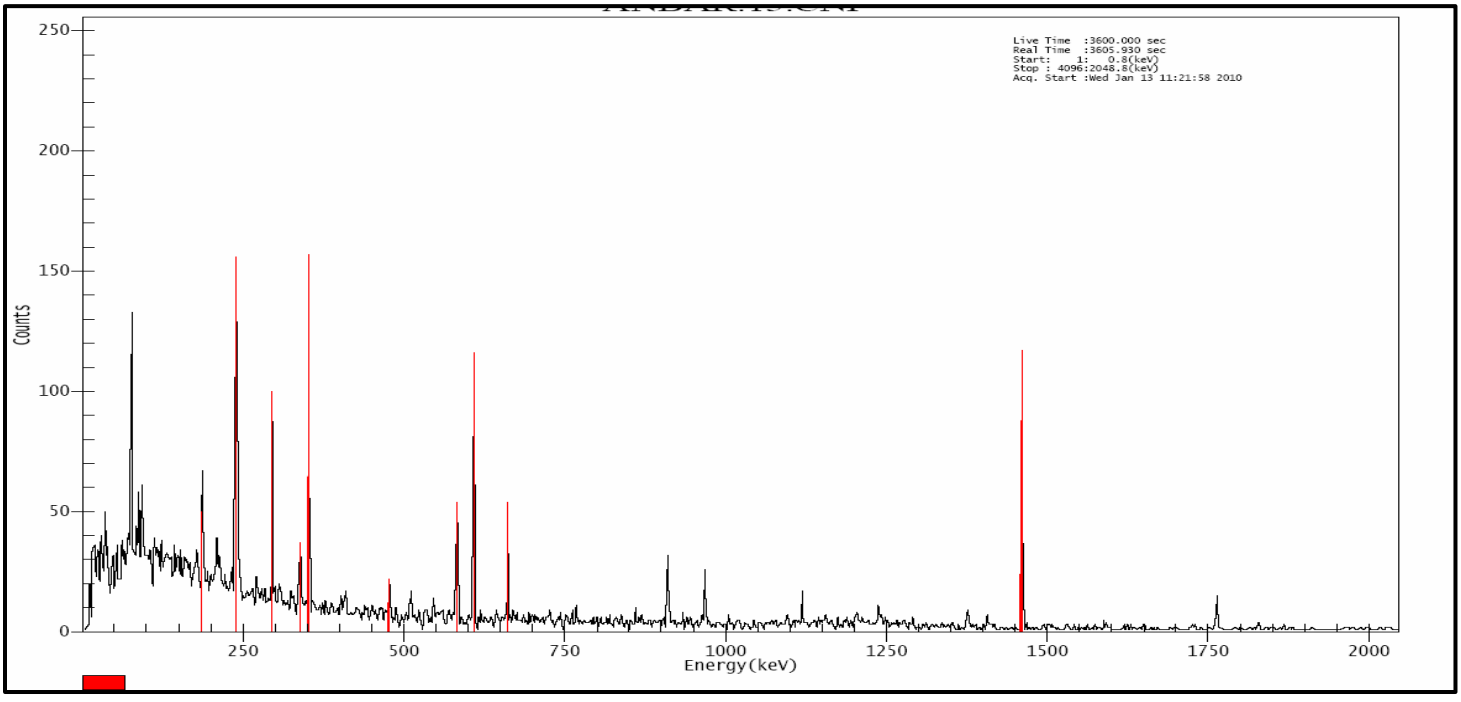

Sample (34): Al-Khayr.

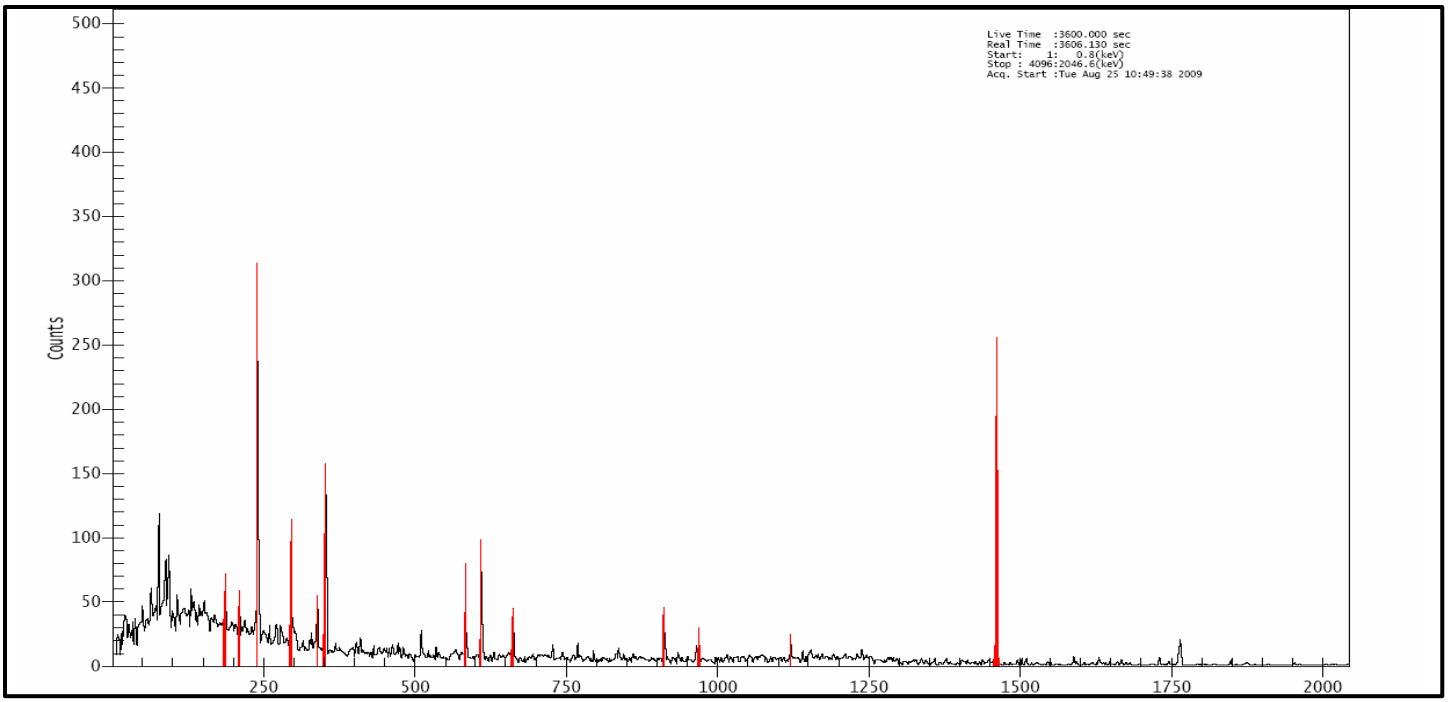

Sample (35): Al-Wadia.

Appendix D

Spectral Analysis of Samples for Kalaat Saleh.

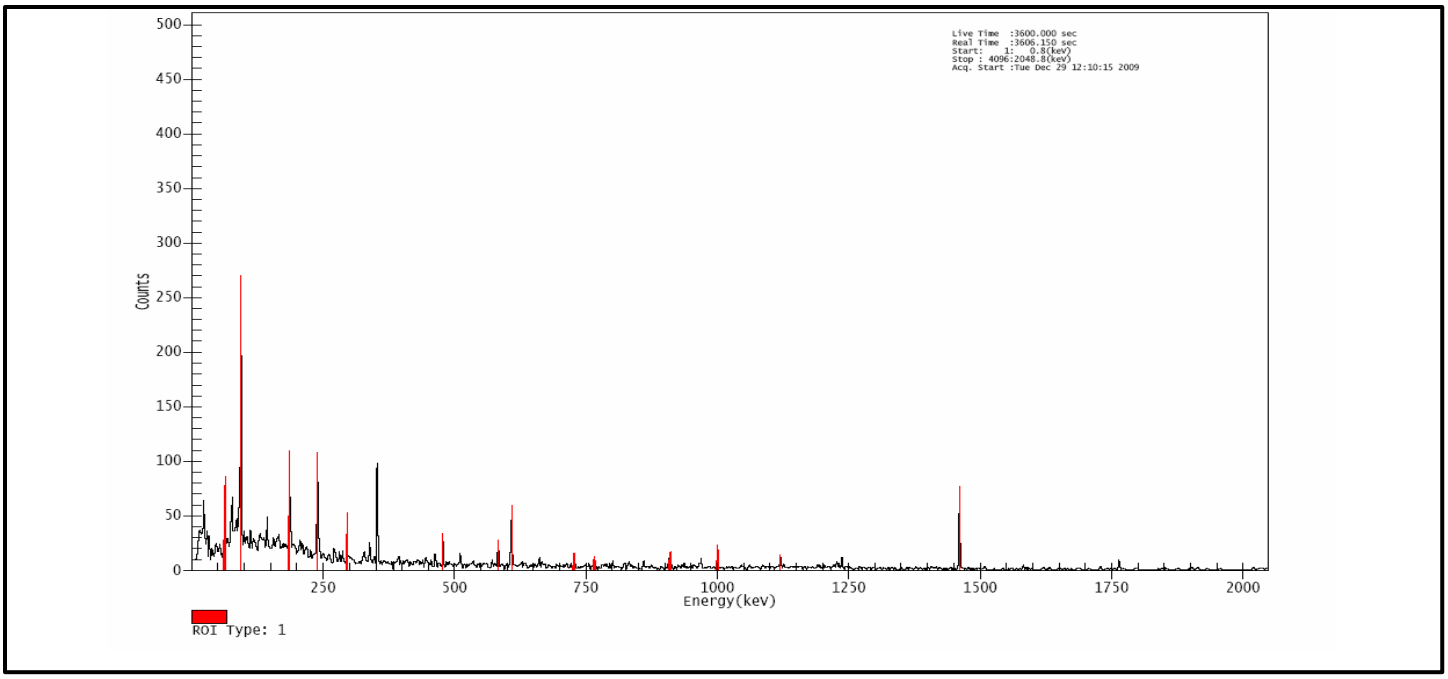

Sample (1): Al-Ghadir.

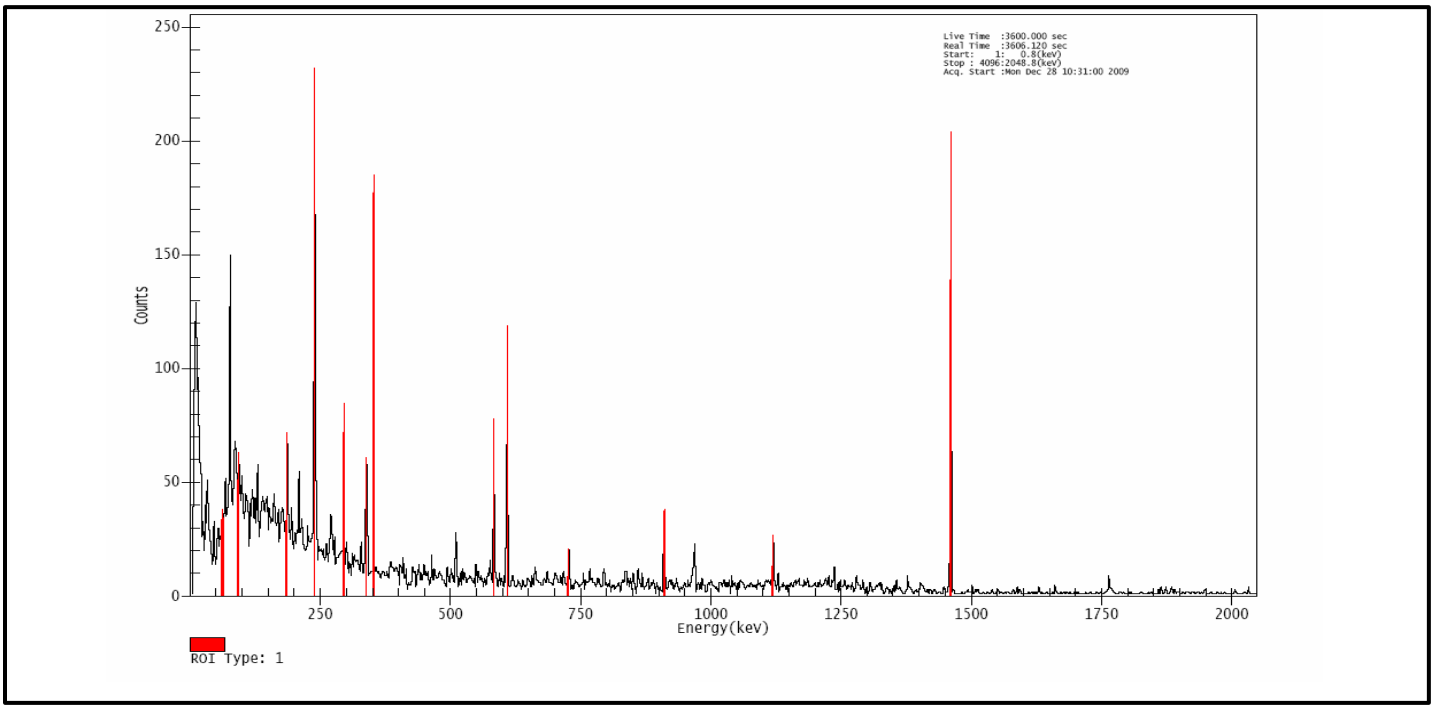

Sample (2): First Karama.

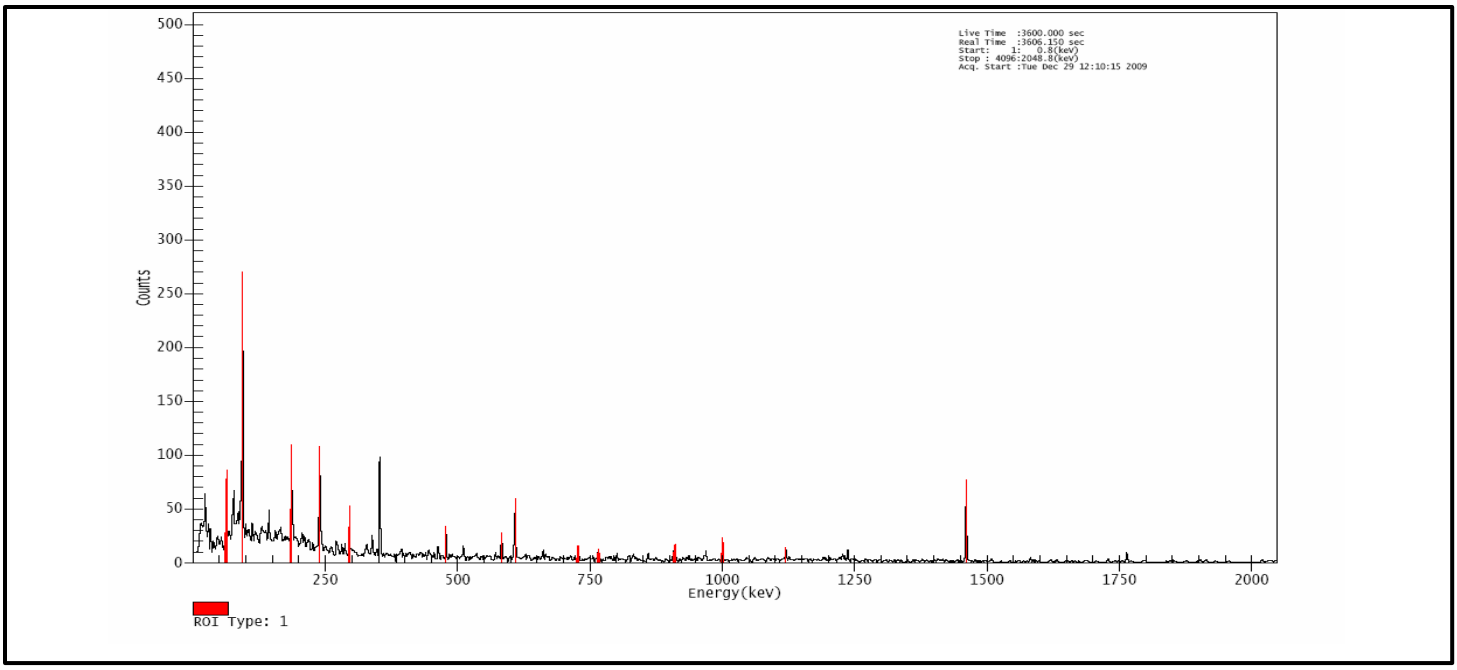

Sample (3): Al-Husaynia (Al-Shibisha).

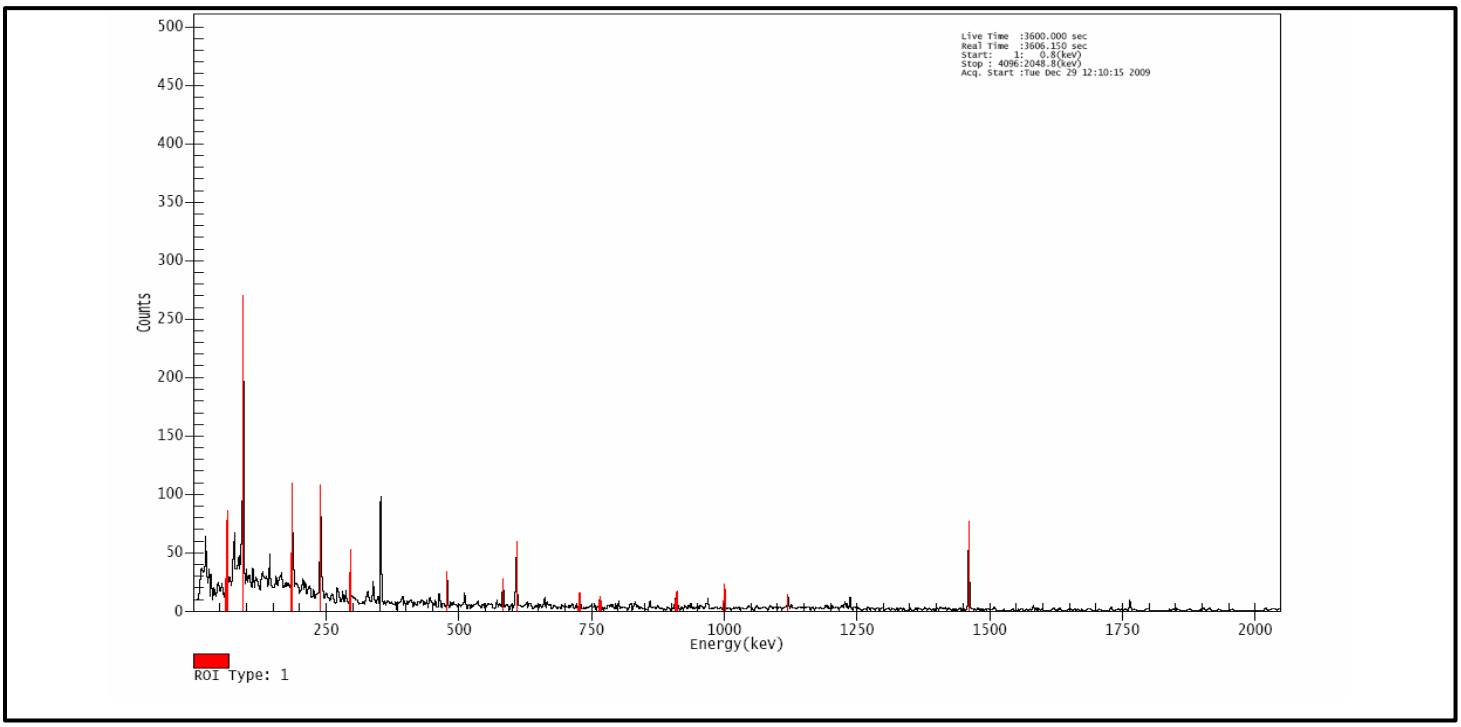

Sample (4): Third Karama.

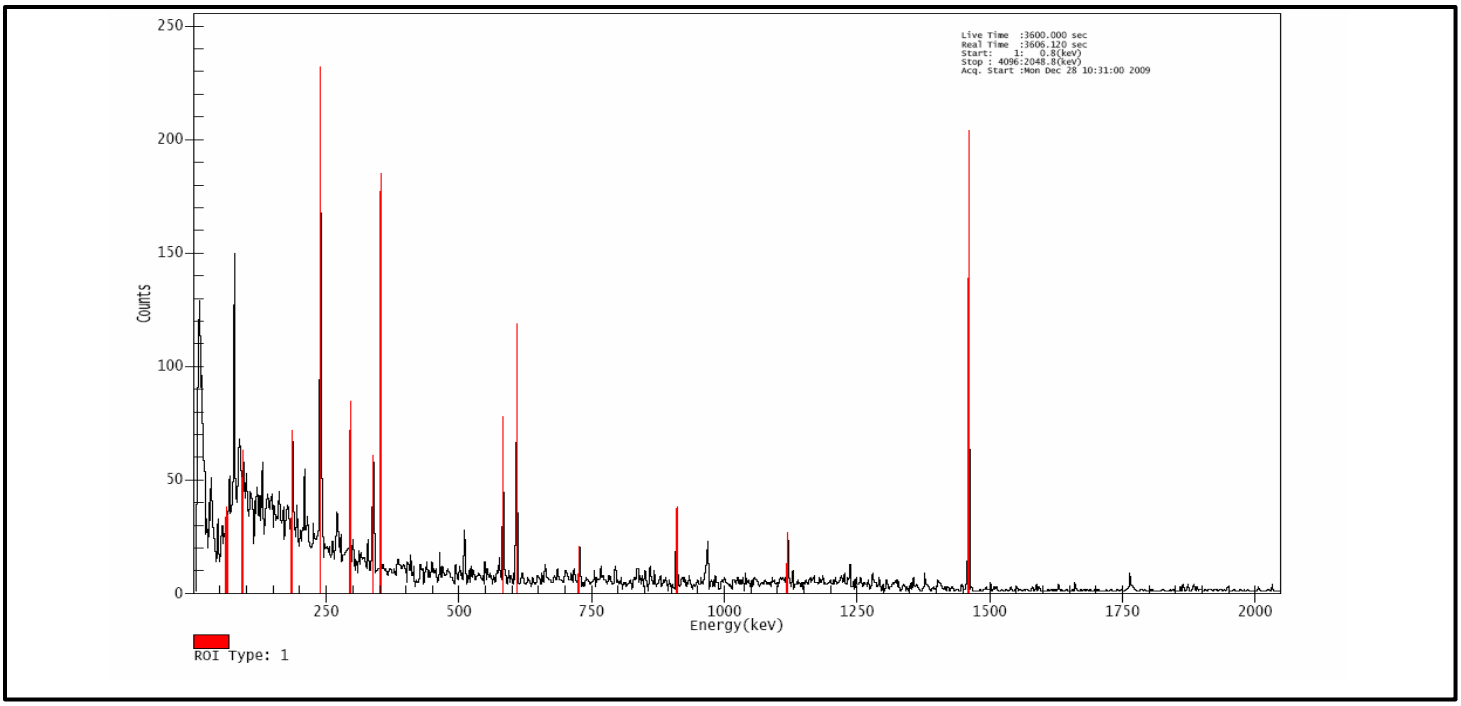

Sample (5): Second Karama.

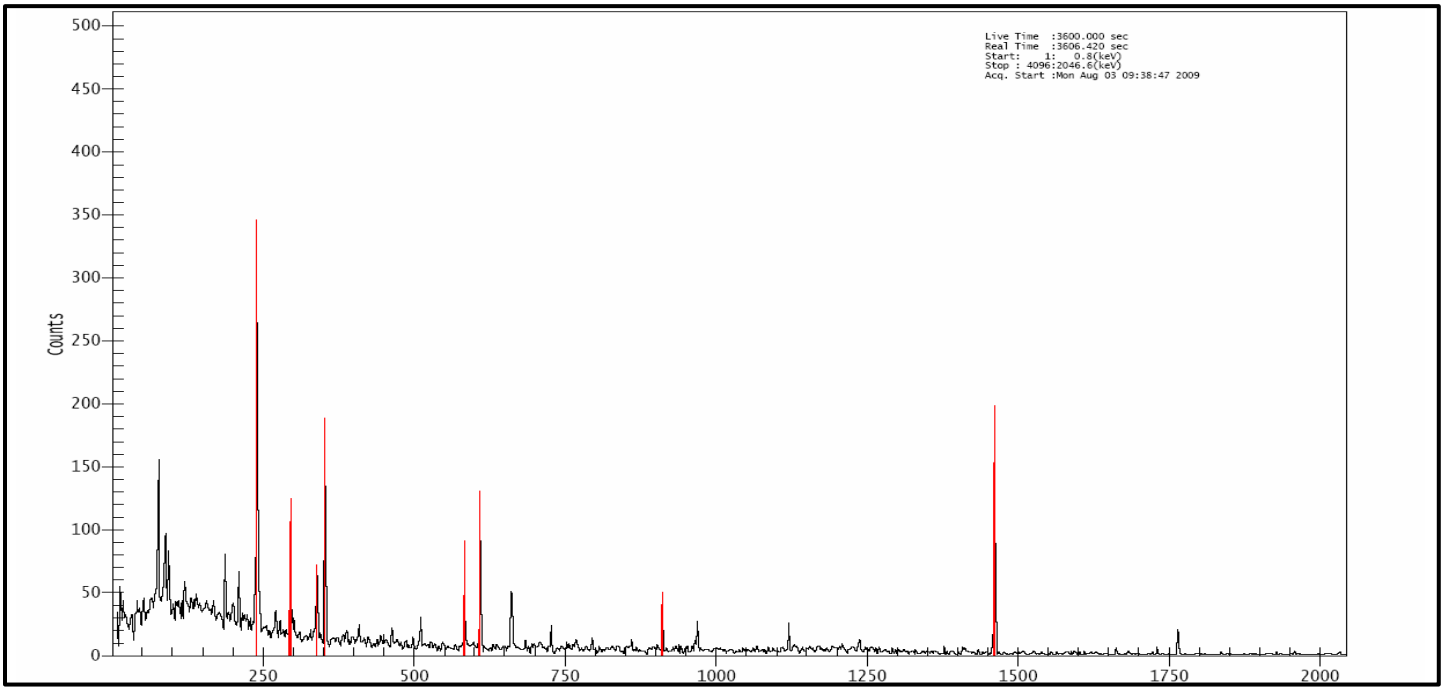

Sample (6): Al-Euruba.

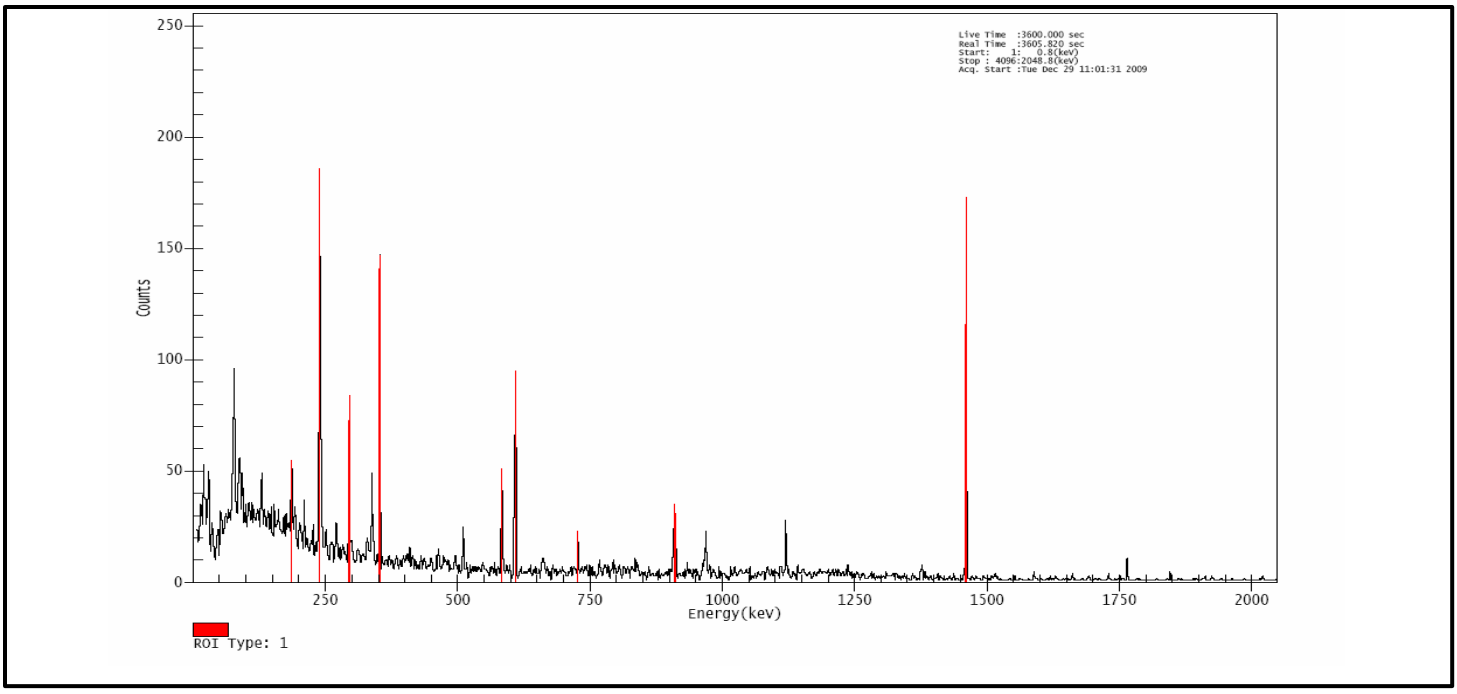

Sample (7): Al-Zahraa (Al-Baeth).

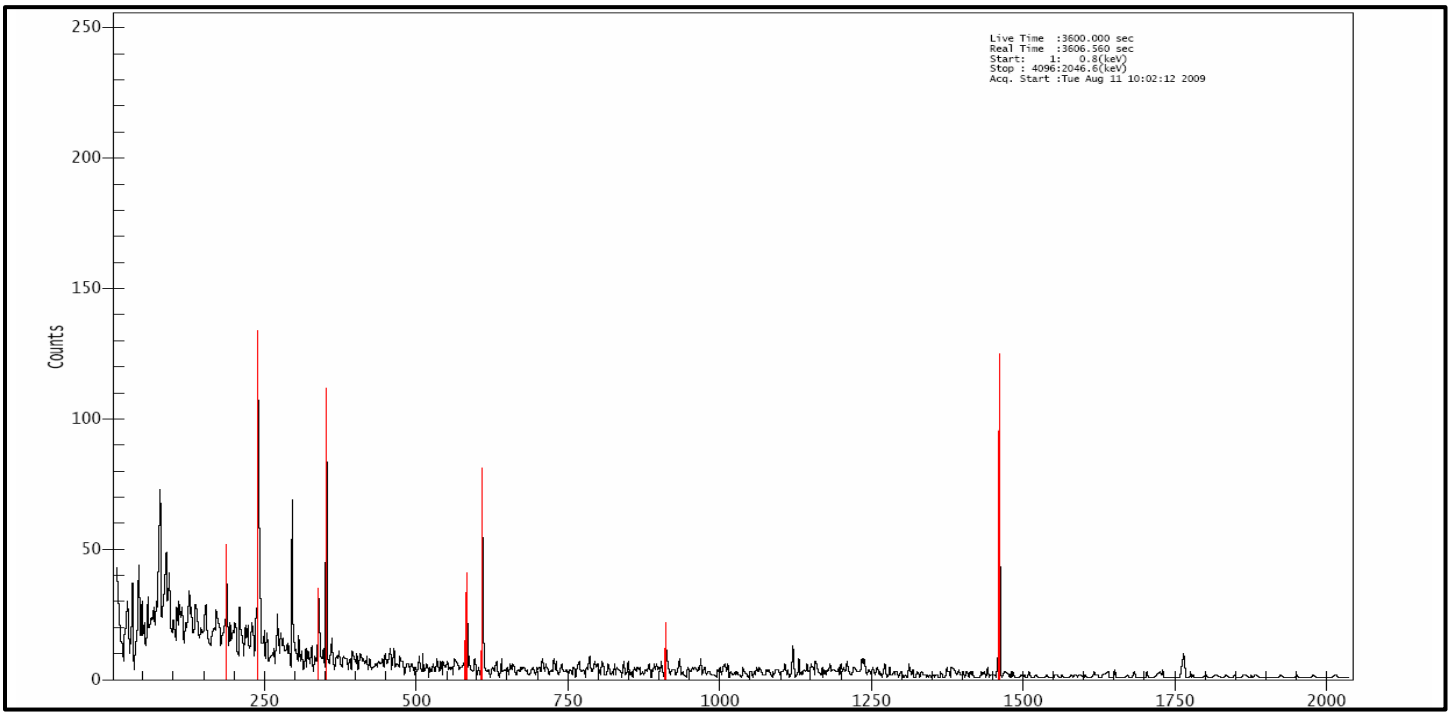

Sample (8): Al-Sadr.

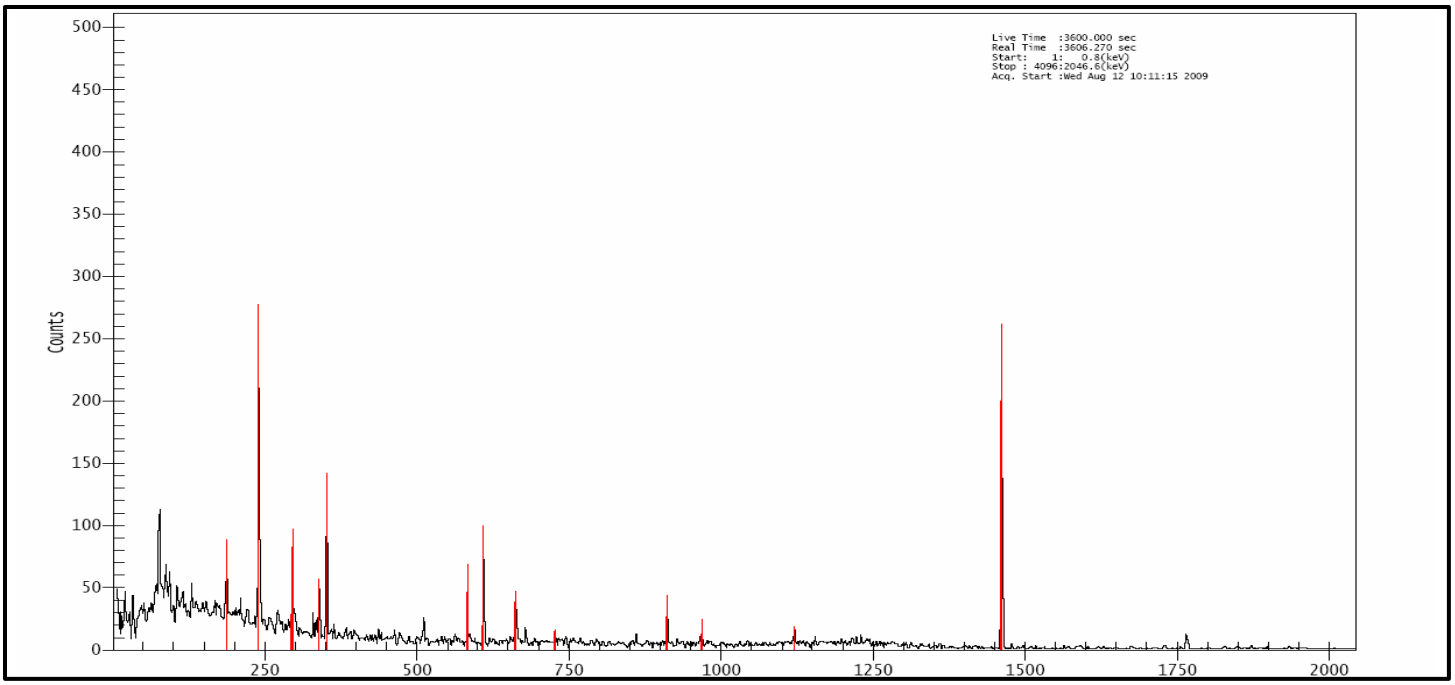

Sample (9): Al-Huriya.

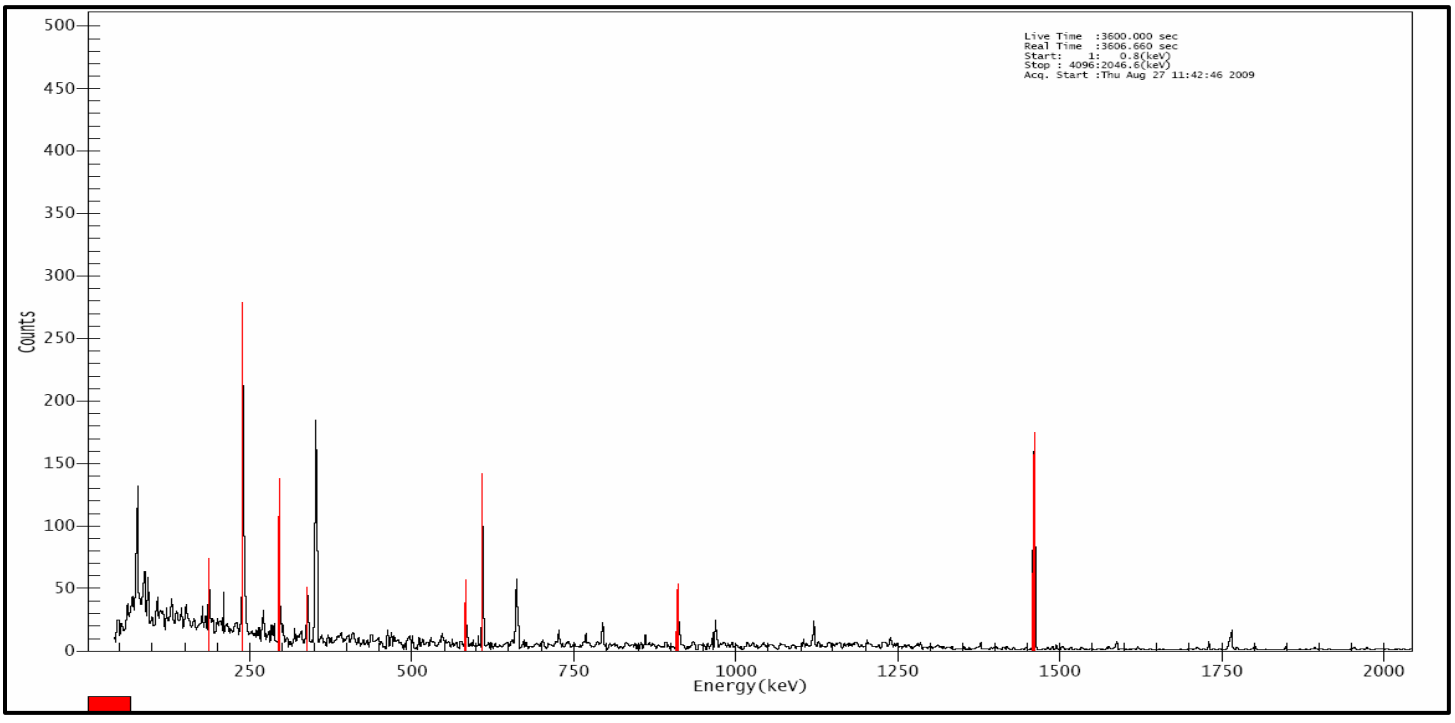

Sample (10): Abu Samej (Al-Firqa).

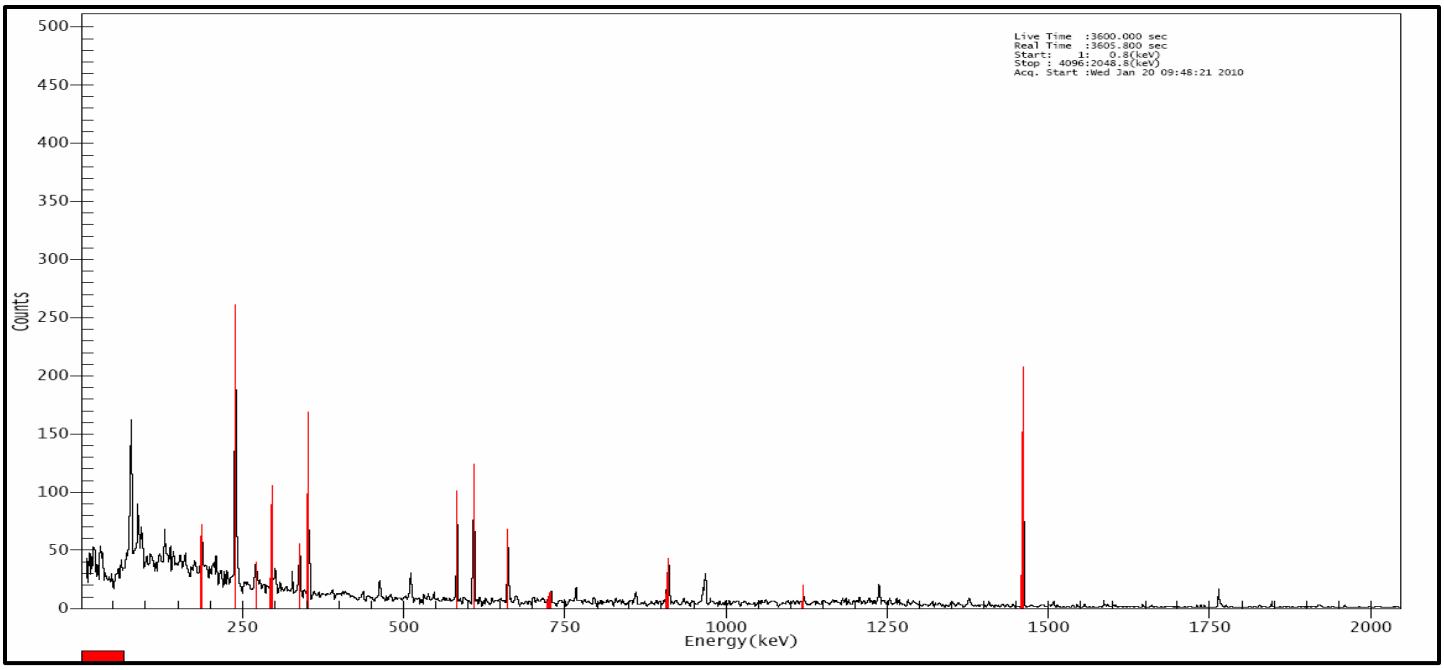

Sample (11): Al-Eizz River.

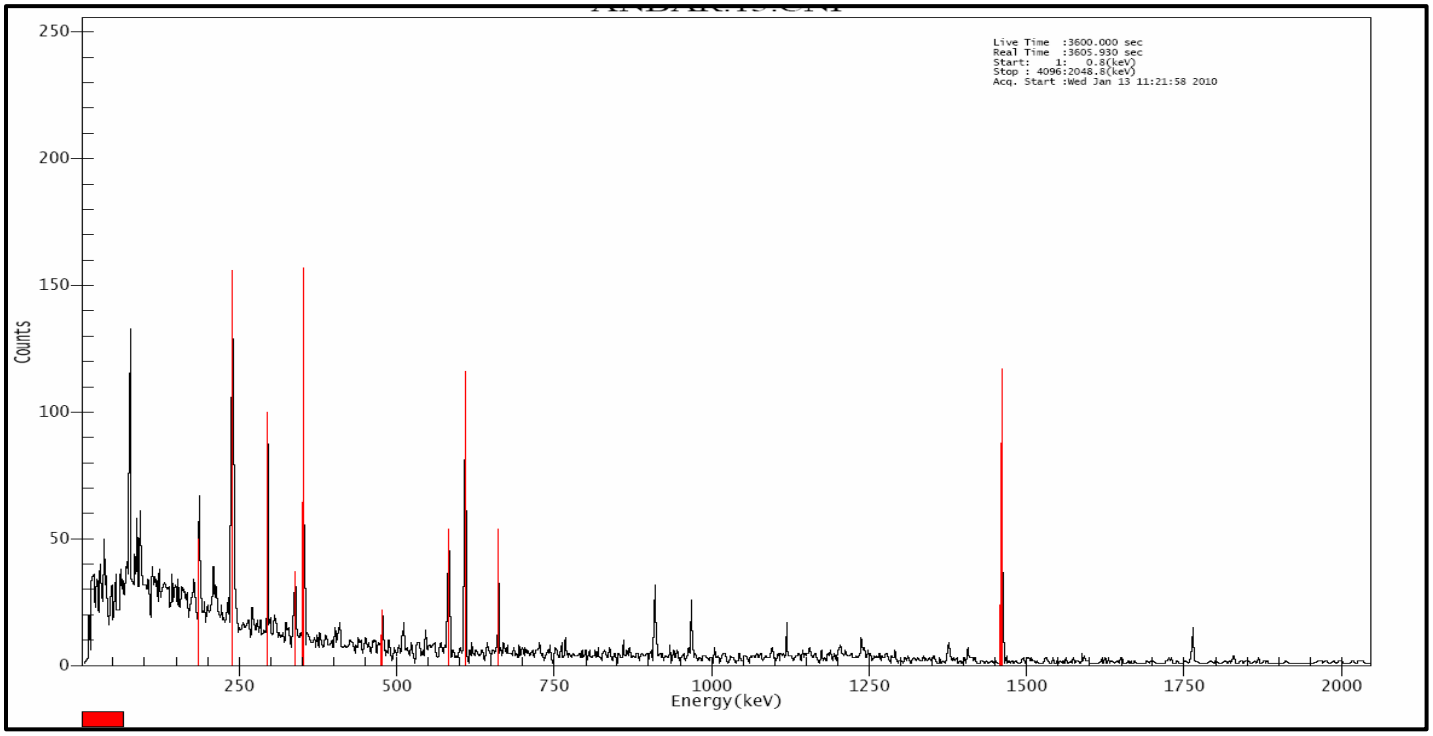

Sample (12): Al-Majaria.

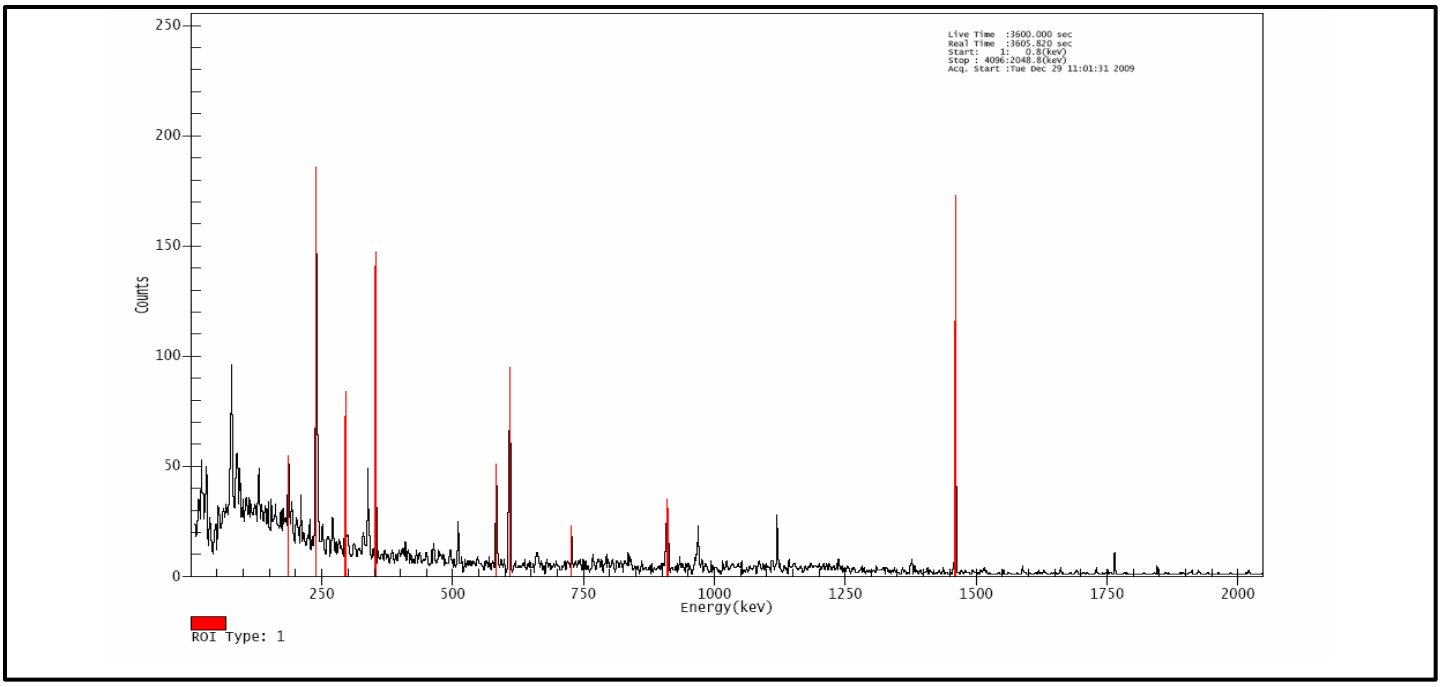

Sample (13): Al-Amir (Al-Easkari).

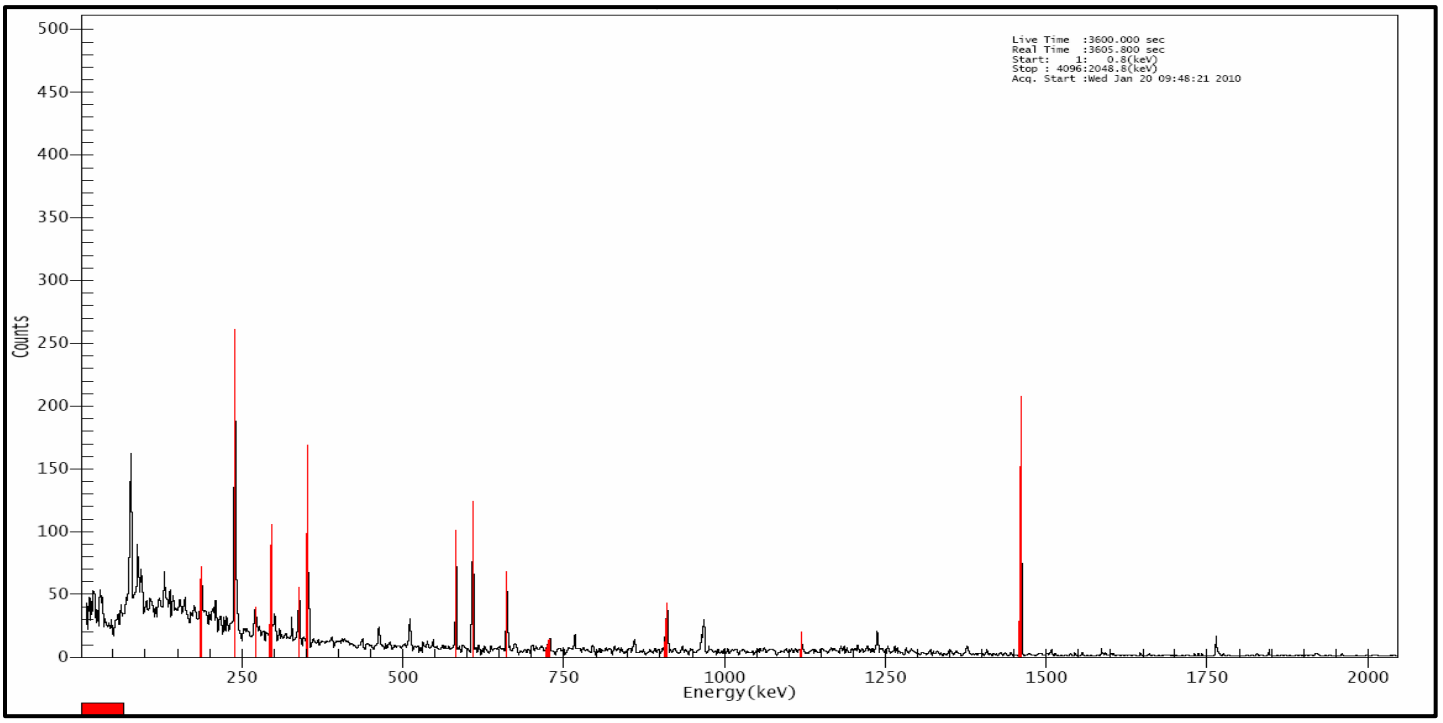

Sample (14): Sulaymaniyah.

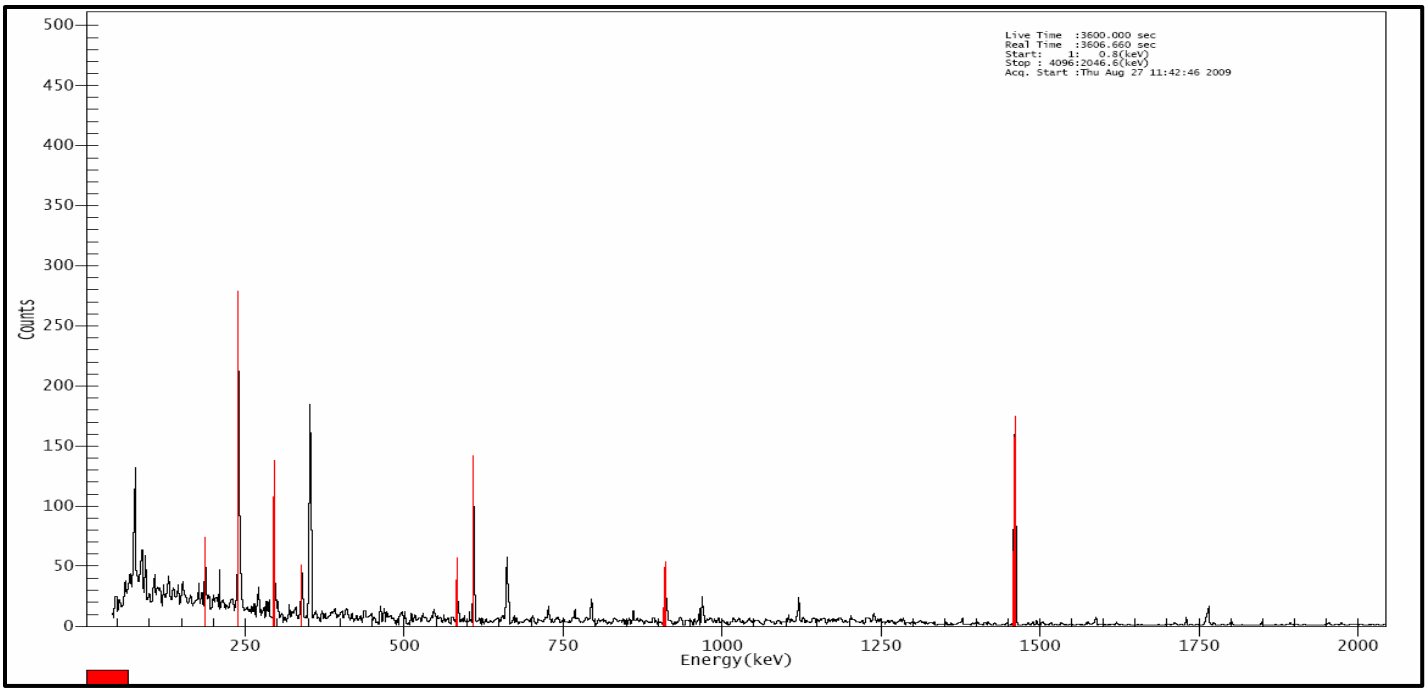

Sample (15): Al-Bayda and Al-Sawda.

الخلاصة

في هذا العمل, تم قياس النويدات المشعة الطبيعية (^{40}K ,^{232}Th, ^{226}Ra) والنويدات المشعة الصناعية (^{137}Cs) في تربتي المجر وقلعة صالح، ميسان – العراق. جُمعت خمسون عينة تربة وحُللت باستخدام مطيافية أشعة كاما المعتمدة على كاشف الجرمانيوم عالي النقاوة (HPGe) .

بلغ متوسط تركيز النشاط الإشعاعي لنظائر الراديوم-226 والثوريوم-232 والبوتاسيوم-40 والسيزيوم-137 في المجر 14.021 ± 4.650 بيكريل/كغم، 14.589 ± 2.521 بيكريل/كغم، 176.791 ± 9.827 بيكريل/كغم، و1.626 ± 0.963 بيكريل/كغم، على التوالي . وفي مدينة قلعة صالح، كانت القيم المقابلة 16.072 ± 5.455 بيكريل/كغم، و20.752 ± 3.650 بيكريل/كغم، و187.813 ± 11.011 بيكريل/كغم، و2.480 ± 1.023 بيكريل/كغم، على التوالي. بالإضافة إلى ذلك، تم حساب مؤثرات الخطورة الاشعاعية في هذا العمل, والتي تشمل النشاط الإشعاعي المكافئ للراديوم (R_{eq})، ومعاملات الخطورة الداخلية والخارجية (H_{ex}، H_{in},)ومعامل الجرعة الممتصة (D_{in}, D_{out} ,D_{tot}), ومكافئ الجرعة الفعالة السنوية الداخلية والخارجية ($AEDE_{in}$, $AEDE_{out}$)، ومعامل دليل أشعة غاما ($I\gamma$)، وخطر الإصابة بالسرطان مدى الحياة ($ELCR_{in}$, $ELCR_{out}$, $ELCR_{tot}$) ،ومعامل الجرعة السنوية للأعضاء التناسلية (AGDE) وجد أنها (48.488 ± 5.749 بيكرل/كغم) ± 0.1688 ,(0.026 و 0.130 ± 0.015)، (0.178 ± 0.019)، (43.260 ± 4.916 نانوجراي/ ساعة، 2.542 ± 22.658 نانو جراي/ساعة، و65.918±7.457 نانوجراي/ساعة)، (0.212±0.024 ملي سيفرت/سنة، 0.027± 0.003 ملي سيفرت/سنة، و0.240±0.027 ملي سيفرت/سنة)، ((0.742± 0.084) × 10^{-3}، (0.097±0.010) × 10^{-3}، و(0.840± 0.095)× 10^{-3})، (159.795± 17.088 ميكرو سيفرت/سنة)، على التوالي في المجر. بينما في قلعة صالح كانت القيم المقابلة (60.209 ± 9.223 بيكريل/كجم)، (0.206 ± 0.037،

و0.162 ± 0.024)، (0.219 ± 0.031)، (52.826 ± 7.844 نانو جراي/ساعة، 27.791 ± 11.945 نانو جراي/ساعة، و80.618 ± 11.945 نانو جراي/ساعة)، (0.259 ± 0.038 ملي سيفرت/سنة، 0.034 ± 0.005 ملي سيفرت/سنة، و0.293 ± 0.0435 ملي سيفرت/سنة)، ((0.907 ± 0.134)×10^{-3}، (0.119 ± 0.017)×10^{-3}، و(1.026± 0.152)× 10^{-3})، و(195.381± 27.988 ميكروسيفرت/سنة)، على التوالي.

أظهرت النتائج أن تركيزات نشاط الراديوم 226، الثوريوم 232، البوتاسيوم 40، والسيزيوم 137 كانت أقل من القيمة الموصى بها من قِبل اللجنة العالمية للأمم المتحدة المعنية بأثر الإشعاع الذري. علاوة على ذلك، كانت جميع معايير الخطر الإشعاعي المقدرة للنويدات المشعة الطبيعية في كلتا المدينتين أقل من الحدود الموصى بها، مما يشير إلى عدم وجود مخاطر صحية ناجمة عن النشاط الإشعاعي في مناطق الدراسة.

جمهورية العراق

وزارة التعليم العالي والبحث العلمي

جامعة ميسان/ كلية العلوم

قسم الفيزياء

قياس مستويات النشاط الاشعاعي وتقييم مؤثرات الخطورة الاشعاعية في ترب مدينتي المجر وقلعة صالح في محافظة ميسان- العراق.

رسالة مقدمة

الى مجلس كلية العلوم, جامعة ميسان

كجزءاً من متطلبات نيل درجة الماجستير في علوم الفيزياء

للباحثة

دعاء محمد كاظم خريبط

بكالوريوس, جامعة واسط ، 2010

بإشراف

أ. د. زهراء عبد الحسين اسماعيل

1448 هـ **2026 م**